EXPERIMENTAL PROGRAM FOR THE DEVELOPMENT OF IMPROVED HELICOPTER STRUCTURAL CRASHWORTHINESS ANALYTICAL AND DESIGN TECHNIQUES. VOLUME I. COMPUTERIZED UNSYMMETRICAL MATHEMATICAL SIMULATION AND EXPERIMENTAL VERIFICATION FOR HELICOPTER CRASHWORTHINESS IN WHICH MULTIDIRECTIONAL IMPACT FORCES ARE PRESENT

Gilbert Wittlin, et al

May 1973

Prepared for:

Army Air Mobility Research and Development Laboratory

May 1973

AD

USAAMRDL TECHNICAL REPORT 72-72A

EXPERIMENTAL PROGRAM FOR THE DEVELOPMENT OF IMPROVED HELICOPTER STRUCTURAL CRASHWORTHINESS ANALYTICAL AND DESIGN TECHNIQUES

VOLUME I

COMPUTERIZED UNSYMMETRICAL MATHEMATICAL SIMULATION AND EXPERIMENTAL VERIFICATION FOR HELICOPTER CRASHWORTHINESS IN WHICH MULTIDIRECTIONAL IMPACT FORCES ARE PRESENT

By
G. Wittlin
M. A. Gamon

May 1973

EUSTIS DIRECTORATE
U. S. ARMY AIR MOBILITY RESEARCH AND DEVELOPMENT LABORATORY
FORT EUSTIS, VIRGINIA

CONTRACT DAAJ02-71-C-0066
LOCKHEED-CALIFORNIA COMPANY
BURBANK, CALIFORNIA

Approved for public release; distribution unlimited.

DISCLAIMERS

The findings in this report are not to be construed as an official Department of the Army position unless so designated by other authorized documents.

When Government drawings, specifications, or other data are used for any purpose other than in connection with a definitely related Government procurement operation, the United States Government thereby incurs no responsibility nor any obligation whatsoever; and the fact that the Government may have formulated, furnished, or in any way supplied the said drawings, specifications, or other data is not to be regarded by implication or otherwise as in any manner licensing the holder or any other person or corporation, or conveying any rights or permission, to manufacture, use, or sell any patented invention that may in any way be related thereto.

Trade names cited in this report do not constitute an official endorsement or approval of the use of such commercial hardware or software.

DISPOSITION INSTRUCTIONS

Destroy this report when no longer needed. Do not return it to the originator.

Unclassified

Security Classification

DOCUMENT CONTROL DATA - R & D

(Security classification of title, body of abstract and indexing annotation must be entered when the overall report is classified)

1. ORIGINATING ACTIVITY (Corporate author)

Lockheed-California Company
Burbank, California

2a. REPORT SECURITY CLASSIFICATION

Unclassified

2b. GROUP

3. REPORT TITLE

EXPERIMENTAL PROGRAM FOR THE DEVELOPMENT OF IMPROVED HELICOPTER STRUCTURAL CRASHWORTHINESS ANALYTICAL AND DESIGN TECHNIQUES, VOLUME I - COMPUTERIZED UNSYMMETRICAL MATHEMATICAL SIMULATION AND EXPERIMENTAL VERIFICATION FOR HELICOPTER CRASHWORTHINESS IN WHICH MULTIDIRECTIONAL IMPACT FORCES ARE PRESENT

4. DESCRIPTIVE NOTES (Type of report and inclusive dates)

Final Technical Report

5. AUTHOR(S) (First name, middle initial, last name)

Gilbert Wittlin
Max A. Gamon

6. REPORT DATE	7a. TOTAL NO. OF PAGES	7b. NO. OF REFS
May 1973	~~225~~ 223	48

8a. CONTRACT OR GRANT NO	9a. ORIGINATOR'S REPORT NUMBER(S)
DAAJ02-71-C-0066	USAAMRDL Technical Report 72-72A
b. PROJECT NO Task 1F162203A52902	
c.	9b. OTHER REPORT NO(S) (Any other numbers that may be assigned this report)
d.	

10. DISTRIBUTION STATEMENT

Approved for public release; distribution unlimited.

11. SUPPLEMENTARY NOTES	12. SPONSORING MILITARY ACTIVITY
Volume I of a two-volume report.	Eustis Directorate U.S. Army Air Mobility R&D Laboratory Fort Eustis, Virginia

13. ABSTRACT

The results of a four-phase study to develop helicopter structural crashworthiness analytical and design techniques are presented. The study consisted of the development of a computer program (KRASH) and the verification of a mathematical model to predict the dynamic response during a survivable accident in which combined vertical and lateral impact velocities are present. Included in the study were a literature survey and evaluation, a detailed analysis of 32 accident cases, a drop test of a UH-1H helicopter with ground impact conditions of 23 fps vertical velocity and 18.6 fps lateral velocity, and parameter studies. It is concluded that program KRASH is capable of accurately predicting the dynamic responses during a multi-directional accident and that the program is a valuable tool with which to perform design trade-off studies. A consistent crashworthiness design criteria approach is illustrated which considers the crash environment, human tolerance limits, structural load deflection characteristics and design cost, weight and geometry penalties, all treated as a system. It is recommended that a combined analytical and test effort be initiated for the purpose of determining structural element nonlinear behavior and that deterministic methods to evaluate crashworthiness capability of present and future helicopters be used. Further recommendations are made regarding mathematical modeling of helicopters other than the UH-1H and for additional R&D effort to reduce the potential of cabin penetration by upper mass items, i.e., transmission, rotor blade.

DD FORM 1 NOV 68 1473

Unclassified

Security Classification

Unclassified
Security Classification

14. KEY WORDS	LINK A		LINK B		LINK C	
	ROLE	WT	ROLE	WT	ROLE	WT
nonlinear behavior						
dynamic response						
crashworthiness						
impact dynamics						
structural dynamics						
design criteria and concepts						
crash environment						
analytical techniques						
experimental program						
accident analysis						
human tolerance						
survivable accident						
load deflection						
energy absorption						
mathematical simulation						
Dynamic Response Index						
structural deformation						
design tradeoff						

i lb

Unclassified
Security Classification

DEPARTMENT OF THE ARMY
U. S. ARMY AIR MOBILITY RESEARCH & DEVELOPMENT LABORATORY
EUSTIS DIRECTORATE
FORT EUSTIS, VIRGINIA 23604

This report was prepared by Lockheed-California Company under the terms of Contract DAAJ02-71-C-0066. The Eustis Directorate technical monitor for this effort was Mr. G. T. Singley III of the Military Operations Technology Division.

The purpose of this effort was to develop (1) a computerized mathematical simulation which can predict the dynamic response of U.S. Army helicopters exposed to a crash environment with combined vertical and lateral impact velocity components, and (2) design techniques which, when implemented, will enhance occupant survival and reduce materiel losses during severe yet survivable helicopter accidents. The contractor achieved these objectives by (1) conducting literature, accident data, and organizational surveys, (2) developing a 40-mass, 240-degree-of-freedom, nonlinear lumped mass mathematical model, (3) tailoring the model to represent the UH-1D/H aircraft, (4) correlating the computerized UH-1D/H mathematical model with the results of a full-scale UH-1D/H drop test, and (5) conducting parametric studies to analyze the effect of design changes on system crashworthiness. This report contains a description of the state-of-the-art surveys, mathematical model, parametric studies, supporting testing, and results obtained.

The conclusions and recommendations submitted by the contractor are considered to be valid.

The report is divided into two volumes. Volume I contains a description of the state-of-the-art surveys, mathematical model, testing, parametric study, and results obtained. Volume II contains abstracts of literature reviewed, a comprehensive description of the mathematical model, a user's guide for the computer program, and the full-scale crash test instrumentation and photographic data.

Task 1F162203A52902
Contract DAAJ02-71-C-0066
USAAMRDL Technical Report 72-72A
May 1973

EXPERIMENTAL PROGRAM FOR THE DEVELOPMENT OF IMPROVED HELICOPTER STRUCTURAL CRASHWORTHINESS ANALYTICAL AND DESIGN TECHNIQUES

VOLUME I

COMPUTERIZED UNSYMMETRICAL MATHEMATICAL SIMULATION AND EXPERIMENTAL VERIFICATION FOR HELICOPTER CRASHWORTHINESS IN WHICH MULTIDIRECTIONAL IMPACT FORCES ARE PRESENT

by

G. Wittlin

M. A. Gamon

Prepared by

Lockheed-California Company
Burbank, California

for

EUSTIS DIRECTORATE
U. S. ARMY AIR MOBILITY RESEARCH AND DEVELOPMENT LABORATORY
FORT EUSTIS, VIRGINIA

SUMMARY

The results of a four-phase study to develop improved rotary-wing aircraft structural crashworthiness criteria and concepts are presented. From a summary of 3657 U. S. Army rotary-wing aircraft accidents that occurred between 1967 and 1971, 92.8% are found to be survivable or partially survivable. Thirty-two survivable accidents are reviewed in detail. The detailed accident investigation results are summarized with regard to kinematics, structural damage, and personnel injury. A literature survey is performed which consists of a review, summary, and evaluation of 32 technical reports and specifications.

During Phase II, both a substructure test and an analysis are performed on a P2V fuselage bumper, and the results are compared to determine the effectiveness of each method in determining energy absorption characteristics of aircraft structure and to ascertain the effect of the rate of loading on the nonlinear load-deflection characteristics of aircraft structure. Included in Phase II is the development of a digital computer program ("KRASH") which is capable of predicting the aircraft structural dynamic responses resulting from a crash environment. A qualitative assessment of the program's capability is satisfactorily performed by comparing analytical results with previous drop test and accident data.

The details of the Phase III UH-1H helicopter drop test are presented, including the test objectives, preparations, instrumentation, cotographic coverage, test procedure, and data reduction. The vehicle ground impact conditions are 23 fps vertical velocity and 18.6 fps lateral velocity. The test included 24 accelerometer signals, 2 strain-gage signals, and a calibrated rod to view deflection of the fuselage. The results of the test are presented in the form of acceleration time histories and peak values. Included is a description and photographs showing postcrash damage. The drop test data is correlated with results obtained analytically using program "KRASH". The 31 lumped mass analytical model used in the correlation is described in the report. The analytical model includes Dynamic Response Index (DRI) measurements at the forward and rear fuselage locations.

Parameter studies performed during Phase IV, are used to ascertain the effect of changes in load level and/or load stroke for the various structural elements, including landing gear skids, lower fuselage, seat system, engine, and transmission mounts on structural and occupant responses. A consistent design criteria approach is proposed in this report, and the results of the parameter variations are used to illustrate the manner in which the concepts can be applied to improve crashworthiness capability of the vehicle to the 75th and 95th percentile potentially survivable accident levels.

The results of the study are presented in 2 volumes. Volume I contains the discussions of the program details and results which lead to the conclusions and recommendations. Volume II contains the supporting test and analytical data as well as a complete description of computer program KRASH including a User's Guide and a sample problem.

FOREWORD

This report was prepared by the Lockheed-California Company under U. S. Army Contract DAAJ02-71-C-0066 (Task 1F162203A52902) . The work was administrated under the direction of the Eustis Directorate, U. S. Army Air Mobility Research and Development Laboratory, Fort Eustis, Virginia, with G. T. Singley, III, acting as Project Engineer.

The Lockheed-California Company Program Leader was G. Wittlin. M. A. Gamon developed the digital computer program "KRASH" and supporting analytical procedures. Digital computer programming was performed by G. Howell under the direction of B. McCorkle. J. Ryan directed the test effort and was assisted by M. Rapko. Substructure analysis was performed by B. Almroth of LMSC. Consultation was provided by Messrs. J. E. Wignot and P. C. Durup.

The results of the study effort were enhanced by the support supplied by the following organizations and personnel:

- U. S. Army Agency for Aviation Safety (USAAAVS), Ft. Rucker, Ala. (Lt. Col. Darrah, Col. Kerfoot, Col. Sutliff, J. Haley and L. Sand.)
- U. S. Naval Safety Center, Norfolk, Va. (Cmdr. Starbuck, J. Coombs).
- U. S. Army Aviation Systems Command (AVSCOM), St. Louis, Mo. (Col. Phillips, R. Oliver and W. Bruggeman).
- U. S. Army Aeronautical Depot Maintenance Center (ARADMAC), Corpus Christi, Texas (Col. Dillard, G. Startz).
- Directorate of Aerospace Safety, Norton AFB, California (Maj. Carbe).
- Dynamic Science (S. Desjardins).

TABLE OF CONTENTS

LIST OF ILLUSTRATIONS

LIST OF TABLES

LIST OF SYMBOLS

Human Tolerance Criteria

AF	amplification Factor
DRI	Dynamic Response Index
$\frac{d}{dt}$, $\frac{d^2}{dt^2}$	first derivative, second derivative
f_n	natural frequency, Hz
$G_{X,Y,Z}$	measured G's in X,Y,Z axis
$G_{X_L}, G_{Y_L}, G_{Z_L}$	limit G's in X,Y,Z axis
G/Sec, g/sec	rate of onset
K	stiffness
m	mass
t	time
δ	deflection
ϵ_p	maximum excitation
π	Pi
τ	rise time
τ_r	time at peak excitation
ω_n	natural frequency, rad/sec
ζ	percent of critical damping

LIST OF SYMBOLS

SUBSTRUCTURE ANALYSIS & TEST

a, b, c	equation constants
CDS	Lockheed Rye Canyon Central Data System
R	radius of shell inner contour
S	arc length along inner contour
STAGS	Structural Analysis of General Shells
w	normal deflection
X, Y, Z	Cartesian coordinates
σ, z	shell coordinate
Δ	incremental or differential
Ω	shell inner contour angle

MATHEMATICAL MODEL & CORRELATION

CDS	Lockheed Rye Canyon Central Data System
c.g	center of gravity
DX	incremental distance
G, g	units of acceleration
fps	feet per second
f_n	natural frequency, Hz
K	stiffness
KR	stiffness reduction factor
msec	milliseconds
PAX	passenger
x, y, z	inertial coordinates

LIST OF SYMBOLS

MATHEMATICAL MODEL & CORRELATION (Continued)

Δ, δ	deflection for seat, masses
π	Pi
ϕ, θ, ψ	Eulerian angles
μ	coefficient of friction
ω_n	natural frequency, rad/sec
ζ	percent of critical damping

INTRODUCTION

BACKGROUND

Current helicopter design criteria are based on independent requirements for structure and/or equipment to withstand acceleration levels. In particular, a helicopter fuselage is designed with the lightest structure which will meet the flight and ground load requirements, yet fulfill specified missions. As a result, human tolerances to acceleration and the rate of change of acceleration far exceed the crashworthiness capabilities of the helicopters now in operation. This deficiency has been attributed, in part, to the need to keep structural weight to a minimum, yet fulfill mission requirements. However, this does not hide the fact that a disproportionately small amount of effort has been applied to a consistent approach to airframe structural crashworthiness design. Ideally, a consistent design for crashworthiness means that the design is such that the various parts of the structure are such that personnel would not be exposed to incapacitating injury prior to expending all of the energy absorption capability of the structure. With consistent structural crashworthiness design as a goal, a considerable improvement can be made toward providing a design that will provide survivability closer to the 95th percentile accident pulse with a modest weight penalty.

The concern for occupant survival in a crash situation has taken on an accelerated pace in recent years. The emphasis has changed from finding the cause of the accident to improving the chances for crash survival. Research conducted by the U. S. Army Transportation Research Command * and aviation crash injury studies, under the auspices of Government agencies, has yielded significant contributions to the understanding of the ability of human bodies to withstand high accelerations. Numerous tests have been conducted to determine the protection afforded occupants by the design and orientation of seats during simulated crash conditions. Considerable insight into the cause of injuries and fatalities has been gained as a result of the crash investigations conducted by the U. S. Army Board for Aviation Accident Research (USABAAR)**, the Federal Aviation Administration (FAA), and the major airframe manufacturers. The knowledge obtained regarding restraints such as seats, belts, and harnesses is important to the understanding of the problem of crashworthiness. However, it is only one ingredient which must be integrated with other areas of significance in order that proper crashworthiness design procedures can be established.

---

* Now the Eustis Directorate, U. S. Army Air Mobility Research & Development Laboratory, Fort Eustis, Virginia.

** Now the U. S. Army Agency for Aviation Safety (USAAAVS), Fort Rucker, Alabama.

The manner in which the aircraft kinetic energy developed in a crash is absorbed can have a significant effect on the safety of the occupant. If absorption is to be accomplished through structural deformation, then it is desirable to make the deformation as large as possible to keep the loads under which the deformation occurs at a constant but tolerable level. Deformation of primary structure, providing no total collapse, will attenuate the forces that are transmitted from the point of contact to the occupant's section. The material properties and uses should be such as to facilitate predicted structural deformation. In addition to material properties, the fabrication technique can influence the ability of the structure to absorb the energy.

The determination of design procedures can, therefore, be seen to be complex due to the fact that the dynamic response of structures is a function of many parameters, including configuration, fabrication technique, material properties, excitation magnitude, shape and duration of loads. Consequently, there has been increased interest in the ability to model the structural characteristics of aircraft and determine the dynamic response to measurable excitation functions. Analyses have been performed and results compared to test data and/or accident evaluation reports. Thus far, gross behavior of aircraft structures can readily be ascertained. However, analysis to describe detailed structural behavior presents some problems. Crash landings result in structural deformation into the plastic region. The "state of the art" of dynamic analysis in this regime has limitations with regard to time, size, and cost of analysis. To complicate the problem further, crash analysis to date primarily has considered the vertical impact loads. However, accident data reveals that the definition of lateral and longitudinal crash loads and, consequently, structural responses to such loads is significant and must be included in a crashworthiness study which is oriented toward the development of design criteria and concepts.

The development of analytical methods which can accurately predict structural crashworthiness in the initial stages of aircraft design provides a valuable means by which improved occupant survival can be achieved with minimum cost and weight penalty. Investigations to date have shown that the following characteristic rotary-wing aircraft structural inadequacies exist:

1. Structure below the fuselage floor and in the fuselage sides permits transmission of injurious deceleration forces to the seated occupant.

2. Inadequate fuselage strength to maintain a protective shell in a lateral "rollover" accident.

3. Insufficient structural strength to resist inward and upward crushing of the lower, forward fuselage in nose-down, longitudinal impacts.

4. Inadequate floor ductility that causes shear and bending fractures especially at occupant seat location.

5. Inadequate transmission and rotor mast tie down strength resulting in penetration into occupiable cabin volume.

Although several analytical and experimental studies have been conducted in recent years, there is still a need to resolve the effect of lateral and longitudinal crash forces when combined with the vertical forces that are present. Design guides that have developed thus far will be limited until such time as the complete dynamic response during crash landings can be analytically modeled and verified through actual test data. To develop design criteria which will enhance occupant survival and reduce material losses during severe yet potentially survivable rotary-wing aircraft accidents, it is necessary to evaluate the existing crash data and current procedures for predicting damage, determine the dynamic behavior of the airframe structure on impact, and determine the potential benefits of modified designs to improving crashworthiness.

PROGRAM OBJECTIVES

The objectives of the program described herein are:

- To develop a computerized mathematical simulation which can predict the dynamic response of U. S. Army rotary-wing aircraft when exposed to a crash environment with a combined vertical-lateral impact velocity.

- To develop design criteria and preliminary design concepts which, when implemented, will enhance occupant survival and reduce material losses during severe yet survivable rotary-wing aircraft accidents.

To facilitate the achievement of the stated program objectives, the study is performed in four technical phases as follows:

I	-	literature survey and accident analysis
II	-	development of a computer program and simulation
III	-	drop test verification
IV	-	parametric analysis

The specific goals of each phase are stated below:

Phase I Goals

- Evaluate and summarize the literature that is pertinent to rotary-wing crashworthiness structural design.

- Relate the cause of injury to structural deficiencies.
- Establish initial impact conditions for the Phase III drop test.
- Provide a means to qualitatively evaluate the analytical program to be developed during Phase II.
- Help define the crash environment and subsequent hazards.
- Investigate areas in which improved design criteria and concepts can be utilized.

Phase II Goals

- Evaluate and compare analytical and test methods which can be utilized to determine energy absorption characteristics of aircraft structure.
- Determine the effect of rate of loading on the load deflection characteristics of aircraft structure.
- Develop an analytical model which will be capable of predicting the aircraft dynamic response resulting from a crash environment.
- Perform a qualitative assessment of the analytical program's ability to perform a crash analysis.

Phase III Goals

- Obtain experimental data which can be used to improve and/or verify prediction methods.
- Establish the degree of accuracy associated with the analytical procedures.
- Show the limitations associated with the analytical method.
- Indicate possible future measurement requirements necessary to further improve design criteria.

Phase IV Goals

- Establish the relative significance of different parameters.
- Show the extent to which different parameters influence the response.
- Develop improved design criteria and concepts.

- Provide a means by which design criteria can be updated.

REPORT FORMAT

The table of contents conveys the general plan of the report. The study is documented in two volumes. Volume I contains the discussions of the program details and results which lead to the conclusions. Volume II presents the supporting test and analytical data.

The background information is presented initially to provide a proper perspective in relation to the objectives of the program, and the goals of each phase which are discussed. Volume I is presented in a manner which is consistent with the chronological order of the four technical phases and includes:

- Crashworthiness Analysis of Survivable Helicopter Accidents and the Survey and Evaluation of Technical Reports.
- Substructure Test and Analysis and the Development of the Digital Computer Program "KRASH".
- Experimental Program and Correlation.
- Parametric Studies and Design Criteria.

The program results are presented in summary form prior to the conclusions and recommendations.

Volume II contains supporting data for the details presented in Volume I. This volume contains abstracts for the 32 technical reports reviewed during the program. Included in the literature survey section is a matrix categorization of the reports by subject and applicable area of interest. A brief description is presented on STAGS, the LMSC computer program used to perform the analysis of the P2V-4 fuselage bumper. A comprehensive description of program KRASH is presented, including the theory, initial conditions, the User's Guide, and a sample problem. Twenty-six channels of recorded test data, thirteen channels of filtered data and forty-eight channels of integrated test data and film data are presented as well as additional analytical data.

CRASHWORTHINESS ANALYSIS OF SURVIVABLE HELICOPTER ACCIDENTS

ACCIDENT REVIEW CRITERIA

Two indices of crashworthiness which are proposed in References (1) and (2) and used consistently throughout the literature are:

1. The degree of cabin collapse under standard crash conditions.

2. The level of acceleration experienced by occupants during the crash.

Basically the structure, to be considered of crashworthy design, must provide a protective shell around the occupant while allowing the structure to collapse to some degree. In addition, the structure must minimize the level of acceleration that reaches the occupant, such that it will be below human tolerance limits.

On the basis of program objectives, indices of crashworthiness, accident types, degree of structural damage, and injuries sustained during crash impacts, the criteria that were established for determining the accident cases to be selected for detailed analysis consisted of the following:

- major injury to personnel
- minimum of one survivor
- helicopter sustained substantial structural damage
- utility type helicopter (UH-1D/H)
- significant information available in the data bank

DEFINITIONS

The various Government agencies from which accident data were obtained provided computerized summaries and narratives of the accident cases. The terminology most commonly used in the accident records is defined below:

Accident Types

Survivable - An accident is survivable if the crash forces imposed upon the occupants are, in the investigator's best judgement, within the limits of human tolerance and all portions of the inhabitable area of the aircraft remain reasonably intact, i.e., are not collapsed sufficiently to impinge upon or crush vital areas of a person in a normal position.

Partially Survivable - Fatal injuries or occupancy of an inhabitable area are not criteria in determining survivability of an accident. For example, if the front seat area of a tandem seat aircraft has been completely demolished, but structures surrounding the rear seat area were virtually intact, the accident would be classified as partially survivable even though the rear seat occupant was fatally injured. The accident would still be classified as partially survivable if the rear seat was unoccupied. Thus, occupancy or non occupancy is irrelevant to survivability.

Nonsurvivable - An accident is nonsurvivable when impact forces exceed human tolerance, and/or all inhabitable areas are collapsed, or disintegrated, by impact to a degree where all occupants would sustain crushing injuries of vital body areas.

Structural Damage Codes

Alpha (destroyed) - loss or damage to the aircraft which renders the aircraft of no further value, except for possible salvage of parts. Includes repairable aircraft which must be surveyed because of inaccessible location, or aircraft for which the cost of repair exceeds the standards for economical repair.

Substantial (major) - aircraft damage when (1) the total direct man-hours required to effect complete repairs to the aircraft, at any level, exceed the substantial damage limits of 500 direct man-hours (for the UH-1), and (2) destruction or damage is beyond economical repair to a major component, requiring its removal and replacement with a new component.

Minor - aircraft sustained damage requiring between 100-499 direct man hours to repair (for the UH-1).

Limited - aircraft sustained damage requiring less than 100 direct man hours to repair (for the UH-1).

Injury Classifications

A. Thermal Fatalities and Injuries - Fatalities are considered to be thermal when the primary cause of death is established as due primarily to thermal injuries. Thermal injuries include all persons who received thermal injuries regardless of degree and exclusive of all other injuries regardless of degree.

B. Nonthermal Fatalities and Injuries - Fatalities are considered to be nonthermal when the primary cause of death is attributed to other than thermal injuries. Nonthermal injuries include all persons who received injuries which did not involve any degree of burn.

C. Major Injuries - Any injury requiring five or more days in the hospital or quarters, or a combination of both, or any of the following without regard to hospitalization:

(1) Unconciousness due to trauma.

(2) Fracture (open or closed) of any bone, other than closed fractures of the phalanges or nasal bones.

(3) Traumatic dislocation of any joint, including phalanges, or internal derangement of the knee.

(4) Injury to internal organs.

(5) Moderate to severe lacerations which cause extensive hemorrhage or require extensive surgical repair.

(6) Third-degree burns.

(7) First- or second-degree burns involving more than 5 percent of the body surface.

D. Other Injuries - Other injuries include the categories of minor and minimal.

(1) Minor injury: any injury which

(a) Results in hospitalization or sick in quarters for at least one day but not more than four days, for military.

(b) Results in loss of regular working time beyond the day or shift in which injury occurs, for civilian personnel.

(2) Minimal Injury: any injury which does not meet the criteria (above) for major or minor injury.

DATA SOURCES

Accident records were obtained from the following three sources:

- U. S. Army Agency for Aviation Safety (USAAAVS), Ft. Rucker, Alabama
- U. S. Naval Safety Center, Norfolk, Virginia
- Directorate of Aerospace Safety, Norton AFB, California

USAAAVS and the U. S. Naval Safety Center were visited at the onset of the

program. The Directorate of Aerospace Safety did not permit access to their files; however, a computer printout of accident narratives was supplied for the study. In addition to the Government agencies noted above, visits were made to the following organizations:

- U. S. Army Aviation Systems Command (AVSCOM), St. Louis, Missouri
- U. S. Army Aeronautical Depot Maintenance Center (ARADMAC), Corpus Christi, Texas
- Dynamic Science, Phoenix, Arizona

From USAAAVS, a summary of 3657 rotary-wing accidents during fiscal years 1967 through 1971 was obtained. The summary included utility, cargo and light-observation helicopters. A computer search performed by USAAAVS for the more recent accidents yielded 30 cases which met the damage and injury criteria established for the accident review. In addition, a study of accident cases compiled by J. Haley of USAAAVS[33], consisting of 135 utility (UH-1D/H), 33 light-observation (OH-6), and 17 cargo (CH-47) helicopters, was also used in the selection of accident cases to be analyzed. From the information presented, details from a total of 25 accident case records were requested for review. All the cases were UH-1D/H helicopter accidents.

At the U. S. Naval Safety Center the data records group had compiled in excess of 1,000 accident narratives for review. From this total, 154 were classified as major accidents in which substantial structural damage or injury occurred. The major accident narratives were reviewed and 20 cases were selected for detailed analysis. A review of the selected cases yielded only 3 cases which were incorporated into the accident analysis. The data obtained from the narratives were used in a summary of mishap causes, types, and phases of operation.

The Directorate of Aerospace Safety at Norton Air Force Base provided an accident data computer summary for the study. Narratives from 20 cases were included. Four accident cases were used in the detailed analysis.

At ARADMAC it was learned that the aircraft that are sent there are selected on the basis of a "cost-to-repair" criterion. If the repair estimates are in excess of $25K for the fuselage, or $140K for the total aircraft, then the aircraft is considered to be "economically" non repairable. On the basis of this cost criterion, the types of structural damage that would be most useful to the analysis to be performed in the program are not available at ARADMAC. It had been anticipated that severely damaged main frames and bulkheads, from which measurable deformation could be obtained and related to modes of failure, would be available for inspection.

Nine aircraft which were considered to be too severely damaged for ARADMAC to repair were visually examined. The observation of these aircraft indicated severe damage to secondary structure, loss of transmission at the mounts, loss of landing skids, and inverted impact. The damage in the forward section of two aircraft was total, indicating severe plowing or longitudinal forces.

ANALYSIS OF ACCIDENT DATA

The analysis of accident records consisted of a review of the accident narratives, witness comments, medical reports, and photographs of the damaged structure. Good photographs in particular are very valuable in accident evaluation. To assist in accident analysis, several guidelines were formulated based on information obtained from:

- Static test data
- Structural design requirements
- Human tolerance limits
- Structural energy-absorbing capability
- Previous crashworthiness studies
- Accident investigation experience

To facilitate the accident review, an accident worksheet was developed for the program. The worksheet is a refinement from a similar format presented in Reference 3. The worksheet shown, Figure 1, provides for a description of the impact conditions, aircraft behavior after ground contact, injury data, and structural damage sustained during the accident.

The accident analysis was conducted using the following information:

35 narratives of accident cases from USAAAVS

154 narratives of major accidents from the U. S. Naval Safety Center

20 narratives of accidents from the Directorate of Aerospace Safety

25 detailed accident cases from USAAAVS

3 detailed accident cases from the Naval Safety Center

4 detailed accident cases from the Directorate of Aerospace Safety

1 summary of 3657 U. S. Army rotary-wing aircraft accidents between the period 1967 - 71

1 summary of 185 U. S. Army rotary-wing aircraft accident cases compiled by J. Haley of USAAAVS

1. Case No.

2. Impact Conditions:

Longitudinal Velocity, fps_____	Flight Path Angle, deg _____
Vertical Velocity, fps _____	Pitch Angle, deg_____
Lateral Velocity, fps _____	Roll Angle, deg_____
	Yaw Angle, deg _____

3. Aircraft Behavior After Ground Contact

Longitudinal Distance, ft _____

Lateral Distance, ft_____

Lateral Roll

Forward Roll

Plowing

Skid/Bounce

Postcrash Fire

Miscellaneous

4. Injury Data Fatal Major Minor None

Total No. Aboard _____ Type of Injury:

Personnel	Injury	Cause

5. Structural Damage

Landing Skid	Tail Rotor Blade
Transmission	Nose Structure
Engine	Upper Fuselage Structure
Seats	Lower Fuselage Structure
Main Rotor Blade	Miscellaneous

6. Comments

Figure 1. Helicopter Accident Data Sheet.

The data was analyzed to determine a summary of:

- Accident causes
- Accident types
- Phases of operation
- Impact conditions
- Structural damage sustained
- Personnel injury experience

The emphasis on the detailed analysis was placed on the UH-1D/H utility type aircraft since the accident analysis was to assist in the development of an analytical model which is to be verified with test data obtained by drop testing a UH-1D/H helicopter.

ROTARY-WING ACCIDENT SUMMARIES

Figure 2 is a summary of mishap causes, types, and phases of operation in which the mishaps occurred. The data is compiled from 174 Naval Safety Center and Air Force accident narratives. Neglecting mishaps attributed to combat, the predominant causes of accidents are pilot factor (40), material failure or malfunction (40), and personnel error or maintenance (25). These causes represent 23%, 23% and 14.5%, respectively, of the total reported. Noncombat type mishaps are associated primarily with system failures (43) and collisions with either the ground, water, or objects, or hard landings (38). These represent 25% and 22%, respectively, of the total cases reviewed. In 31 cases (17%), the type of accident is undefined. The phase of operation is generally in-flight (103), landings (32), or takeoff (16) during field operations. Combined, these represent 87% of the total. The autorotation phase of operation accounts for 5.8% of the cases presented.

In Reference 33, 1045 U. S. Army accidents are summarized for the period between January 1967 and December 1969. Occurrences by phase for these cases are:

Simulated (training) and emergency autorotations	39.2%
Landing	18.1
Reposition	16.5
In Flight	11.0
Takeoff	8.9
Others	6.3

A comparison of the two sets of data (1045 U. S. Army cases and 174 Navy and Air Force cases) indicates different mixes with regard to phase of operation on which reported accidents occurred. The difference in good part is attributed to the manner in which each agency reports accidents.

In the case of the Naval Safety Center records, there are several causes, types, and phases associated with each accident. In some instances the initial cause of the mishap may be misleading. For example, an initial malfunction may be responsible for the pilot's reaching a position whereby the vehicle strikes an object or makes contact with the ground. The initial cause of the accident, under these circumstances, may not be considered the primary cause as reported elsewhere. Another inconsistency between the reporting methods of the agencies is in the use of all-encompassing terms. For example, the "in-flight" phase as denoted by one agency might be segmented into repositioning, training, and in-flight by another agency.

Figure 3 is a summary of 3657 U. S. Army rotary-wing accidents between 1967 and 1971. Survivable and partially survivable accidents account for approximately 89% and 4%, respectively, of all accidents. Thus non-survivable accidents account for 7% of the total number of accidents. These percentage figures are approximately the same as the figures reported by the Army for the time period between 1961 and 1965. A review of survivable accidents reveals that in these types of accidents, 4.3% of the persons receive fatal injuries, 7.3% sustain major injuries, 18.4% experience minor or lesser injuries, and 70% escape injury. These figures compare favorably with injury experience in 2546 U. S. Army rotary-wing accidents reported between 1967 and 1969 in Reference 33. Basically, the mix between survivable and nonsurvivable accidents has not changed in the last decade. The ratio of fatalities and injuries to total persons involved has remained about the same since 1967. Data from 756 survivable Army accidents for the time period 1961-65, reported in Reference 18, reveals that of 2068 occupants involved, 1.5% sustained fatal injuries, 18.5% sustained major or minor injuries, and 80% escaped without injury. These figures reveal that despite increased R & D emphasis on crashworthiness in recent years, the personnel involved in survivable accidents today are no better able to escape serious injury than they were before. Although it is true that the accident rate per aircraft hours utilized has decreased substantially during this time period, the design of a crashworthy aircraft which enhances occupant survivability has not progressed as significantly as one would believe, despite improvements in personnel equipment and restraint systems.

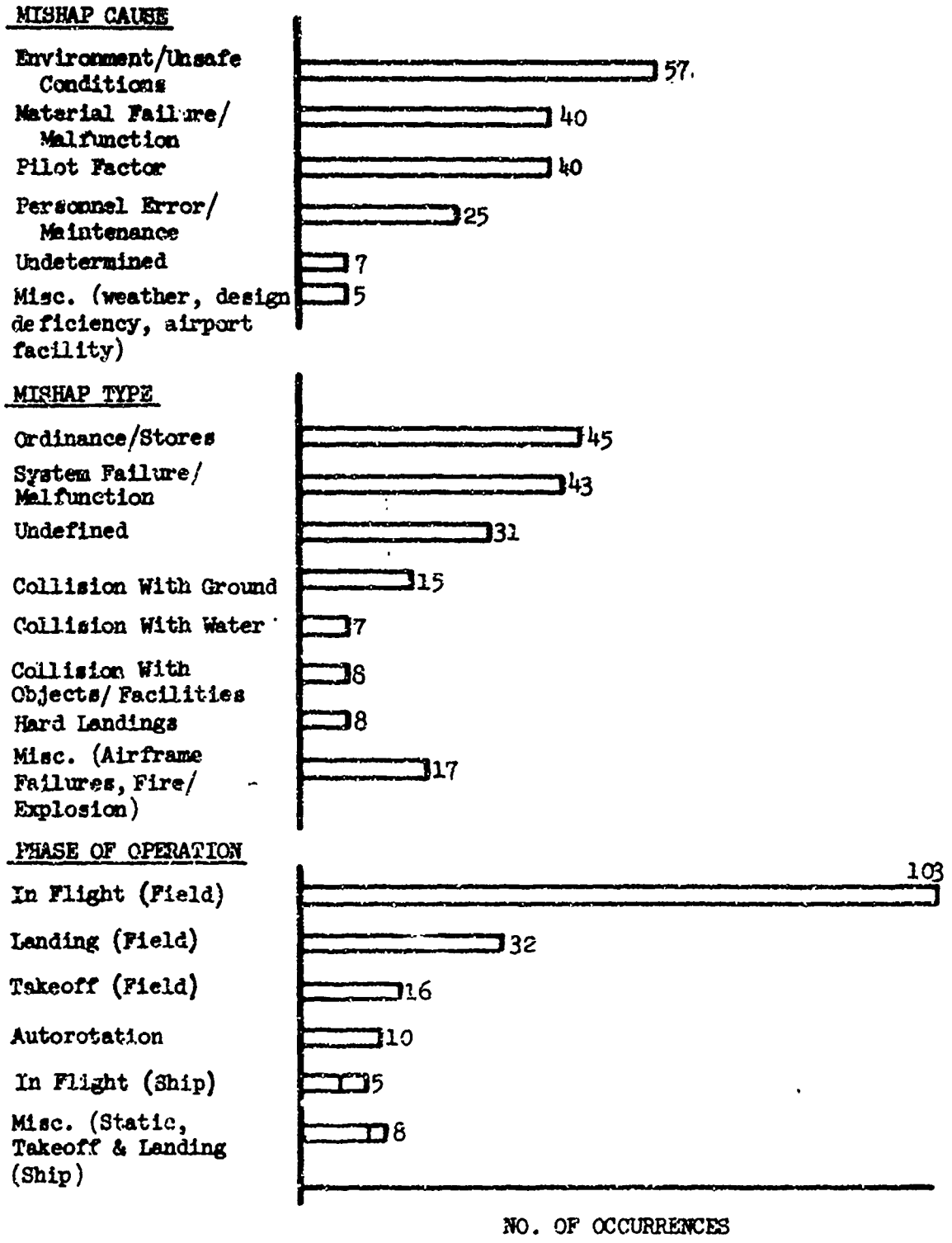

Figure 2. U.S. Navy and Air Force Rotary-Wing Accident Data Summary.

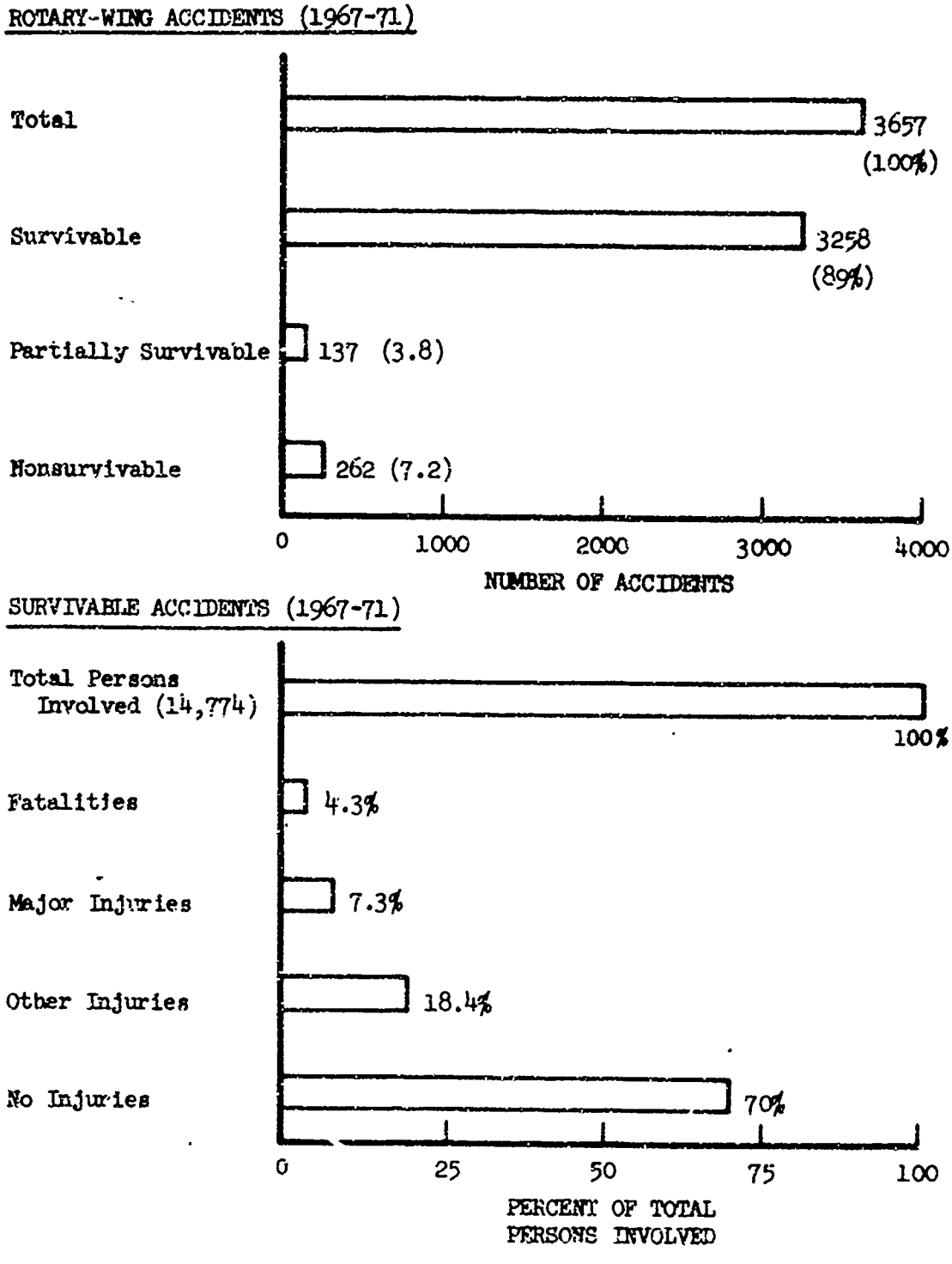

Figure 3. U.S. Army Rotary-Wing Accident Data Summary.

RESULTS OF DETAILED ACCIDENT INVESTIGATION

Table I presents a comprehensive summary of the results of the detailed accident investigation performed using 32 accident cases. The table is divided into several key areas which are considered essential to accident analysis, including:

- kinematics
- structural damage
- personnel injury

The table is segmented as follows:

Column 1, case identification
Columns 2 through 11, impact conditions, including:

longitudinal, vertical and lateral velocities
flight path angle
pitch, roll and yaw angles
yaw rotation notation
operational phase (hovering or autorotation)

Columns 12 through 18, aircraft ground behavior, including:

postcrash fire
lateral or forward roll
nose or inverted impact
plowing
skid or bounce
rotation about vertical axis

Columns 19 through 31, structural damage date, including:

landing skids
transmission
engine
seats
main rotor blade
tail boom
tail rotor blade
nose structure
upper cabin structure
lower fuselage structure
side structure
rotor blade and transmission penetration of cabin

Columns 32 through 36, injury types, including the number of:

persons involved
fatalities
major injuries
minor injuries
no injuries

Columns 37 through 44, primary causes of accidents, including the number attributed to:

deceleration forces
struck by object
transmission or rotor blade penetration
structure crushing and/or collapse
personnel impact with equipment and/or ejection
fire
suspected drowning
unknown

Columns 45 through 49, factors contributing to injury, including:

nonuse or loss of helmet
restraint not used
shoulder harness not used
tie-down chain failure
postcrash egress difficulty

Columns 50 and 51, blade contact with:

object
ground
other aircraft

Columns 52 through 55, terrain at site of accident, including:

water
hard soil
soft soil
trees and brush

Column 56, number of photographs that were available for the case study.

TABLE I SUMMARY OF DETAILED ACCIDENT I

CASE NO.	KINEMATICS																	STRUCTURAL DAMAGE DATA													INJU	
	IMPACT CONDITIONS										A/C GROUND BEHAVIOR																					
	LONGITUDINAL VELOCITY, FPS	VERTICAL VELOCITY, FPS	LATERAL VELOCITY, FPS	FLIGHT PATH ANGLE, DEG	PITCH ANGLE DEG	ROLL ANGLE DEG	YAW ANGLE DEG	YAW ROTATION DEG/SEC	HOVERING	AUTO ROTATION	POST CRASH FIRE	LATERAL ROLL	FORWARD ROLL	INVERTED OR NOSE IMPACT	PLOWING	SKID/BOUNCE	ROTATE	LANDING SKID	TRANSMISSION	ENGINE	SEATS	MAIN ROTOR BLADE	TAIL BOOM	TAIL ROTOR BLADE	NOSE STRUCTURE	UPPER CABIN STRUCTURE	LOWER FUS. STRUCTURE	SIDE STRUCTURE	ROTOR BLADE PENETRATION	TRANSMISSION PENETRATION	PERSONS INVOLVED	FATALITIES
col	2	3	4	5	6	7	8	9	10	11	12	13	14	15	16	17	18	19	20	21	22	23	24	25	26	27	28	29	30	31	32	33
1									X										X						X	X			X	X	4	
2	5/10	25/30	15/20	90		20/40			X		X	X	X						X	X	X	X	X	X	X		X				9	1
3		30/40		90	90								X						X	X	X	X			X						6	
4		20/30	10/20	90		10/20	X		X			X						X	X			X	X	X	X		X				6	1
5	20/30	10/15					X	X		X					X		X	X	X		X	X	X		X			X		X	6	1
6		10/15	10/15	90			20/25		X			X					X	X	X		X	X	X	X	X	X		X	X		4	1
7		20/30	20/30	90			45	X		X					X	X	X	X	X		X	X		X		X	X			X	10	
8		25/35		90				X	X					X					X	X		X	X	X				X			6	2
9	5/10		5/10	0	15/20		90	X									X		X			X		X				X	X	X	4	1
10		15/20	5/15	90	30	10/20	X	X	X			X				X	X	X	X	X		X	X	X			X	X		X	5	
11	150/150			0										X					X	X		X									6	2
12	25/35	25/25	15/20		45	X		X				X			X			X	X		X	X	X			X	X	X			7	
13		25/35	13/25	90			X	X			X	X						X		X	X							X			4	1
14		10/20	10/20	90			X	X	X		X	X										X						X	X		5	1
15	75/100	20/30		20	10/20	10/20				X	X			X		X		X	X	X		X			X						4	1
16		10/20	X	90		X	X	X	X								X	X	X			X	X	X	X	X		X	X		3	
17		30/40		90	90																X		X		X			X			11	10
18	50/75		X	0				X										X	X			X	X	X							2	1

Y OF DETAILED ACCIDENT INVESTIGATION

MAGE DATA						PERSONNEL INJURY DATA																	MISCELLANEOUS						
						INJURY TYPES					PRIMARY CAUSES								CONTRIBUTING FACTORS					BL CONT	TERRAIN					
NOSE STRUCTURE	UPPER CABIN STRUCTURE	LOWER FUS. STRUCTURE	SIDE STRUCTURE	ROTOR BLADE PENETRATION	TRANSMISSION PENETRATION	PERSONS INVOLVED	FATALITIES	MAJOR INJURIES	MINOR INJURIES	NONE	DECELERATION FORCES	STRUCK BY OBJECTS	TRANSMISSION/RB PENETRATION	STRUCTURE CRUSHING/COLLAPSE	IMPACT WITH OBJECT OR EJECTED	FIRE	SUSPECTED DROWNING	UNKNOWN	HELMET NOT WORN/LOSS	RESTRAINT NOT USED	SHOULDER HARNESS NEGLECTED	TIE DOWN CHAIN FAILURE	POST CRASH DIFFICULTY	MAIN ROTOR BLADE	TAIL ROTOR OR BOOM	WATER COLLISION	HARD SOIL	SOFT SOIL	TREES	NUMBER OF PHOTOGRAPHS
26	27	28	29	30	31	32	33	34	35	36	37	38	39	40	41	42	43	44	45	46	47	48	49	50	51	52	53	54	55	56
X	X			X	X	4		1	1	2			2												X		X			1
X		X				9	1	4	4		7	2							4					X					X	2
X						6		1	5		6									2				X					X	4
X		X				6	1	2	2	1				1	2			2	1	2	2	1		X					X	3
X			X		X	6	1	1	3	1	2	2	1						1		2			X			X			4
X	X		X	X		4	1		2	1		2	1												X		X			9
	X	X			X	10		2	1	7	2			1										X				X		2
			X			6	2	3	1		2			2	1			1						X	X				X	0
			X	X	X	4	1		1	2			2											X	X		X			0
		X	X		X	5			1	4	1									1					X				X	5
						6	2	1	2	1							5		1	2	2		3			X				0
	X	X	X			7		2	3	2		1		2	2					1	2			X	X				X	3
			X			4	1	3			2				1	1					1						X			0
			X	X		5	1		1	3	1		1						1					X					X	0
X						4	1	2	1		1			2																X	0
X	X		X	X		3			3			1			1	1		1						X			X			5
X			X			11	10	1						4	4		2	1		1			1C			X				2
						2	1		1							2													X	0

TABLE I. (CONTINUED)

CASE NO.	KINEMATICS: IMPACT CONDITIONS: LONGITUDINAL VELOCITY, FPS	VERTICAL VELOCITY, FPS	LATERAL VELOCITY, FPS	FLIGHT PATH ANGLE, DEG	PITCH ANGLE DEG	ROLL ANGLE DEG	YAW ANGLE DEG	YAW ROTATION DEG/SEC	HOVERING	AUTO ROTATION	A/C GROUND BEHAVIOR: POST CRASH FIRE	LATERAL ROLL	FORWARD ROLL	INVERTED OR NOSE IMPACT	PLOWING	SKID/BOUNCE	ROTATE	STRUCTURAL DAMAGE DATA: LANDING SKID	TRANSMISSION	ENGINE	SEATS	MAIN ROTOR BLADE	TAIL BOOM	TAIL ROTOR BLADE	NOSE STRUCTURE	UPPER CABIN STRUCTURE	LOWER FUS. STRUCTURE	SIDE STRUCTURE	ROTOR BLADE PENETRATION	TRANSMISSION PENETRATION	INJU: PERSONS INVOLVED	FATALITIES
col	2	3	4	5	6	7	8	9	10	11	12	13	14	15	16	17	18	19	20	21	22	23	24	25	26	27	28	29	30	31	32	33
19	5/10	5/10		45					X							X		X									X				4	
20		15/25		90	X	X	X	X			X				X				X			X		X		X		X	X		4	1
21	80/100			0				X				X										X		X	X						7	6
22	35/45	25/35	X	35	X	X	X	X			X	X				X		X		X		X	X		X		X	X			10	6
23						20/30		X		X						X	X						X	X				X			8	1
24		<10			60	35		X		11						X	X							X							2	
25						X					X	X						X	X	X	X	X	X		X	X		X		X	6	1
26		30/40	10/20	90	10/20	10/20		X		X							X	X	X	X	X	X		X	X	X	X	X	X	X	2	
27		5/10	5/10	90	5/15	90/100		X																X							2	
28	5/15	30/40	8/10	80	0/10	X		X		X	X	X						X	X			X		X		X	X	X	X		2	
29	40/45	15/20		20	-30		45								X				X		X	X			X			X			3	
30		20/30	10/15						X						X			X	X	X	X					X	X				8	
31	45/55	25/35		25							X							X				X	X	X							3	
32	70/80	10/15		10												X	X	X	X			X				X				X	5	
tot								18	10	7	10	11	3	3	6	8	10	18	22	11	11	25	15	16	14	11	11	17	<13	>	168	38

Preceding page blank

ABLE I. (CONTINUED)

GE DATA						PERSONNEL INJURY DATA															MISCELLANEOUS						
						INJURY TYPES					PRIMARY CAUSES								CONTRIBUTING FACTORS					BLADE CONTACT		TERRAIN				
UPPER CABIN STRUCTURE	LOWER FUS. STRUCTURE	SIDE STRUCTURE	ROTOR BLADE PENETRATION	TRANSMISSION PENETRATION	PERSONS INVOLVED	FATALITIES	MAJOR INJURIES	MINOR INJURIES	NONE	DECELERATION FORCES	STRUCK BY OBJECTS	TRANSMISSION/RB PENETRATION	STRUCTURE CRUSHING/COLLAPSE	IMPACT WITH OBJECT OR EJECTED	FIRE	SUSPECTED DROWNING	UNKNOWN	HELMET NOT WORN/LOSS	RESTRAINT NOT USED	SHOULDER HARNESS NEGLECTED	TIE DOWN CHAIN FAILURE	POST CRASH DIFFICULTY	MAIN ROTOR BLADE	TAIL ROTOR OR BOOM	WATER COLLISION	HARD SOIL	SOFT SOIL	TREES	NUMBER OF PHOTOGRAPHS
27	28	29	30	31	32	33	34	35	36	37	38	39	40	41	42	43	44	45	46	47	48	49	50	51	52	53	54	55	56
	X				4				4															X		X			0
X		X	X		4	1		3			1						3							X		X			1
					7	6		1		6				1					3								X		0
	X	X			10	6	1	3						1	7		2					7		X			X		0
		X			8	1	1	6						5			1		6	2							X	0	
					2				2														X				X		4
X		X		X	6	1	2	3		3			1	2									X			X	X		4
X	X	X	X	X	2		1	1		2																			3
					2			1	1								1										X		3
X	X	X	X		2		1	1									2												1
		X			3			1	2					1									X				X		2
X	X				8		8						2	2						4							X		6
					3		:		2	4											1					X			1
X				X	5				5	1																X			2
11	11	17	<13	>	168	38	38	52	40	42	11	7	15	21	11	7	14	8	18	15	2	13	13	8	2	3	9	7	11

Kinematics

In developing an understanding of the manner in which a helicopter sustains structural damage and the personnel sustain injuries during a crash, it is important to ascertain the condition under which accidents occur. One of the more interesting determinations from the accident review is that in approximately two-thirds of the cases, the aircraft main rotor blades or tail boom is noted to have made contact with a tree or the ground prior to what is generally considered to be the crash impact. This initial contact by the main blade, or tail section, significantly affects the aircraft pitch, roll and yaw motions and, consequently, influences the helicopter crash environment. For example, the loss of the tail boom deprives the helicopter of its ability to balance a main rotor blade developed torque which is in excess of 10,000 ft-lb. As a consequence of losing the tail boom or rotor, the aircraft will spin uncontrollably. This phenomenon is understandable when one realizes that the aircraft can develop a rotational acceleration of .37 rad/sec^2 due to the loss of torque control and considering the aircraft's yawing mass moment of inertia. The data shows that there is a strong correlation between the aircraft yawing at impact, tail boom or rotor damage, and rotation on the ground after impact. The loss of the tail boom also affects aircraft pitching motion since the tail section accounts for approximately 10% of the total aircraft pitching mass moment of inertia. The damage to the tail section results in a nose-down aircraft attitude, and depending on the proximity of the aircraft to the ground, the main rotor can contact either the ground or the portion of the tail section attached to the helicopter. The damage that the rotor blade imposes upon the structure and/or occupants is dependent upon the location of the blade during its rotation at the time the blade strikes the ground.

Another phenomenon that is noted to occur frequently is a lateral rollover. This condition occurs in approximately one-third of all accidents. Rollovers of this nature are attributed to the presence of side forces resulting from a lateral impact velocity. Similarly, forward rollovers are associated with high-forward-velocity components.

Lateral velocities, estimated from 14 accidents, are shown to have mean and average values of 13 fps and 14.3 fps, respectively. Vertical velocities estimated from 25 accident cases have mean and average values of 22.5 fps and 22 fps, respectively. These values appear to be consistent with information presented in References 2 and 33.

Structural Damage

From Table I the frequency of occurrence of structural damage noted in the cases analyzed is as follows:

Main rotor blade	25
Transmission	22
Landing skids	18
Side structure	17
Tail rotor blade	16
Tail boom	15
Nose structure	14
Transmission or rotor blade penetrated occupant space & structure	13
Lower fuselage structure	11
Upper fuselage structure	11
Engine	11
Seats	11

The frequency of occurrence of rotor blade, transmission, and tail boom damage is attributed to the large percentage (56%) of times that either the rotor blade or the tail boom contacted the ground, an object such as a tree, or another aircraft, consequently causing a crash condition.

Damage to the side of the aircraft structure generally occurs as a result of lateral impacts and lateral rollover conditions. There were several instances noted where the aircraft impacted nose vertically down. However, nose and lower forward surface damage occurs also during high forward velocities and a slight nose-down attitude. Although there were a couple of inverted impacts, upper fuselage or cabin structural damage generally resulted from cabin penetration by rotor blade or transmission and during rollover situations.

Photographs from selected cases are presented in Figures 4 through 16 to illustrate the type of structural damage sustained as a function of the impact conditions. Figure 4 (Case 4) shows damage that is attributed to combined vertical and lateral impact velocity and lateral rollover of the aircraft. Extensive damage to the landing skids and lower fuselage is evidence of severe sink speeds. Buckling of the main frame and collapse of fuselage-cabin and nose structure are evidence of significant side forces. In this particular accident, five of the six persons involved sustained injuries. It is surmised that in this accident the main rotor blade struck a tree, then severed the tail boom, and crashed to the ground with apparent loss of lift and rotational controls.

Figure 4. Side View of Vertical Impact, Lateral Rollover (Accident Case 4).

Figures 5 and 6 (case 6) show a condition in which the tail rotor blade of a hovering aircraft struck the main rotor blade of another helicopter. The loss of tail rotor resulted in an unbalanced condition and nose-down pitch. The aircraft hit hard on the left skid and rolled to the left. In this attitude the rotor blade tip struck the ground. The force was sufficient to pull the mast and transmission forward and to the left. One of the three injuries sustained in this accident is attributed to penetration by the rotor blade.

Figures 7 and 8 (case 7) illustrate the results of an accident in which it is believed that the tail skid impacted with a high sink speed, causing severing of the tail boom. The loss of control resulted in the rotor blade's making ground contact. The rotor blade, hub, and transmission were torn loose and crushed the top cabin and side fuselage structure. The accident records indicate that three of the ten occupants were injured and that the injuries were attributed to deceleration forces and lacerations from contact. However, the photographs would indicate a high probability that penetration of the occupiable space by the transmission or rotor blade or crushing of the structure would contribute to injury. The failure of the tail boom, which shows tensile forces at the lower right fitting and compression at the upper left, further indicates vertical forces acting at the aft section. The final location of the tail boom (perpendicular to the aircraft) and the attitude of the aircraft indicate the presence of side forces during the accident.

Figures 9 (case 17) and 10 (case 25) indicate damage resulting from a severe nose-down or inverted crash. In both accidents the landing skids are intact. The nose structure is severely crushed. In case 17 the impact was made on water, and causes of the 10 fatalities that were incurred are not stated. However, it is anticipated that large decelerative forces and/or severe crushing of the structure into the occupiable area probably occurred. In case 25, all six occupants were injured. Three of the injuries were attributed to high decelerative forces, one to collapse of structure, and two to ejection from aircraft or impact with equipment.

Figures 11 and 12 (case 29) show damage from an accident in which the helicopter impacted in a nose-low attitude. The main rotor contacted the ground and both the main transmission and rotor system separated. The photographs show extensive damage to the nose structure, lower fuselage floor and forward support frame. The position of the separated rotor and transmission indicates that the blades contacted the ground forward of the aircraft. Since the aircraft was hovering prior to the accident, the longitudinal velocity component is not considered to be high.

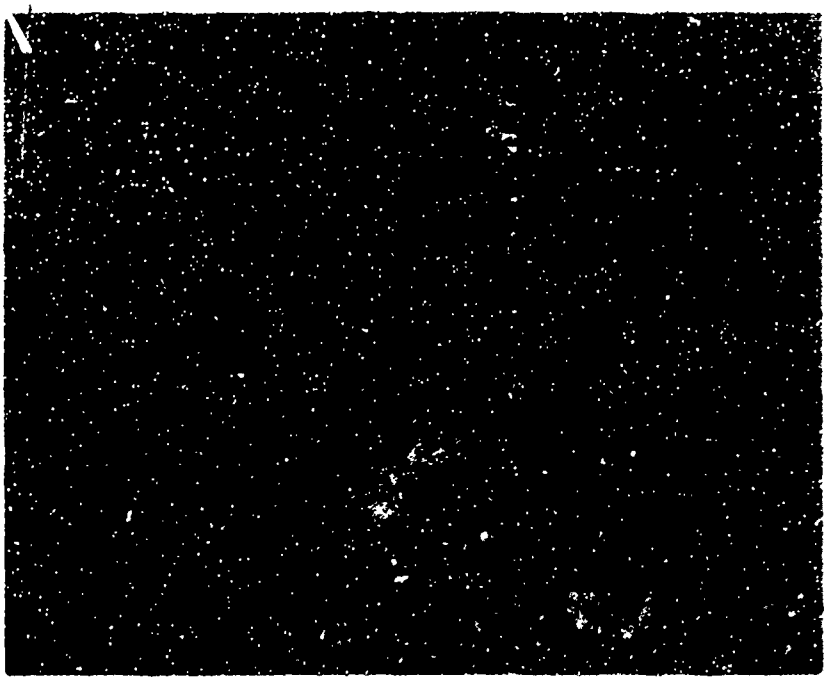

Figure 5. Side View, Rotor Blade Penetration of Cabin (Accident Case 6).

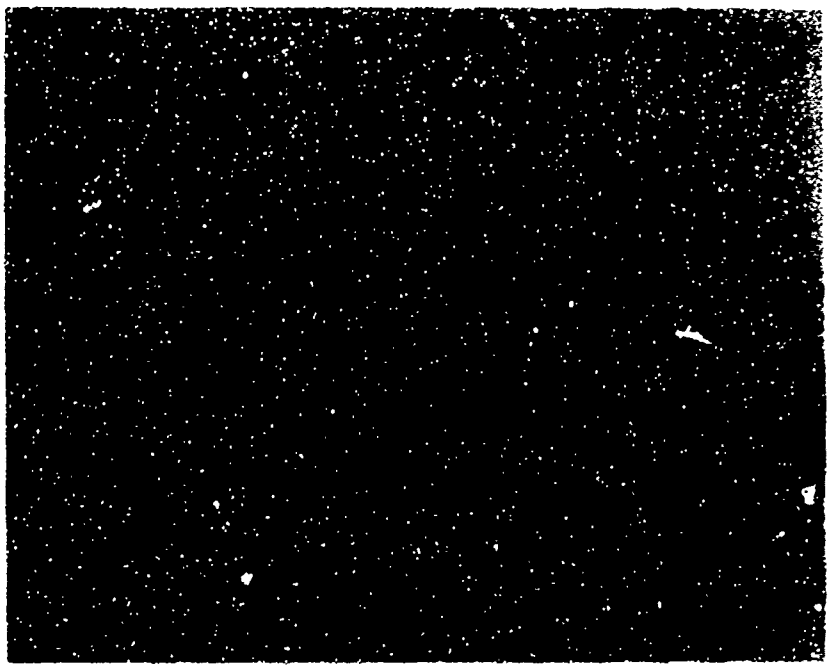

Figure 6. Rear View, Rotor Blade Penetration of Cabin (Accident Case 6).

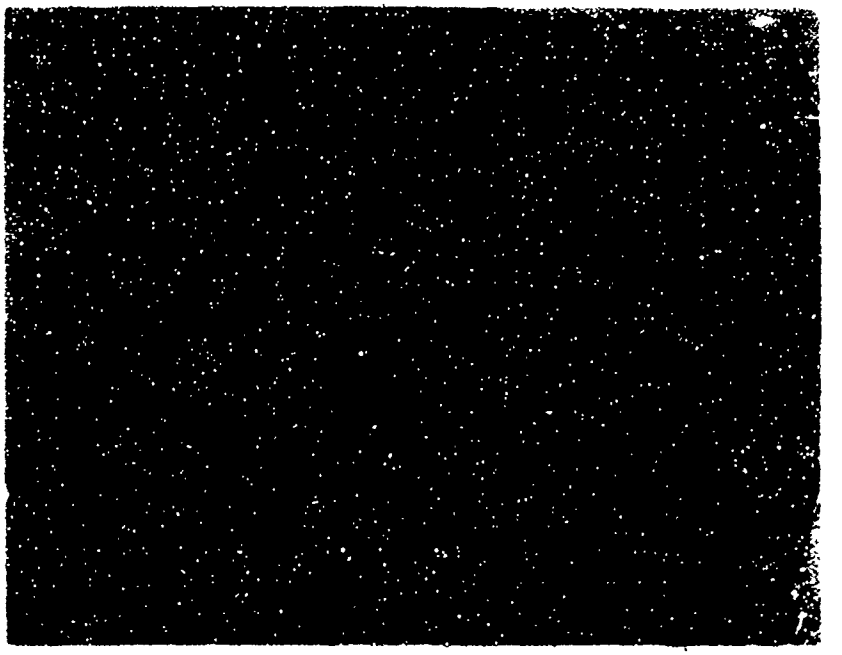

Figure 7. Side View, Rotor Blade and Transmission Penetration of Cabin (Accident Case 7).

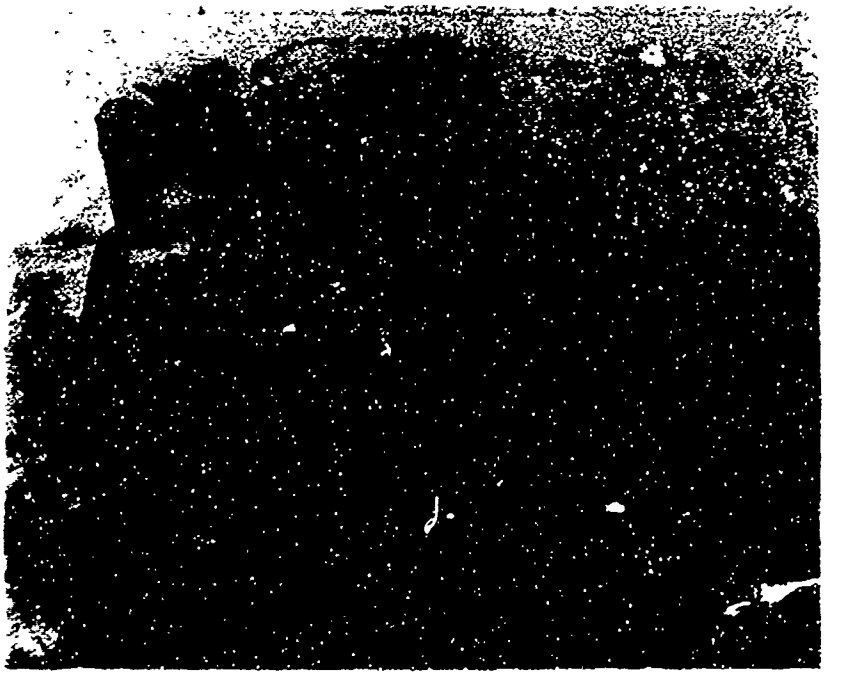

Figure 8. Rear View, Tail Boom Loss (Accident Case 7).

Figure 9. Severe Nose Impact (Accident Case 17).

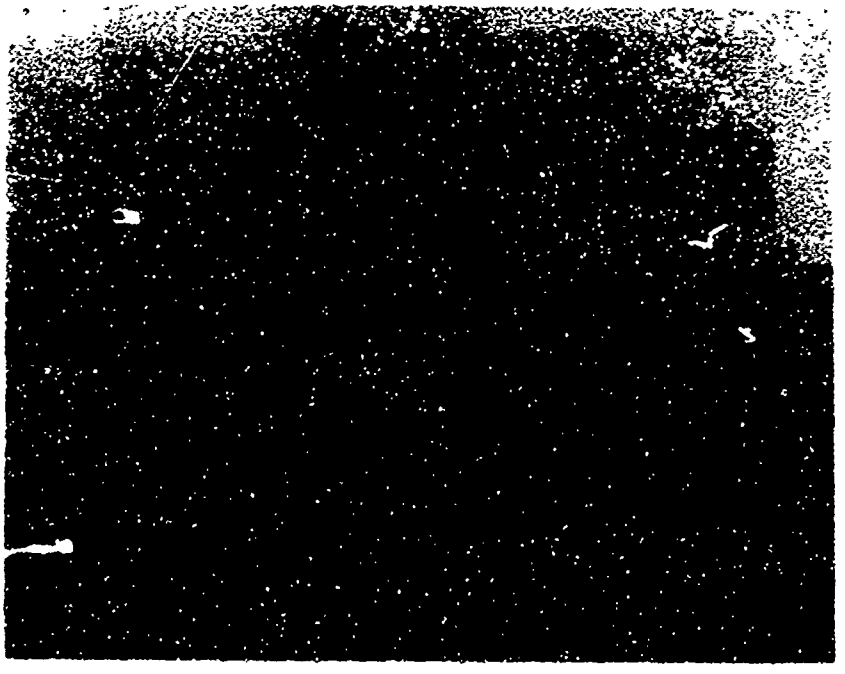

Figure 10. Severe Nose and Inverted Impact (Accident Case 25).

Figure 11. Side View, Side and Front Structural Damage (Accident Case 29).

Figure 12. Front View, Nose Structure Damage, Loss of Rotor System (Accident Case 29).

Figures 13 and 14 (case 30) represent an accident in which the helicopter descended vertically to the ground and stayed in an upright position. The rotor blade and transmission are essentially intact although tilted slightly. The landing skids are bent upward, and both the fuselage section (forward of F.S. 63.3) and tail section (aft of F.S. 248) are collapsed as one would expect in a pure vertical drop. In this particular accident the impact loads were extremely severe.

Personnel Injury Data

The injury data in Table I shows the following breakdown of injuries and fatalities for the 168 personnel involved in the cases analyzed:

Fatalities	38
Major injuries	38
Minor injuries	52
No injuries	40

The prime causes of injuries for this 32-accident sample are noted to be:

Deceleration forces	42
Occupant impact with equipment or ejection from aircraft	21
Collapse or crushing of structure	15
Unknown	14
Occupant struck by an object	11
Fire	11
Penetration of occupant space by transmission or rotor blade	7
Suspected drowning	7

The injuries due to decelerative forces accounted for approximately one-third of the injuries recorded in the cases analyzed. Since the term "decelerative forces" is a broad classification for many types of injuries in Army accidents, it is expected to represent a substantial percentage of reported injuries. Injuries resulting from deceleration forces noted in the accident cases are generally associated with back and vertebra compression type injuries. Figures 13 and 14, taken from case 30, show the results of a crash in which there is a predominantly high vertical descent speed. In this accident, at least 4 of the 8 occupants were considered to suffer injuries attributable to high deceleration forces. Evidence of the decelerative forces can be seen in the upward displacement of the landing skids, the buckling of the support frame, and the damage to the seat supports. The rotor blades in this accident remained intact.

Figure 13. Side View, High Vertical Rate of Descent (Accident Case 30).

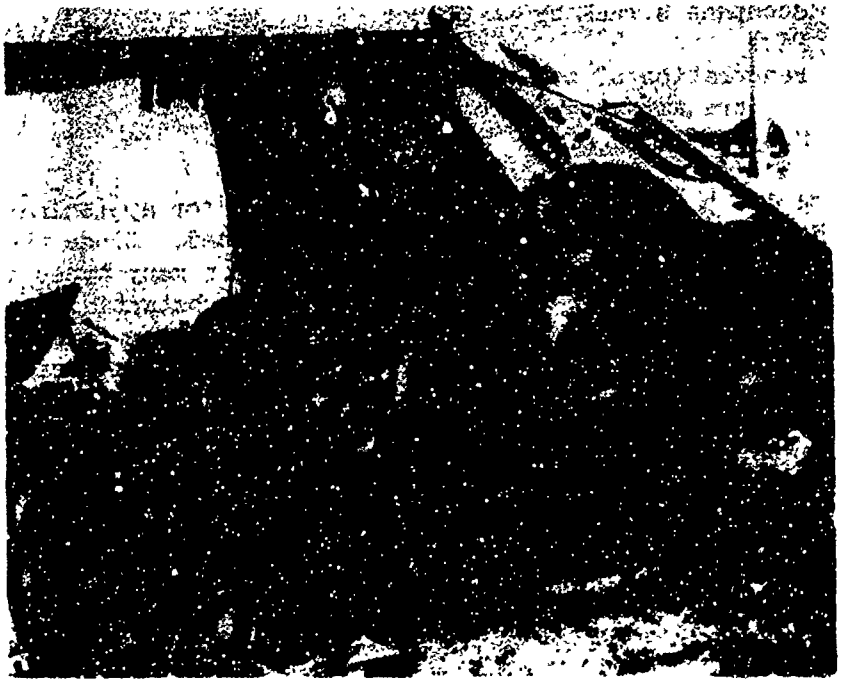

Figure 14. Close-Up View, High Vertical Rate of Descent (Accident Case 30).

The transmission and main rotor blade were damaged in approximately 70% of the cases analyzed. They were suspected of penetrating the occupiable space in 40% of the accidents studied, and their recorded contribution to injuries was about 5.5% of the total. Figures 5 through 8, discussed earlier, illustrate structural damage resulting from penetration by the rotor blade and/or transmission.

Figures 15 (case 30) and 16 (case 12) illustrate accidents in which collapsing of the occupant's liveable space occurred. In case 12, there were 5 injuries, of which 2 were attributed to collapse of the structure. There was no penetration of the cabin by either a rotor blade or a transmission, but the impact forces were significant enough to cause buckling of the floor and collapse of the seat support structure. In case 30, there were 8 major injuries, of which 2 were a result of the crushing of the structure. In this particular accident there was primarily a vertical impact velocity present.

The preceding discussion on the causes of injuries is based on a 32 accident sample and as such should not be interpreted as being statistically significant. References 2, 17, 18, 25 and 33 are several reports which provide additional pertinent data with regards to the causes of injuries.

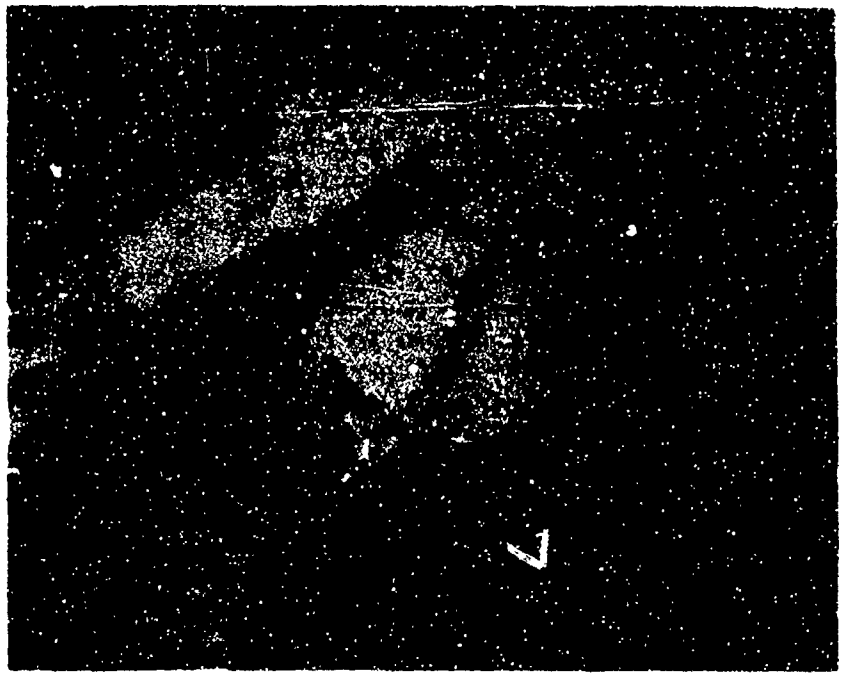

Figure 15. Collapse of Cabin Structure, High Vertical Rate of Descent (Accident Case 30).

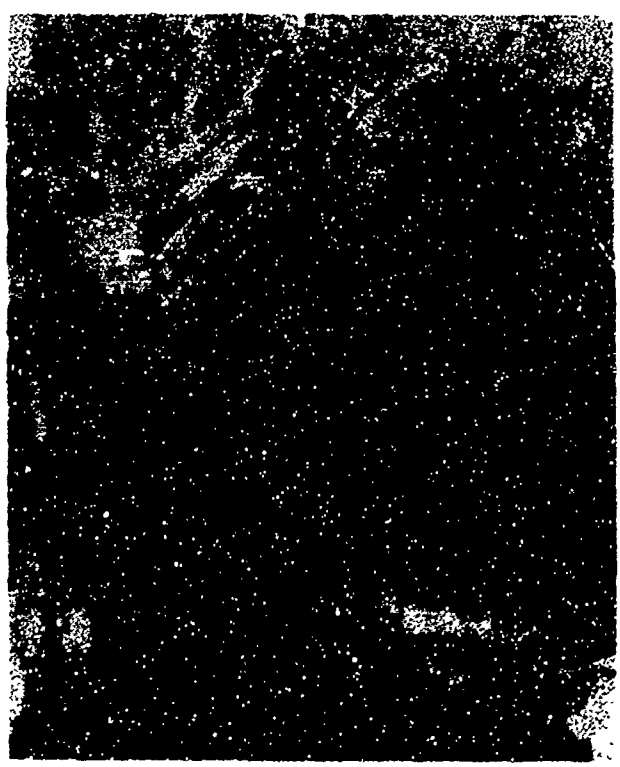

Figure 16. Collapse of Cockpit Structure, Buckling of Floor Structure (Accident Case 12).

SURVEY OF TECHNICAL PUBLICATIONS

GENERAL DISCUSSION

In this program, technical publications were reviewed and their contents categorized to assist in future reference as needed, in accordance with the various aspects of developing improved crashworthiness criteria and concepts. A review and evaluation of 32 publications, including USAAMRDL, FAA, and NASA technical reports and MIL Specifications, are presented herein. A complete listing of the publications which comprise the literature survey is presented in Volume II. The literature is reviewed with regards to the impact on rotary-wing aircraft crashworthiness design. In particular, emphasis is placed in the following areas:

- Crash Loads and Environment
- Design Criteria and Principles
- Human Tolerance Criteria
- Analytical Methods
- Accident and Injury Data
- Crash Test Data and Methods
- Energy Absorption
- Structural Behavior and Failure Modes
- Restraint and Escape Systems
- Military Specifications

For each of the subject areas listed above, an evaluation is performed which shows the literature applicable to that particular subject, the contribution of each report briefly stated, and a composite summary of the pertinent aspects of the literature.

Volume II, which provides additional literature survey information, consists of a summary or abstract for each report and a literature survey subject index which contains a matrix categorization of the contents of the technical reports. The matrix categorization lists the reports by number and associates each report with an area of specific content or applicability. All report numbers in this section refer to the reference numbers as they are listed under LITERATURE CITED.

EVALUATION

Crash Loads and Environment

The data presented in the literature indicates that the crash environment

is highly dependent upon the aircraft structural configuration and crash conditions. Rotary-wing and fixed-wing aircraft crash-impact at different velocities and attitudes, which contributes to differences in loads that are experienced by each type of aircraft. Test data shows that rotary-wing aircraft generally experience higher peak loads than the heavier fixed-wing aircraft. However, the peak loads occur for shorter durations in rotary-wing aircraft as compared to fixed-wing aircraft. The vertical "G" load is considered a critical condition in causing injuries, or fatalities, to the occupant. The longitudinal loads, by comparison, are generally approximately half the level of the vertical load. In the longitudinal direction, sliding friction absorbs a significant amount of energy, whereas in the vertical direction, all the energy must be absorbed by the structure. In addition, it has been shown that the human can tolerate higher acceleration in the longitudinal direction than in the vertical direction. However, as discussed in later sections, excessive vertical "G" loading is only one of many causes of injuries and fatalities.

The crash environment is currently stated in terms of the 95th percentile survivable accident velocity change and floor acceleration level for longitudinal, vertical and lateral impact directions. A summary of this data for two classes of aircraft ((a) rotary and light fixed-wing aircraft, and (b) fixed-wing transport aircraft) obtained from report (2) is presented in Tables II and III. This data represents the present structural design goals for aircraft crashworthiness.

Reports (2), (3), (10) and (26) describe the crash environment obtained from tests and accident records and are applicable to rotary-wing aircraft. Reports (1), (2), (5), (6), (7), and (21) discuss the crash environment for fixed-wing aircraft. Reports (28), (29) and (31) are MIL Specifications in which crash load requirements are stated.

The crash environment data presented in report (2) and reproduced in Tables II and III are based on the following:

a) average floor acceleration estimates
b) comparison of accident configuration and damage with test data
c) observation of failure and nonfailure of seat belts, shoulder harness and seats of known strength
d) comparison of injuries with generally accepted human tolerance limits

Report (10) shows H-25 crash test data. The recorded accelerations are higher in magnitude but shorter in duration than the fixed-wing aircraft test data. The H-25 airframe vertical and longitudinal accelerations reached 100 G's and 50 G's, respectively, at the floor. The pilot experienced 60 G's and 40 G's peak loads in the vertical and longitudinal directions, respectively. Report (3) presents the results of a recent drop test performed with a UH-1D/H

helicopter. In this test the aircraft impacted with a 30-fps vertical velocity and experienced peak vertical accelerations of between 70 and 110 G's at the rear and forward floor locations. Report (26) discusses structural damage obtained from OH-6A tests and relates to the damage to the sink speed and G's that the cockpit experiences. The report compares load factors vs deformation for equal crash energy absorption.

TABLE II. SUMMARY OF DESIGN PULSES CORRESPONDING TO THE 95TH PERCENTILE ACCIDENT OF ROTARY-AND LIGHT FIXED-WING AIRCRAFT (REPORT 2)

Impact Direction	Velocity Change (fps)	Peak G*	Average G	Pulse Duration "T" (sec)
Longitudinal (Cockpit)	50	30	15	0.104
Longitudinal (Passenger Compartment)	50	24	12	0.130
Vertical	42	48	24	0.054
Lateral (Light Fixed-Wing)	25	16	8	0.097
Lateral (Rotary-Wing)	30	18	9	0.104

*Assuming an equilateral triangle pulse shape.

TABLE III. SUMMARY OF DESIGN PULSES CORRESPONDING TO THE 95th PERCENTILE ACCIDENT OF FIXED-WING TRANSPORT AIRCRAFT (REPORT 2)

Impact Direction	Velocity Change (fps)	Peak G*	Average G	Pulse Duration "T" (sec)
Longitudinal (Cockpit)	64	26	13	0.153
Longitudinal (Cabin)	64	20	10	0.200
Vertical	35	36	18	0.060
Lateral (Cockpit)	30	20	10	0.093
Lateral (Cabin)	30	16	8	0.116

* Assuming an equilateral triangle pulse shape.

Reports (1), (5), (6) and (7) show fixed-wing crash test floor and passenger measured acceleration data. In general, the peak lateral accelerations, vertical accelerations and longitudinal accelerations are 20 G's, 40 G's and 25 G's, respectively. However, test data from (1) notes peak longitudinal accelerations of 77 G's at the cockpit, decreasing to 28 G's at the aft section of the aircraft.

Design Criteria and Principles

The principles presented in these reports indicate that to achieve crashworthy capability one must design such that:

- The structure surrounding the occupants remains intact without significantly reducing the living space.

- The structure crushes and deforms in a controlled, predictable manner so that the forces imposed on the occupants are minimized.

The design for crashworthy structure should take into consideration the fact that the energy-absorbing requirements of the structure differ for longitudinal and vertical impacts. In the longitudinal direction, friction assists in the absorption of energy. The energy from vertical impacts, on the other hand, must be absorbed by the structure and in a very short time period.

Materials play a very significant role in the development of crashworthy structure. Where possible, the materials should have sufficient ductility to insure crushing, twisting and buckling without rupture. Consideration must be given to material elongation, tear resistance, crack propagration and stress concentrations as well.

At present there are some firmly established criteria and principles which, if properly implemented, could enhance occupant survivability under crash conditions. These criteria and principles should be used to develop a consistent crashworthy design which requires that the occupant space not collapse during the period that the landing gear and the fuselage structure crushes during response to the 95th percentile impact velocity, while the loads imposed, through the behavior of the seat support structure, do not exceed human tolerance.

Reports (1), (2), (4), (8), (25) and (26) present information which is pertinent to crashworthy design criteria and concepts. Reports (1) and (2) discuss design concepts in detail. In particular, methods to achieve improved fuselage design for fixed-wing vehicles are presented. The five methods outlined are:

- Increase in energy absorption capacity of structure forward of the occupiable area.
- Alteration of structure to reduce scooping and gouging of soil.
- Reinforcement of cabin structure.
- Modification of structure to insure breakaway.
- Modification of structure to permit increased deformation in unoccupied areas.

Report (4) discusses the importance of material and detail design considerations in the design for crashworthiness. Report (8) shows the results of analysis for improving fuselage design. Improvements are shown to be obtained by strengthening, redistribution of bending material, and incorporating energy-absorption features. The analytical results are verified by test results.

Report (25) refers to experimental and developmental crashworthy design configurations which use controlled deformation and "load limit" techniques to absorb a maximum amount of energy in the very limited crushing distance available. Several proposals for improved helicopter fuselage designs are presented. Minimum helicopter design crash conditions are recommended.

Report (26) compares variations of load factor and deformation for equal crash energy absorption and shows that a structure designed to minimum strength and maximum deformation is a more desirable crashworthy design than a structure designed to maximum strength and minimum deformation. The report discusses factors which must be considered in providing attenuation for the vertical component of the crash impact. Future crash survivability design objectives are presented.

Human Tolerance Criteria

The problem of providing acceptable acceleration limits in the design for the survivability of occupants is complex and involves the ability to determine and measure the dynamic relationship between the structural system (airframe and restraint system) and the human system (occupant). Data which is used to establish present criteria requires improvement in the following areas:

- Definition of the dynamic response of the restraint system to ascertain the influence on the occupant acceleration levels. Current criteria are based on acceleration measurements at the seat and not on the subject.

- Improved modeling of the human system to account for the critical body modes. Data in this regard is limited and, consequently, so is verification of analytical methods with experience.

- The literature points out that tolerance limits are a function of (a) peak acceleration, (b) duration of acceleration, and (c) rate of onset of initial acceleration that the occupant experiences. The occupant's posture, position, direction relative to the acceleration forces, and the manner in which the occupant is restrained influence the acceleration levels that are experienced by the occupant.

Report (15) is a comprehensive survey of the literature regarding the subject of human tolerance to rapidly applied accelerations. The information presented in this report is used throughout the literature as a basis for relating the crash environment to human tolerance levels. The acceleration peaks, durations and rates of acceleration onset for various directions of acceleration are summarized in Table IV.

TABLE IV. SUMMARY OF HUMAN TOLERANCE LEVELS FOR PEAK VALUES, DURATION AND RATES OF ACCELERATION (REPORT (15))

Acceleration Direction	Peak Acceleration (g) (Voluntary Human Exposure)	Duration of Acceleration (sec)	Rate of Acceleration Onset (g/sec)
Sternumward (fwd)	35	.1	1150
Spineward (aft)	45	.04	600
Headward (up)	16	.04	115
Tailward (down)	10	.01	80

The direction of the acceleration forces obtained from Report (2) is presented in Figure 17.

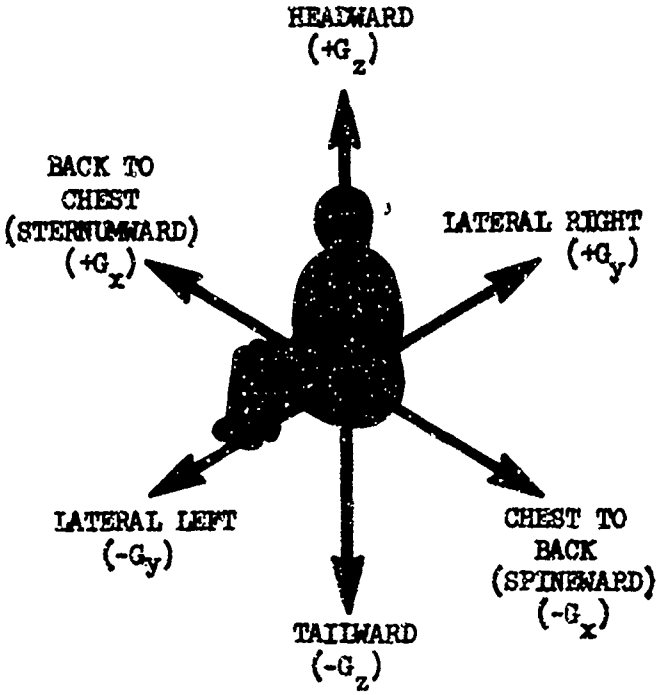

DIRECTION OF DECELERATIVE FORCE

VERTICAL

Headward - Eyeballs down
Tailward - Eyeballs up

TRANSVERSE

Lateral Right - Eyeballs left
Lateral Left - Eyeballs right
Back to Chest - Eyeballs in
Chest to Back - Eyeballs out

Note:

The decelerative force on the body acts in the same direction as the arrows

Figure 17. Decelerative Forces on the Body.

In addition to report (15), there are several reports listed in the index which provide significant information with regard to the establishment and measurement of acceptable human tolerance criteria. These reports are (7), (12), (14), (22) and (27). Reports (2), (3), (10), (11), (13), (19), (20), and (31) relate to human tolerance levels but are based on the information presented in the prime references.

Several methods of relating response measurements to human tolerance criteria are presented. Most notable of these are the Dynamic Response Index (DRI) (22), Mechanical Impedance Systems (14), lumped mass parameters (12), and shock spectra (7). All of the above methods except the use of shock spectra involve modeling the human body or a portion of the human system. The modeling of the human system has, thus far, been limited due to a lack of experimental data. The lack of data is obviously hampered by the inability to perform destructive tests with the subject. The development of mechanical impedance functions for the human system requires verification of the method with data, particularly to determine if the system's mechanical impedances obtained from sinusoidal vibration can be related to random vibrations and

impact forces. The use of shock spectra represents a tool which may be useful as a qualitative means of comparing the response of different systems. However, before using shock spectra as a quantitative means of establishing criteria, one must be aware of the method's limits with regard to system nonlinearity, simultaneous vector components, system damping, restraint systems and pulse rates.

Report (12) presents a comprehensive description of the problems associated with human tolerance modeling and limits. This report discusses: (a) basic body dynamics, (b) the application of human body dynamics, (c) sources of data on body dynamics, and (d) dynamic models. The basis of human body dynamics is stated as being that biological structures respond to applied loads and accelerations in exactly the same manner as any other physical or mechanical system. The report suggests that due to such variables as bone stiffness and body weight, one must take into account statistical procedures to estimate the lowest strength limits. The basic problem is defined as the requirement to relate the input acceleration time history to injury or some other practical limit. The parameter of major interest is the peak force developed in the elastic material of the body. The force can be conveniently described as a Dynamic Response Index which is equal to the force divided by the body weight. Report (12) states that the primary sources of data are:

- Drop tests - performed by the Civil Aeromedical Research Institute, the FAA, the USAF Aerospace Medical Research Laboratory, and Stanley Aviation.
- Vibration tests - permit the determination of frequency and damping. The three test methods are (1) voluntary exposure to frequency and amplitude, (2) measurement of impedance, and (3) measurement of amplitude transmissibility.
- Structural tests - the major effort to date has been on the characteristics of the vertebral column.
- Sled tests
- Accident data
- Ejection seat data
- Animal tests

Report (27) proposes a concept whereby limits are set by the force exerted per unit area on the body by the restraint or support system at maximum deceleration. In this concept, acceleration levels, rate of onset, and duration time are all dependent variables, while the impact force per unit area, the delta velocity change and the impact pulse define the tolerance envelope.

Analytical Methods

There are several methods which are applicable to the development of a computer program which is capable of predicting the dynamic crash behavior with sufficient accuracy for the purpose of developing design criteria and preliminary concepts for improved crashworthiness of rotary-wing aircraft. These methods are classified as lumped mass, normal mode and finite element. Thus far, the lumped mass and normal mode approaches have been used in analyzing the behavior of complete aircraft structures during a crash condition. The lumped mass approach appears to be more capable of predicting general large-scale deformation than the normal mode approach. The normal mode approach requires a redefining of the element stiffnesses (also required in the lumped mass method) and then a recomputation of the system frequencies and modes shapes for every increment of time in the nonlinear regime. The determination of frequencies and mode shapes requires the solution of coupled equations which necessitates a time consuming matrix inversion. Since in a crash analysis the nonlinear deflections is the most important aspect of the problem, the additional computational requirements of the normal mode approach will be more inefficient and will introduce potentially significant inaccuracies as compared to the lumped mass method. The use of the finite element method in conjunction with a lumped mass system would appear to offer some potential. The finite element solution is essentially the same as a lumped mass solution, i.e., it involves converting continuous mass elements into discrete mass elements interconnected by springs. However, a finite element program is written such that the input is in terms of the characteristics of common structureal elements such as beams and plates. The main concern in using a finite element solution would be the ability to handle nonlinearities easily and perform the analysis within a reasonable program run time.

Reports (3), (8) and (9) are the only ones containing significant information concerning dynamic analyses during crash landing.

In report (8) the fuselage of a typical fixed-wing transport during crashing is modeled. The airplane is allowed to pitch and translate vertically. A series of nonlinear partially restoring springs represents the crushing of the lower fuselage. Up to six fuselage bending normal modes are input. Longitudinal motions are not considered; hence, no plowing or friction drag forces are computed. The program numerically converts the input load-deflection curves into load-time curves and utilizes closed-form solutions for the degrees of freedom within each time increment. No aerodynamics are included. Test case results using six normal modes indicate that structural flexibility does play an important role in crash load determination.

Report (9) deals with modeling the Lockheed Constellation 1649 for crash landing. A symmetrical model (pitch, plunge, fore-aft) is employed, with one fuselage vertical bending normal mode. Vertical springs are distributed longitudinally along the bottom of the fuselage. Each spring constant is a function of vertical deflection, with three separate deflection

regions defined. These regions are the initial elastic range, the plastic range, and an increasing stiffness range representative of floor and wing stiffening at large vertical deflections. Ground plowing and friction forces are included, as are fuselage longitudinal vibrations. The results shown in report (9) indicate that the inclusion of structural flexibility has little effect on the results; rigid-body motions tend to dominate. This conclusion differs with that presented in (8).

In contrast to the previous two reports, which involve quite similar models, report (3) utilizes a lumped mass model directly (no normal modes are computed). This model is intended to represent a UH-1D helicopter during crashing. Fourteen lumped masses with a total of 23 degrees of freedom are included. Only pitch and plunge motions are allowed. The lumped masses are interconnected with partially restoring nonlinear springs in parallel with viscous dampers. Two types of springs are provided: springs which can restrain tensile rebound and those that cannot. The lumped-mass degrees of freedom are solved for directly using numerical integration.

Comparison of experimental results from a helicopter drop test with computer program analytical results showed reasonably good correlation of floor accelerations, indicating accurate modeling of the landing skid and lower fuselage structure. Transmission response comparison is not as good; it appears that a rotational degree of freedom for the transmission is necessary to correctly predict its crash behavior.

Of the above mechanical models, only the lumped-mass helicopter model of report (3) appears capable of predicting general large-scale deformation. The other airplane models require linear structural behavior (except for the lower fuselage) to allow the use of normal modes; thus, only cases involving lower fuselage deformation that do not result in large deformations (or failure) elsewhere can be analyzed.

Accident and Injury Data

Survivable accidents are deemed to constitute approximately 95% of all rotary-wing accidents. Since survivable accidents account for 22% of all fatalities and practically all the injuries sustained during rotary-wing accidents, it is reasonable to assume that improvements in crashworthiness design which enhance the occupant's chance for survivability present a goal worth striving for.

One of the potential means available for the development of improved structural design for crashworthiness is the utilization and interpretation of accident and injury data. Accident data analysis in its present form is very limited. With current techniques, only gross judgements concerning impact velocities and accelerations can be made. Until such times as refinements in the techniques to analyze accident data can be achieved, the benefits obtained from the use of accident information will not be fully realized. Refinements in accident investigation techniques require

more thoroughness in the determination of impact kinematics at the site of the investigation and the application of analytical or semiempirical means by which aircraft behavior and large structural deformations can be related to the sequence of structural damage and injuries sustained during a crash.

The accident data presented in the literature indicates that the causes of major injuries and/or fatalities are numerous. Although excessive vertical acceleration levels are generally thought to be the prime cause of injuries, the reports reviewed show that cockpit crushing, postcrash fire, dislodgement of the occupant, dislodgement of unsecured objects, and flailing of the occupant's head and extremities contribute heavily to the injury toll.

It is also interesting to note that several of the articles discuss the need to protect personnel from lateral impacts or crushing during aircraft rollover accidents. Yet, the crash environment as compiled to date is least defined with regard to the lateral loads imposed during an impact. The accident records, in general, are not very comprehensive, thus making an accurate assessment of impact kinematics and deceleration forces difficult. The crash environment acceleration loads are stated for a location at approximately the center of the fuselage floor. However, peak loads at critical locations, i.e., pilot, passenger, engine, and transmission, can be much different from that at the fuselage floor, depending on the amount and type of structure available.

Reports (2), (3), (17), (18), (20) and (25) present accident data obtained from rotary-wing and light fixed-wing aircraft experience. Reports (2) and (21) present accident data for heavy fixed-wing aircraft.

Reports (2) and (3) are more recent analyses of accident data performed for the purpose of defining the crash environment. In report (2) the 95th percentile velocity changes and acceleration levels in different directions from 373 survivable accidents are presented. These values are summarized in the "Crash Loads and Environment" evaluaton. In report (3) UH-1H Army and Air Force accident cases are analyzed for the period between 1966 and 1968. These cases represent approximately 15% of the total of UH-1H accident records available at USAAAVS and the Directorate of Aerospace Safety for that time period. The accident data was summarized in the form of injury data and injury factors. The leading injury factors were deemed to be (a) aircraft rolled on side, (b) postcrash fire, (c) occupant crushing or entrapment, and (d) excessive vertical G's. Based on the results of the helicopter accident records, report (2) concluded that over half of the injuries and fatalities occurred in rollover accidents and that more fatalities were caused by impact force injuries than by postcrash fire thermal injuries in survivable accidents.

Report (17) discusses major, minor and incident accident cause factors. In all instances, the predominant cause factor is attributable to the pilot. Material and maintenance are also shown to be substantial causes of accidents. Report (18) shows that between 1961 and 1965, survivable accidents accounted for 95% of all accidents. Report (20) compares the crash environment for rotary-wing aircraft to human tolerance levels. The report suggests that the 95th percentile crash data indicates survivability due to crash G's, and their time durations are within the human survival limits for present structures. However, to ascertain the severity of the environment relative to human tolerances, one must determine the extent to which substructure will affect the peak loads. In report (25) helicopter crash performances between 1967 and 1969 are reviewed. Fatalities are shown to result from multiple extreme injuries (60.8%), burns and complications (29.9%), drowning (5.2%), and unknown (4.1%). Occupant injuries were deemed to be caused by accidents which involved aircraft rolling on the side, crushing, thrown out occupants, postcrash fire, transmission and main rotor penetration, and excessive G's.

Report (21) discusses 183 major accidents of cargo and transport type aircraft and lists various injury factors. In this report, many injuries are noted even though the acceleration levels are not considered to be unduly high.

Report (32) is a preliminary draft which indicates that crashworthy features can potentially become cost effective in the UTTAS in approximately 5.5 years. The report takes into consideration the accident history of the UH-1, the cost to the Government of personnel injuries and fatalities, the savings potential on aircraft repair and replacement costs and increased operating costs as a result of increased empty weight due to the incorporation of improved crashworthy design.

Crash Test Data and Methods

Correlation between test and analysis shows that the basic problem in developing analytical models is the ability to realistically describe the structural behavior under loads which will result in large deformations. The test data shows that it is important that fuselage structure exhibit plastic deformation characteristics in both the longitudinal and vertical directions. Tests have shown that unless sufficient energy absorption capability is included in the design of fuselage structure, the pilot and passengers can be expected to experience intolerable acceleration forces. Test programs have provided valuable information which has been used to develop airframe design and restraint systems which better attenuate crash forces. At present, full-scale test techniques provide more valuable design information than do analytical methods. However, the expense of conducting full-scale tests is a formidable obstacle in evaluating the large amount of design considerations for all types of rotary-wing aircraft.

Reports (3), (10) and (23) describe crash test programs performed with rotary-wing vehicles. Reports (1), (5), (6), (7), and (24) present the results of test programs which were conducted with fixed-wing aircraft. Report (16) discusses tests with crushable structures and is applicable to both rotary-wing and fixed-wing aircraft.

Report (3) describes a recent vertical drop test program conducted with a UH-1D helicopter. The program results indicated that the structural representation of the aircraft requires numerous assumptions and estimates regarding the structural behavior of the helicopter. The correlation between analysis and test shows that additional effort is required to refine the analytical model to show agreement with the experimental data. Report (10) describes tests performed on an H-25 helicopter in which accelerations were measured at the cockpit floor, passenger floor, and pilot restraint system, and on dummies representing the pilot and passengers. The pilot experienced accelerations in the headward direction which were shown to exceed the estimated human tolerance limits. The helicopter experienced accelerations which were larger in magnitude and shorter in duration than corresponding accelerations that were obtained during NACA fixed-wing aircraft tests. These tests, being the first of their kind on helicopters, proved invaluable in that they pointedly showed inadequacies in structural design of helicopters for crash impacts. Report (23) describes full-scale crash tests with a CH-21 helicopter for the purpose of evaluating an energy absorption experimental troop seat concept. The two test methods employed in this program were the drone and crane drop tests.

Report (1) describes the results of controlled full-scale tests performed with fixed-wing aircraft to demonstrate the effectiveness of simple structural changes in achieving improved crashworthiness design. The test program was partially successful in reaching its objectives. The program demonstrated the effectiveness of a nose modification in reducing earth scooping and thus reducing the severity of the crash environment. However, the test results regarding the effectiveness of increasing upper cabin compressive strength in reducing cabin collapse due to fuselage bending associated with the rapid pitch-up for longitudinal crashes were inconclusive. The test program described in reports (5) and (6) were performed under the same contract with two different large fixed-wing aircraft (DC-7 and Lockheed Constellation 1649). The programs were directed toward determining the overall acceleration environment, fuel spillage studies, and cockpit, crew and passenger seat experiments during potentially survivable crashes. The tests were designed to simulate crash conditions for three types of potentially survivable accidents. The three conditions were:

- Hard landing with high rate of sink
- Wing low impact with the ground
- Impact into large trees in off-airport forced landing.

Due to a failure in the recording system, the program on the DC-7 did not meet all of the test objectives. However, the tests with the Lockheed 1649 which were successfully recorded showed that the structural damage and deformation of the fuselage that occurred in the crash were relatively mild, particularly in the occupiable portion. The damage was most severe in the lower forward fuselage where primary impacts were concentrated.

In report (7), FAA and NACA test data are reviewed to determine crash severity and the significance and limitation of component tests. A severity index is established by which acceleration levels are compared to human tolerance levels, and a quantitative evaluation is made of the severity of the impact. Data from seven full-scale crash tests are used in this report to develop severity indexes. The severity index in only one case indicated that human tolerance levels would be exceeded, and that occurred at only one station.

Report (8) compares analytical results with tests performed on representative fuselage structure, and report (24) describes the evaluation of the limits of seat belt protection during crash deceleration.

Energy Absorption

There is general agreement throughout the literature that the design of a crashworthy structure requires that a logical sequence of structural failure be planned. The use of seats capable of taking a high "G" loading would not be logical if the design requirements for the airframe and major mass items (i.e., transmission, engine) are such that failure could cause collapse of the occupant's liveable space, causing injury or fatality, while the seat remains intact. On the other hand, the design of an airframe sufficiently strong to hold occupants in place under high impact velocities while the airframe is undergoing very little deformation would be as undesirable as a structure which collapses easily, since the occupant would be subjected to intolerable acceleration magnitudes. The incorporation of energy absorption capability into the structure will help to alleviate the aforementioned design inadequacies since energy absorbers can serve the following functions:

a) Reduce the nontolerable deceleration pulses on the occupant.

b) Permit seat structures to yield to short-duration high-acceleration pulses.

Energy absorbers can be incorporated prudently throughout the airframe to improve the structure's crashworthiness capability. However, as is the case in any design solution, there exists a trade-off among performance, cost, weight and space. Thus, the use of energy absorbers to improve aircraft crashworthiness requires a determination of:

a) Where energy absorption is most critically needed.

b) The amount of energy absorption required.

c) The type of energy absorber that will best serve the needs.

d) The cost in terms of weight and/or space that can be tolerated.

Reports (1), (2), (4), (8), (16),(19) and (20) present information which is pertinent to the subject of energy absorption.

Reports (1) and (2) show that the kinetic energy of the impacting aircraft is equal to the energy deformed in the soil and the structure. The controllable factors are:

- Average force developed in the collapse of the structure
- Linear deformation of the structure
- Deformation energy in structure other than the cabin. The reduction in the deceleration forces requires a corresponding increase in deceleration distance and, consequently, crushable material.

Report (4) discusses the crash environment and how it pertains to energy absorption. The terrain is considered to be the most important parameter in determining the causes of structural collapse. With soft ground, energy is primarily dissipated due to soil plowing or compression. However, on a hard surface, friction between the structure and surface is the means of dissipating energy. Energy absorbed by failure of landing gears, pods and pylons is considered to be insignificant due to their small mass relative to the total structure for longitudinal velocity impacts. For a large transport, the report concludes that kinetic energy cannot efficiently be absorbed by structural collapse and still retain a survivable shell.

Report (8) is oriented toward determining how aircraft kinetic energy is dissipated and what are the most critical areas for crash loading. Analysis indicates that the longitudinal kinetic energy cannot be absorbed by axial collapse of fuselage structure alone, due to the amount of structure required. Friction forces are important in absorbing energy in this direction. Vertical impact energy must be absorbed by crushing of the lower fuselage.

Report (16) discusses the use of foam plastics and aluminum honeycomb as energy absorption material. Foam plastics, as expected, may require considerable depth to satisfactorily reduce acceleration levels, whereas the aluminum honeycomb material stiffness may result in high onset rate.

In report (19) it is concluded that: (a) it is completely impractical, through the use of energy absorbers, to significantly reduce the longitudinal acceleration level for occupants in accidents involving a large change

in velocity in a single deceleration pulse; (b) it is practical to provide energy absorption to limit vertical acceleration in the order of 20-25G in accidents occurring at descent rates ranging from 40-50 fps, assuming some vertical deformation of the structure; (c) it is possible to reduce short-duration (.005 to .010 sec) peak loads to lower values in order to prevent seat failures due to exceedance of design strength. Report (20) discusses the use of energy-augmented alighting gears for helicopters which will absorb appreciable elastic energy. In addition, the use of a load limiter between the pilot seat and structure is investigated. This concept provides additional crushing distance for the pilot over that provided by the airframe.

Structural Behavior and Failure Modes

The information obtained in the literature tends to show agreement on the requirement for progressive damage in a controlled manner in order to achieve improved crashworthiness design. The structural failures which are primarily responsible for resulting in occupant injury, or fatality, are considered to be:

- Longitudinal crushing loads on the cockpit
- Vertical crushing loads on the fuselage shell
- Transverse bending of the fuselage shell
- Buckling deformation of the floor structure
- Landing gear penetration of the fuselage structure
- Rupture of flammable fluid containers
- Transmission or rotor blade penetration of the cabin structure
- Lateral collapse of the fuselage structure

Modifications to the structure and structural design concepts have been presented in many of the reports. Potential improvements consist of increased energy absorption capability, design for breakaway, transferral of major mass items, improved equipment tiedown, and strengthening of cabin structure. The literature distinguishes between the design for longitudinal and vertical impacts in terms of their different structural energy requirements. In the longitudinal impact, unlike in vertical impacts, there exists a high-force-level energy absorption (friction) exterior to the aircraft, and the velocity change can be accomplished in a relatively long time interval.

Analysis of aircraft structural failure modes is hampered by the inability to conveniently describe large nonlinear deformations that take place during an impact in which the crash environment is complex. Aircraft behavior after impact is a function of the impact conditions and the structural characteristics of the airframe and components. Although the determination of the failure mode of various components or airframe segments

provides valuable information, there exists a need to adequately describe in sequence the structural behavior and failure modes during a crash in order to develop improved design criteria. The ability to understand what is happening sequentially is an important aspect in developing a consistent approach to crashworthiness design.

Reports (1), (2), (4), (8), and (20) contain information which is applicable to the areas of structural behavior and failure modes.

Reports (1) and (2) discuss structural modifications which offer promise of improved survival in aircraft accidents. The contribution of the suggested modifications are reviewed in light of the influence of structural energy absorption, earth gouging and scooping phenomena, and change in effective mass upon the two crashworthiness indices:

- extent of cabin collapse
- floor acceleration levels

Improved structural crashworthiness in longitudinal impacts is deemed possible by:

- Reducing impulsive earth scooping
- Reinforcing cabin structure to prevent its collapse within occupiable areas
- Where practical, reducing the strength of the fuselage structure to insure failure in unoccupiable areas
- Improving energy absorption characteristics in the structure forward of the occupiable area
- Increasing deformation and energy absorption in unoccupiable areas

Improved structural crashworthiness in vertical impacts can be achieved by:

- Transferring mass from the top of the fuselage to the cabin floor
- Strengthening of cabin structure so as to increase it resistance to vertical collapse
- Modifying the cabin structure such that elastic energy absorption is increased or plastic energy absorption is provided at loads less than the general collapse load
- Increasing energy absorption in the subfloor structure realizable at load levels below the cabin collapse load

Report (4) discusses the influence that material properties have on crashworthy designs. It is essential to design the bottom and front of the fuselage to buckle and crush as opposed to tearing or rupturing when impacted. The ductile structure, although crushed, will continue to resist load and absorb energy. In addition, the use of ductile material will reduce peak loads transmitted to the occupants or equipment. Report (8) describes the manner in which aircraft kinetic energy is absorbed or dissipated and discusses the critical areas of structure for crash impacts.

Report (20) describes the use of the breakaway design concept and its impact on crashworthy designs. The paper shows that a crew compartment in an experimental Sikorsky S-60 was designed such that the pilot and crew were placed in a pod with no gear structure below them. The canopy and its carry-through structure were constructed in such a manner as to effect a partial breakaway capsule. In 1961 this experimental aircraft crashed. The pilot's crew compartment held intact and tore away from the main airframe, and there were no injuries.

Restraint and Escape Systems

The literature points out the need to think in terms of a total restraint system which includes the seat, the seat anchorage, and the floor structure as opposed to considering the seat by itself when discussing crashworthy design. In addition, recognition is given to the importance of dynamic considerations in the development of strength criteria. Several means by which occupant deceleration levels can be reduced are discussed, including proper seat belt design, energy absorption capability between the seat, seat belt and seat attachment, and the incorporation of progressive plastic collapse properties in the design of seat structure.

Reports (2), (13), (15), (19), (24), (28), and (31) present data applicable to restraint and escape systems.

Reports (28) and (31) are Military specifications for crashworthy design of ejection and nonejection seat systems, respectively. These specifications are discussed under the next subject area (MIL Specs).

Report (24) discusses the limits of seat belt protection during crash decelerations. Three accident cases are reviewed in this report. The report states that the estimates of tolerance limits associated with standard seat belts are a matter of speculation and can range from 15 to 50 G's. The following conclusions are presented:

a. Static strength is not indicative of a seat belt's behavior and strength under a dynamic condition.

b. Seat belt characteristics should be determined in combination with the system of which it forms a part and the typical pulse of the vehicle in which it is used.

c. Many times, protection offered by seat belt restraint is not limited by "G" factors but by injurious aspects of the occupant's environment.

Military Specifications (MIL Specs)

The MIL Specs present very little in the way of useful design requirements for airframe structural crashworthiness. Several of the specifications investigated included requirements for subsystem or component crashworthiness. Of these, one specification was limited to crash-resistant fuel tanks (29), while another specification was for aircraft ejection seat systems (28). A third specification (30), although a helicopter structural design requirement specification, left the quantification of the crash requirement up to the various procuring agencies.

Report (29) is a specification for aircraft crash-resistant fuel tanks. The crash impact test requires that the fuel cells be dropped 65 feet (~65 fps vertical impact) onto a nondeformable surface without resultant spillage.

Report (30) is a helicopter structural design requirement specification. The crash requirement states that the engines, transmissions, equipment and useful load items, and their carry-through structure are to be designed such that their failure would not result in injury to personnel. However, the ultimate inertia load factors are to be specified by the procuring agency. Report (31) is the only specification studied that considered the crash impact environment, dynamic response considerations, and human tolerance limits. The specifications reviewed indicated that design requirements for crashworthiness are incomplete and unsystematic in their approach to the problem and that a great deal of inconsistency exists due to requirements set forth by different agencies.

Report (31) is a recent Military specification for crashworthy design on an aircraft nonejection seat system. This specification incorporates many of the design concepts presented in report (2) and discussed in reports (4), (13) and (19). In particular, the specification describes dynamic testing requirements based on accident data acceleration pulse and velocity changes for the forward side and vertical directions. The specification requires that the occupant not experience acceleration in excess (magnitude and/or duration) of a specified acceptable tolerance level in the vertical direction. The requirements do not specify acceptable human tolerance levels in the transverse directions, nor do they explicitly distinguish between downward and upward tolerances. A third factor pertinent to human tolerance levels, rate of acceleration onset, is not explicitly stated. Report (28) is a Military specification for design of an aircraft upward ejection seat system. This specification defines ultimate crash loads for forward, side and vertical directions. The crash requirements of report (28) are not directed toward human tolerance limits and consequently differ from the requirements stated in report (31).

SUBSTRUCTURE TEST

TEST OBJECTIVE

The purpose of this test was to determine the energy absorption characteristics of a fuselage bumper structure under dynamic loading conditions for correlation with static loading conditions and analytical studies.

TEST SPECIMEN

The test specimen was a P2V-4 Fuselage Bumper Assembly (No. 134171-12). The fuselage bumper was chosen for the test program for the following reasons :

- The fuselage bumper exhibits static load deformation characteristics which indicate that this structure is a candidate for future studies regarding energy absorption.
- The availability of static load deformation data from a previously conducted program (Reference 34) provides an expeditious means by which the effect of the rate of loading on the load deflection characteristics for the structure can be determined.
- The fuselage bumper represents the type of structure for which the current "state-of-the-art" analytical methods should be applicable.

The test specimen is shown in Figure 18.

INSTALLATION

The test was performed in a shock test machine at the Lockheed Rye Canyon Structures Laboratory. Figure 19 shows a schematic of the test arrangement. The shock machine consists of a rigid frame having a roller-guided carriage to which a ballasted impact head is attached. The ballast impact head weighed 2960 lbs for this test. A solenoid-actuated release hook suspended at the carriage at the desired drop height of 25-1/2 inches. The total anticipated energy for this weight drop free-fall, height and anticipated structural deformation was approximately 105,000 in-lb. The input energy for the impact test was set at approximately 10% higher than that estimated for the previously conducted static tests (Reference 34) to insure that the structure would collapse a minimum of 10 inches.

The specimen was supported on the machine base by rubber-padded blocks, which were located in the fore and aft ends of the specimen and at intermediate locations in line with specimen internal stiffeners. Figure 20 shows the test setup for both the static test, described in Reference 34, and the dynamic test, described in this report.

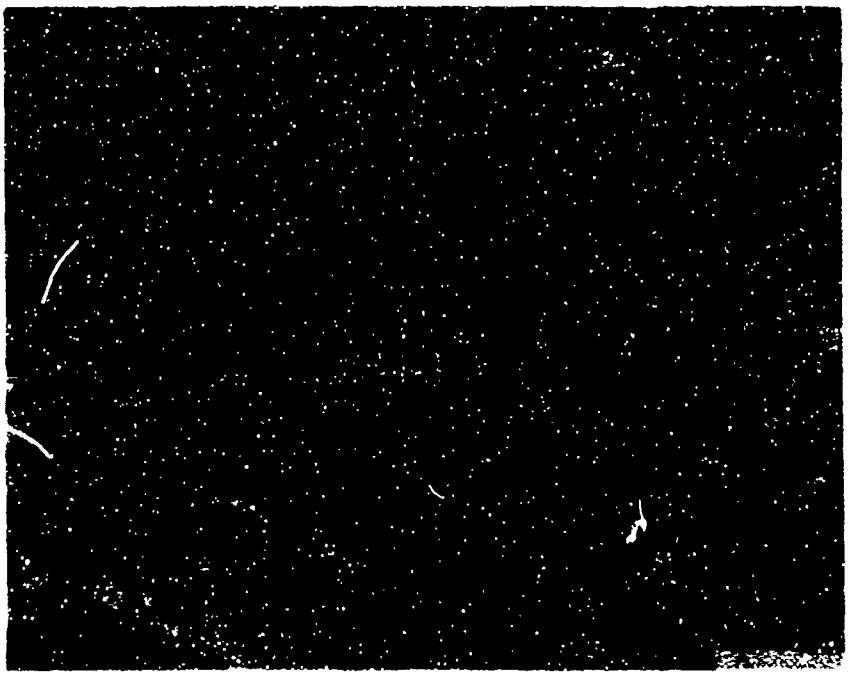

Figure 18. Fuselage Bumper Test Specimen.

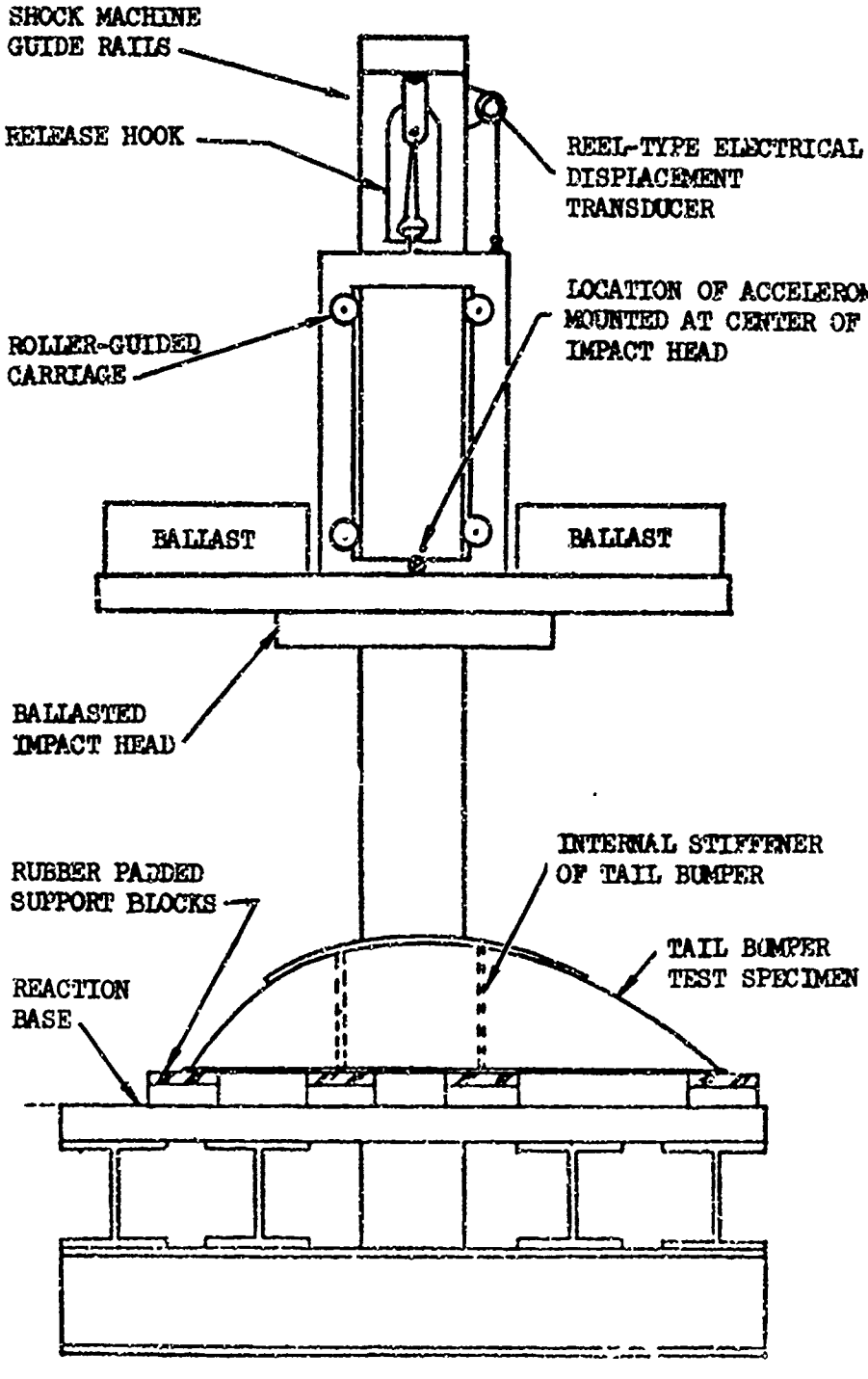

Figure 19. Fuselage Bumper Test Installation.

(a) Static Test Setup.

(b) Dynamic Test Setup.

Figure 20. Comparison of Static and Dynamic Test Specimen Setup.

INSTRUMENTATION

The sensing instrumentation consisted of an accelerometer located on the impact head, a displacement transducer arranged to measure the relative motion between the machine frame and the carriage throughout the entire period of mass excursion, and a supplementary displacement rod to measure the deformation of the structure. The accelerometer (10g Statham) had a frequency response >150Hz. The displacement transducer consisted of a spring-loaded rotary pot driven by a thin wire cable, which generated an output signal faithfully representative of the vertical motion of the impact head. The sensors were calibrated immediately prior to testing, through procedures traceable to the National Bureau of Standards. Accelerometer and displacement transducer outputs were recorded directly in the Lockheed Central Data System (CDS) as time histories of acceleration and displacement. Cross plots of acceleration versus time were obtained from the recorded data.

PROCEDURE

The following procedure was followed during the fuselage bumper impact test:

1. The carriage was raised to engage the release hook at a height which would position the impact head approximately 25-1/2 inches above specimen contact.

2. Instrumentation zero-reference levels were adjusted as required.

3. The oscilloscope and recording switches were actuated, and the release hook solenoid was energized to permit free-fall of the test mass.

4. At the conclusion of the test, the specimen was visually inspected. Multiview photographs of the deformed specimen were obtained.

RESULTS

The time histories of the acceleration and deflection are shown in Figures 21 and 22 respectively. The high-frequency oscillations at impact (time = 2.32 seconds) are attributed to the accelerometer natural frequency ($\approx$ 400 cps). The total deformation is shown to be approximately 11.5 inches. The acceleration versus deflection is cross plotted in Figure 23 for the time period of interest (t = 2.32 sec to t = 2.46 sec).

To compare the results of the dynamic impact test with the results of the static test, the accelerations were transformed to loads by adding 1G and then multiplying each acceleration level by the weight (2960 lbs) of the

ballasted impact head. These results are shown in Figure 24 for both the static and the dynamic test. The load deflection curves, in general, show additional peaks, particularly after the structure has deformed in excess of 5 inches. The peak load levels for the dynamic test reached approximately 13,000 lbs compared to 11,000 lbs during the static test. However, as can be observed in Figure 24, the energy absorbed for both tests shows excellent agreement. The additional input energy supplied in the dynamic test is reflected in the results since the specimen deformed 11.5 inches during the dynamic test as compared to 10 inches during the static test.

The deformed structure for both the static and dynamic tests is shown in Figure 25. The structure deformed in much the same manner in both tests, although from Figure 25 it does appear that the structure had flattened out more during the dynamic test. However, a review of the test setups (Figure 20) indicates that the shape of the impact head used in the dynamic test could have contributed to this "flattening" effect. It would also account for the higher energy peaks noted after the structure had deformed several inches.

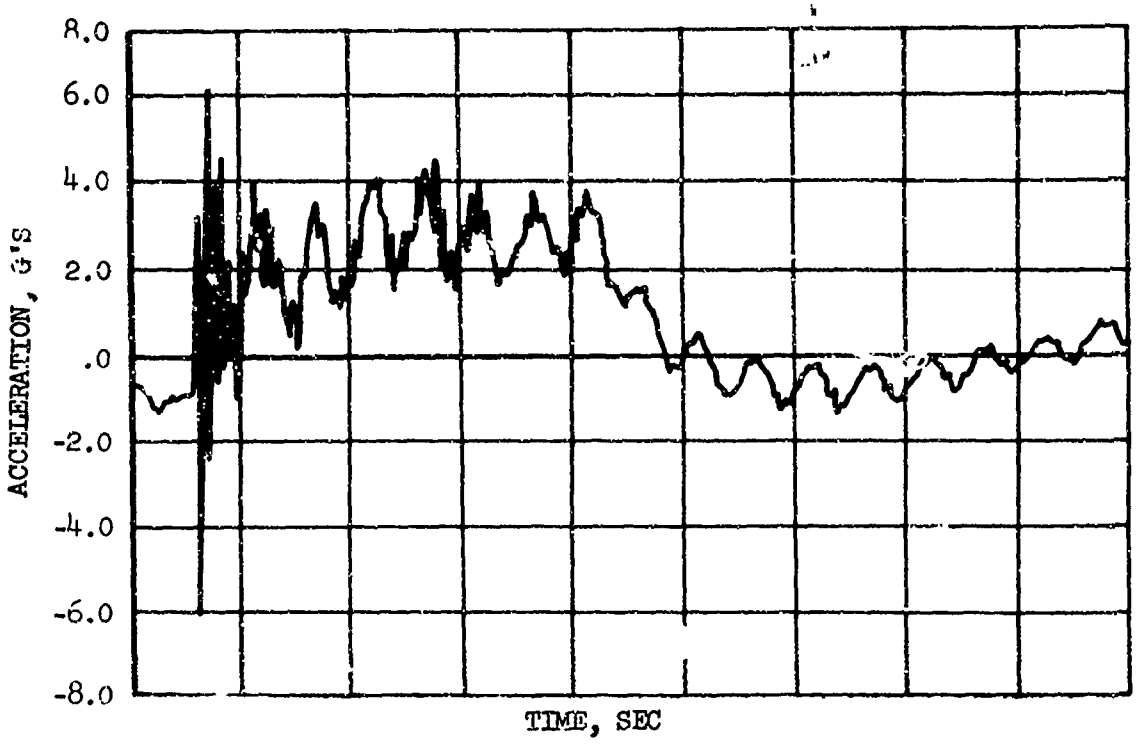

Figure 21. Acceleration vs Time, Fuselage Bumper Dynamic Test.

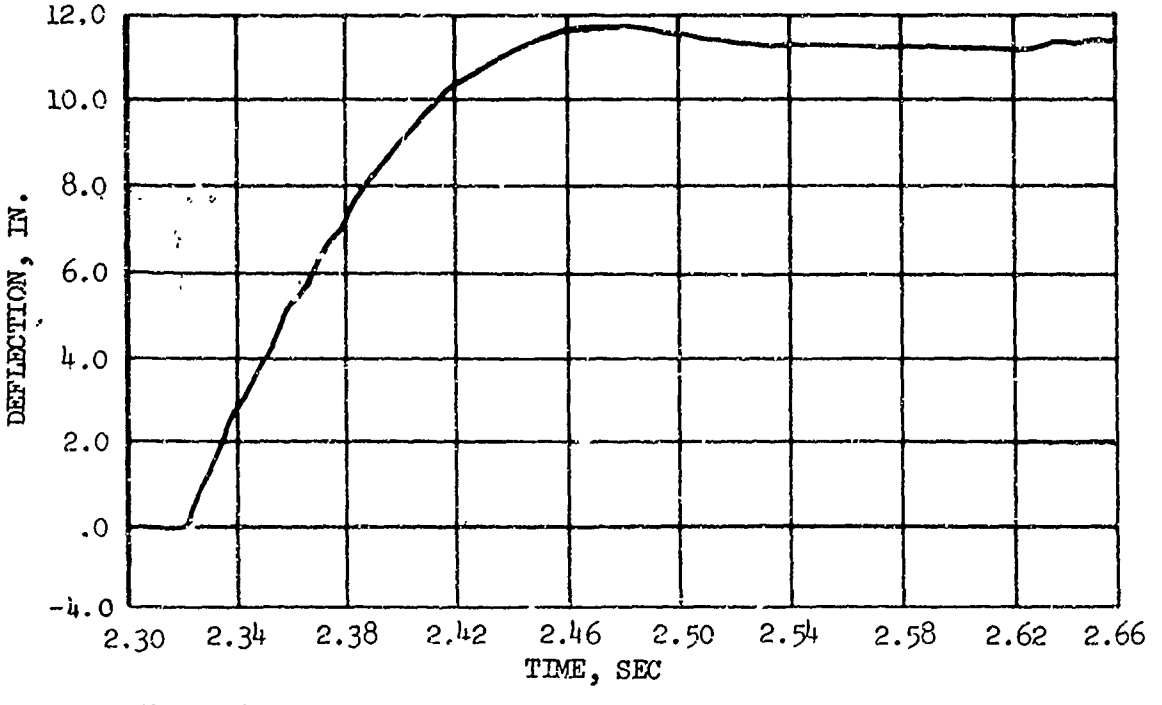

Figure 22. Deflection vs Time, Fuselage Bumper Dynamic Test.

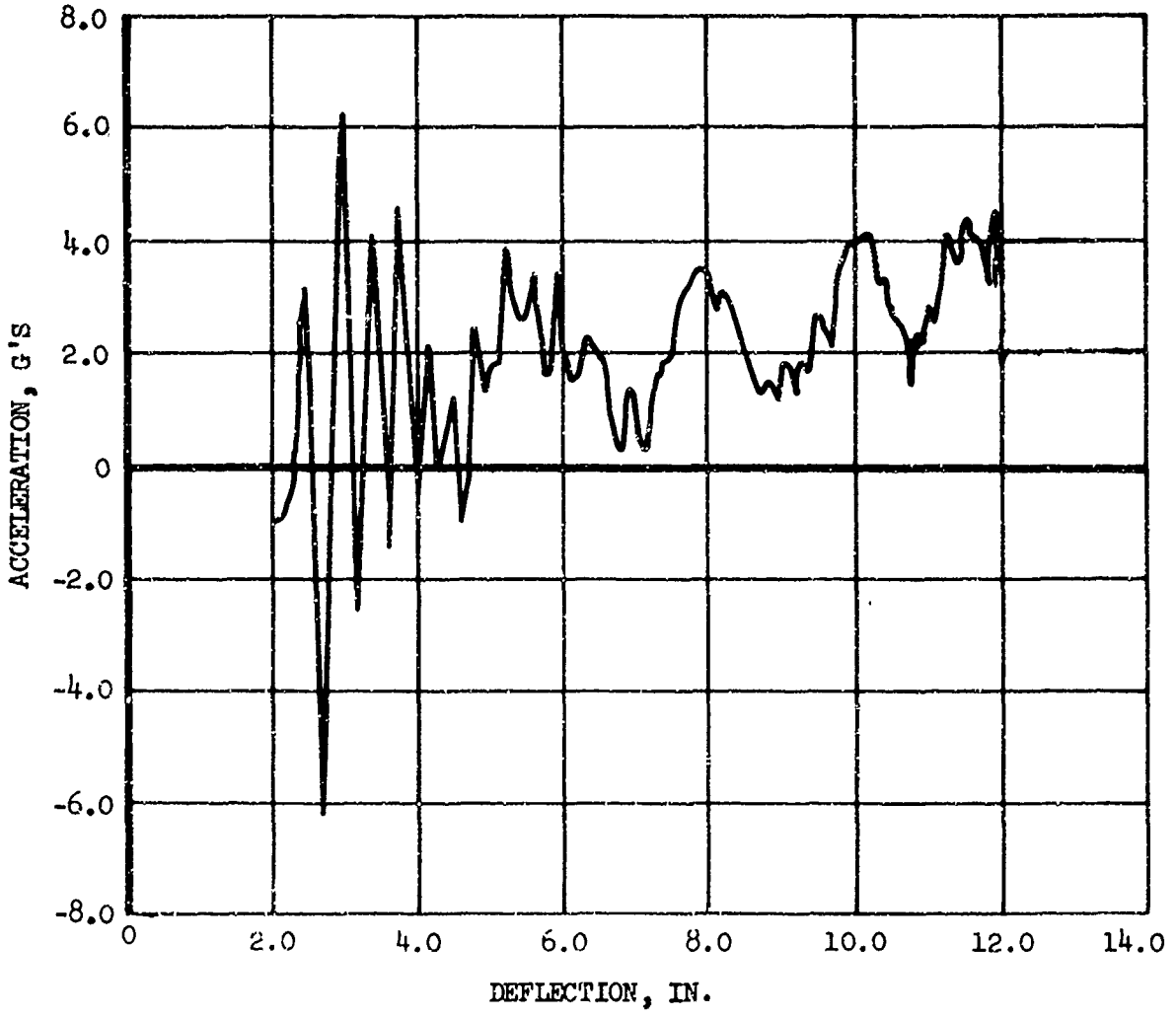

Figure 23. Acceleration vs Deflection, Fuselage Bumper Dynamic Test.

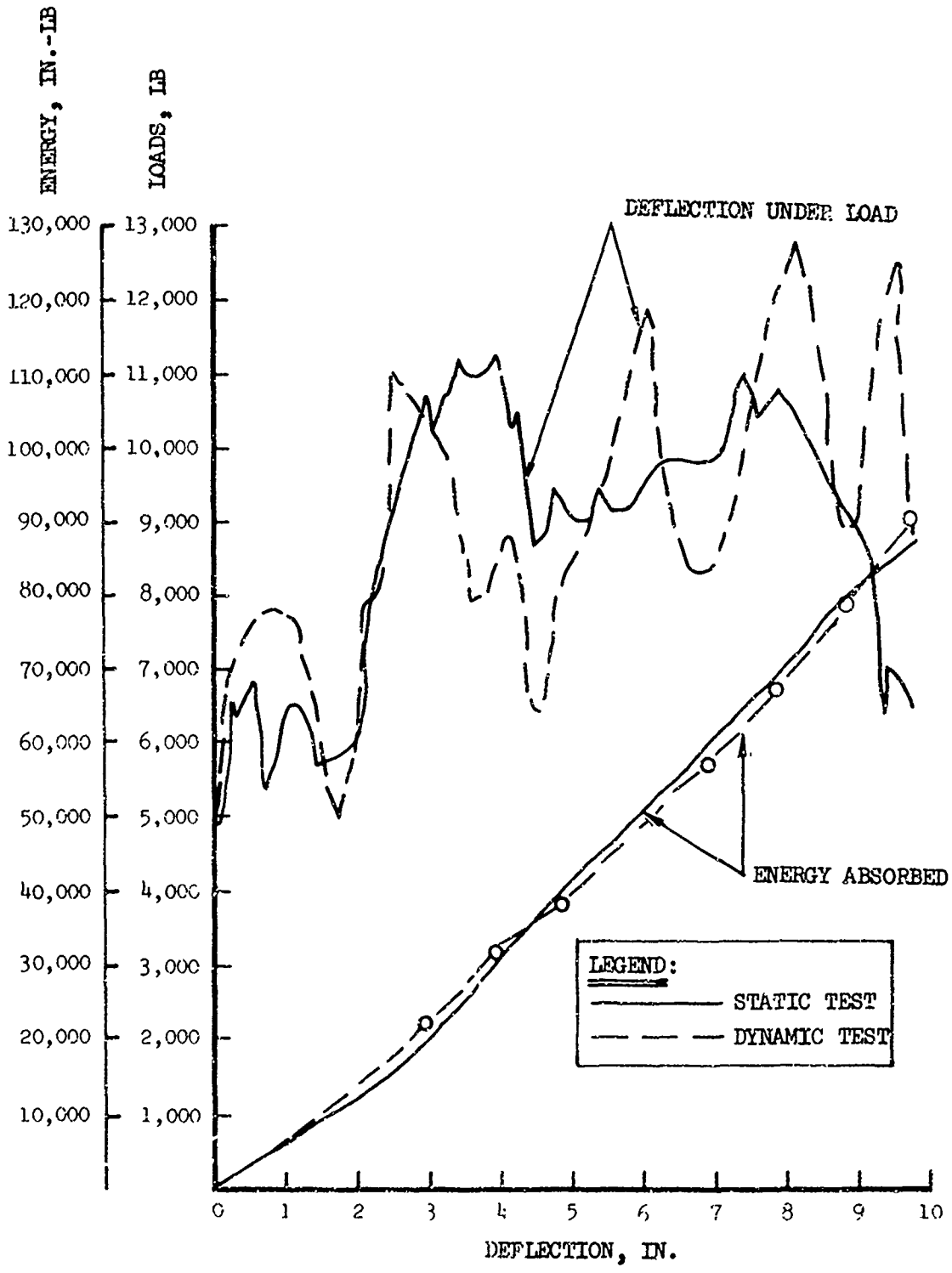

Figure 24. Load Deflection and Energy-Absorbed Results for Static and Dynamic Fuselage Bumper Tests.

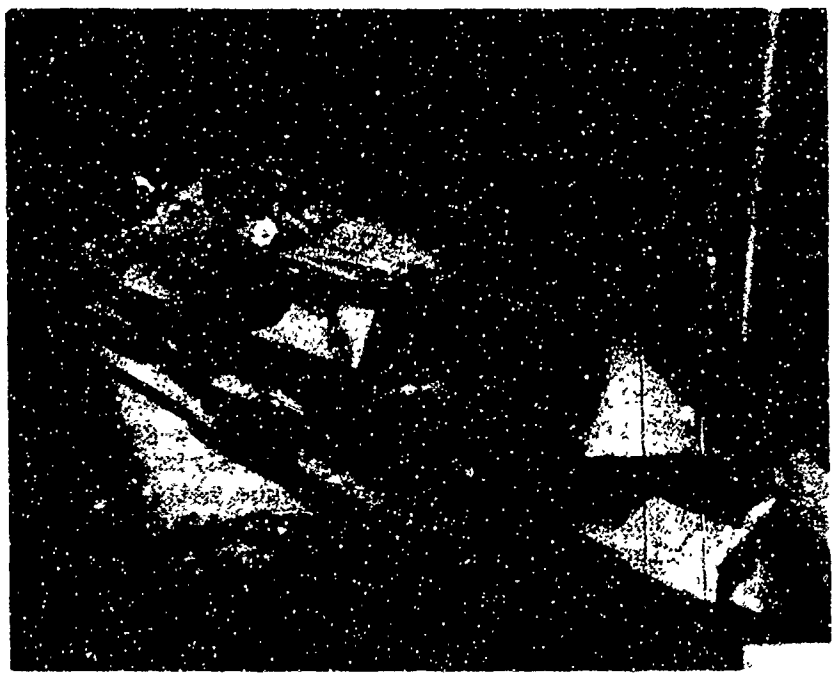

(a) Static test, Deflection = 10 Inches.

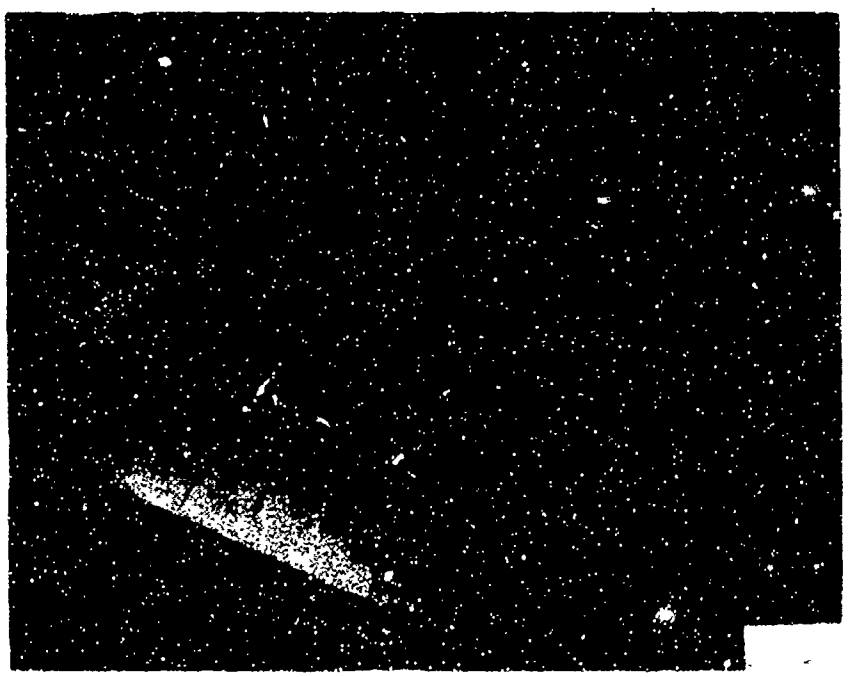

(b) Dynamic test, Deflection = 11.5 Inches.

Figure 25. Static and Dynamic Load Test Specimens Deflected.

SUBSTRUCTURE ANALYSIS

OBJECTIVE

The objective of this analysis was to determine the feasibility of using existing computer program capabilities to obtain load deformation characteristics of aircraft structure which experiences large nonlinear deflections.

METHOD

The fuselage tail bumper, described previously, was analyzed using an existing LMSC* computer program , "STAGS"** STAGS is a general program for the analysis of shells in which the principle of minimum potential energy is used in conjunction with the finite difference method. STAGS performs nonlinear stress and stability analysis for general shells and is capable of treating large deflections. Volume II contains a more detailed description of STAGS.

PROCEDURE

The local displacement curves obtained by static test and shown in Figure 24 indicate that buckling (in the form of a first sharp peak) occurs first at approximately 5000 lbs. Buckling is followed by a gradual crushing of the top of the bumper under a practically constant load. At a deformation of 2 inches, the curve starts to rise again. This is attributed to the fact that the bulkheads at that point start to take load through direct contact. A sketch of this loading situation is shown below.

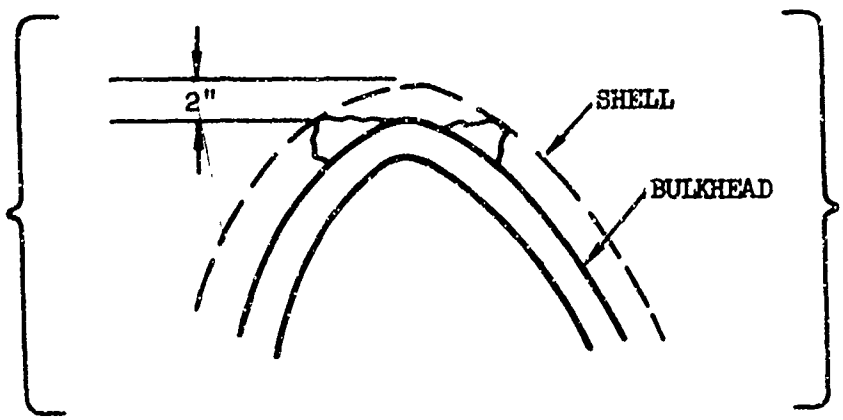

The load increases to approximately 10,000 lbs and thereafter stays reasonably constant up to 8 or 9 inches of deformation.

The analysis using STAGS assumes that the crushing of the shell and the crushing of the bulkhead both take place under constant load.

*Lockheed Missile and Space Company, Inc., Sunnyvale, Calif.
**Structural Analysis of General Shells

Shell Analysis

An initial step in the application of STAGS requires that the geometry of the midsurface be defined analytically. That is, for a point on the surface, the coordinates in a Cartesian system are given in terms of the values of the set of shell surface coordinates which generate the finite difference mesh. The shell surface coordinate system is defined in Figure 26. The geometry corresponding to this definition is shown in Figure 27. The model was assumed to be symmetric about the plane Z = 0. Although the bumper is not quite symmetric about the Z = 0, this simplification saves a considerable amount of computer time and, in view of the approximate nature of the analysis, is justified. The grid lines shown in Figure 27 are obtained from the program's automatic plotter.

In the first effort of analysis, a point force was applied at the apex of the bumper with an inward direction. The nonlinear analysis indicated a maximum in the load displacement curve of about one-third of the load at which the static test showed rapidly increasing displacements. The primary reason for this relatively poor result appeared to be that the load was applied at one point rather than over a flat surface at the top which increases in size with the increase in load. An effort was made to apply a distribution of point forces such that at the load level corresponding to collapse, the bumper is relatively flat and such that the loads are applied approximately over this area. Apparently, collapse of the shell occurs at about 3500 lbs total load on the bumper. Figures 28a and 28b show a "buckling mode", i.e., the difference in displacement between the last two load steps. The most important reason for a deviation between the analytical (3600 lbs) and experimental (5000 lbs) appears to be that the doubler cap was not included in the analysis and that the stiffener (Figure 29a) as modeled as shown in Figure 29b; it is possible that the analytical and theoretical results would have been in good agreement if the model was improved in these two respects.

Bulkhead Analysis

The geometry of the bulkhead as modeled for STAGS analysis is shown in Figure 30. The coordinate "S" here is the arc length along the inner contour. The bulkhead is .060-in.-thick aluminum material. The analytical description of the shell surface is:

$$0 \leq \sigma \leq R\,\Omega$$

$$X = (R - x) \cos (S/R)$$

$$Y = (R - x) \cos (S/R)$$

$$Z = 0$$

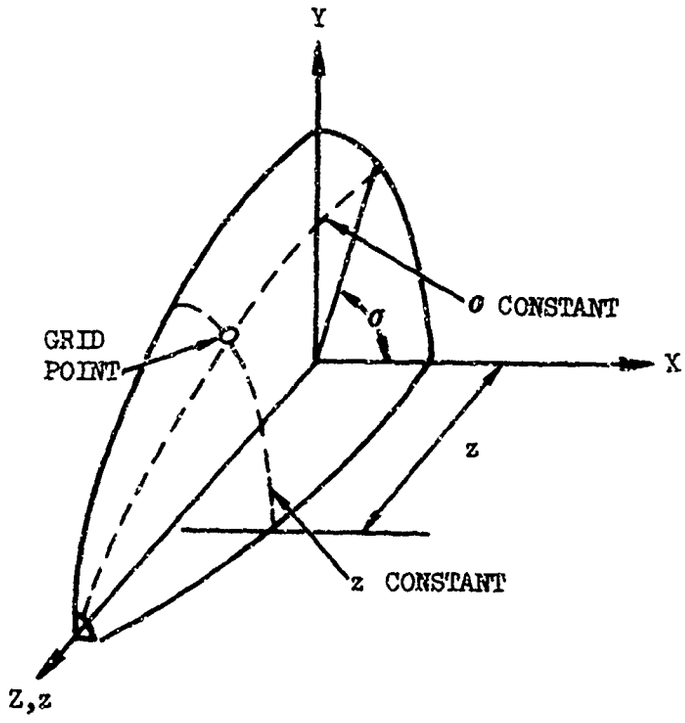

EQUATIONS:

$$Y = a - b_X^2 - c_Z^2$$

$$z = Z$$

$$\tan\sigma = Y/X$$

$$X = \left[-\tan\sigma + \sqrt{\tan^2\sigma - 4b(c_z^2 - a)} \right] / 2b$$

$$Y = X \tan\sigma$$

$$a = 13 \quad b = .333 \quad c = .-19$$

X, Y, Z ARE COORDINATES IN THE CARTESIAN SYSTEM

σ, z ARE SHELL COORDINATES

Figure 26. STAGS Shell Surface Coordinate System.

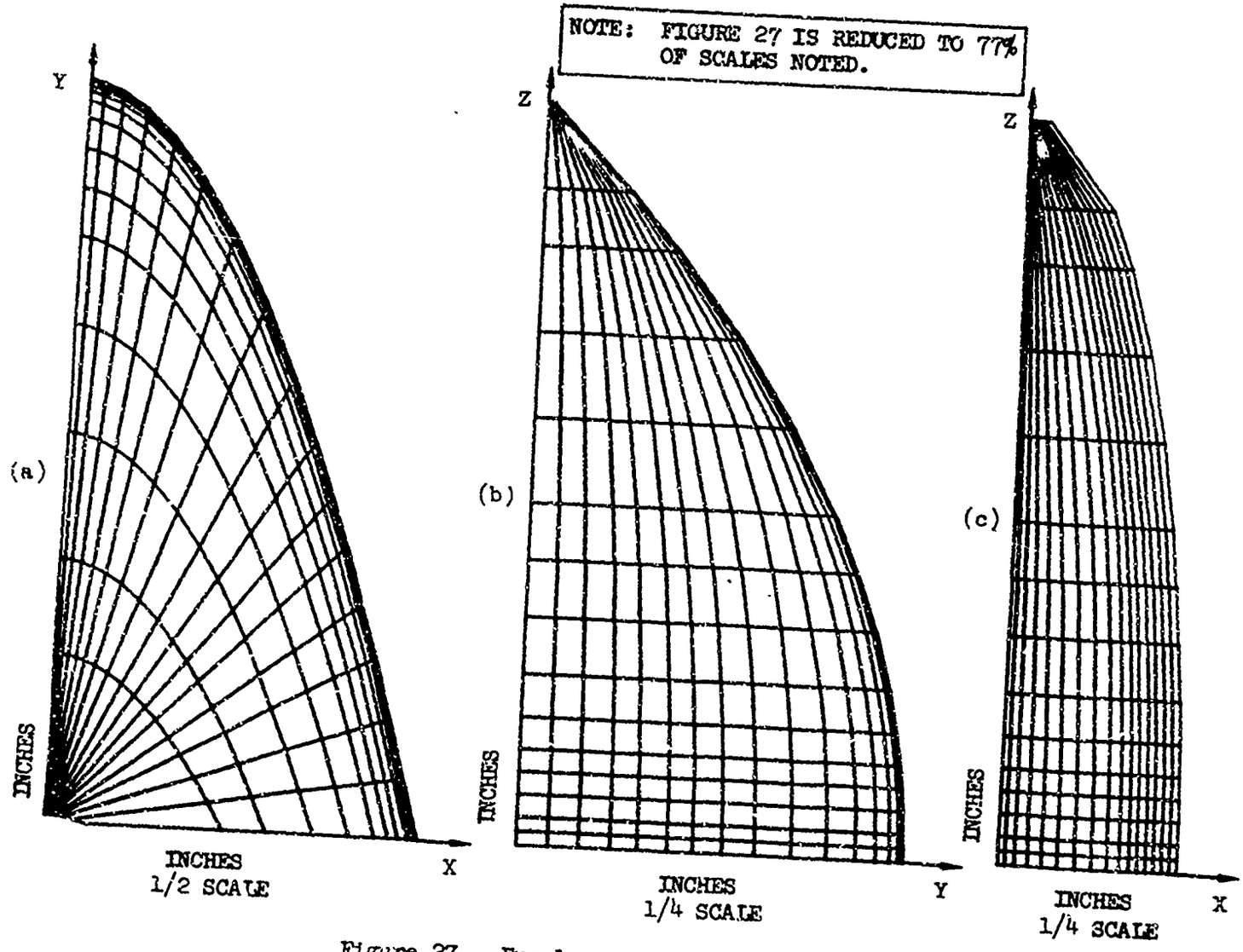

Figure 27. Fuselage Bumper Grid Line.

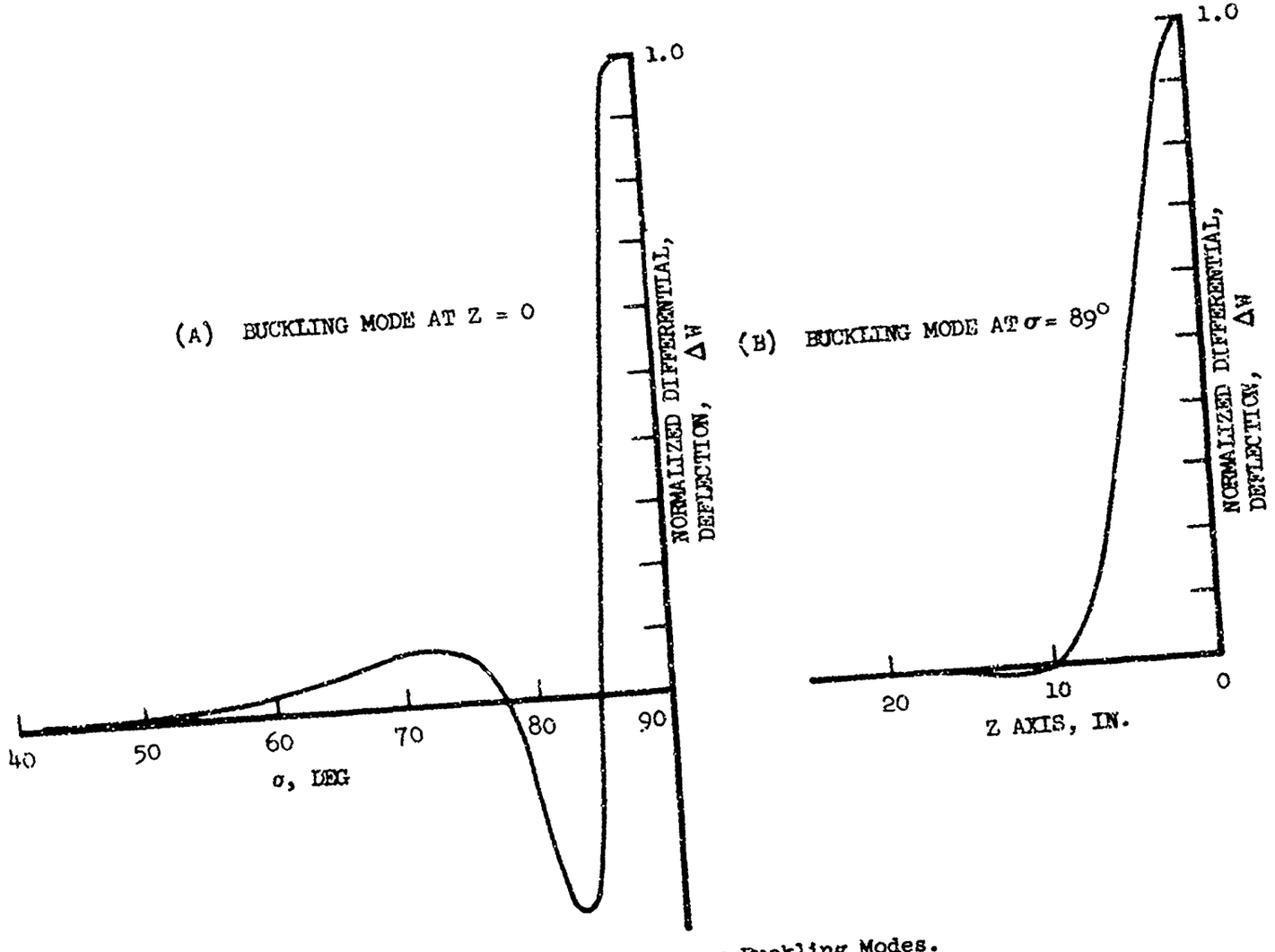

Figure 28. Fuselage Bumper Buckling Modes.

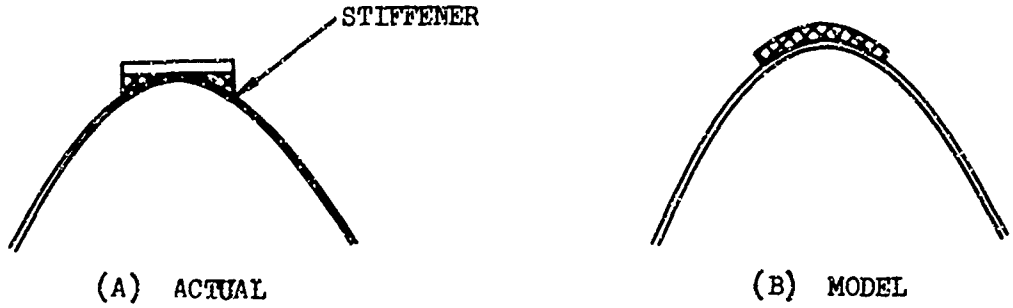

Figure 29. Stiffener, Actual and Model.

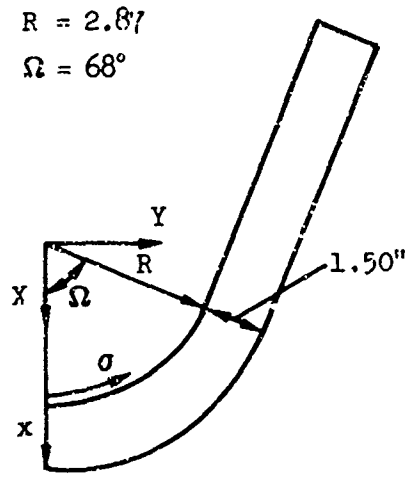

x,σ ARE SHELL COORDINATES

X,Y,Z ARE COORDINATES IN THE CARTESIAN SYSTEM

R = RADIUS TO INNER CONTOUR

S = ARC LENGTH ALONG INNER CONTOUR = Rσ

Figure 30. STAGS Analytical Model of Bulkhead.

$\sigma > R\Omega$

$$X = (R - x)\cos\Omega - (S - R\Omega)\sin\Omega$$
$$Y = (R - x)\sin\Omega + (S - R\Omega)\cos\Omega$$

The flanges were represented as eccentrically attached stiffeners. At the line of intersection with the shell (outer edge for $0 \geq \Omega$), it is assumed that displacements normal to the bulkhead are restrained but that rotations and in-plane displacements are not hindered. A point load was applied at the apex of the bulkhead with an inward direction. The biggest problems in modeling here seem to be connected with lateral restraint at the top of the bulkhead. Friction is probably sufficient to prevent the shell from sliding against the bulkhead, but the badly crumpled shell provides only partial restraint against deformation.

In the first attempt a point force was applied, and it was assumed that the bulkhead was completely free at the point of load application. It appears from the load displacement curve that the maximum definitely lies below 2000 lb (total load on two bulkheads). As efforts were made to continue the run, severe convergence difficulties were encountered. These appear to be due to the formation of a buckle just below the applied load. The case was not further pursued, as it was considered unrealistic to apply the load at a point and to assume that the contact point was free in the lateral direction. In a less conservative analysis it was was assumed that the load was distributed as shown in Figure 31 and that the bulkhead was restrained from lateral displacements but free to rotate at the mid-point.

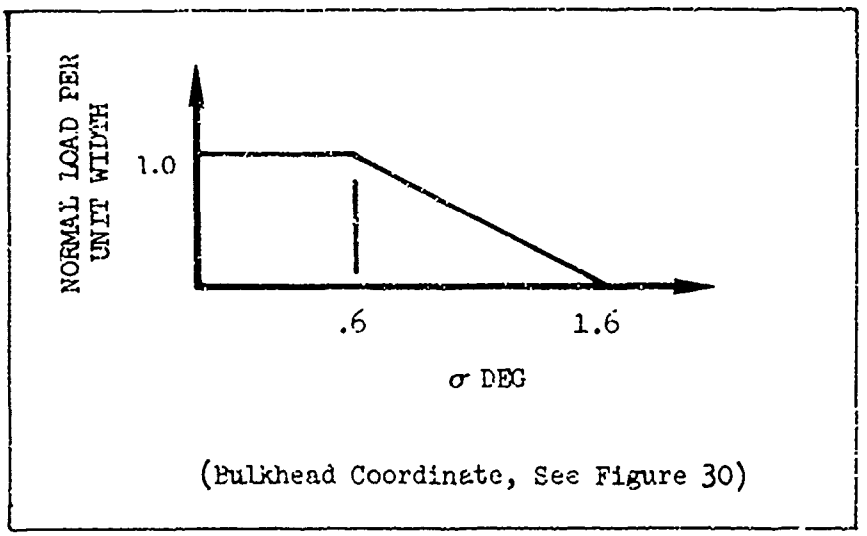

Figure 31. Load Distribution.

The elastic analysis showed no collapse of the bulkhead in a run up to about 10,000 lb load. However, this load level corresponds to very high stresses. As presently the inelastic version of STAGS does not take plastic deformations in the stiffener into account, a more accurate analysis cannot at this time be performed. To assume that a cutoff at the load level at which the proportionality limit is reached or at the yield strength of 38,000 psi would be too conservative. As a plastic hinge may form at the center plane and as the stresses are moderate elsewhere in the bulkhead, it seems possible that even a cutoff at the ultimate stress (61,000 psi) may result in a conservative analysis. However, the latter choice appears to represent the best that can be done at present. The biggest stress is a tension stress in the hoop direction at $x = \sigma = 0$. This stress reaches a level of about 60,000 psi as the applied load (total on two bulkheads) equals 3000 lb (almost linearly). It is possible that the actual buckling load is lower, but more likely it goes the other way, and an analysis including plasticity may indicate good agreement between test and theory.

RESULTS

Figure 32 shows a comparison between the theoretical and static test results. The analysis shows that approximately 60,000 in.-lb-of energy is absorbed in 10 inches of deformation as compared to appro..ately 90,000 in.-lb- of absorbed energy during the static test. A major difference between the analysis and test results exists in the determination of the load which causes initial buckling of the shell. In the analysis, this load is 3500 lb, versus 6000 lb during the test. This difference which accounts for approximately 25,000 in.-lb of energy throughout the 10 inches of deflection is the most significant discrepancy noted in the comparison. After nearly 2 inches of deflection, the bulkheads start to take the load through direct contact. The analysis shows that the bulkheads take an additional constant 3000 lb over the latter 8 inches of deformation. The analytical results for the bulkhead loading are reasonably close to the test data, which indicate an additional average of 3500 lb in the last 8 inches of deflection.

It is anticipated that the analysis can be refined to better represent the fuselage bumper, particularly the doubler cap and stiffener. Additional effort in the choice of grid representation, load distribution, and boundary conditions could also enhance the analytical results. However, improvements of this nature undoubtedly would require additional engineering time and computer expense.

The nonlinear analysis of general types of shells has only recently become feasible, and as such the prediction of energy absorbed during crushing is a formidable task. Although STAGS is considered to perform the nonlinear analysis of shells in an efficient manner, it has several limitations which prevent an accurate prediction of the manner in which a shell wrinkles as

we get into the range of very large deformations. For one, the basic equations for STAGS are valid for only moderate ($\leq 20^{\circ}$) rotations. Also, as a sharp peak is reached in the load displacement curve, it is generally impossible to find converged solutions beyond this peak. Another limitation in the present version of STAGS is that it cannot account for plastic deformation of the structure.

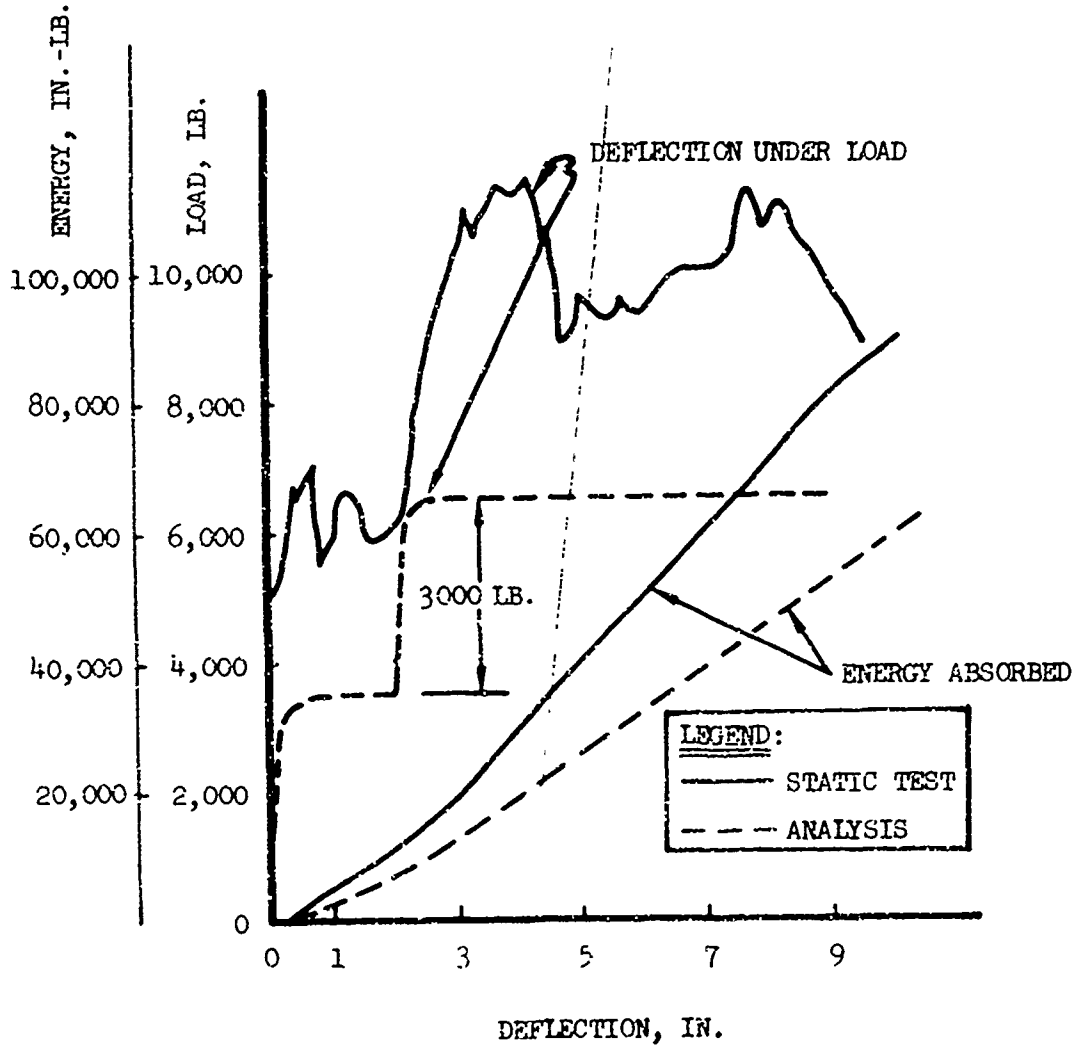

Figure 32. Comparison of Test and Analytical Load-Deflection Curves.

MATHEMATICAL MODEL DESCRIPTION

PROGRAM "KRASH" DESCRIPTION

Program "KRASH" was developed during Phase II of the study described herein. It computes the time history response of N arbitrarily interconnected lumped masses. Each mass is allowed six degrees of freedom defined by inertial coordinates x_i, y_i, z_i and Eulerian angles ϕ_i, ϑ_i, ψ_i, $i = 1,2,\ldots N$. Euler's equations of motion are written for each mass. The equations of motion are integrated numerically to obtain velocities, displacements and rotations. Angular momentum terms, due to rotor angular velocity, are included in the equations of motion.

The following loads (forces and moments) act on each lumped mass:

1. Gravity forces
2. Aerodynamic forces
3. Internal forces and moments
4. External forces and moments

The gravity forces are self-explanatory. The aerodynamic forces consist of a simple lift force on each mass held constant throughout the run. This force is computed for each mass as an input fraction of the total vehicle weight.

The internal forces and moments result from the deformation of structural members, termed "beams", which interconnect the various lumped masses. The degree of interconnectivity, i.e., which of the N masses are interconnected, is specified in the input. Each beam's properties are specified in terms of a 6 x 6 linear stiffness matrix relating the forces and moments at mass j to the relative deflections and rotations of mass j with respect to mass i.

The actual internal forces are computed on an incremental basis. Each increment is just the incremental linear force determined from the stiffness matrix, times the incremental deflection, multiplied by a stiffness reduction factor KR. For each beam element there are six different KR's, one for each relative deflection. For a given relative deflection, say axial deflection, the corresponding KR applies to all six possible loads due to this deflection. Each KR is input as a tabular function of the corresponding deflection. For small deflections, KR = 1 so that a linear analysis is obtained; for larger deflections, KR $\neq$ 1 so that general plastic deformations are allowed. Since the forces are computed incrementally, KR is simply the slope of the appropriate load-stroke curve. The structural element is assumed to behave the same under the influence of positive and negative loads.

In addition to the above, the internal load computation is written such that unloading and subsequent reloading occurs along a linear elastic line. Once any of the six deflections exceeds an input value, the member is assumed to have failed completely (fracture) and the interconnecting forces are set to zero for the remainder of the run. The program equation provides for the inclusion of viscous damping for all of the internal elements.

The external forces result from the crushing of structure which is external to the lumped masses. Each lumped mass is allowed to have as many as three mutually perpendicular "springs" which radiate outward from the mass. Obviously, only those masses on the exterior of the vehicle will use these springs. When any spring contacts the ground, an axial spring compression load is calculated from an input table of spring axial load versus axial compression.

Unloading (extending) and reloading follow an elastic line whose stiffness is input, so that energy is absorbed in permanent deformation. In addition, beyond an input maximum deflection, further loading - unloading proceeds along a steep elastic line (input constant). This is to represent the finite crushing distance available, beyond which the stiffness increases drastically. The external springs do not develop tensile loads and do not fracture as do the internal "beams".

A ground drag load is computed at the ground contact point for each spring. This load is just a constant input friction coefficient times the normal component of the axial spring loads. The direction of the drag load is opposite to the velocity vector of the contact point. The contact surface (ground) is assumed to be flat and rigid.

Program "KRASH" has a built-in routine which will determine when an identified mass penetrates a defined occupiable volume. In addition, the program will obtain the Dynamic Response Index (DRI) for desired personnel locations. Program KRASH uses a modified predictor-corrector integration routine and includes an initial condition subroutine which provides for a balanced vehicle at the start of the analysis.

The complete theory for both the initial condition subroutine and the main program, as well as a user's guide and sample problem, is presented in Volume II.

QUALITATIVE ANALYSIS

Prior to conducting the helicopter drop test, a qualitative analysis was performed using program KRASH for the purpose of showing that the program is capable of predicting structural responses to combined vertical-lateral crash impacts. The UH-1H helicopter that was modeled is sketched in Figure 33. The analytical model representing the UH-1H that was used to perform

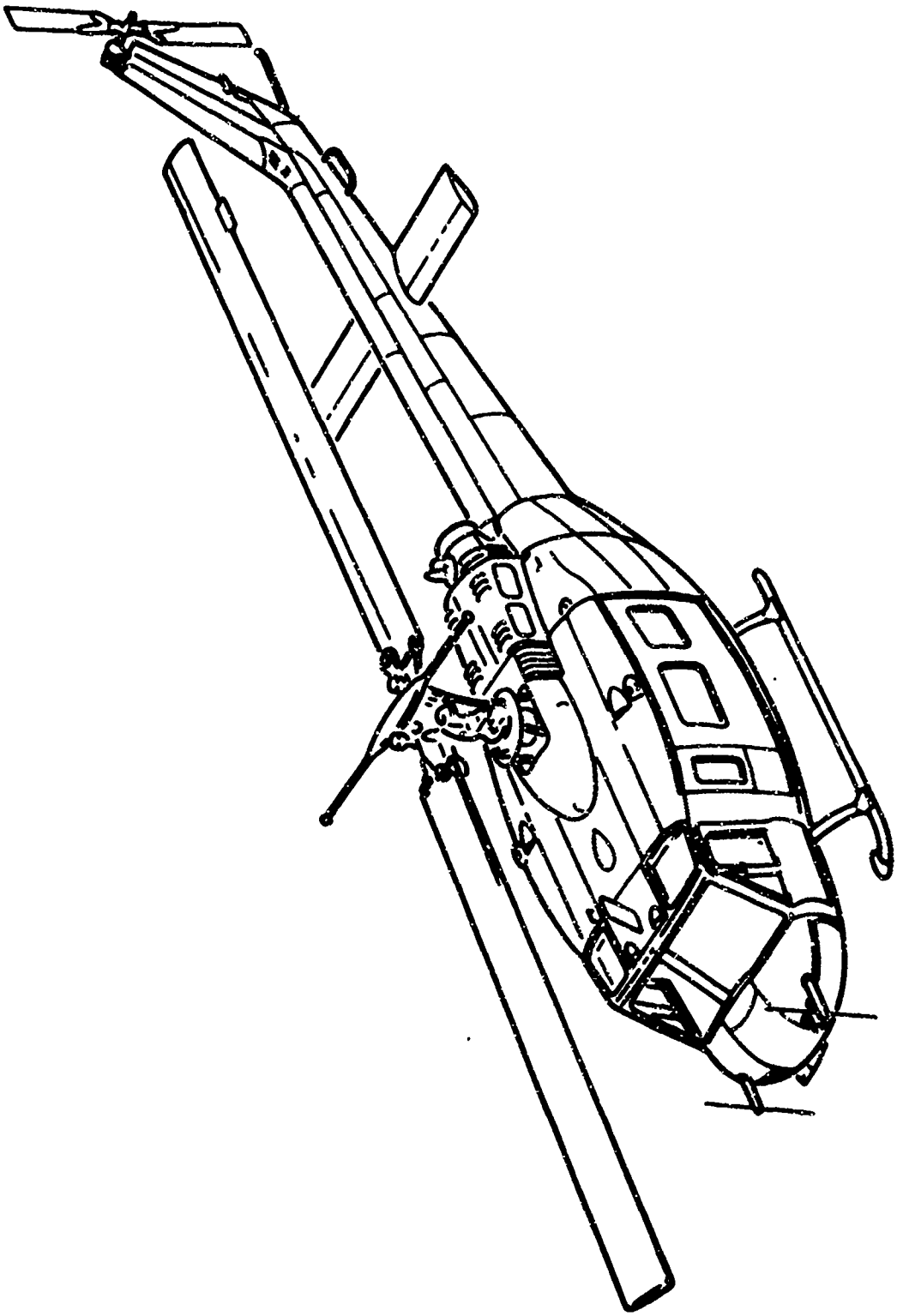

Figure 33. Helicopter Model UH-1H.

the qualitative analysis consisted of 25 masses and 32 internal beam elements and is shown in Figure 34. The description of the model masses, mass locations and weights for the qualitative analysis is shown in Table V. Crushing of the fuselage was obtained by representing the fuselage with nonlinear external springs at stations 10 through 19, 22 and 23.

The analysis was performed for the following impact conditions:

- 10 fps vertical velocity
- 30 fps vertical velocity
- 30 fps (vertical) and 20 fps (lateral) velocities and 10° roll angle

Each computer run was performed for a representative 100-millisecond crash condition. The 100-millisecond duration was chosen for the analysis for the following reasons:

- The time is consistent with previous analysis and test data.
- Significant impact responses are expected in this initial time period.
- Significant trends can be seen in this time duration.

For the landing skids and tail boom, the program option to indicate member failure was exercised. However, for the engine and transmission, it was decided to allow the loads and deflections to exceed the anticipated limiting values in order to obtain additional information. In this instance, failure of the mass item is judged qualitatively by ascertaining from the time history whether limiting deflections are exceeded.

The results of the computer analysis are shown in Table VI, which summarizes the failures, peak G loads, and structural deformations obtained for the three cases analyzed.

The results of the vertical impact cases compare favorably with the data published by Dynamic Science. In particular, the trends for low and high-energy impacts are consistent with expectations. Table VII shows a comparison between the qualitative results obtained from program KRASH and the results from Dynamic Science[3] for 10 fps and 30 fps vertical impacts. The results from KRASH generally show lower decelerations and greater fuselage deformation than the Dynamic Science results. The model used to perform the qualitative analysis with program KRASH has softer external spring characteristics than does the Dynamic Science model which results in lower deceleration and greater fuselage deformation from KRASH. It is anticipated that the use of stiffer fuselage external springs in KRASH would result in higher floor G loads and less fuselage deformation. The output data from KRASH indicates that the vehicle pitches slightly

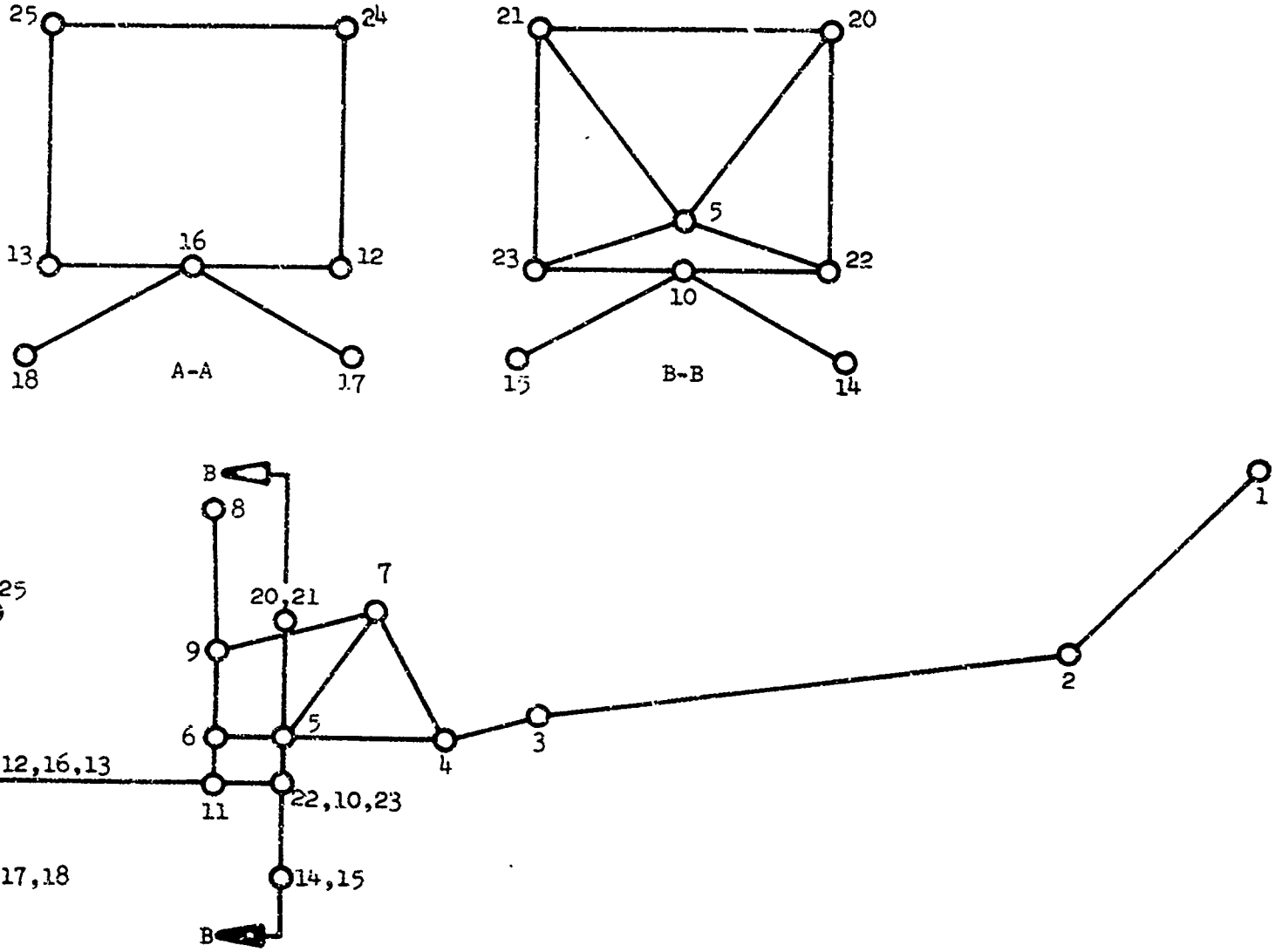

Figure 34. 25-Mass Helicopter Model Representation Used in the Qualitative Analysis.

TABLE V - QUALITATIVE ANALYSIS MODEL GRID POINT IDENTIFICATION

NUMBER	Approx. Location			Spring Length (in.)	Mass Weight (lb)	Simulated Mass Item
	FS	BL	WL			
1	460	0	132		139	Tail Rotor
2	404	0	72		85	Tail Boom
3	241	0	47.5		62	Aft Fuselage and Tail Boom
4	211	0	38.5		172	Aft Fuselage Section, Aft Base for Engine Struts
5	163	0	38.5		278	Aft Fuselage Section, Fwd Base for Engine Struts, PAX
6	141	0	38.5		932	Pylon Support Structure, PAX
7	187	0	79		731	Engine
8	136	0	90		1412	Main Rotor, Blade, Hub and Transmission
9	141	0	67		90	Pylon Support Structure
10	163	0	22	22.5	257	Lwr Fuselage, Center, PAX
11	141	0	22	22.5	2120	Lwr Fuselage, Fuel Tank Location; Passengers
12	71.6	-45	22	22.5	175	Lwr Fuselage, Right Side
13	71.6	45	22	22.5	175	Lwr Fuselage, Left Side
14	163	-50.8	-8	2.25	24	Aft Landing Gear, Right Side
15	163	+50.8	-8	2.25	24	Aft Landing Gear, Left Side
16	71.6	0	22	22.5	1140	Lwr Fuselage Structure, Center, Pilot, Copilot, PAX
17	71.6	-50.8	-8	2.25	24	Fwd. Landing Gear, Right Side
18	71.6	50.8	-8	2.25	24	Fwd. Landing Gear, Left Side
19	23	0	22		307	Nose Structure
20	163	-45	76		31	Aft Top Cabin Structure, Right Side
21	163	+45	76		31	Aft Top Cabin Structure, Left Side
22	163	-45	22	17	166	Lwr Fuselage Structure, Right Side
23	163	+45	22	17	166	Lwr Fuselage Structure, Left Side
24	71.6	-45	76		28.5	Fwd. Top Cabin Structure, Right Side
25	71.6	+45	76		28.5	Fwd. Top Cabin Structure, Left Side
26	163	0	22		55	Troop Seat, Aft
27	71.6	0	22		70	Pilot/Copilot Seat Forward
28	163	0	42		120	10 Hz Man - Weight of Upper Torso - Aft
29	73	0	42		120	10 Hz Man - Weight of Upper Torso - Fwd.
30	163	0	42		120	8 Hz Man - Weight of Upper Torso (DRI) - Aft
31	73	0	42		120	8 Hz Man - Weight of Upper Torso (DRI) - Fwd.

TABLE VI. SUMMARY OF QUALITATIVE ANALYSIS RESULTS

RESULT	Impact Velocity		
	Vertical 10 fps	Vertical 30 fps	Combined Vertical (30) Lateral (20) fps *
Did landing skid fail	yes	yes	yes
Did boom contact ground	no	no	no
Did boom fail	no	yes	no **
Did fuselage contact ground	yes	yes	yes
Did transmission fail	no ***	yes ***	yes ***
Did engine fail	no	yes ***	yes ***
Max. deformation of fuselage (in)	2	11.7	11
Max. vertical accel. of engine ****	5.5	44	34
Max. vertical accel. of transmission	6.8	36	34
Max. vertical accel. of fuselage	22	42	42
Max. lateral accel. of engine	0	0	13
Max. lateral accel. of transmission	0	0	12
Max. lateral accel. of fuselage	0	0	10
Occupant deceleration/crushing injury	no	yes	yes

* 10° roll angle

** Boom rotations were less than established limiting values; however, at the end of the computer run (100 ms), the rotation was approaching the estimated failure point.

*** No failure of the engine was programmed; however, the deflections noted in the time history exceed the anticipated limiting values. Results from previous trial runs showed that the transmission mount would bottom at a vertical impact of 30 fps in approximately .050 seconds. Softer springs representing the transmission mounts do not bottom during the low-level impact (10 fps).

****Maximum accelerations are in "G" units.

TABLE VII. COMPARISON OF QUALITATIVE RESULTS WITH REFERENCE 3 DATA

DESCRIPTION	10 fps Vertical Impact		30 fps Vertical Impact	
	Ref. 3	KRASH	Ref. 3	KRASH
Maximum Acceleration of Engine*	4.2	5.5	65	44
Maximum Acceleration of Transmission*	2.9	6.8	42.5	36
Maximum Relative Deformation of** Fuselage	.1	2	2.4	11.7
Maximum Relative Deformation of** Landing Gear	7.4	9.	9.0	9.0
Did Landing Gear Break	no	yes	yes	yes
Did Boom Break	no	no	yes	yes
Did Fuselage Contact Ground	yes	yes	yes	yes
Did Boom Contact Ground	no	no	no	no
Did Transmission Fail (Mounts Bottom)	no	no	yes	yes

*Units of acceleration are G's

**Units of deformation are inches

(2-1/2 degrees) during the vertical impact. However, yaw and roll angles remain insignificantly small, which for a symmetrical vertical impact condition is to be expected.

During the combined vertical-lateral impact, the lateral G loads reach peak values of 13, 12 and 10 for the engine, transmission and fuselage, respectively. The associated deflections for the engine and transmission are considered to be sufficiently large to cause failure of these items in either the vertical or the lateral direction.

The combined vertical-lateral impact velocity crash analysis was compared to several accident cases described earlier, in which estimates were made of the initial impact conditions. In particular, cases 4, 6 and 7 (Table I) were reviewed. In general, the results of the analysis show qualitatively that, as in the cases of the accidents, severe damage to the landing skids and transmission can be expected. The acceleration levels sustained at the floor are sufficiently large to cause injuries due to decelerative forces or collapse of structure. The analysis indicates that failure of the engine mounts by both lateral and vertical forces is to be expected. The accident pictures, Figures 4 through 8, do not show apparent engine damage. However, it is difficult to assess engine-mount damage due to the lack of a clear view of the detail structure. The analysis does not show the degree of forward fuselage or cabin collapse indicated in the accident photographs. One reason for this discrepancy is that the initial conditions of 10^{0} roll and $\mu = .1$ are perhaps too mild to cause a rollover. The actual accident initial impact rotational displacements and velocities are undoubtedly different from the analytical case. The commentary on the accident cases indicates that, to some degree, damage to the rotor blades and/or tail boom can occur prior to the ground impact. Additionally, one must recognize that the impact surfaces have substantially different coefficients of friction which influence postimpact behavior of the vehicle. The number of people (crew and troops) involved in the three accident cases varied from 4 to 10, which represents a potential weight variation of up to 1300 lb and, consequently, changes the amount of energy that is to be absorbed by the structure during the crash impact.

CORRELATION MODEL

The mesh model used in the qualitative analyses was refined during the correlation studies to incorporate the following changes:

- The model was expanded to 31 masses and 38 internal beam elements so as to include the Dynamic Response Index (DRI) model. The DRI model used during the correlation study is described in detail in the next section.
- The representative collapsible length of the skids prior to contact with the fuselage underscale, was increased from 9.5 inches to 14 inches to be more consistent with the correct vehicle geometry.

- The external springs were revised to more correctly represent their energy absorption capability as indicated by the test results.
- Nonlinear load deflection characteristics of the engine and transmission mounts were modified to more accurately depict their failure modes.

The math model that was used to correlate with test data is shown in Figure 35. The description of the model masses, mass locations and weights is shown in Table VIII. Crushing of the fuselage was obtained by representing the fuselage with nonlinear external springs at several fuselage stations. The free lengths of these springs are shown in Table VIII. The characteristics of the external springs are shown in Figure 36. The springs were chosen so as to simulate fuselage deformation and floor deformation and floor accelerations, as determined from the test data, while reproducing measured engine and transmission responses. The engine and transmission support structure was determined from available U. S. Army, Bell Helicopter and Dynamic Science data and modified as required. The following publications provided information which was used to model the UH-1H:

- Bell Helicopter Reports

  205-099-991, "Basic Structural Design Criteria"(Reference 45)

  205-099-003, "Structural Description Report" (Reference 46)

  205-099-004, "Unit Inertia Loads - Weight and Inertia Distribution Data" (Reference 40)

  205-099-007, "Stress and Loads Analysis" (Reference 47)

  205-099-401, "Skid Gear Drop Tests" (Reference 48)

  205-099-403, "Static Tests of the UHY-1D" (Reference 44)

- USAAVLABS Technical Report 70-71, January 1971 (Reference 3)

The external springs are represented as having the following load deflection regimes; elastic, plastic and a second elastic stiffness. The plastic regime represents crushing at constant load. The final elastic regime represents the end of the finite crushing distance available, beyond which point the structure becomes stiff. Fuselage centerline masses 10 and 16 are considered stiffer than the sides. The landing skid deflections of 1.2 inches represent crushing of the lower tubular cross-section, not overall skid deflections. The dashed lines in Figure 36 indicate the unloading path used after the second elastic region is reached. A ground coefficient of friction of .3 was used for all external springs.

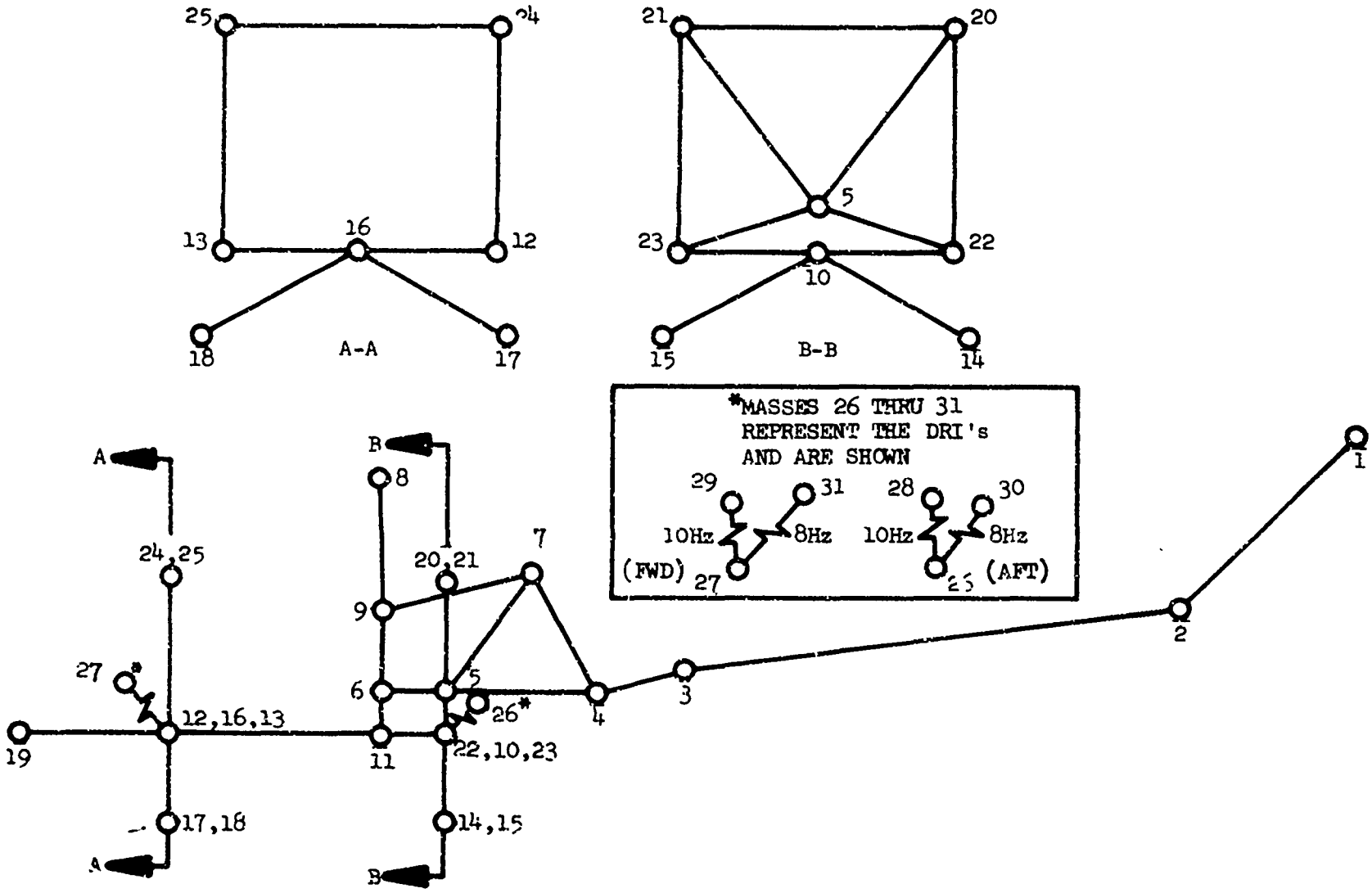

Figure 35. 31-Mass Helicopter Model Representation Used in the Correlation Study.

TABLE VIII. CORRELATION STUDY ANALYTICAL MODEL GRID POINT IDENTIFICATION

NUMBER	Approx. Location			Spring Length (in.)	Mass Weight (lb)	Simulated Mass Item
	FS	BL	WL			
1	460	0	132		139	Tail Rotor
2	404	0	72		85	Tail Boom
3	241	0	47.5		62	Aft Fuselage and Tail Boom
4	211	0	38.5		172	Aft Fuselage Section, Aft Base for Engine Struts
5	163	0	38.5		278	Aft Fuselage Section, Fwd Base for Engine Struts, PAX
6	141	0	38.5		932	Pylon Support Structure, PAX
7	187	0	79		731	Engine
8	136	0	90		1412	Main Rotor, Blade, Hub and Transmission
9	141	0	67		90	Pylon Support Structure
10	163	0	22	17	257	Lwr Fuselage, Center, PAX
11	141	0	22	17	1823	Lwr Fuselage, Fuel Tank Location; Passengers
12	71.6	-45	22	17	175	Lwr Fuselage, Right Side
13	71.6	45	22	17	175	Lwr Fuselage, Left Side
14	163	-50.8	-14	2.25	23	Aft Landing Gear, Right Side
15	163	+50.8	-14	2.25	24	Aft Landing Gear, Left Side
16	71.6	0	22	.17	950	Lwr Fuselage Structure, Center, Pilot, Copilot, PAX
17	71.6	-50.8	-14	2.25	24	Fwd. Landing Gear, Right Side
18	71.6	50.8	-14	2.25	34	Fwd. Landing Gear, Left Side
19	23	0	22		307	Nose Structure
20	163	-45	76		31	Aft Top Cabin Structure, Right Side
21	163	+45	22		31	Aft Top Cabin Structure, Left Side
22	163	-45	22	17	166	Lwr Fuselage Structure, Right Side
23	163	+45	76	17	166	Lwr Fuselage Structure, Left Side
24	71.6	-45	76		28.5	Fwd. Top Cabin Structure, Right Side
25	71.6	+45	76		28.5	Fwd. Top Cabin Structure, Left Side
26	163	0	22		55	Troop Seat, Aft
27	71.6	0	22		70	Pilot/Copilot Seat Forward
28	163	0	42		120	10 Hz Man - Weight of Upper Torso - Aft
29	73	0	42		120	10 Hz Man - Weight of Upper Torso - Fwd.
30	163	0	42		120	8 Hz Man - Weight of Upper Torso (DRI) - Aft
31	73	0	42		120	8 Hz Man - Weight of Upper Torso (DRI) - Fwd.

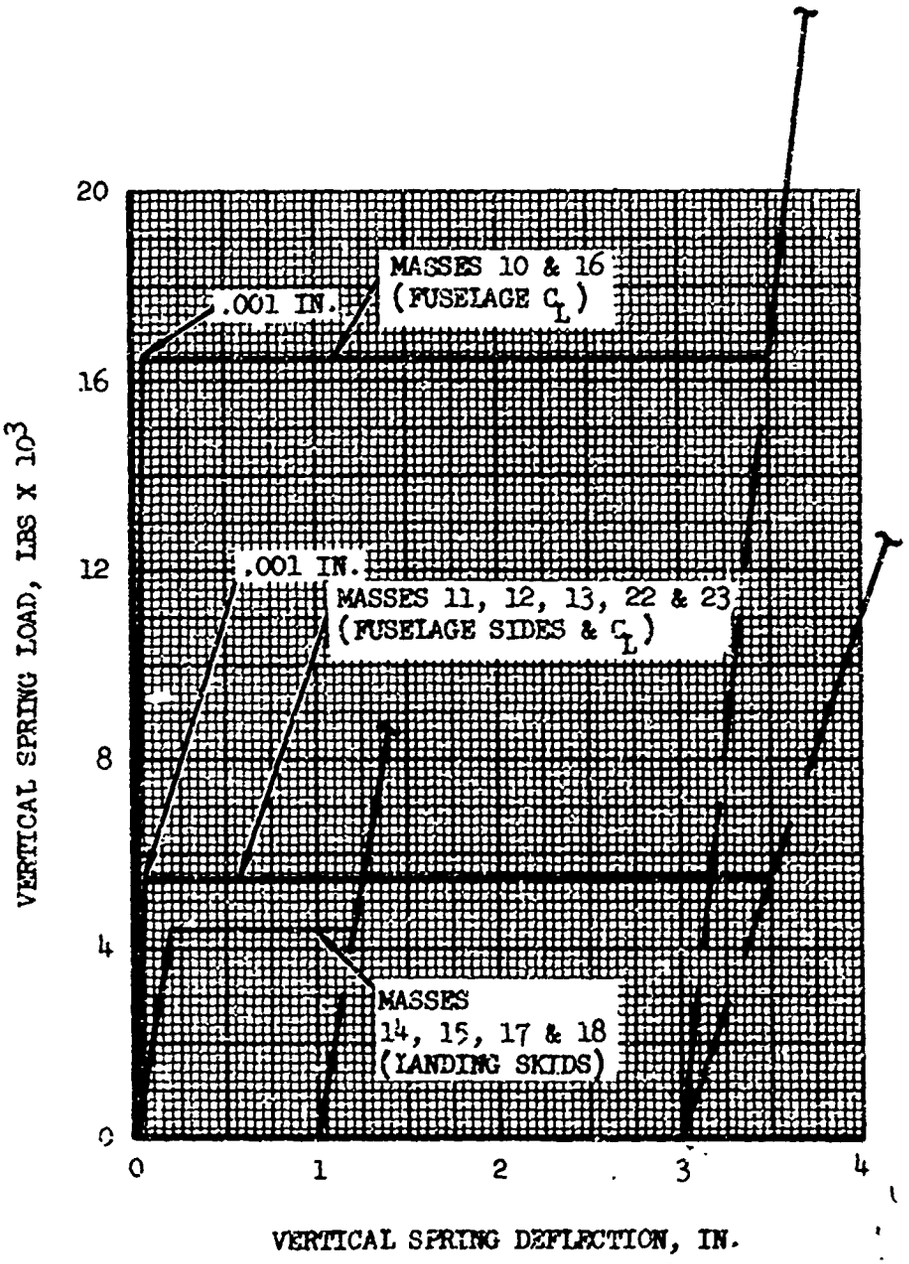

Figure 36. External Springs.

Figures 37 through 42 show the load deflection curve and stiffness reduction factors (KR) applied to the internal beams supporting the engine and transmission, landing skids and tail boom. The actual instantaneous beam stiffness is the product of the linear input stiffness and the KR factors in the figures. Normally, KR is initially equal to 1, representing linear behavior, and then decreases to zero or even negative values. Zero KR corresponds to a flat load-stroke curve, negative KR corresponds to decreasing load with increasing deflection. The units of DX's shown in the figures are inches for deflections (x, y, z) and radians for rotations (ϕ, θ, ψ).

Some of the engine and transmission support beam KR's drop to zero and then increase to .2. This represents a stiffness change resulting from interference with adjacent structure, such as the engine compartment floor. The landing skid KR's in Figure 41 drop from 1 to -3.33. This is done so that when the skids rupture in the analysis, the load in the skid is near zero (the area under the KR curve is zero). If this is not done, a large transient response occurs when the skids rupture, due to the sudden imbalance in the system. While this transient response would be representative of a brittle fracture, it is felt that the failure of the skids is more gradual. The same reasoning applies to the tail boom, Figure 42, in the non-axial directions.

The transmission axial (vertical) KR, shown in Figure 39, is the only one that doesn't start at 1. This starts at a very low value corresponding to the soft transmission mounts, then increases to 1 representing the much stiffer basic structure beneath the transmission. Note that the axial direction for element 8-9 is essentially vertical.

DYNAMIC RESPONSE INDEX (DRI)

Six masses (26 through 31) were added to the qualitative analysis model (Figure 33) to represent the DRI's at the vehicle aft and forward sections. The Dynamic Response Index (DRI) measurement is described in detail in References 35 and 36. The occupant seat and main response is modeled in program KRASH as shown in Figure 43.

The 10 Hz man is modeled to obtain the seat response, and then independently the seat response is used to find the response of an 8 Hz man. In program KRASH the response of masses 26, 28 and 30 are found simultaneously; however, mass 30 is not permitted to feed back responses to mass 26.

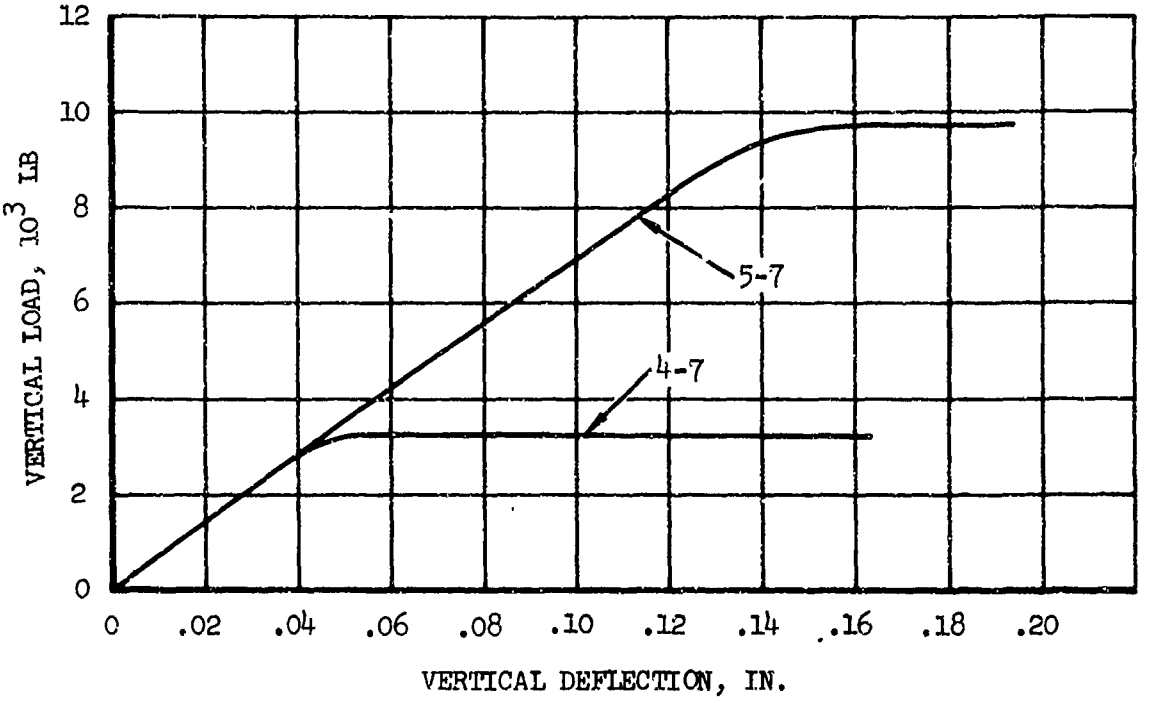

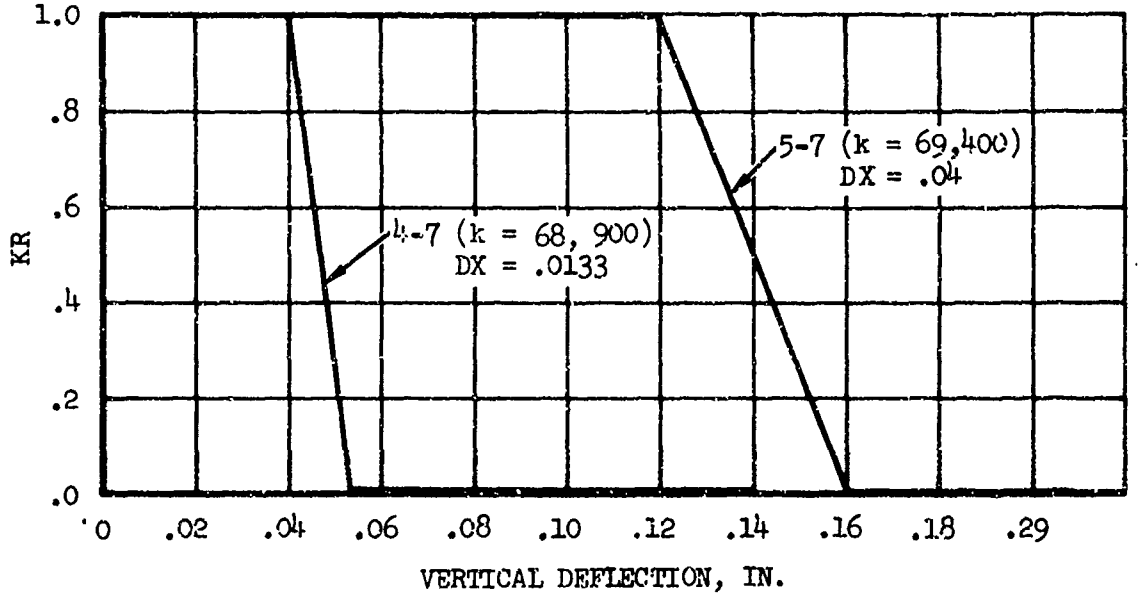

Figure 37. Engine Vertical Stiffness and Stiffness Reduction Factor.

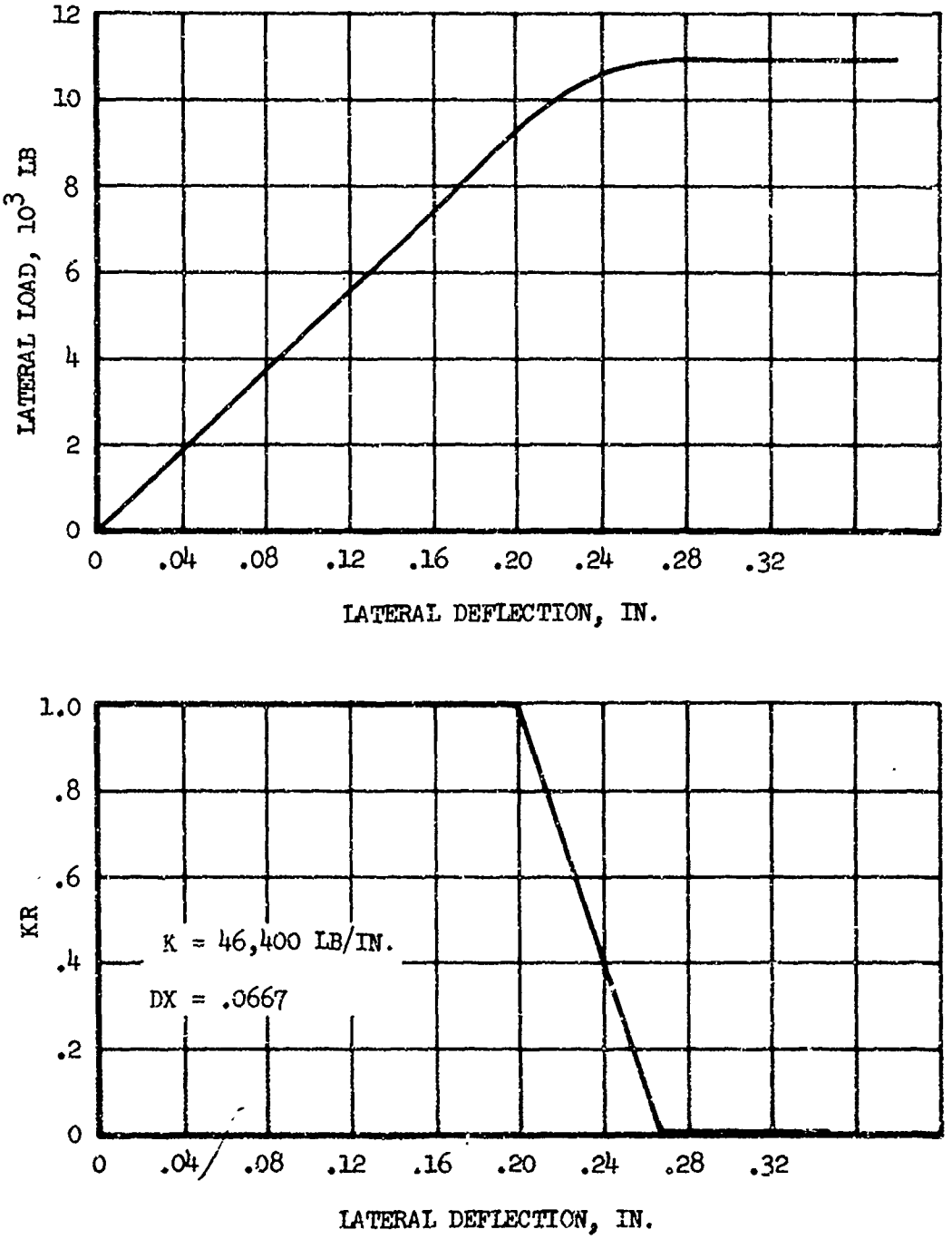

Figure 38. Engine Lateral Stiffness and Stiffness Reduction Factor.

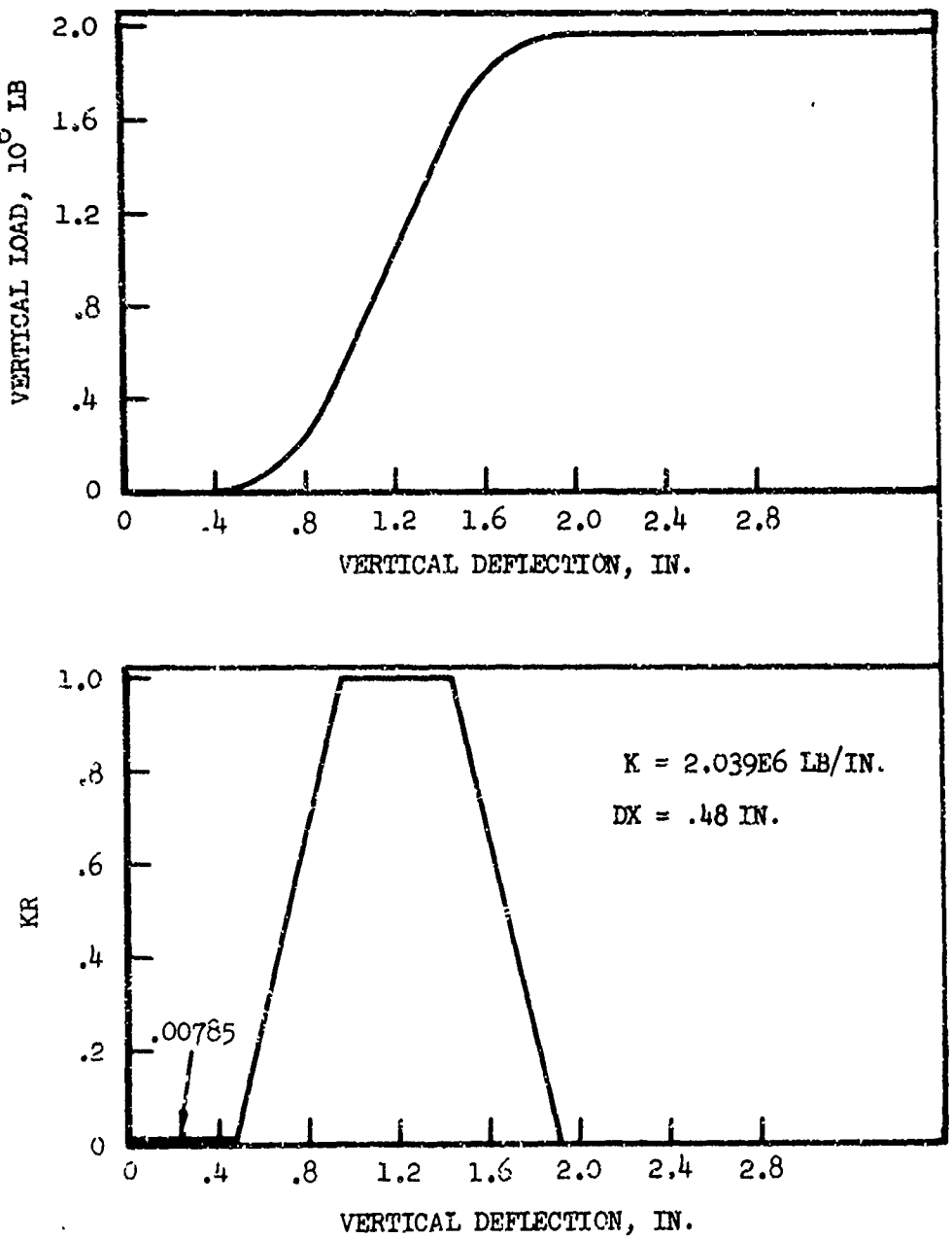

Figure 39. Transmission Vertical Stiffness and Stiffness Reduction Factor.

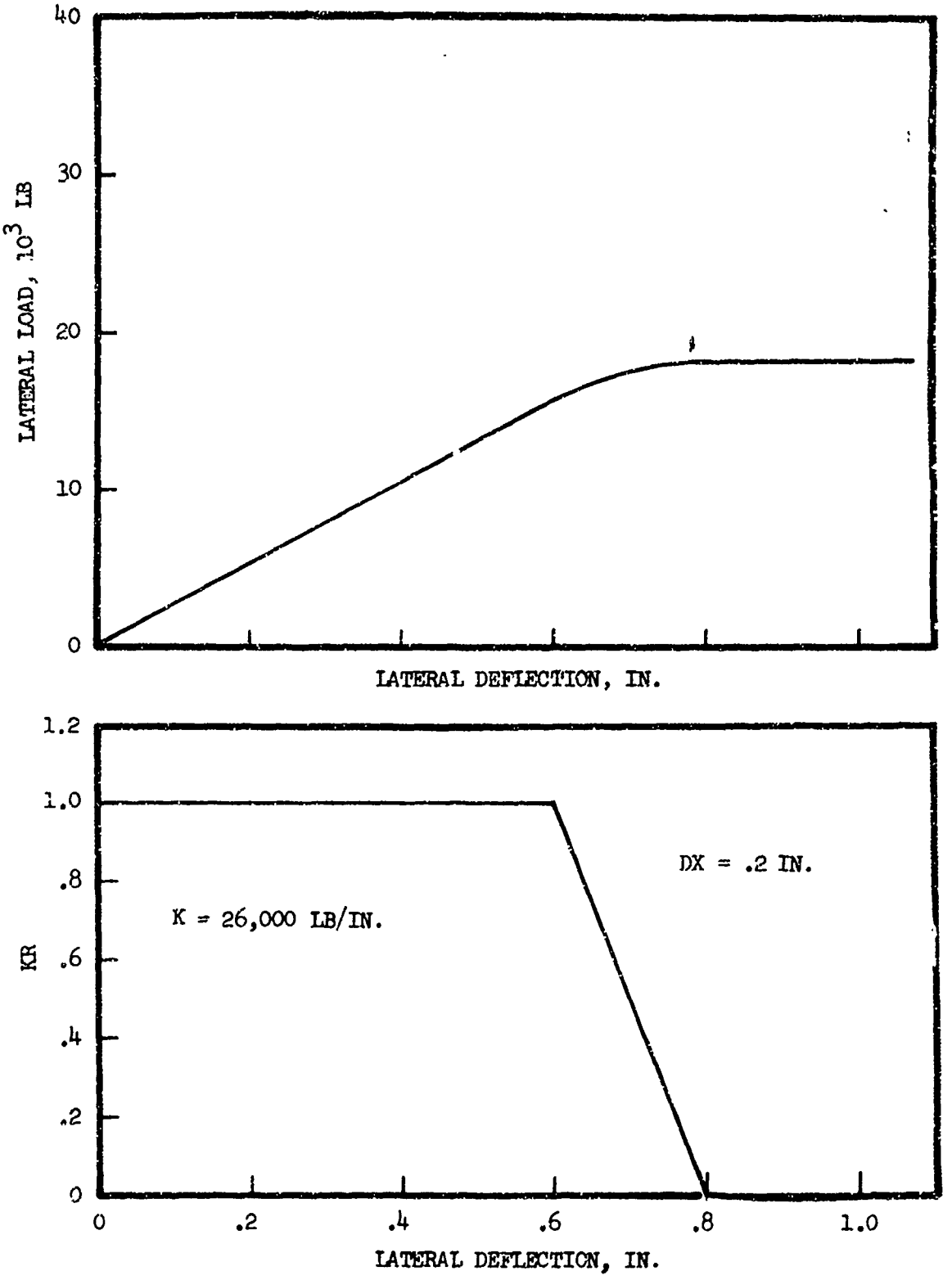

Figure 40. Transmission Lateral Stiffness and Stiffness Reduction Factor.

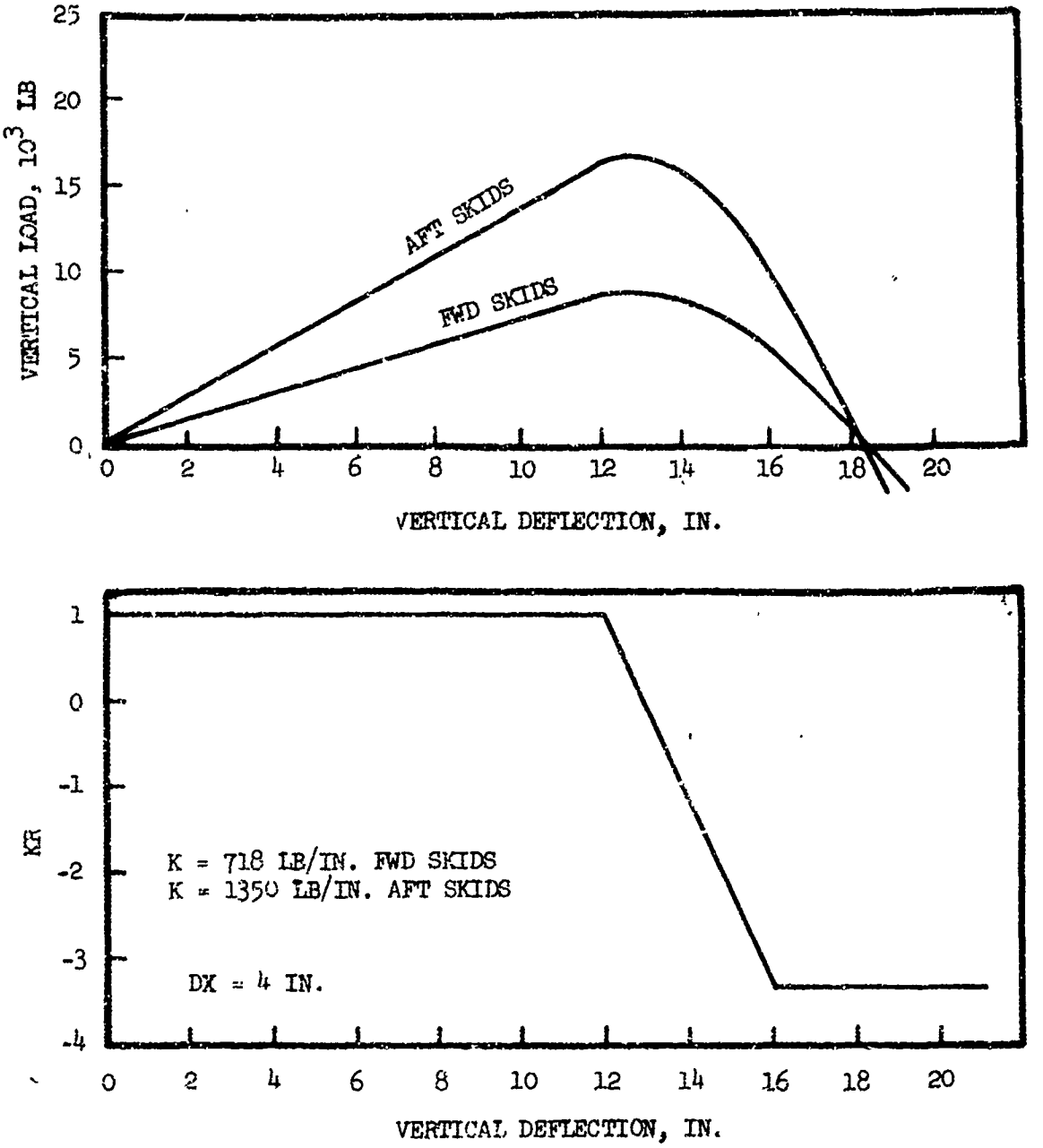

Figure 41. Landing Gear Skids Vertical Stiffness and Stiffness Reduction Factor.

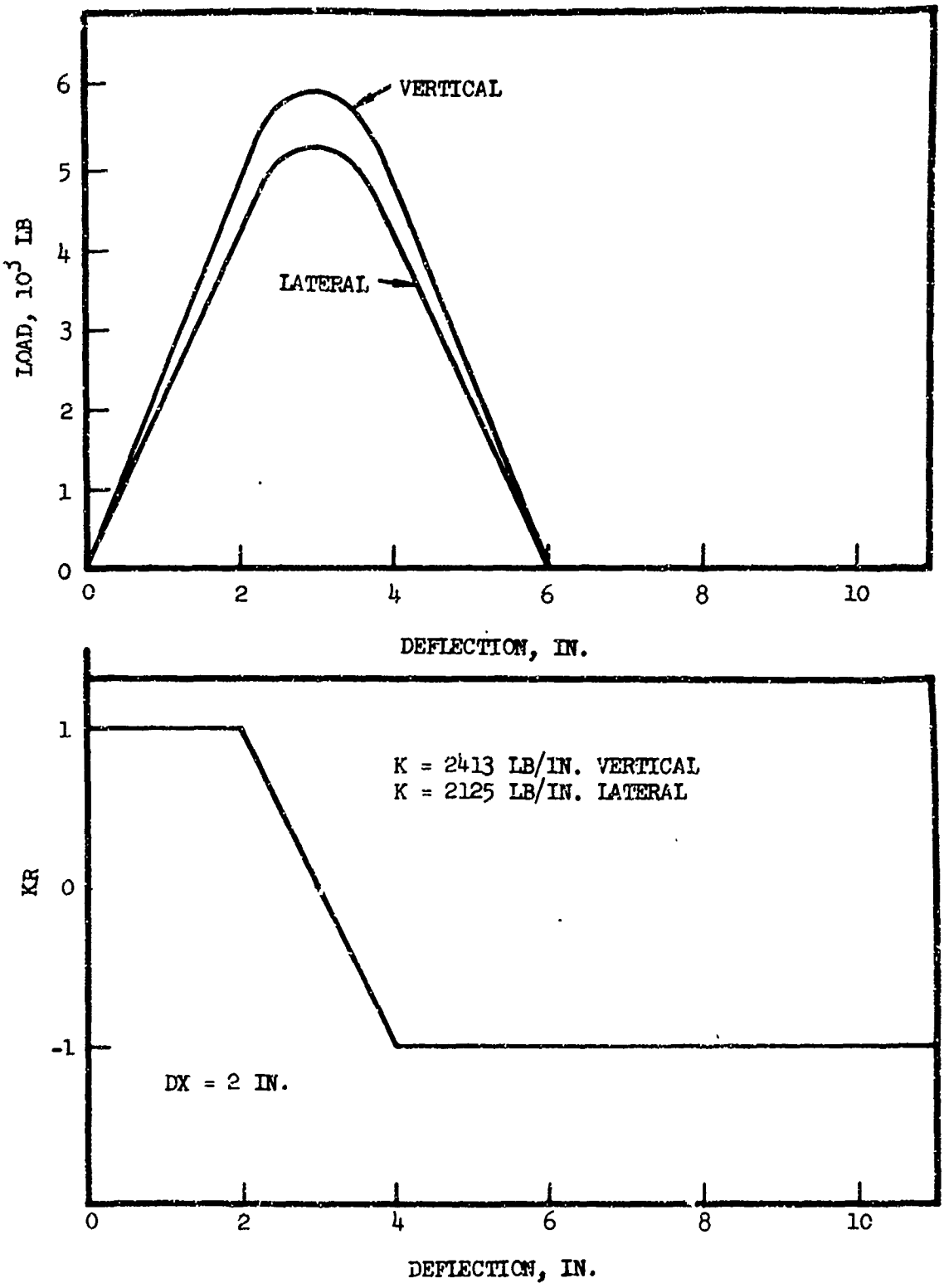

Figure 42. Tail Boom Stiffness and Stiffness Reduction Factor.

The model coefficients obtained from cadaver tests for spinal injury and presented in reference 35 are:

ω_n = 52.9 rad/sec (natural frequency)

ζ = .224 (damping)

The model coefficients for the 10 Hz man needed to obtain the seat response presented in reference 36 are:

ω_n = 62.8 rad/sec (natural frequency)

ζ = .3 (damping)

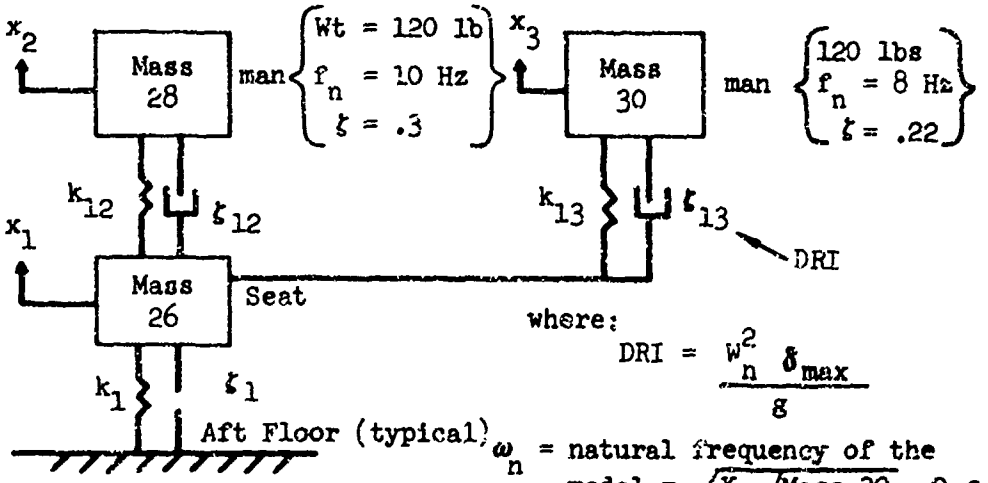

where:

$$DRI = \frac{W_n^2 \, \delta_{max}}{g}$$

ω_n = natural frequency of the model = $\sqrt{K_{13}/\text{Mass } 30} = 2\pi f_n$

δ_{max} = maximum deflection

g = 386 in/sec^2

ζ = % critical damping

Figure 43. Dynamic Response Index (DRI) Model.

EXPERIMENTAL PROGRAM

TEST OBJECTIVE

A drop test was performed with a Government-furnished UH-1H for the purpose of:

1. Ascertaining the accuracy of the mathematical simulation developed during Phase II.
2. Providing a basis for improvement of the computer program.
3. Providing data which will enhance the development of improved design criteria and concepts.

SITE PREPARATION

The test site was the Lockheed Rye Canyon Laboratory Facility. Preparation for the test site included the use of some existing structure as well as the fabrication of new major test support items. The layout of the test setup, shown in Figure 44, notes the various significant items. A brief description of those items which were fabricated specifically for this program follows.

Concrete Pad

A 24 - ft - x - 36 - ft x 6 - in.- thick concrete pad reinforced with a steel rod was installed for the drop test as the impact surface for the test vehicle. The surface was chosen to more closely represent the infinitely rigid surface used in the computer simulation.

Swing Support Boom

The boom is an "A" frame structure 39 ft long and 10 ft across the base. The boom consists of a welded assembly of 10-inch-square steel tubing with a hinge at the base, where it attaches to an existing drop tower, and a clevis device at the apex end, where the boom, a crane pickup, and the constraint loads connect through a single pin. The boom was used to stabilize the upper pivot of the swing 54 ft above the ground when supported by a derrick crane.

Swing Hanger-Release Mechanism

This assembly, shown in Figure 45, consists of two 10-in. box beams, each 5 ft long, and a solenoid release hook device. The swing hanger beam (upper beam), attached to the swing straps, and the mast hanger beam (lower beam), attached to the helicopter mass, are nested together under a preload acting through a release mechanism.

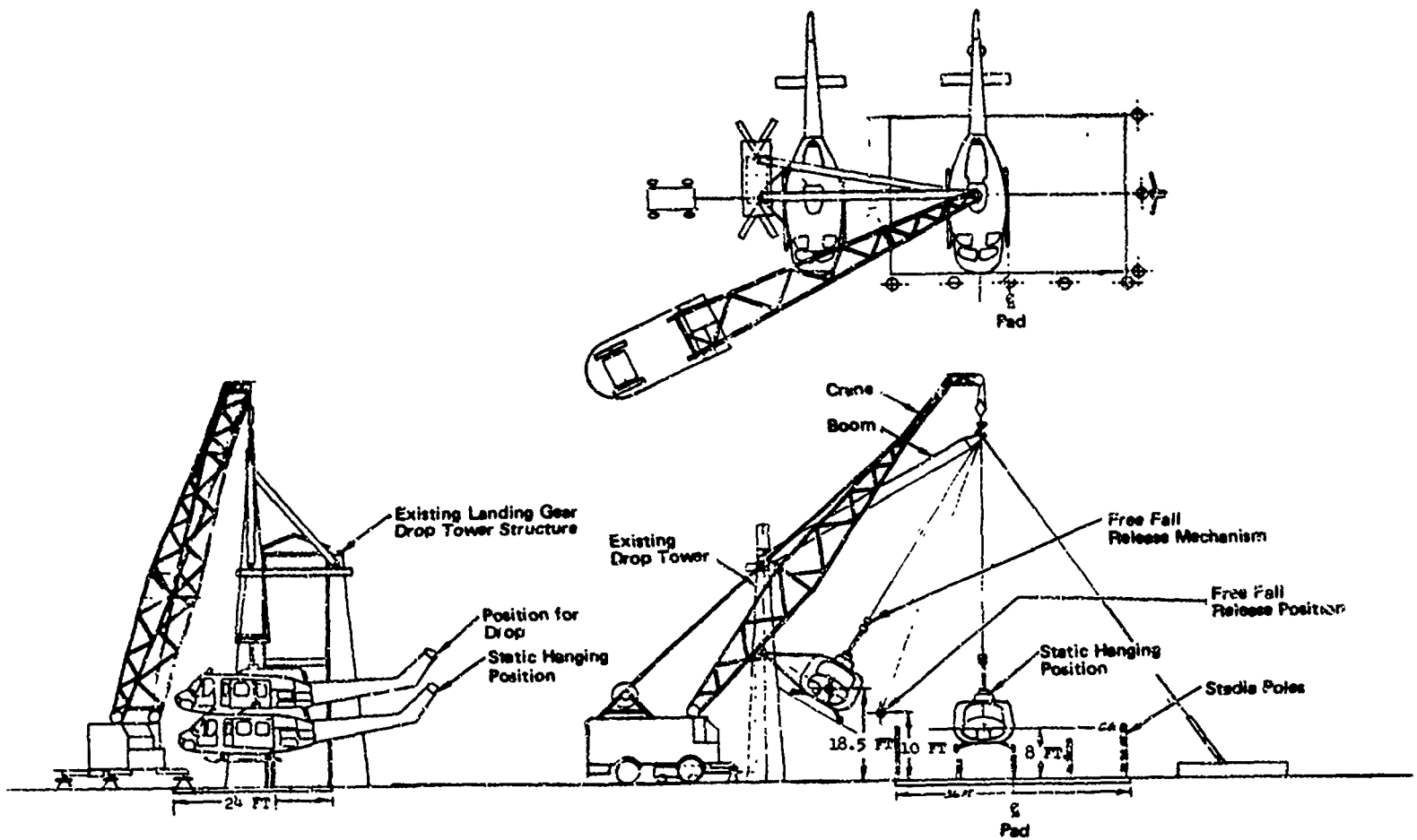

Figure 44. Site Preparation.

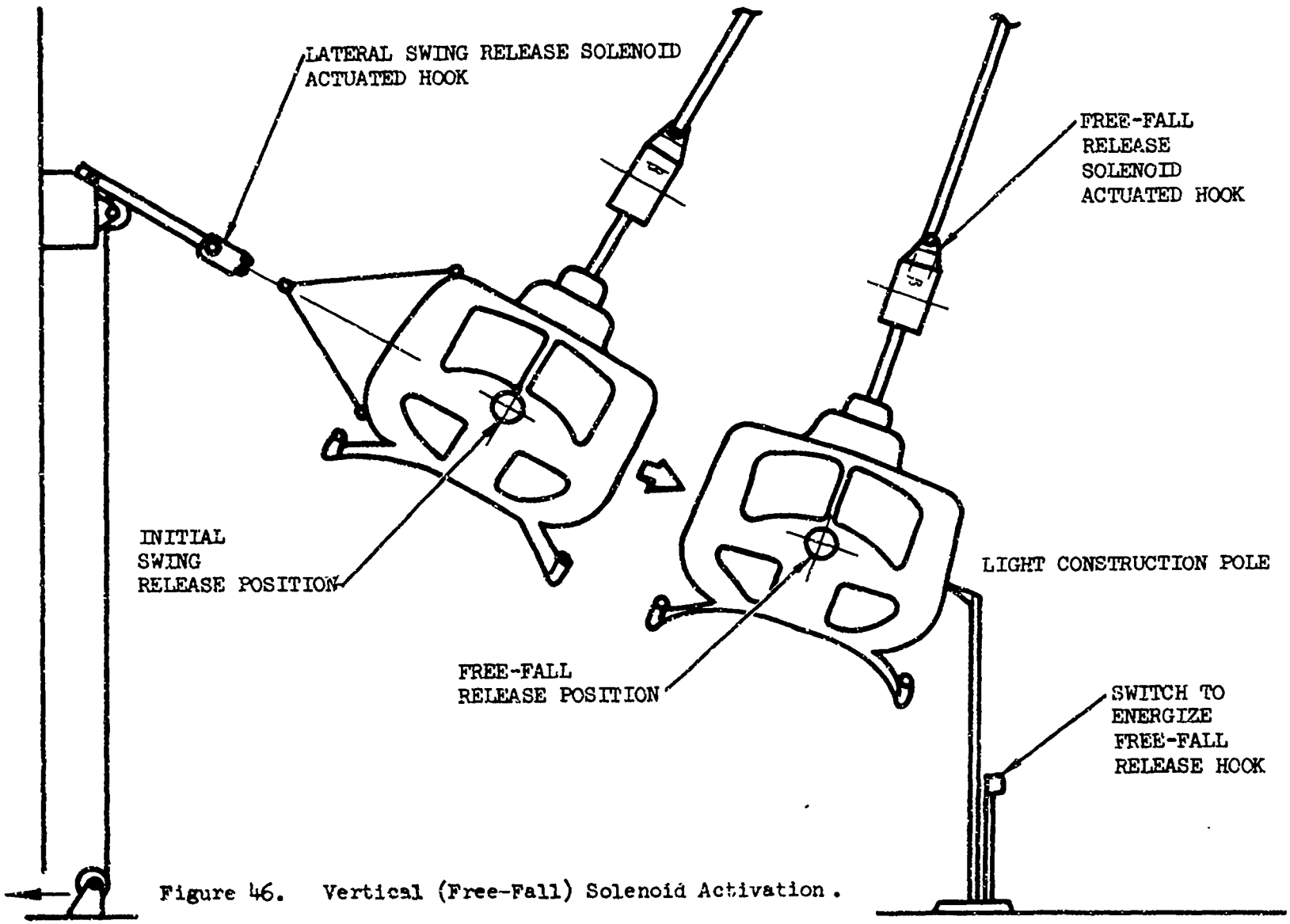

Figure 46. Vertical (Free-Fall) Solenoid Activation.

These last two items are not significant for structural strength considerations. The mast hanger beam represents the weight of the main rotor hub arm assembly within ± 10%. The helicopter weight and c.g. were measured to be 8500 lb and F.S. 135, respectively.

Fuel

The helicopter was loaded for testing by filling the fuel cells two-thirds full (150 U. S. gallons) of dyed water to simulate on-board loading of the aircraft's full fuel load capability of 224 U. S. gallons.

On-Board Loading

Thirteen anthropomorphic dummies, weighing up to 200 lb each, were properly placed in the seats. Two Government-furnished cameras were installed on board to take motion pictures of the cabin interior. Figures 47 and 48 are photographs showing the dummies installed in the vehicle. The rear-mounted cameras can be seen in the latter photograph. The locations of the various anthropomorphic dummies are shown in Figure 49.

INSTRUMENTATION

The Lockheed Rye Canyon Central Data System (CDS) is the primary facility for data recording and processing.

Instrumentation consisted of the following:

- 24 accelerometers
- 2 strain gage bridges
- 1 fuselage deflection indicator

Accelerometers

Twenty-four accelerometer channels with signal conditioning amplifiers were used to record dynamic response of the structure and pilot during the test. The signals were fed directly into the CDS computer storage (memory disc). The accelerometers are of piezo resistive type (Endevco, CEC and Statham), with an assortment (depending on location of the test vehicle) of dynamic ranges up to 250 g's. The frequency responses of the accelerometers range from 300 Hz to 2000 Hz. Figure 49 shows the various locations of the accelerometers throughout the vehicle. Table IX describes the accelerometer locations, sensing directions and recording data. Figures 50 through 58 show typical accelerometer mountings. All the data were recorded directly into the CDS system (24 channels); 13 of these channels were simultaneously recorded on tape, to provide a degree of redundancy.

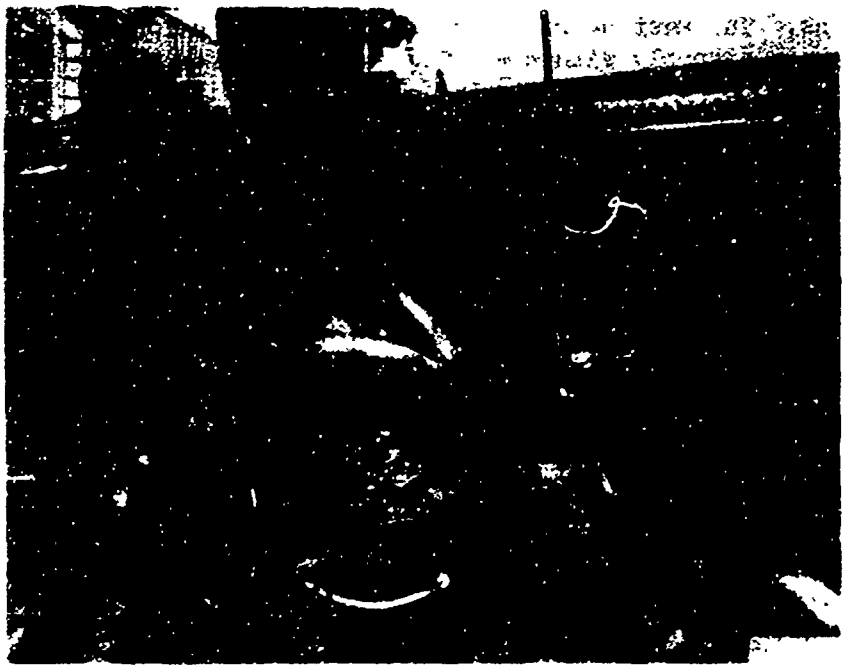

Figure 47. Cabin Interior, Right Side.

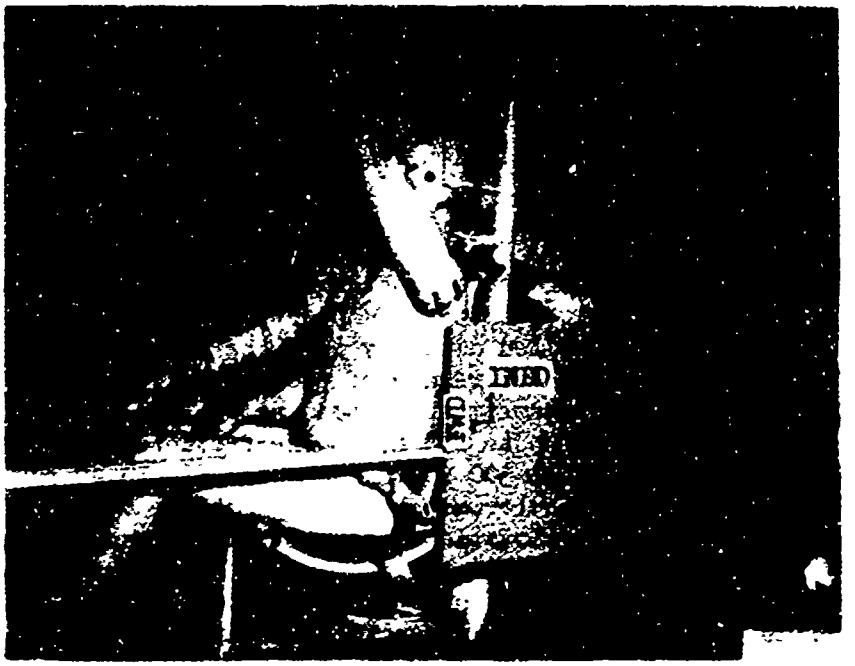

Figure 48. Cabin Interior, Left Side.

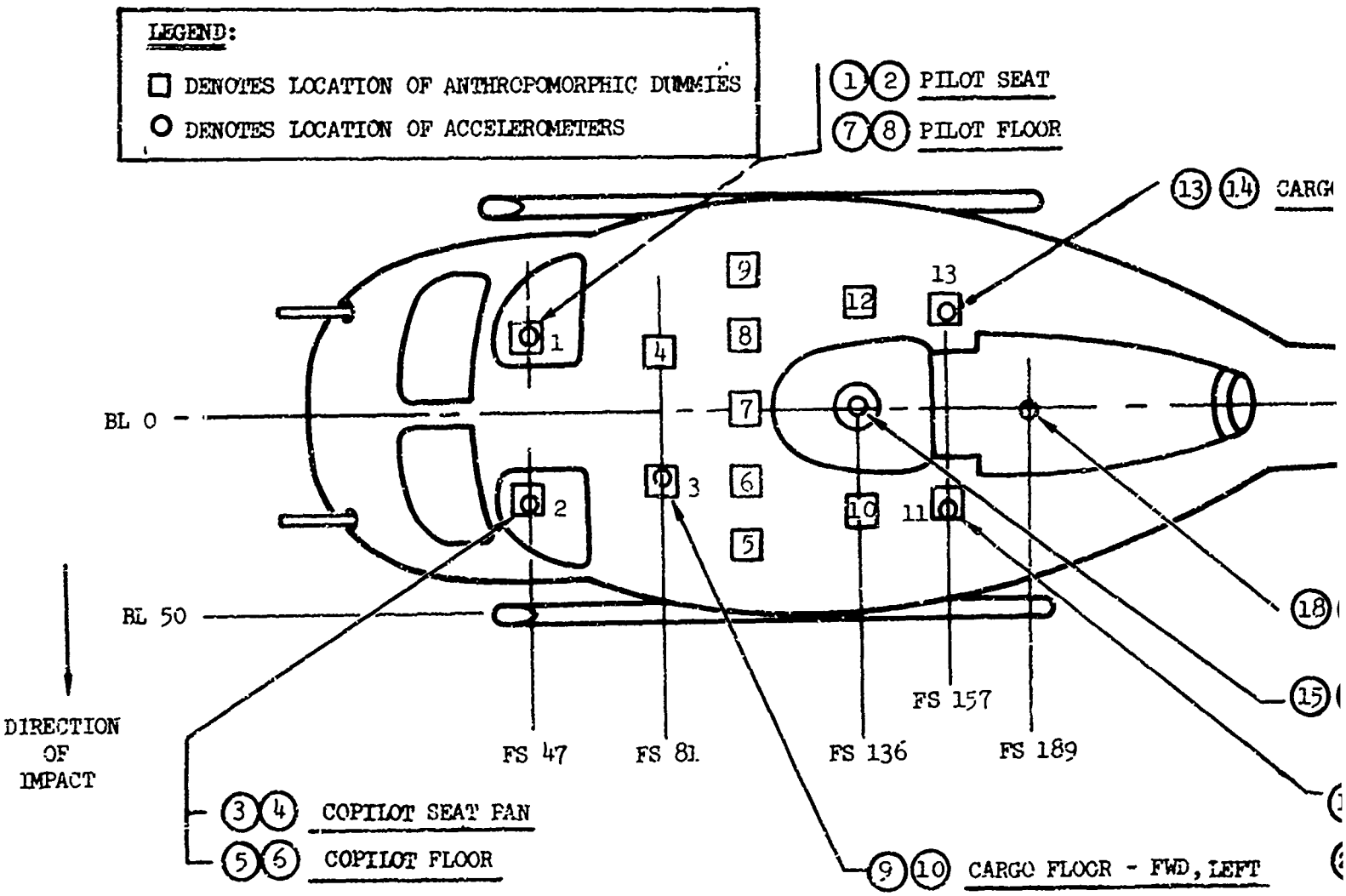

Figure 49. Accelerometer and Passenger Locations - Helicopter Drop Test.

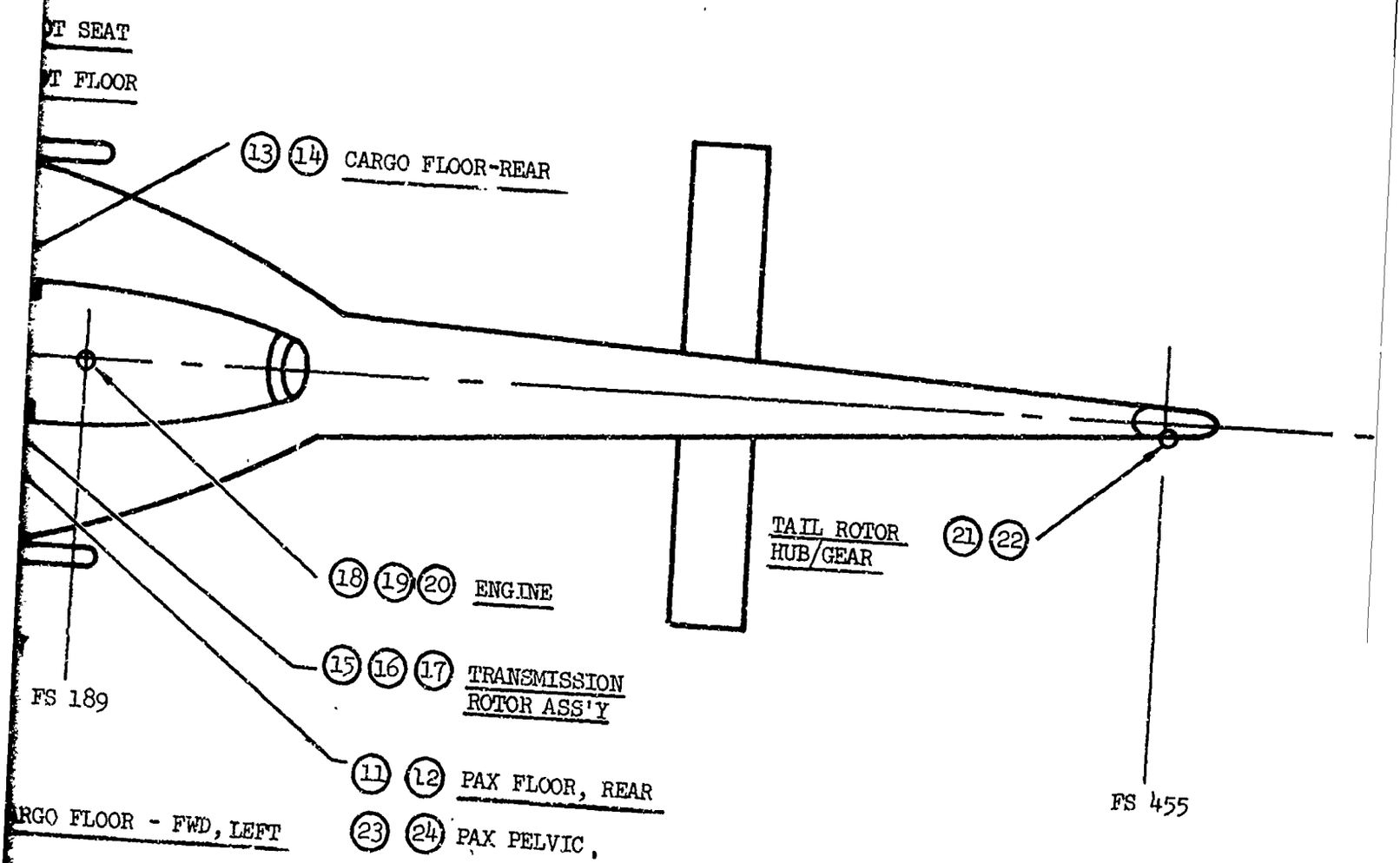
T SEAT
T FLOOR
13 14 CARGO FLOOR-REAR
18 19 20 ENGINE
15 16 17 TRANSMISSION ROTOR ASS'Y
11 12 PAX FLOOR, REAR
RGO FLOOR - FWD, LEFT
23 24 PAX PELVIC
TAIL ROTOR HUB/GEAR
21 22
FS 189
FS 455

TABLE IX. ACCELEROMETER LOCATIONS AND SENSING DIRECTIONS

No.	Identification	Approximate Location			Direction of Measurement			Tape Recorder	Approximate Peak Acceleration Required
		FS	WL	BL	Vertical	Lateral	Axial		
07	Pilot Seat Pan	47	29	-22	X			X	100
08	Pilot Seat Pan	47	29	-22		X		X	50
09	Copilot Seat Pan	47	29	22	X			X	100
10	Copilot Seat Pan	47	29	22		X		X	50
30	Floor, Copilot Location	47	22	22	X			X	100
31	Floor, Copilot Location	47	22	22		X		X	100
32	Floor, Pilot Location	47	22	-22	X				100
33	Floor, Pilot Location	47	22	-22		X			100
34	Cargo Floor, Fwd., Right	81	22	-15	X				150
35	Cargo Floor, Fwd., Right	81	22	-15		X			100
36	PAX* Floor, Rear, Left	157	22	+24	X			X	100
37	PAX* Floor, Rear, Left	157	22	+24		X			50
38	Cargo Floor, Fwd., Left	81	22	+15	X				100
39	Cargo Floor, Fwd., Left	81	22	+15		X			50
40	Xmsn, Rotor Assy.	136	87	0	X			X	100
41	Xmsn, Rotor Assy.	136	87	0		X		X	50
42	Xmsn, Rotor Assy.	136	87	0			X	X	50
43	Engine	189	78	0	X			X	50
44	Engine	189	78	0		X		X	50
45	Engine	189	78	0			X	X	50
46	Tail Rotor Hub/Gearbox	455	136	-14	X				50
47	Tail Rotor Hub/Gearbox	455	136	-14		X			50
48	PAX*	157	47	+24	X				50
60	PAX*	157	47	+24		X			50

*PAX - Passenger

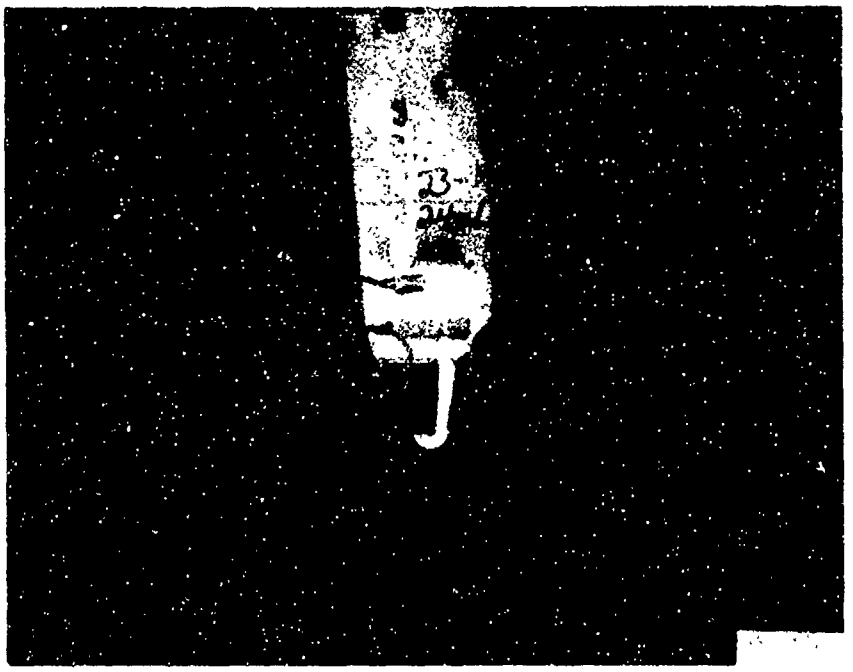

Figure 50. Accelerometer Location, PAX Pelvic.

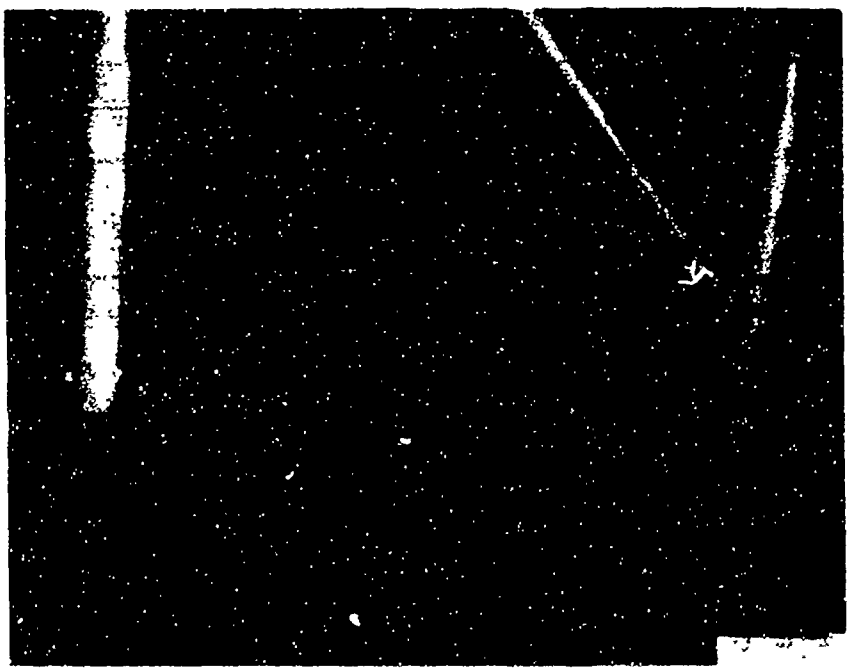

Figure 51. Accelerometer Location, PAX Floor.

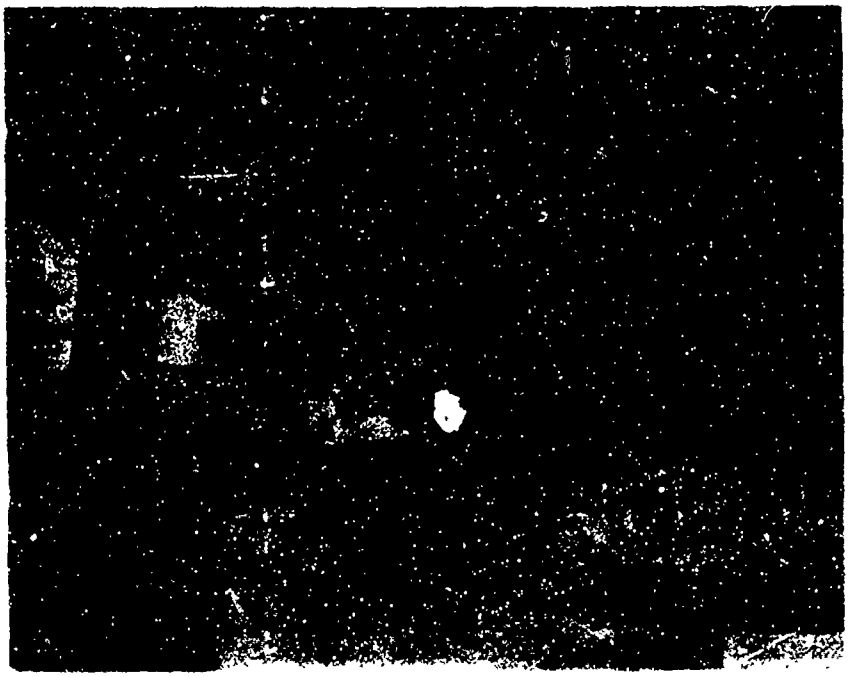

Figure 52. Accelerometer Location, Cargo Floor - Forward Right.

Figure 53. Accelerometer Location, Cargo Floor - Forward Left.

Figure 54. Accelerometer Location, Transmission.

Figure 55. Accelerometer Location, Engine.

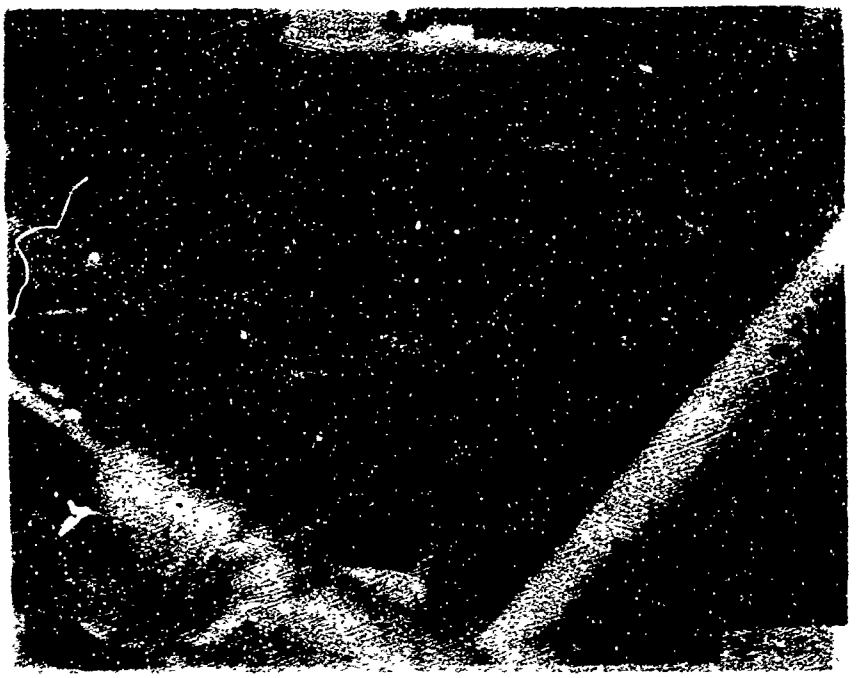

Figure 56. Accelerometer Location, Copilot Seat.

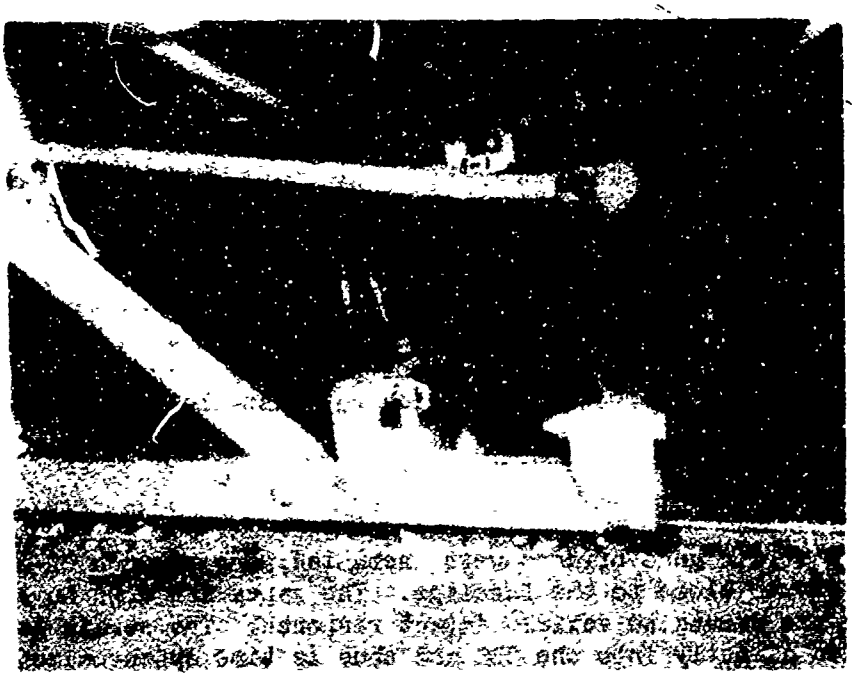

Figure 57. Accelerometer Location, Pilot Floor.

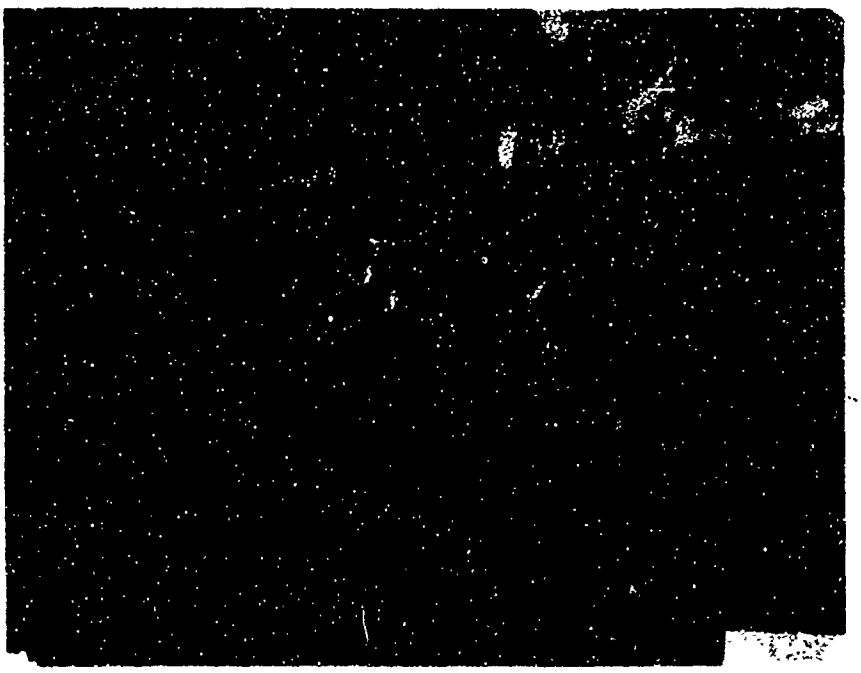

Figure 58. Accelerometer Location, Tail Rotor Gearbox.

Fuselage Deflection Indicator

Center fuselage deformation was measured by means of a single deflection indicator rod positioned diagonally across the fuselage with the lower end attached to the fuselage structure at the floor and the upper end equipped with a scale target projecting through the skin. One of the ground cameras provided continuous coverage of the above-described deflection measurement. The camera was synchronized with the accelerometer and strain gage measurements, thus providing time correlation. Figure 59 shows the deflection rod which was installed at approximately F. S. 68.

Strain Gages

Two bending strain gage bridges were installed, one on each of the left-hand skid struts close to the fuselage. The gages are used to correlate bending in the struts to vehicle impact response. The strain gage data was recorded directly into the CDS and thus is time synchronized with the accelerometer data. Figure 60 shows the strain gage installation on the aft strut.

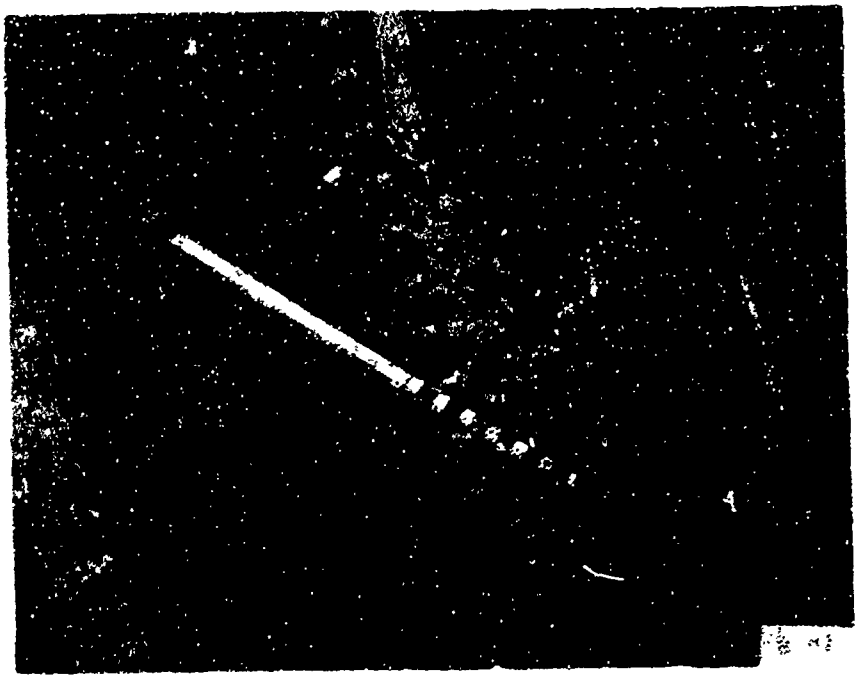

Figure 59. Fuselage Deflection Rod.

Figure 60. Strain Gage, Aft Strut.

PHOTOGRAPHY

Nine high-speed cameras and two normal-speed documentary cameras were used to record the trajectory of the helicopter and the impacting action. Two of the high-speed cameras (provided by the U. S. Army) were installed onboard the helicopter. One camera faced forward covering the pilot and copilot, and one camera faced rearward to cover the passengers. The remaining seven high-speed cameras were positioned on the ground to record the aircraft impact action with the aid of stadia poles that were used as position references.

The normal-speed cameras covered the overall scene for documentary purposes. The high-speed cameras were remotely controlled and synchronized against a time base common to the CDS recording system. For the purpose of identifying deformation of major structures, stripes were painted on the structure inside the cabin and on the outside. Still photographs were taken of the test setup and instrumentation prior to the drop test structural damage to the vehicle and components and the final positions of the anthropomorphic dummies after the test.

Figure 61 is a layout showing the camera coverage, types of cameras, and the frames and lens setting associated with each camera.

TEST PROCEDURE

Pretest Check-Out

Prior to the planned drop test, several preliminary checks were made with the helicopter placed in the test position. These tests were performed to determine the following:

- instrumentation calibration
- instrumentation, equipment and photographic synchronization
- swing separation from the tower
- vehicle balance and motion
- predicted trajectory evaluation

The following preliminary tests were performed:

Initial Swing Performance Tests - The helicopter was raised vertically to a height less than 1 foot off the concrete pad and from this position was laterally displaced 23° with the side pull system. The helicopter was released to swing freely for purposes of observing all body motion of the test vehicle. The vehicle motion was filmed. A review of the tests and the film indicated that no significant undesirable yaw or roll motion was present. However, on the backswing (safety bolts were installed in the swing hanger block which prevented a vertical release)

No.	CAMERA	F.P.S.	LENS (mm)	COVERAGE
1	Hycam	1000	13	Side
2	Hycam	1000	10	Front
3	Hycam	1000	10	Overall front quarter
4	Photosonics	500	5.3	Onboard rear
5	Photosonics	500	5.3	Onboard front
6	Locam	400	25	Overall rear quarter
7	Locam	400	10	Overall rear quarter
8	Locam	400	12.5	Overall total
9	Locam	24	13	Documentary
10	Hycam	1000	50	Deflection rod
11	Arriflex	24	13	Documentary

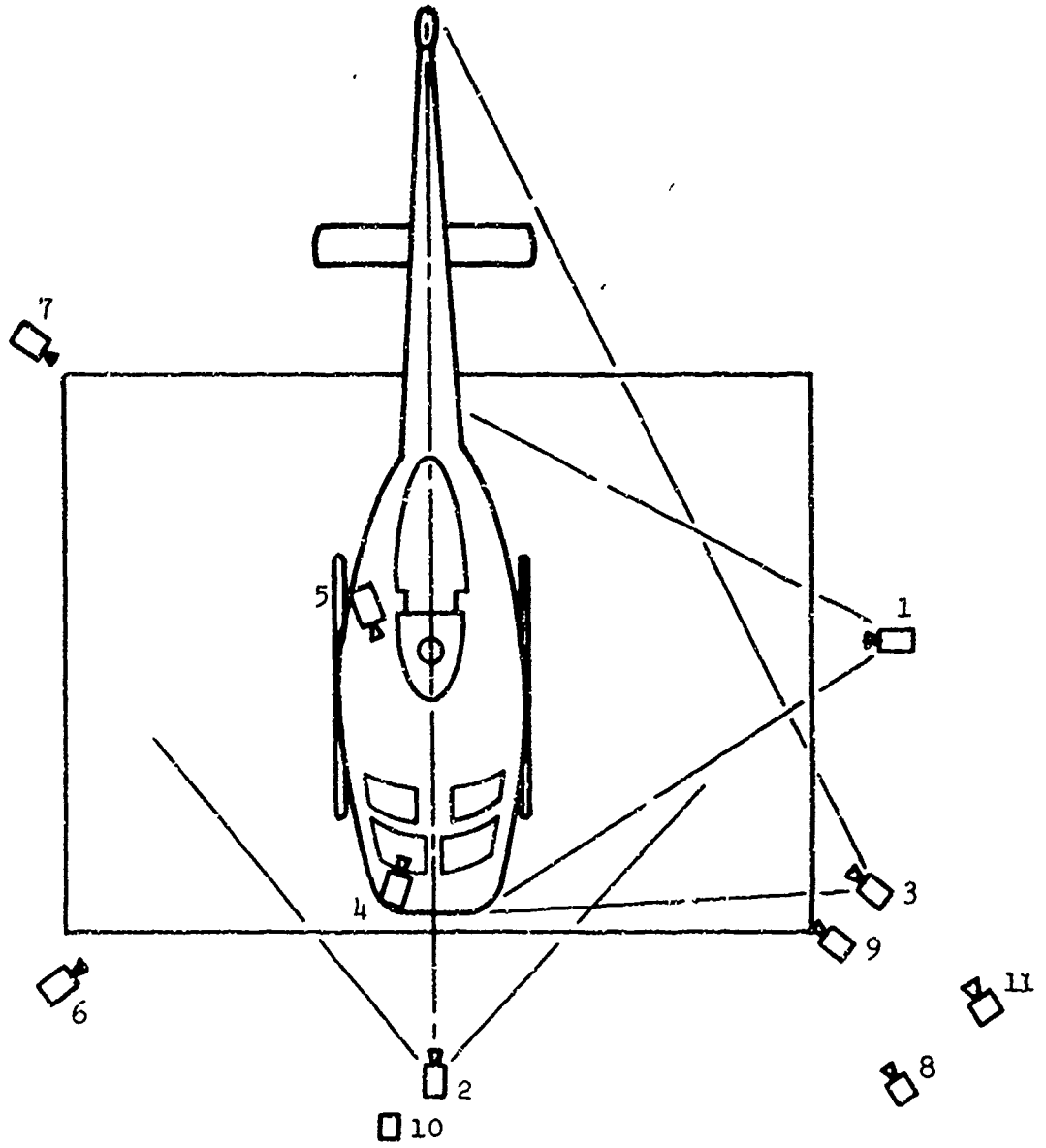

Figure 61. Photographic Coverage Layout.

the vehicle developed a yawing motion which, on subsequent traverses, increased. The yawing motion was considered to be large enough to present a potential problem, in the event of a failure of the vertical release mechanism to operate during the test. Thus, as a safety precaution, it was decided to add stainless steel straps for the purpose of arresting the vehicle motion during an overswing. The straps were of sufficient length to allow the vehicle freedom of motion for at least 10 feet after impact. This is considered sufficient distance so as not to distort the test data. The vehicle, although not swing tested, was placed at its full 40° position for check-out of the test alignment. Figures 62 and 63 show the vehicle at the 23° vertical release and at the full 40° lateral release positions, respectively.

The swing tests were repeated with the stainless steel straps in place. The improvement in vehicle motion on the backswing, from a safety aspect, was considered to be significant, and the test was planned with the use of arresting straps. The straps are shown in Figure 64. During the preliminary swing tests the release microswitch was activated and operated satisfactorily each time.

The preliminary swing tests also provided an opportunity for the test personnel to familiarize themselves with the test procedures.

Low-Level Drop Tests - The helicopter, installed on the swing, was raised vertically to a height approximately 3 inches above the concrete pad (4 fps vertical impact) with the skids level. The vehicle was dropped to check out the instrumentation system and the vertical separation system (solenoid release mechanism for free-fall). A height of 3 inches was chosen for the pretest based on Army-supplied landing skid strain gage data from drop tests which indicated that the strain developed at this drop level is the threshold value above which the skids would experience permanent set. The results of this low-level test were recorded in CDS. Immediately after the tests, the results were available on a scan; and within 2 hours after the tests, hard-copy plots of all measured parameters were available. The results were compared with acceleration predictions using computer program KRASH and Army-supplied landing skid strain gage data. The first run indicated that several accelerometers and strain gages were interchanged and that some accelerometer polarities were reversed. Changes were made to the instrumentation setup, and the low-level drop test was repeated. The test data obtained from the second low-level test was satisfactory.

Figure 62. Vehicle at 23° Position.

Figure 63. Vehicle at 40° Position.

Figure 64. Arresting Straps.

Drop Test

Initial Conditions

The initial conditions upon ground impact as described in the test plan were:

vertical velocity (fps)	28 ±2
lateral velocity (fps)	17.5 ±2.5
longitudinal velocity (fps)	0
pitch angle (deg)	0 ±5
yaw angle (deg)	0 ±5
roll angle (deg)	15 ±5

Test Sequence

The helicopter drop test was conducted according to the following procedural step:

- Raised the test vehicle, installed on swing, to a vertical height of approximately 4 feet off the pad.

- Laterally displaced the vehicle to an offset swing position angle of approximate 23° to set up the free-fall release mechanisms.
- Laterally displaced the helicopter to the maximum offset position angle of approximately 40° and prepared to start the test with data acquisition system and cameras ready on signal.
- Started the Test:
  1. - Data recording systems on
  2. - Normal-speed camera on
  3. - High-speed camera on
  4. - Swing-release latch energized
- Activated microswitch upon contact by laterally swinging vehicle.
- Energized solenoid and initiated free fall.
- Impacted with concrete pad.
- Shut down test photo/instrumentation.

TEST RESULTS

General

A review of the test setup and the high-speed film coverage indicated that the vehicle impacted with the following conditions:

vertical velocity (fps)	23.0
lateral velocity (fps)	18.6
longitudinal velocity (fps)	0
pitch angle (deg)	1 (nose down)
yaw angle (deg)	0
roll angle (deg)	10 (right side up)

Figure 65 shows the drop sequence photographed at 2 frames/sec. Upon impact, the skid leading edge at the forward strut contacted the ground first. The vehicle pitched nose-up after impact and rolled onto the skid trailing edge. There was extensive damage to the fuselage left side and underside and the cabin structure forward of the pilot and copilot. The troop seats at fuselage stations 117, 139 and 158 totally collapsed, and the final positions of the anthropomorphic dummies reflected a shift of the dummies in the direction of impact. The tail boom experienced a

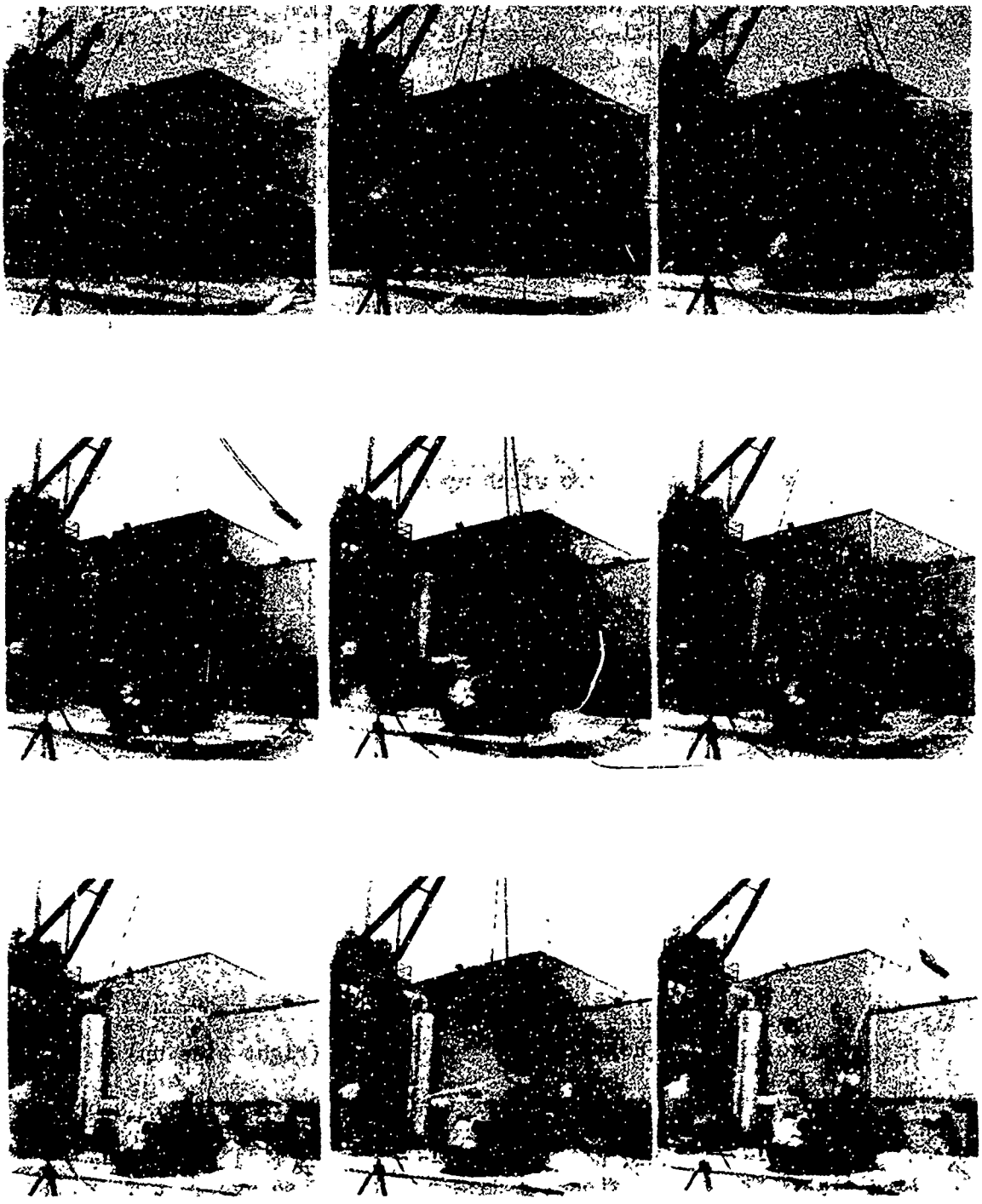

Figure 65. Drop Sequence.

fracture at F. S. 316. The engine and transmission appeared to survive the impact in good condition. Although there was no noticeable failure of either the engine or the transmission, there was a slight yaw rotation of the engine. The floor experienced extensive buckling. Buckling of the fuselage cabin was also noted in the posttest inspection. The impact vertical velocity was lower than stated in the test plan, and the difference is discussed in the TEST DATA section of Volume II.

All the high-speed cameras functioned during the test; however, the rear-mounted on board camera did not activate until after the impact, thus providing limited data. All the accelerometers and strain gages performed properly during the test. However, after impact, two amplifiers were overdriven by G forces which exceeded their peak acceleration settings. The accelerometers affected were installed near the passenger pelvic area (lateral) and on the forward floor (lateral).

A left side (impact side) view of the posttest crash is shown in Figure 66. Figure 67 presents a view looking from the rear, showing the vehicle's final position. In both photographs fuel spillage is quite noticeable. Figures 68 through 78 depict some of the damage sustained during impact.

A summary of the damage sustained by the troop seats and structure is presented in Tables X and XI, respectively.

Landing Gear Skids

The leading edge of the left skid made initial ground contact at impact. The sequence of subsequent skid contact was approximately as follows, from the time of initial impact;

- full left skid at 11 msec
- right skid front at 45 msec
- full right skid at 52 msec

The skids were damaged extensively and collapsed, as was to be expected. Figures 68 and 69 show the damaged left and right landing skids, respectively.

Fuselage Structure

The fuselage underside was estimated from the high-speed films to have contacted the ground at approximately 109 msec after initial ground impact. At approximately 143 msec after impact, the films indicated that the fuselage reached a maximum deflection of between 4 and 4.5 inches. Posttest inspection revealed that at several locations, most notably at the juncture of the fuselage and skids, there was as much as 2 to 3 inches of permanent deformation. A posttest inspection of the deflection rod

TABLE X. PASSENGER AND SEAT TEST RESULTS

	Passenger (PAX)	Wt. (Lbs.)	Passenger (PAX) Position After Crash	Seat Condition After Crash	Reference Figure(s)
Cockpit F.S. 47	1 Pilot	203	No Change	No Change	
	2 Copilot	198	No Change	No Change	73,77
First Row F.S. 91.8	3 Left PAX.	148	No Change	Seat Fabric Torn	73,77
	4 Right PAX.	108	Leaning 30° to Left	Left Rear Seat Post Floor Attach. Fitting Separaced Downward from Floor	74
Second Row F.S. 117	5 Left PAX.	130	Sitting on Floor Leaning 30° to Left	Complete Seat Collapse	73,76
	6 Lt. Center PAX.	202	Sitting on Floor Leaning 10° to Left	Complete Seat Collapse	73,76
	7 Center PAX.	103	Leaning 45° to Left	Left Side of Seat Partially Collapsed	73,76
	8 Rt. Center PAX.	130	Sitting on Floor	Complete Seat Collapse	73,75
	9 Right PAX.	188	Sitting on Floor	Complete Seat Collapse	73,75
Rear Left Row	10 Fwd. PAX. F.S. 138.8	206	Sitting on Floor	Complete Seat Collapse	73
	11 Aft. PAX. (Instru- F.S. 157.8 mented)	202	Sitting on Floor	Complete Seat Collapse	73
Rear Right Row	12 Fwd. PAX F.S. 138.8	194	Sitting on Floor	Seat Rear Fabric Rod on Floor	74
	13 Aft PAX. F.S. 157.8	196	Sitting on Floor	Seat Rear Fabric Rod on Floor	74
	Total Wt.	2297			

[1] All passengers had seat belts fastened. Only pilot and Copilot had shoulder belts.

TABLE XI. HELICOPTER STRUCTURE TEST RESULTS

Structure Section	Damage Description	Reference Figures
FUSELAGE COCKPIT AREA (Fwd. of F.S. 64)	(1) Windshield corner post left side - broke from roof (2) Roof section fwd. left corner (above Copilot) - set downward - 2.0" (3) Windshield-left side - 75% broke away	66
FUSELAGE FWD. CARGO (F.S. 64 to F.S. 120)	(1) Floor area above the two main fore & aft floor beams (between F.S. 64 and F.S. 104) buckled upward max. deflections @ F.S. 74, W.L. 14 - 1.63" & @ F.S. 102, W.L. - 106"	66
	(2) Fuselage diagonal deflection @ F.S. 68 between floor (W.L. 22) & roof (W.L. 80) was measured with an indicator during & after test - total dynamic deflection 3.25", permanent set - 2.45"	66
	(3) Fuselage underside deformation - left side - approx. 2.0" to 2.5"	70
FUSELAGE - AFT CARGO (F.S. 120 to F.S. 166)	(1) Lower fuselage section - left side (fwd. of F.S. 166) raised 3.5" with respect to fuselage section aft of rear engine firewall (2) Seat support post floor attachment fitting broke from floor downward - post end - 2.5" below normal position on floor (3) Fuselage underside deformation - left side - approx. 2.0" to 3.0"	71
TAIL BOOM	(1) Tail boom @ F.S. 316 broke - skin (0.032" thk.) (2) Stringers failed in tension on right side and upper left side	67,72
LANDING GEAR - SKIDS	(1) Both skids rotated outward with struts fully imbedded in fuselage (2) Right forward skid strut broke off completely 16" from skid	68,69
ENGINE	Engine center line shifted 3/8" to left and 3/8" downward. Forward shroud on engine shifted 1.5-2" to the left 3/8" bow in center of forward engine support strut on the right side.	79
TRANSMISSION	No noticeable damage. Distance from mast beam to floor approximately (1/4") the same before and after the test. Mounts appear undamaged.	77

Figure 66. Posttest Damage, Left Side View.

Figure 67. Posttest Damage, Rear View.

Figure 68. Posttest Damage, Left Landing Skid.

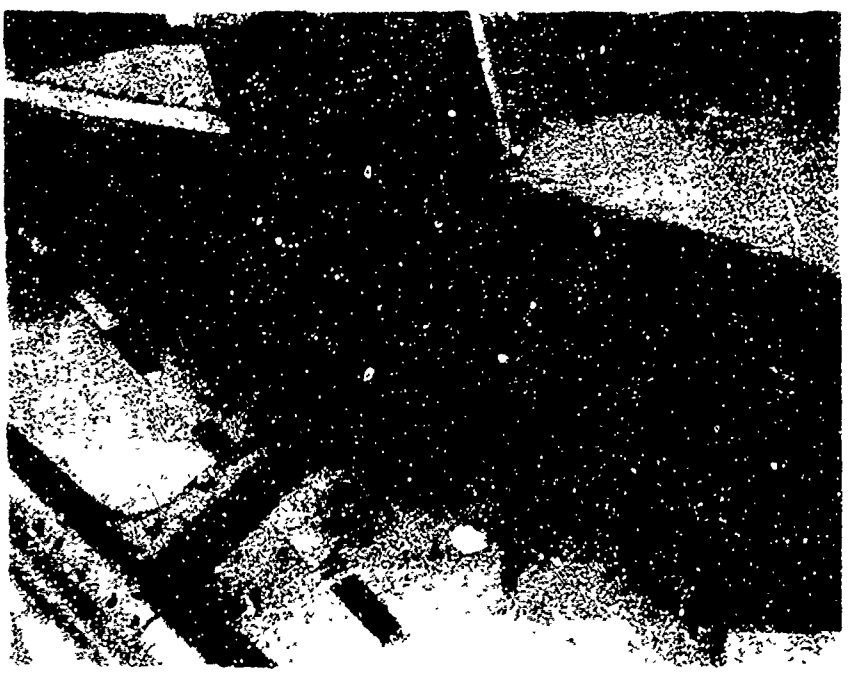

Figure 69. Posttest Damage, Right Landing Skid.

Figure 70. Posttest Damage, Fuselage Underside.

Figure 71. Posttest Damage, Fuselage Side.

indicated that the fuselage experienced a maximum deflection of approximately 3.2 inches, of which 2.4 inches was permanent. The floor was noted to have buckled approximately 2 inches in several sections near mid fuselage. Figures 70 and 71 are two views of the fuselage underside depicting deformation.

Tail Boom

The tail boom fractured at approximately F. S. 316. From the high-speed films, the boom was noted to start bending at 225 ms after initial ground impact, and the boom tip contacted the ground at just slightly over 400 ms after initial ground impact. Figure 72 shows a close-up view of the tail boom damage.

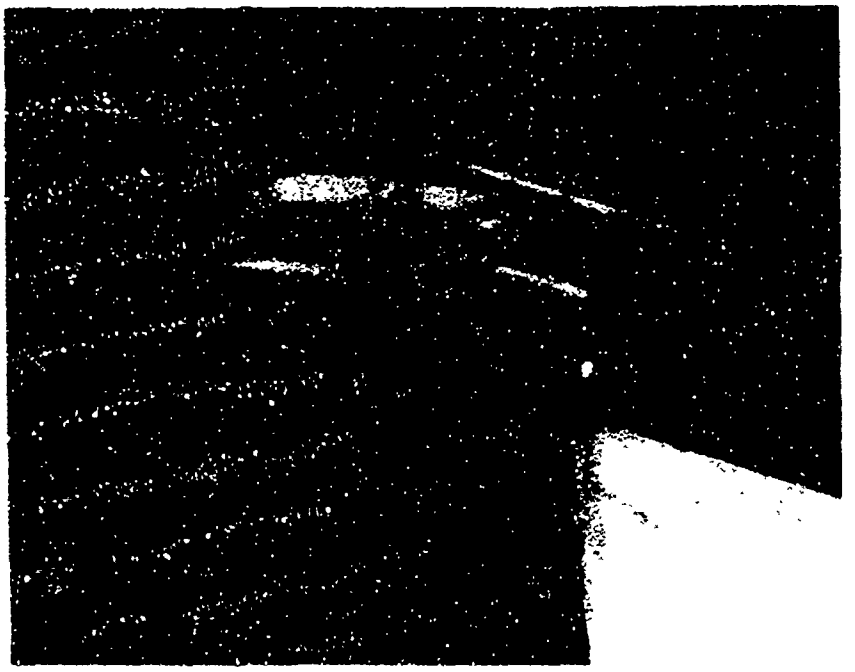

Figure 72. Posttest Damage, Tail Boom F.S. 316.

Crew Seats and Anthropomorphic Dummies

The seats located at F. S. 117, 139 and 158 collapsed totally as a result of the impact. The instrumented dummy (medical attendant) located at the rear left seat (F.S. 158) ended up seated on the floor with the knees raised (Figure 73). The final position of the various dummies indicated

a left-leaning tendency which is consistent with the direction of impact. The cross bar rearward of the five passengers at F. S. 117 indicates a high potential of injury to the occupants due to possible impact at or near the neck. Figures 73 through 76 show, in detail, the damage to the seats and the final positions of the dummies. The floor below these occupants also appeared to survive the impact in good condition. Figures 77 and 78 show close-up views of a troop seat at F. S. 81.8 and the co-pilot seat, respectively.

Figure 73. Posttest Damage, Left Side Seats and Troops.

Figure 74. Posttest Damage, Right Side Seats and Troops.

Figure 75. Posttest Damage, Passenger Second Row, Right Center, and Right.

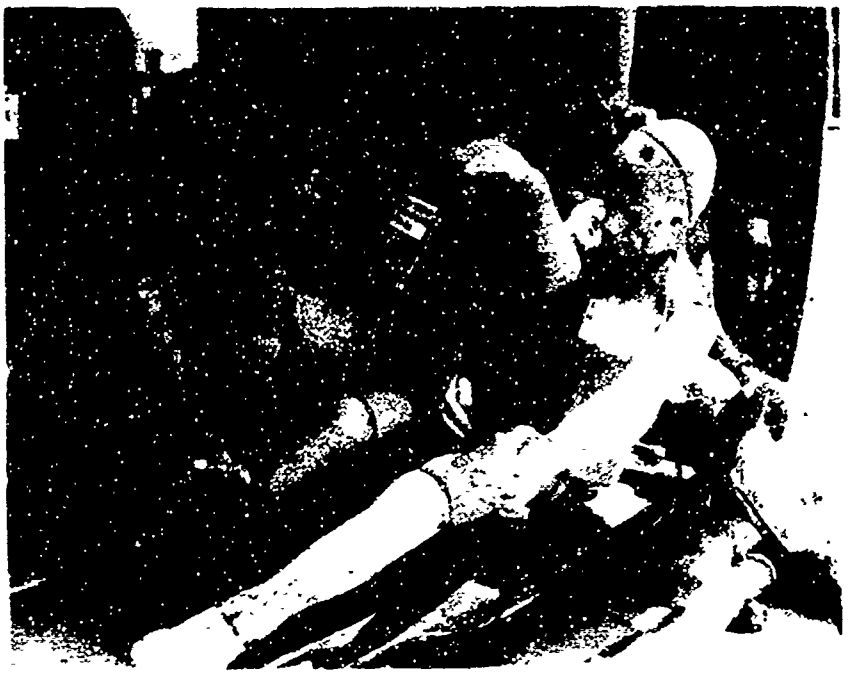

Figure 76. Posttest Damage, Passenger Second Row, Center, and Left Center.

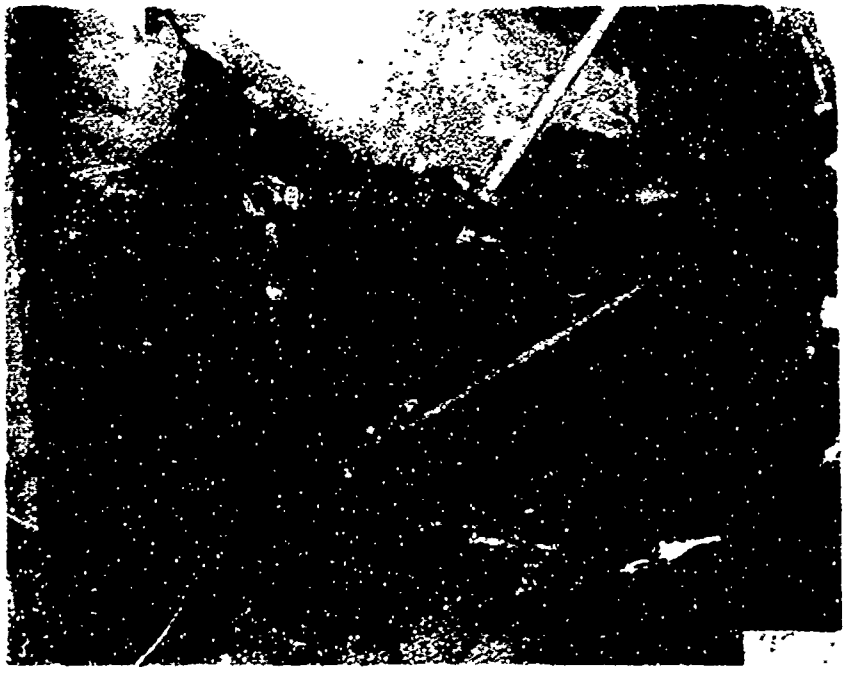

Figure 77. Posttest Damage, Troop Seat F.S. 81.8, Left Side.

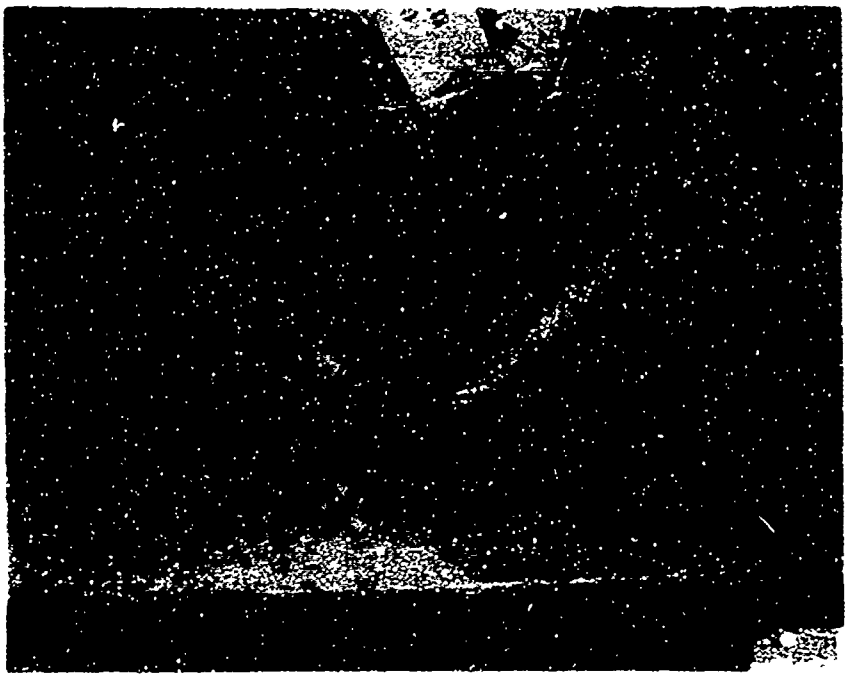

Figure 78. Posttest Damage, Copilot Seat, Left Side.

Power Plant

The engine appeared to survive the impact in good condition. The posttest inspection revealed a slight yaw rotation to the left where the engine connects to the housing. The right mounts show a slight distortion. The posttest view of the engine is shown in Figure 79.

Figure 79. Posttest Damage, Engine.

Transmission

The transmission, which is shown in Figure 80, experienced no noticeable damage.

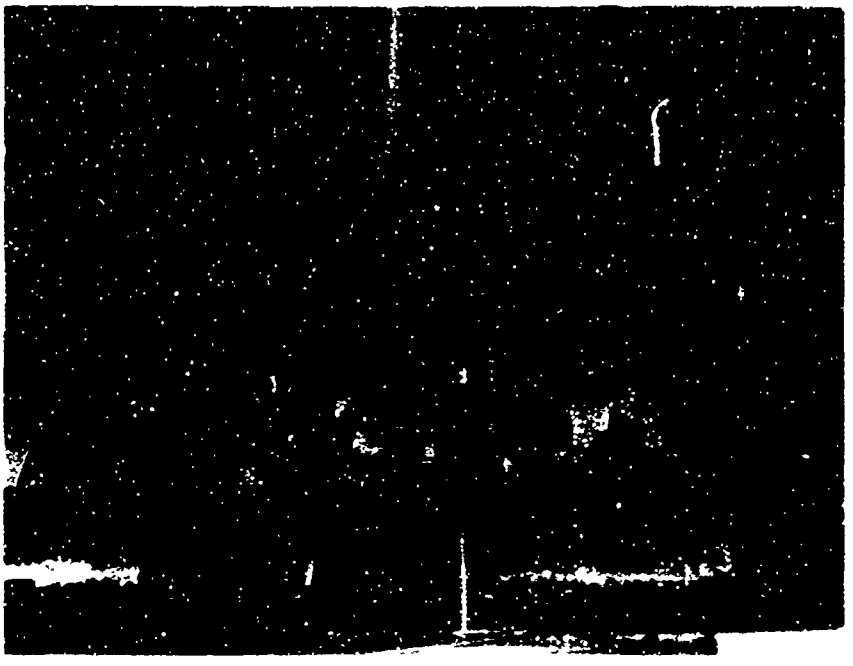

Figure 80. Posttest View, Transmission.

DATA REDUCTION

The responses (24 accelerometers and 2 strain gages) were recorded directly into the Lockheed Central Data System (CDS). This data is digitized and was used to obtain numerically integrated velocities and displacements. The recorded accelerations and integrated velocities and displacements are presented in Volume II. Thirteen of these responses were simultaneously recorded on a backup tape system. These data were filtered using 100-cps filters (down 3 db @ 100 cps). The filtered accelerations are presented in Volume II.

A summary of the peak decelerations, recorded during the test, is shown in Table XII.

TABLE XII. SUMMARY OF TEST MEASURED PEAK DECELERATIONS

Test Trace No.	Accelerometer Location	Fuse-lage Station	CDS Data G's***/Time*	Filtered**** G's***/Time*
07	Pilot Seat Pan, Vertical	47	-40/110 -65/140	-25/100 -20/140
08	Pilot Seat Pan, Lateral	47	70/140	35/115-135
09	Copilot Seat Pan, Vertical	47	-110/115	-60/105
10	Copilot Seat Pan, Lateral	47	45/115	20/125
30	Floor Copilot, Vertical	47	-48/100	-30/90
31	Floor Copilot, Lateral	47	55/105	27/102
32	Floor, Pilot, Vertical	47	-78/140	-45/100
33	Floor, Pilot, Lateral	47	32/140	-
34	Cargo Floor Fwd, Right Vertical	81	-125/110	-
35	Cargo Floor Fwd, Right Lateral	81	50/100	-
36	PAX Floor Left, Vertical	87	-100/95	-
37	PAX Floor Left, Lateral	87	50/120	-
38	Cargo Floor Fwd, Left Vertical	81	-170/100	-
39	Cargo Floor Fwd, Left Lateral	81	66/115**	-
40	Transmission, Vertical	136	-30/110	-26/100
41	Transmission, Lateral	136	10/100	6.8/130
42	Transmission, Axial	136	+8/100	+5/100
43	Engine, Vertical	189	-25/110	20/100
44	Engine, Lateral	189	+15/160 -15/105	+12/150 -10/95
45	Engine, Axial	189	+12/100	+10/95
46	Tail Boom, Vertical	455	20/135	-
47	Tail Boom, Lateral	45	15/120	-
48	PAX Pelvic, Vertical	157	-25/110	-
60	PAX Pelvic, Lateral	157	-64/115**	-

*Time after impact in milliseconds

**Amplifiers overdriven during test

***Positive G's are down, to the right and forward

****100-cps low-pass filter

CORRELATION

GENERAL

The math model used in the correlation studies is presented in Figure 35 and Table VIII and discussed in the section entitled CORRELATION MODEL.

The initial conditions used for the correlation computer analysis are as follows:

Initial Velocity	-	23 fps vertical (down)
		18.6 fps lateral (left)
		26.4 deg/sec roll velocity (right side down)
Initial Attitude	-	10 deg roll (left side down)
		1 deg pitch (nose down)

The analysis shows good agreement with test results in the following essential areas:

- sequence of events
- vehicle motion
- time of occurrence of peak responses
- fuselage maximum deflection and permanent deformation
- changes in vertical and lateral velocity
- fuselage peak vertical deceleration
- engine and transmission peak deceleration
- engine and transmission deflections
- passenger dynamic response

From observations of the high speed films, the deflection rod markings, and posttest measurements, it is estimated that the maximum lower fuselage deflection with respect to the floor during the test was between 4 and 4.5 inches and that the permanent deformation was between 2 and 3 inches. The analysis indicates a maximum deflection of 2.3 inches at the forward fuselage (mass point 16) and 5.0 inches at the aft fuselage (mass point 10). The permanent deformation obtained in the analysis was approximately 1.8 inches forward and 3 inches aft. Table XIII shows a summary comparison of the analysis and test impact sequence and fuselage deformation. The test data was obtained primarily from nominally 1000 frames/sec film data which translates into approximately 1 millisecond (msec) per frame. At a sink speed of 23 fps, the vehicle is moving approximately 1/4 inch every 1 msec. Thus, differences of several milliseconds between the test and analysis data are not considered significant. For example, a full 10 millisecond time shift can be accomplished by altering the external spring lengths by 2.5 inches, which is less than 15% of the free length of 17

inches used in the analysis. The analysis assumes an initial roll velocity of .4615 rad/sec and a ground coefficient (μ) of .3 which, if different than the test conditions could contribute to the slight differences in time, noted in Table XIII, between the analysis results and the test observations.

TABLE XIII. COMPARISON OF ANALYSIS AND TEST IMPACT TIMES OF OCCURRENCE AND FUSELAGE DEFORMATION *

Event	Test	Analysis
Time After Impact (msec)		
Left Front Skid Impact	0	0
Full Left Skid Impact	11	7
Right Front Skid Impact	45	56
Full Right Skid Impact	53	61
Maximum Fuselage Underside Deflection	143	128 **
Maximum Deflection (Mass 10)	4" - 4.5"	5.0"
(Mass 16)		2.3"
Permanent Deformation (Mass 10)	2" - 3"	3.0"
(Mass 16)		1.8"

* Time after impact in Milliseconds (msec)

** Average of masses 10 (aft) and 16 (forward)

ACCELERATIONS

The correlation between analysis and test measured accelerations is presented in Table XIV and Figures 81 through 86. The analytically determined peak deceleration levels shown in Table XIV compare very favorably with the test results. The peak deceleration levels obtained by analysis generally occur slightly later than indicated by test data.

The transmission vertical deceleration results give excellent agreement in both peak values and time of occurrence. The engine, although agreeing in peak value, shows a peak response occurring 9 to 19 milliseconds later than noted in the test (129 msec vs 110-120 msec). The floor vertical accelerations, obtained by analysis, are slightly lower than measured and they occur approximately 9 to 14 milliseconds later than noted in the test. The pilot seat pan vertical acceleration test data agrees with the analysis in amplitude (4%) and time (4 msec). The passenger peak vertical response

is within 4% of the test value but occurs more than 28 milliseconds later. The aft passenger location in the mathematical model is located near the engine and the time of occurrence of peak vertical response for both the passenger and engine are very similar. The comparison of test and analysis vertical acceleration time histories are shown in Figures 81, 82 and 83 for the floor, transmission and engine, respectively. Figures 84, 85 and 86 show the correlation between test and analysis for the passenger floor (rear left), passenger pelvic and pilot seat pan, respectively. The peak responses of the transmission, engine and rear seated occupant are shown by analysis to occur 3 msec, 15 msec and 34 msec after the occurrence of peak floor accelerations, respectively. The test data indicates that the peak floor accelerations occur approximately 15 msec prior to the peak accelerations for the aforementioned masses. By considering the relative times to peak responses for the various masses the correlation results between analysis and test are shown to be extremely close.

The lateral peak acceleration correlation shows good agreement for the transmission and engine. Although the transmission analytical peak value is greater than the test value, the time of occurrence of the peak response is in agreement. The engine peak responses, analytical and test, show excellent agreement. However, the predicted value occurs much earlier than the test value. A softened lateral engine mount representation was included in the parameter study phase of the study and the results indicated that the time differential between the analysis and the test is reduced to approximately 28 msec from 45 msec. With the softer engine mounts the peak accelerations obtained by analysis still shows good agreement with the test. The engine mount stiffness is apparently softer than that indicated in Figure 38 . The lateral floor peak accelerations do not show good agreement with the test data. The time of occurrence is consistent with the other data comparisons, in that the analytical results indicate 6 to 26 msec lag as compared to the test results. At the floor the analysis shows a peak response of -10 G's versus -40 G's (unfiltered test data). However, it is surmised that 100 cps low-pass filtering of this data would reduce the response level to less than 20 G's, based on reductions obtained from other filtered data. The mathematical model floor accelerations are expected to be lower than test data because the model represents the floor with several lumped masses, whereas the test installed accelerometers, although mounted as close as practical to rigid surfaces, do in fact measure local responses. The model, on the other hand, by the choice of relatively large masses, inherently has a lower frequency response ($\approx$ 6-10 cps) than that recorded by the corresponding accelerometers. However, although the accelerations may differ, the model accounts for the proper forces being transmitted to the upper mass components (transmission and engine) as noted by their respective responses. The transmission and engine provide rigid masses upon which to mount accelerometers.

TABLE XIV. COMPARISON OF ANALYSIS AND TEST PEAK DECELERATIONS*

Response Parameter	Test		Analysis*****		Difference between Test and Analysis********	
	G_{Peak}***	Time**	G_{Peak}	Time**	G_{Peak}***	Time**
VERTICAL						
Engine	-24/-26****	110/120****	-26	129	+2/0	-19/-9
Transmission	-27/-30****	110/115****	-30	117	+3/0	-7/-2
Forward Floor	-26	105	-22	114	-4	-9
Aft Floor	-45	100	-27******	114	-18	-14
Passenger Pelvic	-26	100-120****	-25	148	-1	-28 to -48
Seat Pan (Pilot)	-26	100	-25	104	-1	-4
LATERAL						
Engine	+11	150	12.5 11.6	110******* 127*******	+1.5 +.6	+40 +23
Transmission	+6.8	125	12	132	+5.2	-7
Forward Floor	+27	100	4.8/7.5	114/126	-19.5 to -22.2	-14 to -26
Aft Floor	+40	110	10 24 (transient)	117 94	-30 -16	-7 +16

*100 CPS low-pass filtered test data unless otherwise noted

**Time in msec after initial impact

***Vertical acceleration is positive down. Lateral acceleration is positive to the right.

****CDS data

*****Analytical forward floor accelerations are obtained from mass 16. Analytical aft floor accelerations are obtained from mass 10. Analytical engine accelerations are obtained from mass 7. Analytical transmission accelerations are obtained from mass 8.

******Peak transient response of 60 g's at 0.094 sec.

*******Softer engine lateral mount stiffness

********Negative G_{peak}(time) indicates that the analytical peak value is lower (occurs later) than the test peak value.

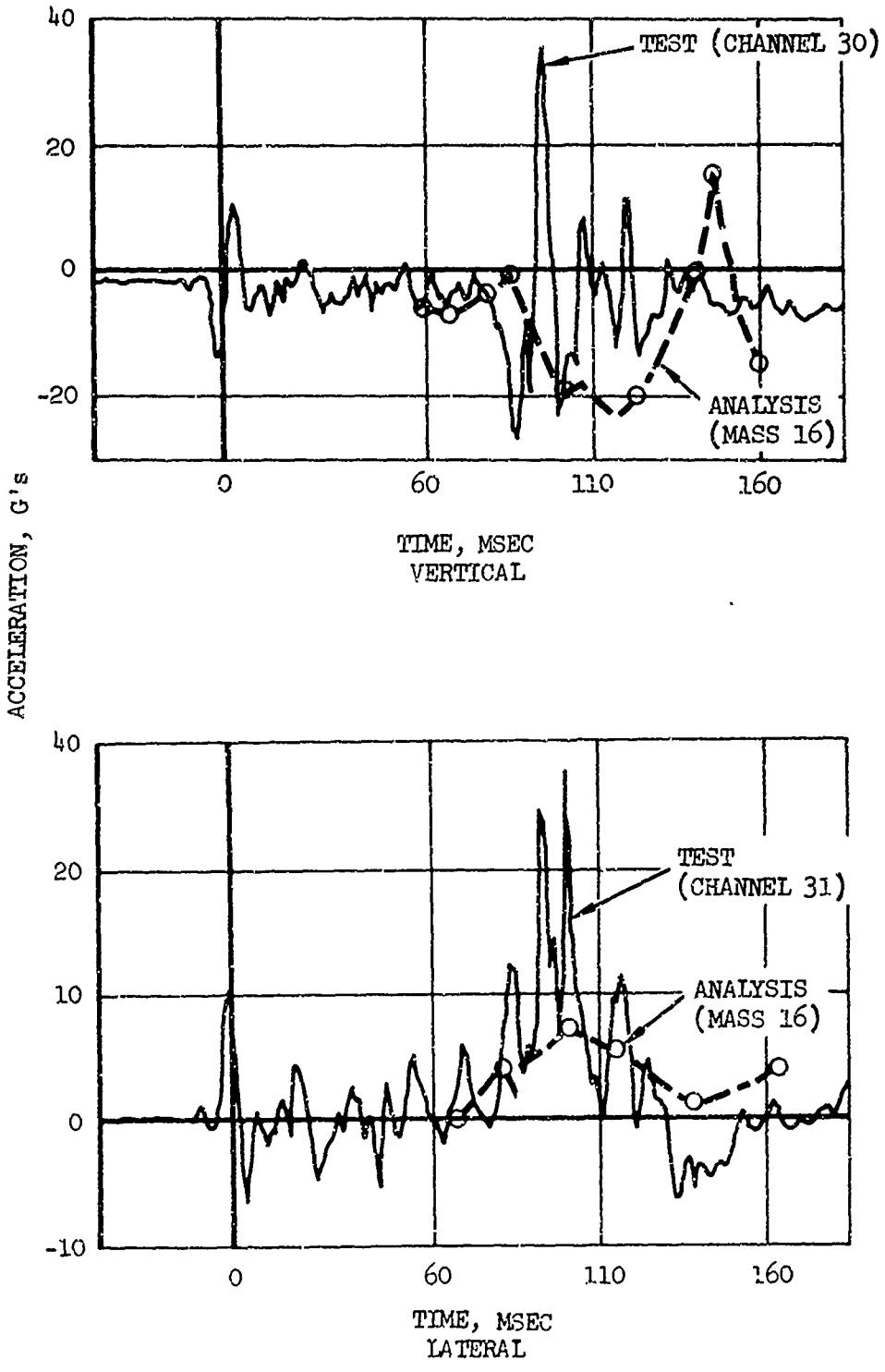

Figure 81. Correlation of Floor Accelerations at Copilot Location.

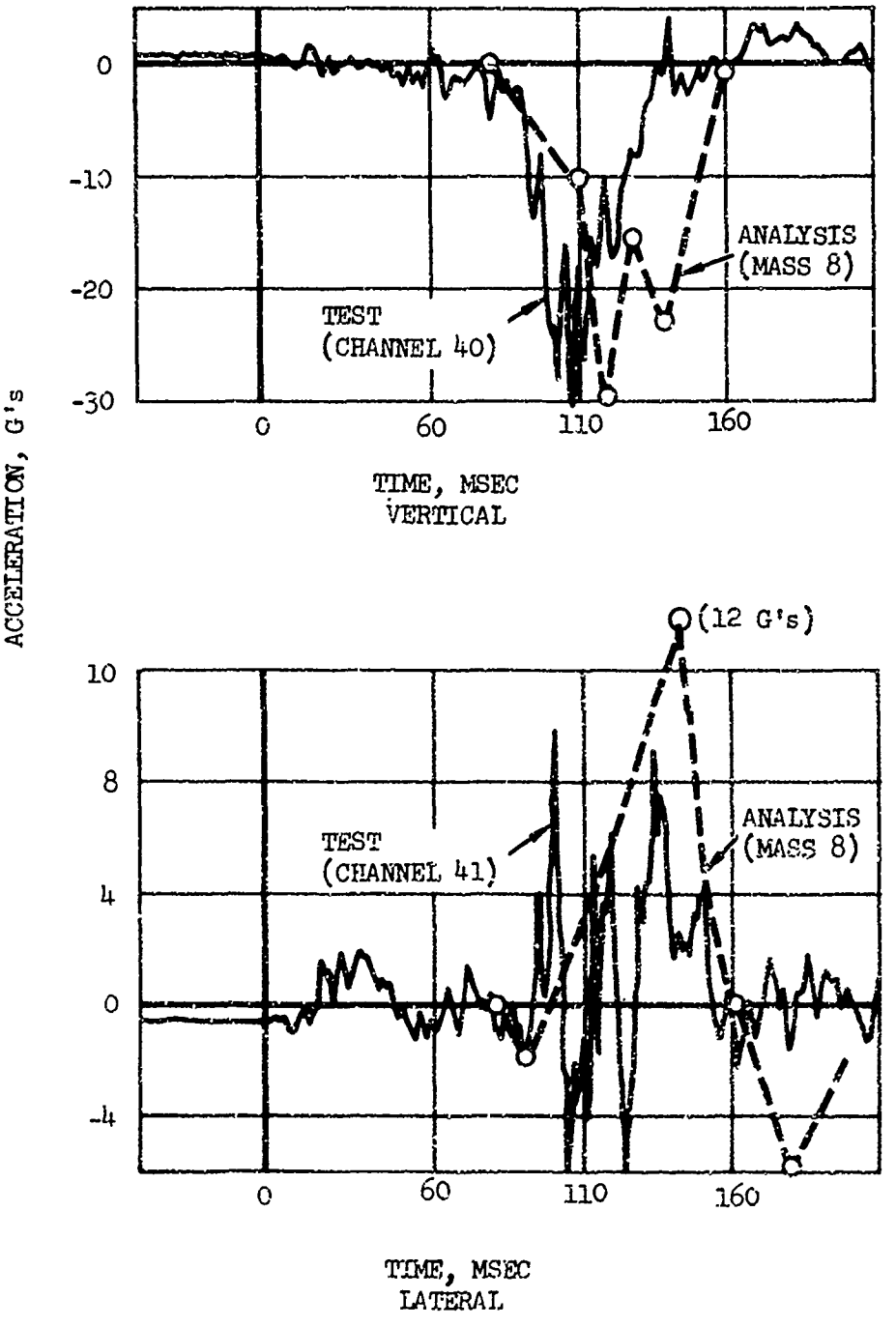

Figure 82. Correlation of Transmission Rotor Housing Accelerations.

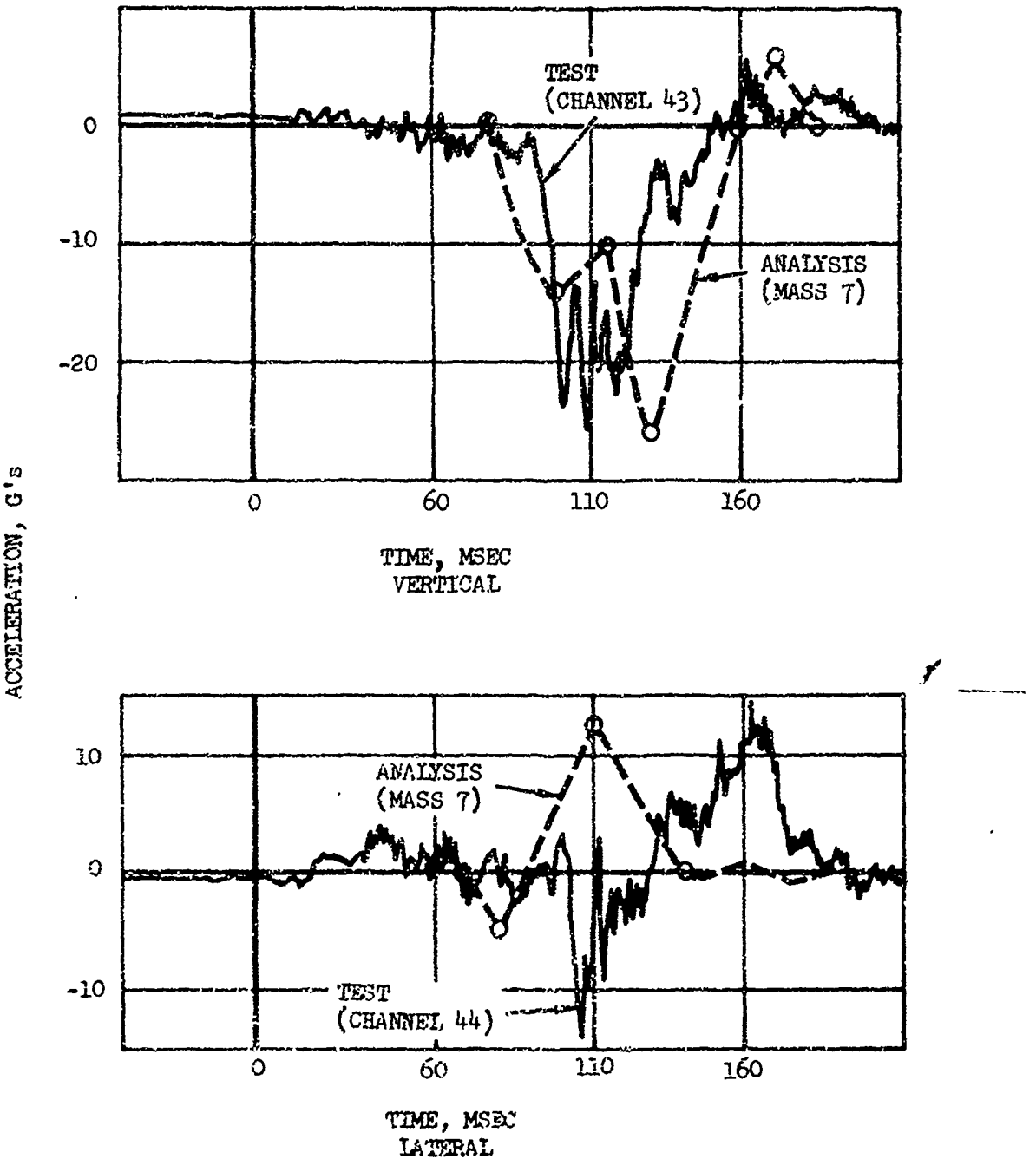

Figure 83. Correlation of Engine Accelerations.

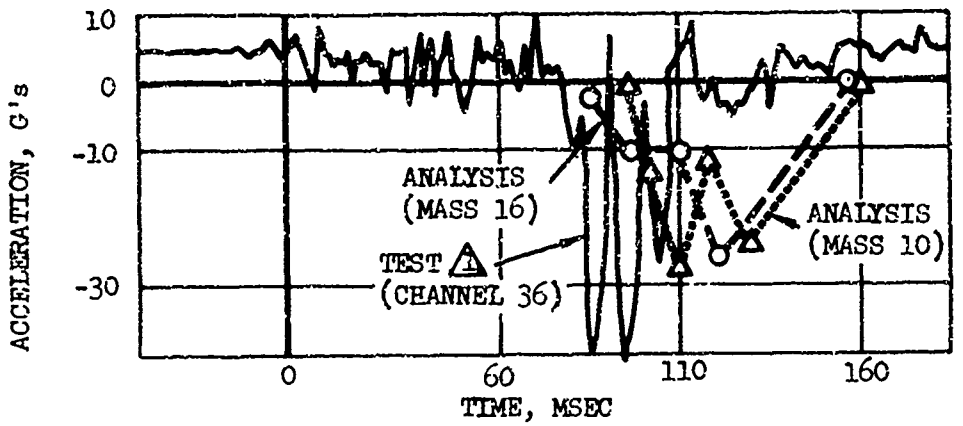

Figure 84. Correlation of Passenger Floor Rear Left Vertical Accelerations.

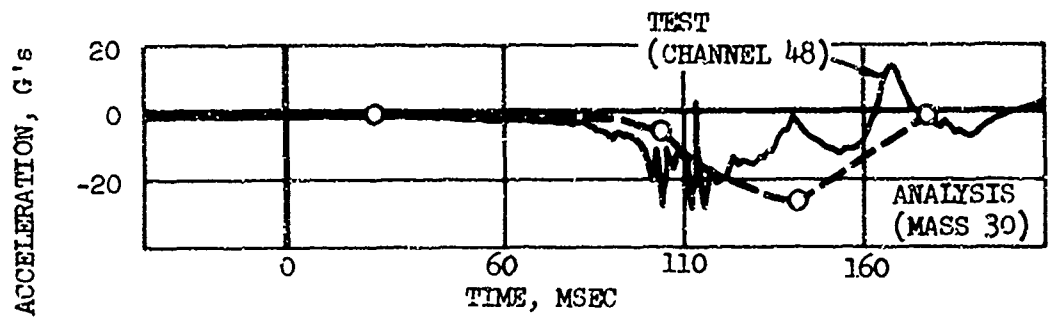

Figure 85. Correlation of Passenger Pelvic Vertical Accelerations.

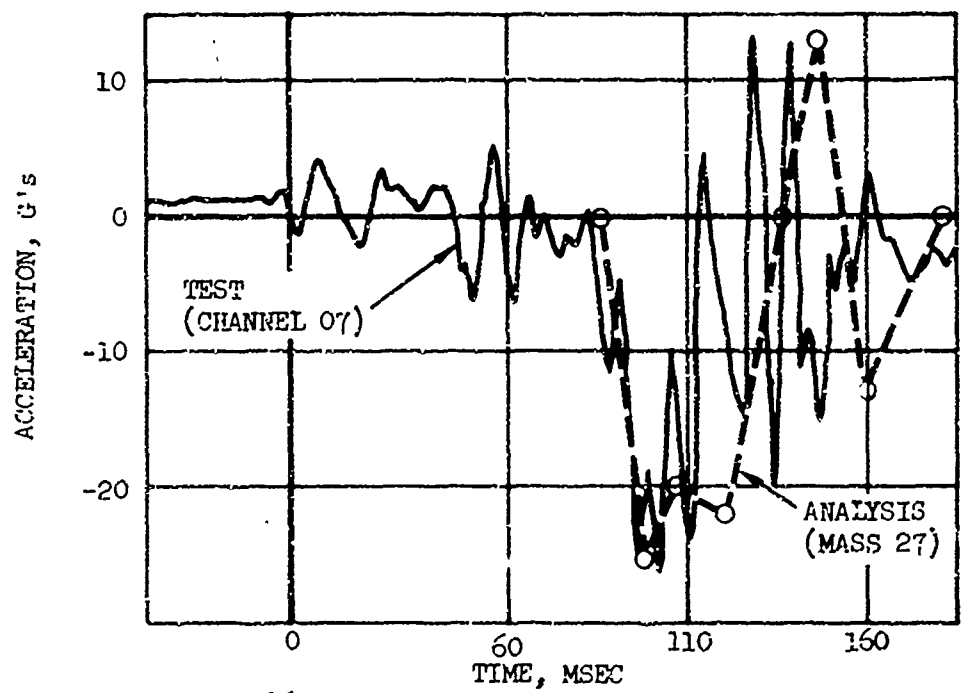

Figure 86. Correlation of Pilot Seat Pan Vertical Accelerations.

The comparison of analysis and test axial acceleration for the engine transmission as well as velocities and displacements is presented in the ANALYTICAL DATA section of Volume II. No attempt was made to improve the results in the axial direction since the purpose of the study is to develop a model to investigate combined vertical and lateral impacts.

The maximum engine and transmission member deflections are shown in Table XV. The values noted are in agreement with the summary of structural damage described earlier in Table XI.

TABLE XV. MAXIMUM MEMBER DEFLECTIONS OBTAINED BY ANALYSIS

	Vertical (in.)	Lateral (in.)
Engine - Member 4-7	.04	.17
Member 5-7	.13	.17
Transmission - Member 8-9	1.17	.48

VELOCITIES

The test velocities were obtained by numerically integrating the recorded accelerations. A trapezoidal rule was used which incorporated a .008 sec integration time interval. The integration routine required an input of initial velocities which were obtained from a review of the high-speed films. The integrated velocities are considered to provide valuable information regarding trends and for evaluating consistency of data. The absolute velocity values, however, must be viewed with caution since small offset accelerations due to structural damage, passenger and seat movement or channel noise, can show up as significant velocity values. For example, a 1G offset could alter the velocity after .2 sec by as much as .64 fps.

The correlation velocities are shown in Figures 87 through 90 for the floor vertical, floor lateral, transmission and engine, respectively. The trends are consistent with expectations. The analysis shows a slightly higher velocity change over the .2 sec time span of comparison.

DISPLACEMENTS

The test displacements represent total movement of the respective locations and were obtained by numerically integrating the recorded accelerations twice. The initial displacement, at impact, was assumed to be zero. Any errors in obtaining integrated velocities will also show up in the displacements. For example, the same .1G acceleration offset which

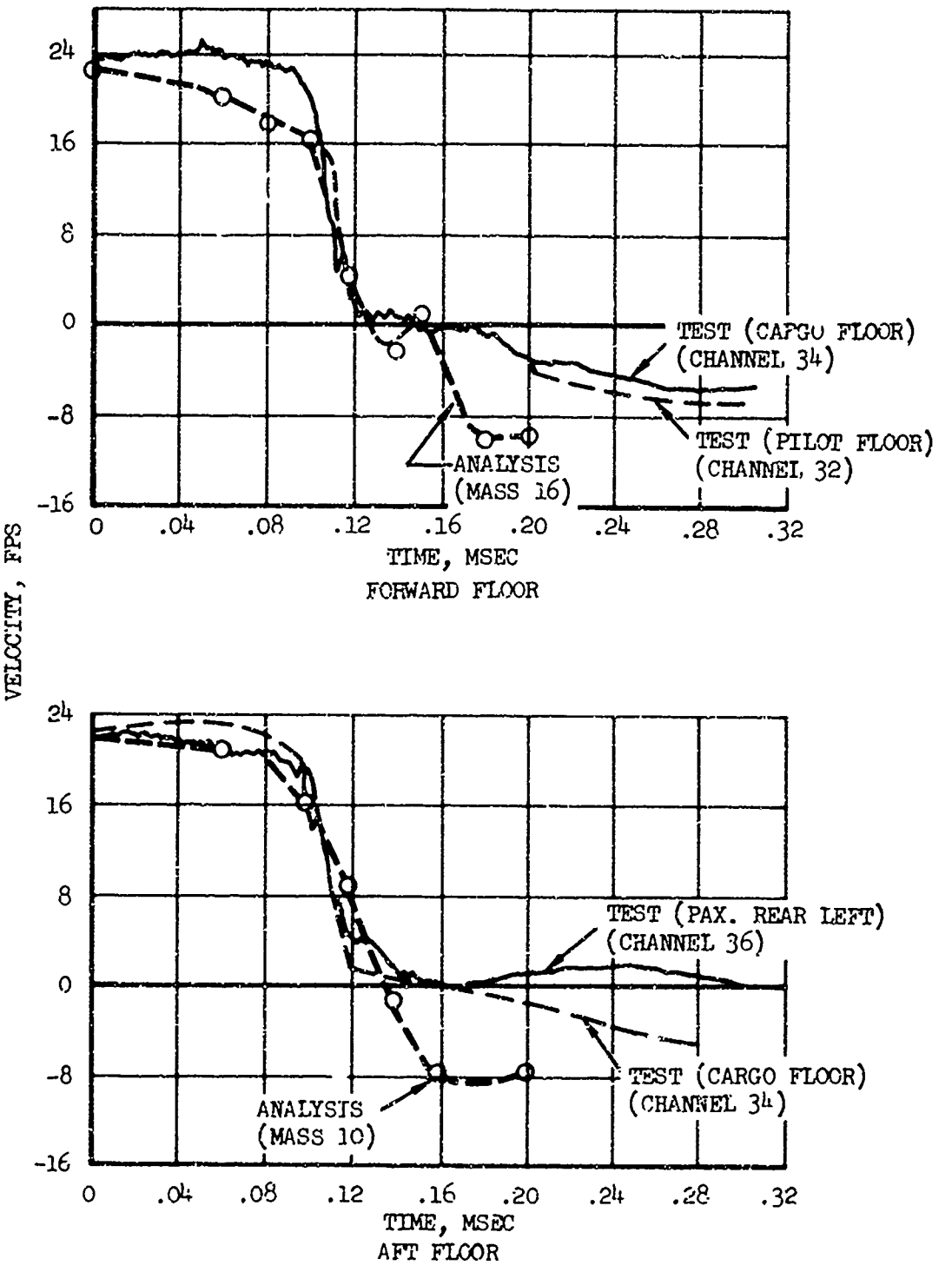

Figure 87. Correlation of Floor Vertical Velocities.

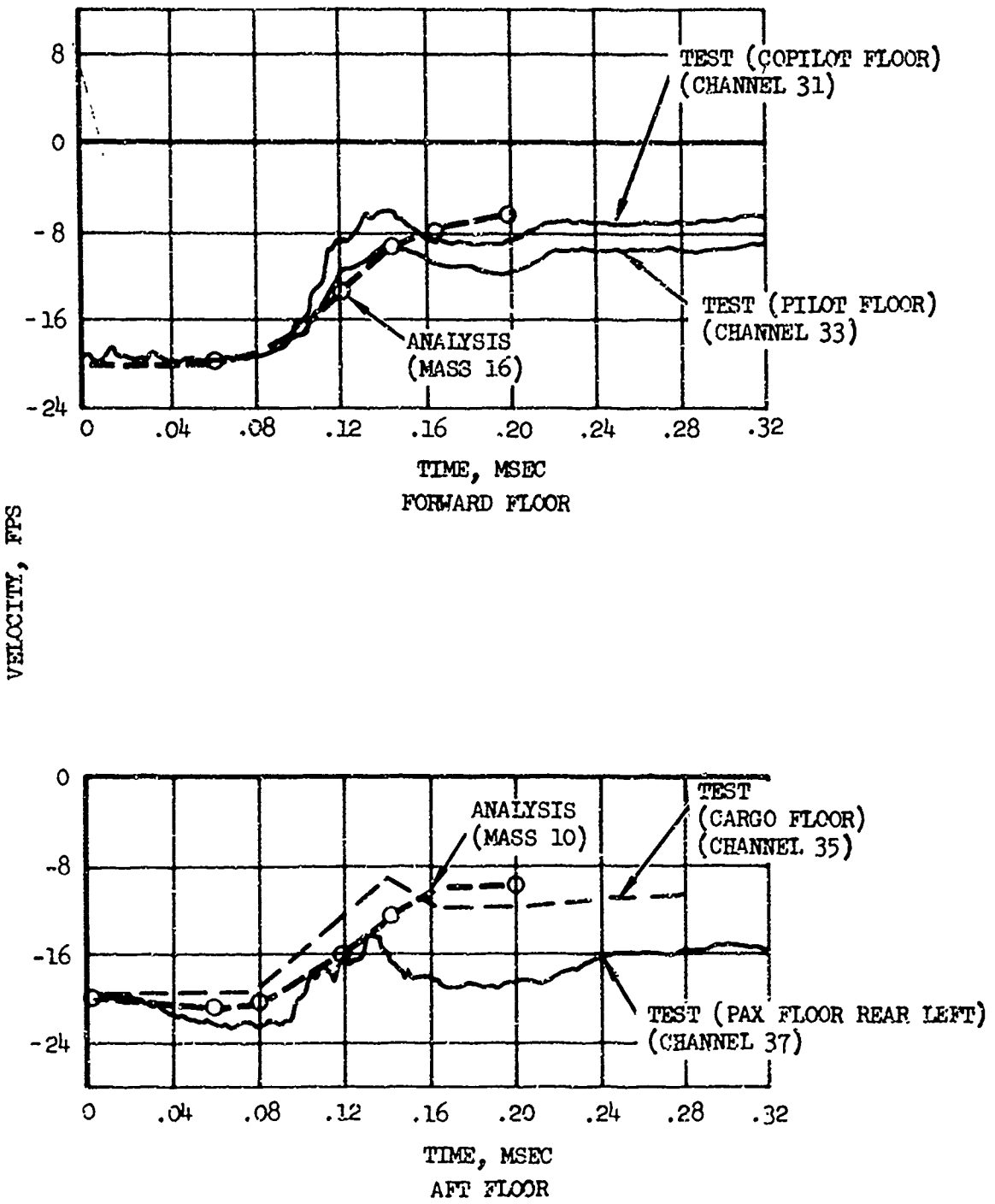

Figure 88. Correlation of Floor Lateral Velocities.

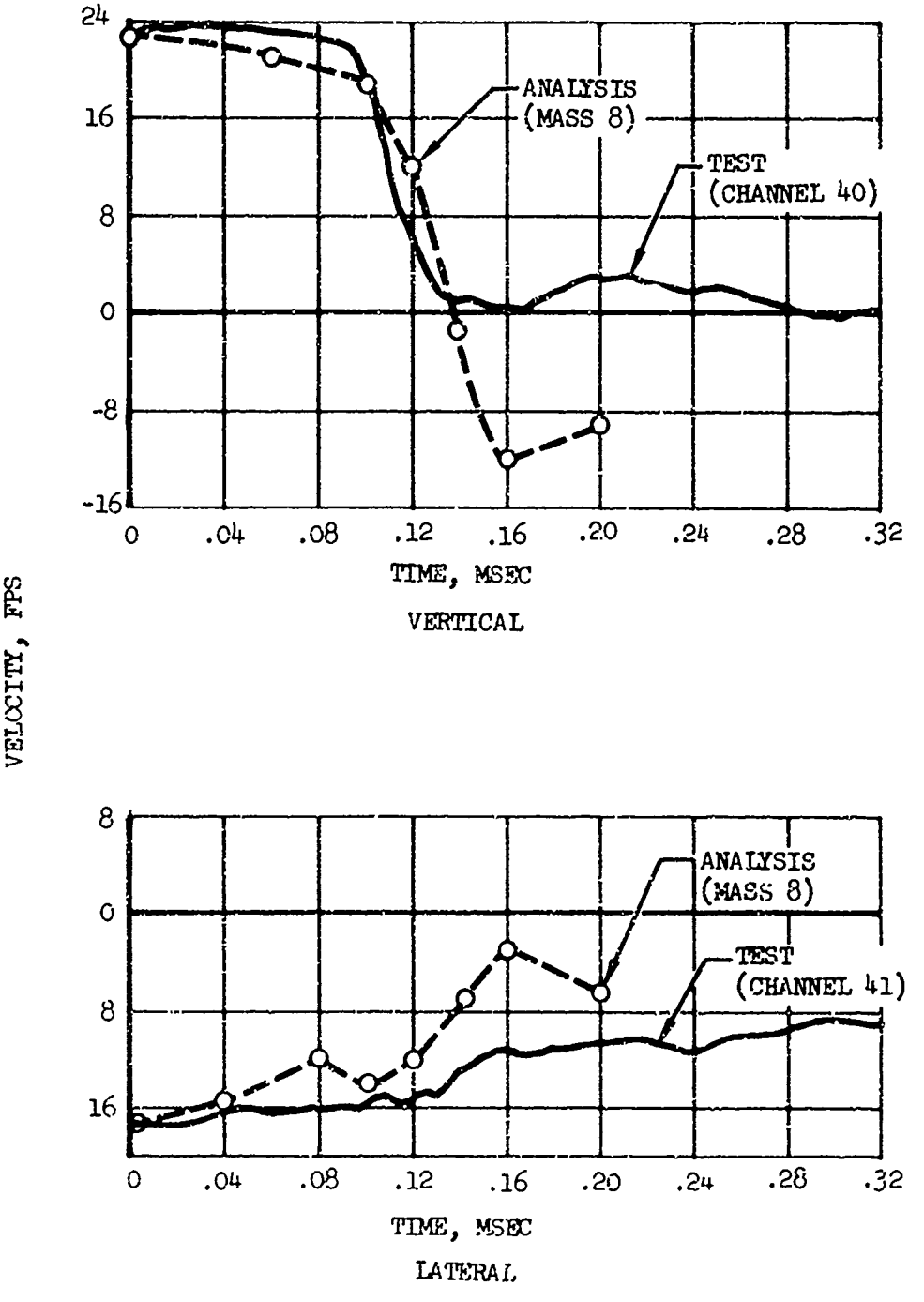

Figure 89. Correlation of Transmission Rotor Housing Velocities.

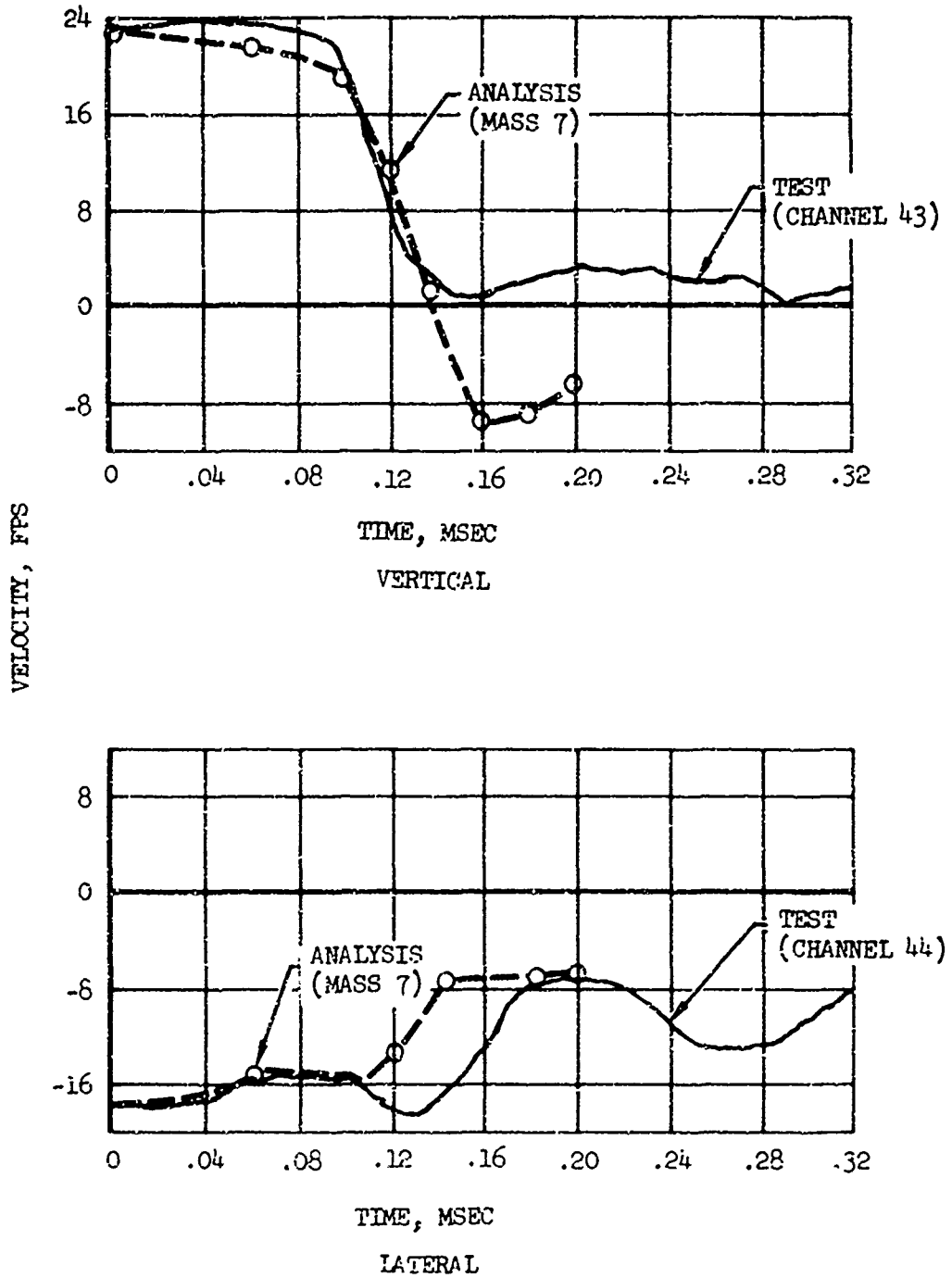

Figure 90. Correlation of Engine Velocities.

produced a .65-fps velocity difference after .2 sec will result in a .77-inch incremental displacement. For longer time periods the discrepancy can become quite pronounced.

Figures 91 through 94 show a comparison of test and analysis displacements for the floor vertical, floor lateral, transmission and engine, respectively.

The results compare very favorably in terms of rate of change and maximum displacements. The vertical displacements in the analysis reach a peak displacement at approximately 120 msec after impact and then return, indicative of rebounding. The test results show a steep rate of change for approximately 120 msec after impact; however, afterwards, there is either a gradual decline or a slight continuation of the increase. It is believed that the test data reflects a lower change in velocity than is being experienced. If one examines the velocity changes in Figure 87 and hypothesizes slightly reduced velocities (crossing zero) the effect will be to reduce the integrated displacements.

The complete set of test data, including recorded accelerations and strains, filtered acceleration data, integrated velocities and displacements, is presented in Volume II under TEST DATA. Also contained in Volume II is the output data from program KRASH which was utilized in the correlation.

DYNAMIC RESPONSE INDEX (DRI)

The comparison of the analysis results using the DRI model described previously in the section entitled DYNAMIC RESPONSE INDEX MODEL is shown, and the test data is shown in Table XVI.

Based on cumulative probability data of injury curves in Reference 2 (Figure 1-12) it could be expected that the probability of spinal injury, based on operational data, varies from .3 at the forward floor to $>.50$ at the aft floor. The cumulative probability of injury curves [2] are shown in Figure 95.

The following section contains further analysis concerning human tolerance criteria and utilizing the test data obtained from this program.

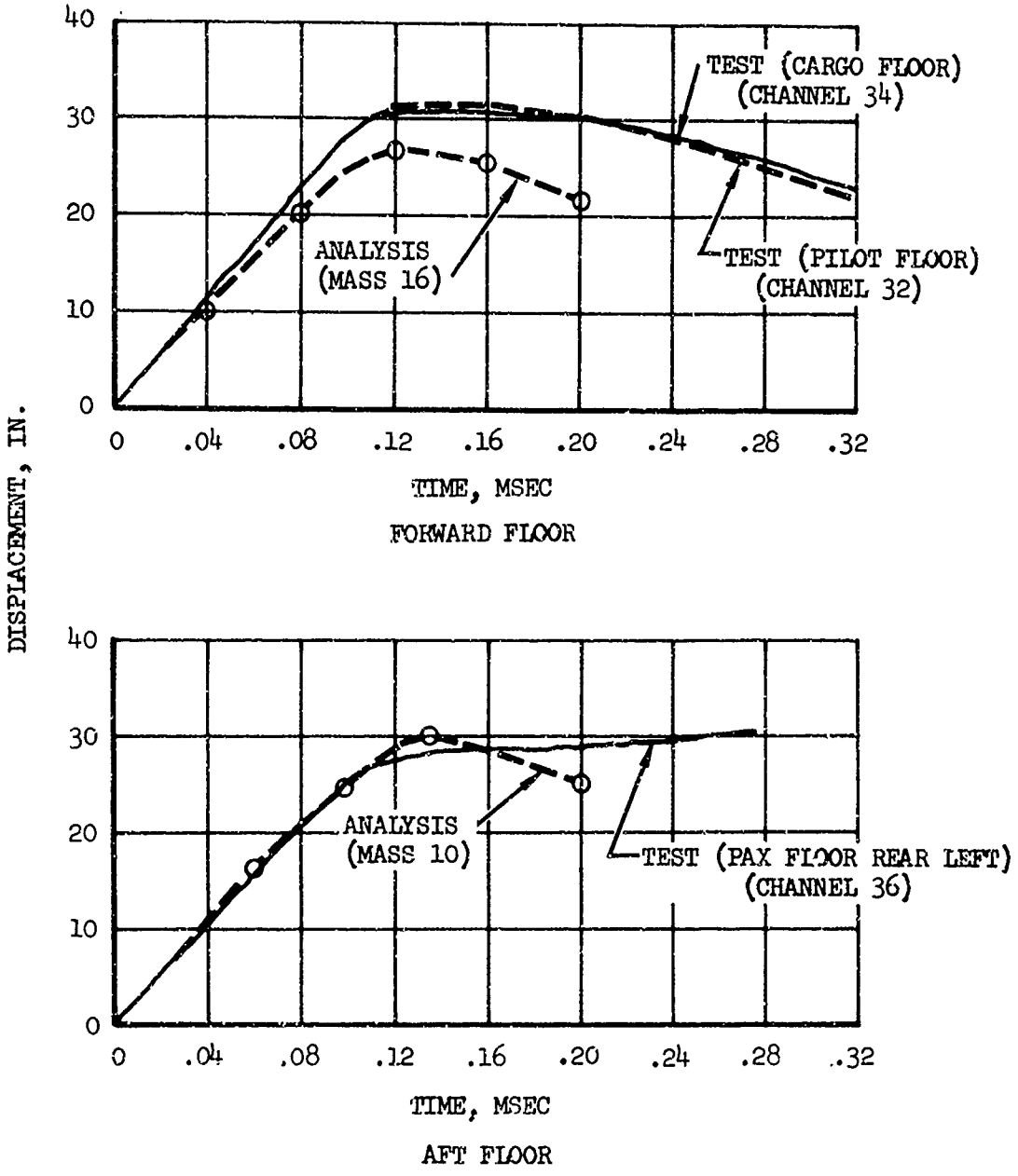

Figure 91. Correlation of Floor Vertical Displacements.

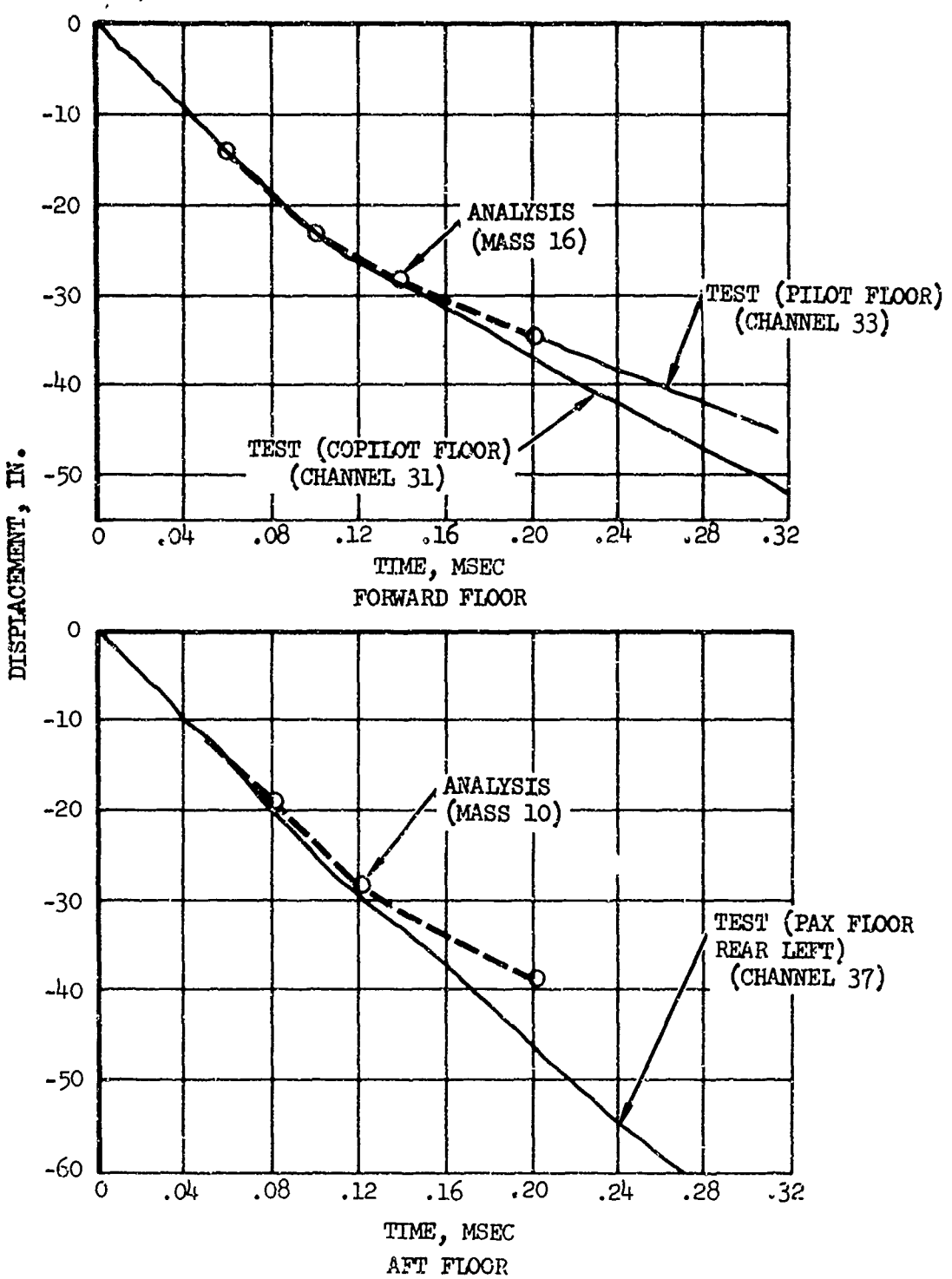

Figure 92. Correlation of Floor Lateral Displacements.

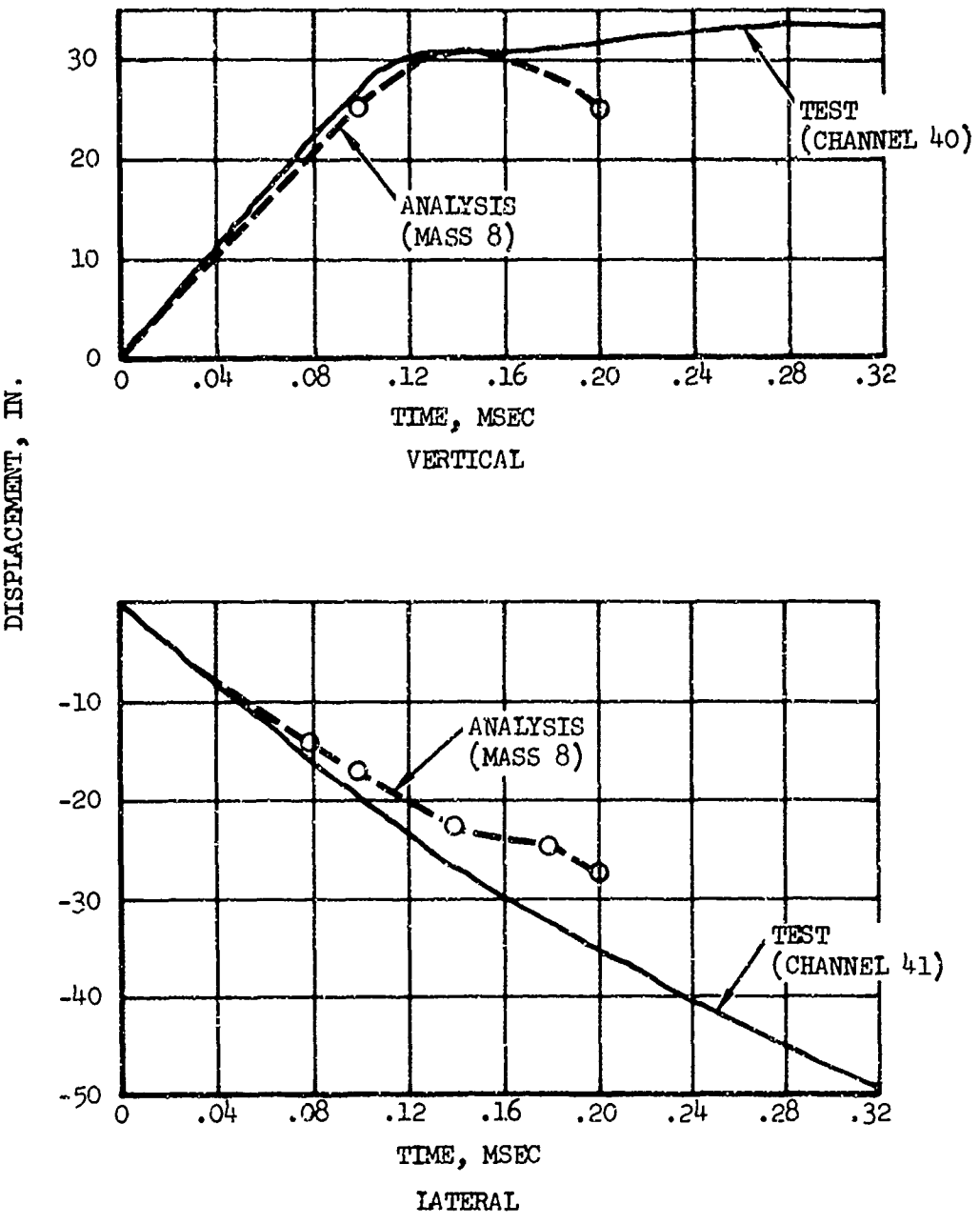

Figure 93. Correlation of Transmission Rotor Housing Displacements.

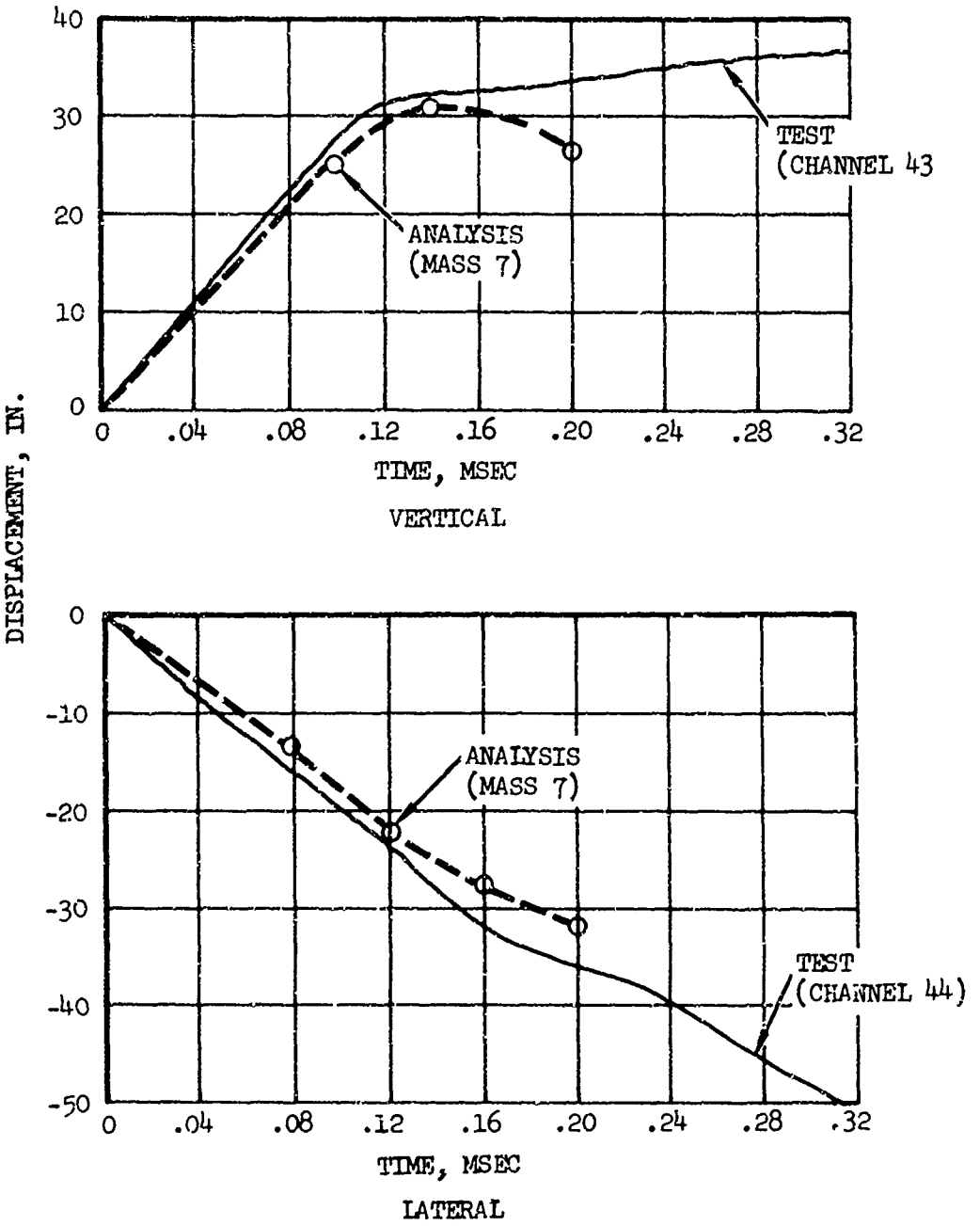

Figure 94. Correlation of Engine Displacements.

TABLE XVI. COMPARISON OF ANALYSIS AND TEST OCCUPANT RESPONSES AND DRI'S

	Peak Acceleration (G's)	DRI $\delta_{max}\left(\omega_n^2/g\right)$
Aft Mass 26 - Seat	23.2	-
28 - 10 Hz man	25.4	-
30 - DRI Model	24.7	27
Fwd Mass 27 - Seat	25	-
29 - 10 Hz man	24.7	-
31 - DRI Model	20.5	22
Passenger Pelvic (aft), Test Data	26	30

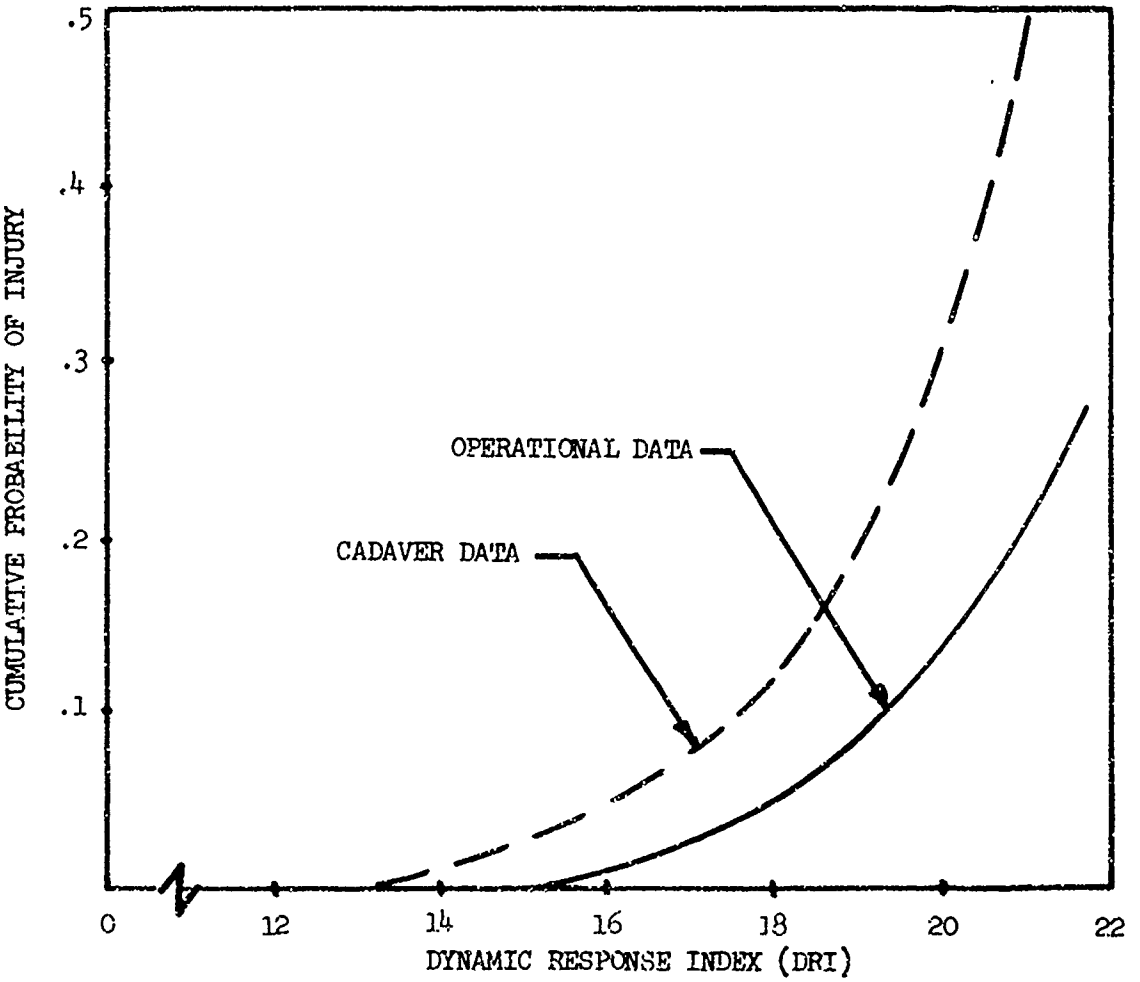

Figure 95. Probability of Spinal Injury Predicted from Cadaver Data Compared to Operational Experience (Figure 1-12, Reference 2)

HUMAN TOLERANCE CRITERIA CALCULATIONS

To assess the potential injury that the occupants would experience at the impact levels obtained during the drop test, the data was analyzed using the following severity indices:

- Dynamic Response Index
- The Air Force MIL-S-9479A Ejection Seat Acceleration Environment (28)
- Human Survival Limits Summarized in NASA Memo 5-19-59E (15)

Dynamic Response Index

The Dynamic Response Index (DRI) analysis was performed using the filtered test data obtained from the helicopter test. The upper torso of the human body was modeled as the single-lumped-mass, damped system shown in Figure 96. Assuming that the body mass acts upon the vertebrae to cause deformation, the response of the lumped mass was determined by idealizing the excitation as either a half sine pulse or a trapezoidal pulse. The DRI calculations in this section are based on the assumption that the seat is rigid and that the lumped mass represented the upper torso of the body. The equation of motion governing the dynamics of the problem obtained from Reference 41 is:

$$\frac{d^2\delta}{dt^2} + 2\zeta\omega_n \frac{d\delta}{dt} + \omega_n \delta = z$$

half sine pulse: (Figure 96)

$$z = \epsilon_p \sin \frac{\pi t}{\tau} \qquad 0 \leq t \leq \tau$$

trapezoidal pulse: (Figure 97)

$$z = \epsilon_p \frac{2t}{\tau} \qquad 0 \leq t \leq \tau/2$$

$$= \epsilon_p \qquad \tau/2 \leq t \leq \tau/2 + \tau_r$$

$$= -\epsilon_p \frac{2t}{\tau} \qquad \tau_r + \tau/2 \leq t \leq \tau_r + \tau$$

$$= 0 \qquad t \geq \tau + \tau_r$$

where τ = rise time

ϵ_p = maximum excitation

τ_r = time at peak excitation

t = time

ω_n, δ, ζ are defined in Figure 96

The model coefficients obtained from cadaver tests and presented in Reference 2 are:

ω_n = 52.9 rad/sec

ζ = .224

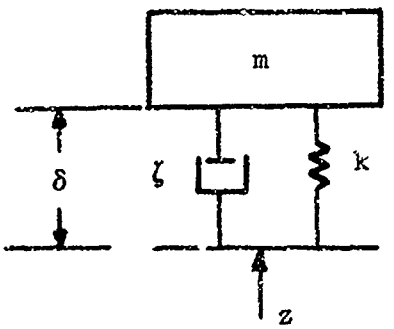

m = mass (lb-sec^2/in.)

δ = deflection (in.)

ζ = damping ratio

k = stiffness (lb/in.)

z = acceleration input (in./sec^2)

* DRI = $\frac{\omega_n^2 \cdot \delta_{max}}{g}$

ω_n = natural frequency of the model = $\sqrt{k/m}$ (rad/sec)

g = 386 in./sec^2

*Dynamic Response Index

Figure 96. Spinal-Injury Model (from Reference 2).

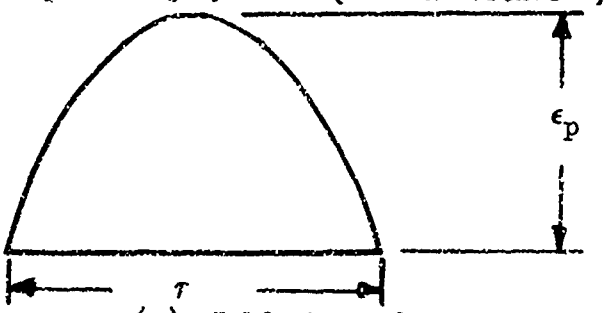

(a) Half sine pulse

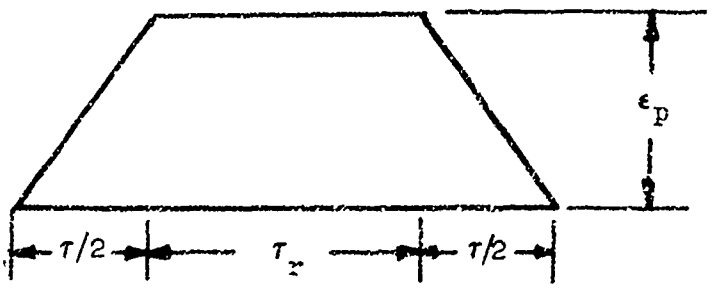

(b) Trapezoidal pulse

Figure 97. Idealized Pulse Shapes.

The results of the DRI analysis are shown in Tables XVII, XVIII and XIX. Table XVII summarizes the response parameters, τ, τ_r, Peak G's, and rate of onset for the filtered acceleration data of the pilot, copilot and instrumented passenger. Table XVIII presents the results of DRI calculations for the vertical accelerations at several locations (pilot and copilot seat pan and floor, and passenger floor) and compares this data with the measured passenger pelvic response.

Table XIX shows the probability of spinal injury as determined from Ref. 2 (Figure 1-12). Based on measured passenger (medical attendant) response data, the probability of spinal injury is between 30% (operational data) and 80% (cadaver data). DRI calculations from floor measurements located near the passenger indicate a higher probability of spinal injury (between 50% and 99.9%). DRI calculations based on pilot and copilot floor accelerations indicate a probability of injury up to 15%. The stiffness and damping coefficient for the anthropomorphic dummy representing the medical attendant are not known. However, it is highly unlikely that they are in agreement with the DRI model coefficients.

MIL-S-9479A (USAF) (28)

The Air Force bases the allowable ejection seat acceleration limits on the following expression (Reference 28):

$$\sqrt{\left(\frac{DRI_z}{G_{z_L}}\right)^2 + \left(\frac{G_y}{G_{x_L}}\right)^2 + \left(\frac{G_x}{G_{x_L}}\right)^2} < 1$$

Table XX presents results utilizing DRI calculations with a trapezoidal/triangular-shaped pulse and laterally measured floor accelerations. The axial accelerations are deemed to be relatively small compared to a minimum limit value of 20. In all cases the combined accelerations exceed 1, indicating excessive acceleration magnitude. Two of the values shown in Table XX are based on seat pan measurements which are consistent with the MIL Specification and are appropriate for accelerations measured on the seat.

Human Tolerance Limits (NASA Memo 5-19-59E) (15)

The test results were compared to data published in NASA Memo 5-19-59E (Reference 15). A comparison of the peak acceleration obtained during the test and estimated durations with headward acceleration vs. duration of applied acceleration curves of Reference 16 (Figure 17) indicates that the copilot, pilot and medical attendant would all incur at least moderate injuries. The passenger could be expected to sustain severe injury. A

TABLE XVII. RESPONSE PARAMETERS - TRAPEZOIDAL DATA

DATA CHANNEL	ACCELERATION LOCATION	τ	τ_r	PEAK G'S	RATE OF ONSET G/SEC
07	Pilot Seat Pan - Vertical	25	15	25	2000
08	Pilot Seat Pan - Lateral	80	20	34	860
09	Copilot Seat Pan -Vertical	6	4	60	16600
10	Copilot Sea Pan -Lateral	60	30	19	640
30	Copilot Floor Vertical	25	15	24	1920
31	Copilot Floor Lateral	90	10	25	555
36	Passenger Floor Vertical	25	15	42	3300
48	Passenger Pelvic Vertical*	40	20	26	1100

*All data except the passenger pelvic vertical acceleration is based on 100-cps filtered test data. The passenger pelvic acceleration data is obtained from the raw data.

**τ, τ_r units are in msec.

TABLE XVIII. DYNAMIC RESPONSE INDEX - VERTICAL ACCELERATIONS*

ACCELEROMETER LOCATION	DATA CHANNEL	HALF SINE PULSE**				TRIANGULAR/TRAPEZOIDAL PULSE			
		(msec)	τ/T	AF	DRI	τ/T	τ_r/T	AF	DRI
Pilot Seat Pan	07	40	.32	.6	15	.2	.11	.75	18.3
Copilot Seat Pan	09	10	.065	.25	15	.05	.03	.25	15.0
Copilot Floor	30	40	.32	.6	15	.2	.11	.75	18.
Passenger Floor	36	40	.32	.6	25.2	.2	.11	.75	31.5
Passenger Pelvic Accel. (measured)	48	--	--	--	26	--	--	--	26.

NOTES:

τ, τ_r - defined in Figure 97, units are in msec

AF - amplification factor

DRI - dynamic response index

T - natural period of response = .125 sec

* - Reference 2 (page 26)

** - Reference 41 (pages 8-30 and 8-48)

TABLE XIX. PROBABILITY OF SPINAL INJURY*

ACCELERATION LOCATION	DATA CHANNEL	HALF SINE PULSE		TRAPEZOIDAL PULSE	
		P(O)	P(C)	P(O)	P(C)
Pilot Seat Pan	07	0	.02	.07	.15
Copilot Seat Pan	09	0	.02	0	.02
Copilot Floor	30	0	.02	.07	.15
Passenger Floor	36	.5	.99	.99	.999
Passenger Pelvic	48	.3	.8	.3	.8

NOTES:

P(O) - Probability of Spinal Injury predicted from operational data.

P(C) - Probability of Spinal Injury predicted from cadaver data.

* - Reference 2

TABLE XX. DYNAMIC RESPONSE - MIL-S-9479A (USAF)*

ACCELEROMETER LOCATION	G_y/G_{y_L}	DRI/G_{z_L} ****	$\sqrt{\Sigma \text{ SQUARES}}$ **
Pilot Seat Pan	2.3	3.0	3.75
Copilot Seat Pan	1.3	2.5	2.8
Copilot Floor	1.67	3.0	3.4
Passenger Floor	2.0 ***	5.25	5.6

NOTES:

G_x, G_y, G_z = Measured G's in x, y, z axis

G_{X_L}, G_{y_L}, G_{z_L} = Limit G's in x, y, z axis

G_{y_L} = 15, G_{z_L} = 6 ($\tau/2 < 40$ msec), G_{z_L} = 12 ($\tau/2 > 40$ msec)

* Reference 28

** $\sqrt{\Sigma \text{ Squares}} = \sqrt{\left(\frac{G_x}{G_{x_L}}\right)^2 + \left(\frac{G_y}{G_{y_L}}\right)^2 + \left(\frac{DRI}{G_{z_L}}\right)^2}$

*** Estimated from raw data plots

**** DRI values obtained from Table XVII for triangular/trapezoidal pulse

similar comparison shows that (Reference 15, Figure 20) for acceleration versus initial rate of change of headward acceleration, all the responses either exceed a tolerable situation or result in permanent injury, depending on the occupant's seating location. The occupants in the test vehicle had different supports from those that the reference test data is based on; thus, exact comparisons are difficult.

A comparison of data in the lateral direction is difficult due to a lack of reference material. The human tolerance limits for spineward acceleration can be applied for the rear passengers only since they face the direction of impact. The test data for the rear passenger floor indicates that the passenger can experience moderate to severe injury due to the acceleration levels. In addition, due to the rate of onset acceleration, the passenger may experience severe shock.

CORRELATION WITH ADDITIONAL TEST DATA

To obtain additional information with which to improve program KRASH's capability to determine structural response during a crash, a comparison was made between 30 fps vertical velocity test data, published in Reference 3, and the analytical results using the 31-mass correlated math model. Refinements to the input data were made, as required, to improve the vehicle representation. The 30 fps vertical velocity test data provides information at a potentially higher percentile accident level than the 23 fps impact velocity data obtained during Phase III drop test and, thus, affords an opportunity to exercise additional program logic. The comparison with published data from Reference 3 was satisfactory in the following respects:

- the time of occurrence for peak floor accelerations
- peak floor acceleration levels (taking into account the effect of low-pass filtering)
- initial peak transmission and engine acceleration levels
- maximum transmission mount deflection

However, the time of engine and transmission peak accelerations does not agree with the published data.

The published test data for the engine and transmission is a time history of the respective responses. Whereas one would expect initial peak decelerations to occur shortly after peak floor decelerations are experienced (70 msec after impact), the test data indicates that the engine experiences its first peak deceleration 140 msec after impact. The transmission test data shows peak decelerations of approximately -40 G's at 115 msec after impact before it experiences -70 G's at 170 msec after impact. The time of occurrence of the initial engine and transmission peak deceleration, obtained by the analysis, appears more consistent with expectations.

The analysis also differs from the test data in that the engine-mount analytically determined deflections, using the correlation model, are much lower than observed in the test photographs.

A peak vertical deflection of 2.8 inches was obtained using a softer engine mount representation than that shown in Figure 37. However, the peak acceleration levels were lower than desired. A more detailed discussion on the modeling of engine mounts is presented in the RESULTS OF THE PROGRAM Section under CORRELATION.

The comparative results between the analysis and 30 fps vertical velocity drop test data are shown in Table XXI.

TABLE XXI. COMPARISON OF ANALYSIS AND PREVIOUS 30 fps VERTICAL VELOCITY DROP TEST DATA

	Test Data	Analytical Results
Peak Acceleration (G's)		
Engine	50*	48.2****/26*****
Transmission	40/70	37.5/61.2
Floor	75	44 to 51.4
Time of Occurrence (msec)		
Engine	145	82
Transmission	120/175	68/88
Floor	55 to 70	56 to 72
Peak Deflections (in.)		
Engine Mount	2 - 3**	.3****/2.8*****
Transmission	2.5 - 3***	1.62

NOTES:

* A second peak acceleration of 90 G's occurs at 160 msec after impact.

** Obtained from review of posttest damage photographs (average of left and right side).

*** Noted in Reference 3 text.

**** Using engine mount as modeled in Figure 37. At a 42-fps vertical velocity the analysis shows a 2.06-inch deflection.

***** Using a soft engine mount described in the RESULTS OF THE PROGRAM Section under CORRELATION.

PARAMETER STUDIES

GENERAL

The mathematical model of the UH-1H helicopter, refined during the correlation with drop test data, was used in the parameter studies. The parameter variations were performed to ascertain the structural behavior of the airframe due to changes in the load carrying capability of the structural elements, particularly the landing skids, lower fuselage, seat system, engine and transmission mounts. The results of the parameter studies are closely linked to the development of improved design criteria and concepts. Parameter studies were conducted for potentially survivable accident levels between the 50th and 95th percentiles. The initial roll, pitch and yaw angles and angular velocities are zero so as to minimize the number of variables that can affect the final results. Further rationale for this decision is that while the crash environment (impact velocities) is statistically determined, the initial angles and angular velocities are not clearly defined. The effect of changes in these initial conditions, although worthy of consideration, would require a substantially larger matrix of parameter variations and presents difficulties in substantiating the probability of occurrence from experience.

The parameter studies encompass the following:

- The response acceleration for pure vertical velocity impact at the 50th, 75th and 95th percentile potentially survivable accident.
- The response acceleration for combined vertical and lateral velocity impact in which each of the velocity impacts are simultaneously at their respective level for the 50th, 75th and 95th percentile potentially survivable accidents.
- The potential of spinal injury as measured by the DRI as a function of the impact speed over the range of the 50th to 95th percentile potentially survivable accident.
- The effect on response accelerations and/or stroke requirements of changes in load-stroke characteristics of the landing skid, lower fuselage, seat system, engine and transmission.
- The relationship between incremental weight and cost associated with structural changes necessary to achieve a more crashworthy design at the higher (75th and 95th) percentile potentially survivable accidents.

From the review of the 32 accident data cases, performed in Phase I, twelve cases were noted to have simultaneous vertical and lateral ground impact velocities. Figure 98 represents an envelope of vertical velocity versus lateral velocity. At the extremes are the current 95th percentile levels for a vertical impact (42 fps) and a lateral impact (30 fps). The data from the accident cases presented in Table I are plotted on the figure. A first approximation indicates the envelopes for 50th, 75th and 95th percentile potentially survivable accidents. For purposes of this report the envelope shown in Figure 98 will be referred to as the 50th, 75th and 95th percentile for a combined vertical-lateral potentially survivable impact. It is recognized that the limited accident data obtained in Phase I does not allow for an accurate statistical representation of the envelopes, however, for comparative purposes, it does allow the parameter studies to be put in proper perspective.

Therefore, the parameter studies are identified by the following conditions:

TABLE XXII. ACCIDENT CONDITIONS INVESTIGATED

Condition	Velocities (fps) Vertical	Lateral	Approximate Potentially Survivable Accident Percentile
A	24	0	50th - vertical
B	30	0	75th - vertical
C	42	0	95th - vertical
D	24	17.1	70th - combined vertical-lateral
E	30	22.4	95th - combined vertical-lateral
F	42	30.0	95th vertical - 95th lateral
G	23	18.5	70th - combined vertical-lateral (Phase III drop test level)

The correlation results obtained during Phase III of this program provided analytical verification at approximately the 70th percentile potentially survivable accident level for a combined vertical-lateral impact condition. Comparison of analysis with previous vertical drop test data at the 75th percentile potentially survivable accident level indicated that the model understated the engine deflections obtained during the test. The lack of additional test data to verify major element lateral and rotational stiffnesses, failure modes and structural unloading and reloading paths at the higher impact energy levels indicates that the major significance of the parametric studies is in developing trends and is not to be viewed as a precise measure of dynamic response. However, to be meaningful the parametric studies should be related to quantitative measures. Table XXIII sets forth some quantitative yardsticks by which the results of the parametric studies are evaluated. The deflections noted in Table XXIII, obtained from the results of the correlation studies, are intended as a

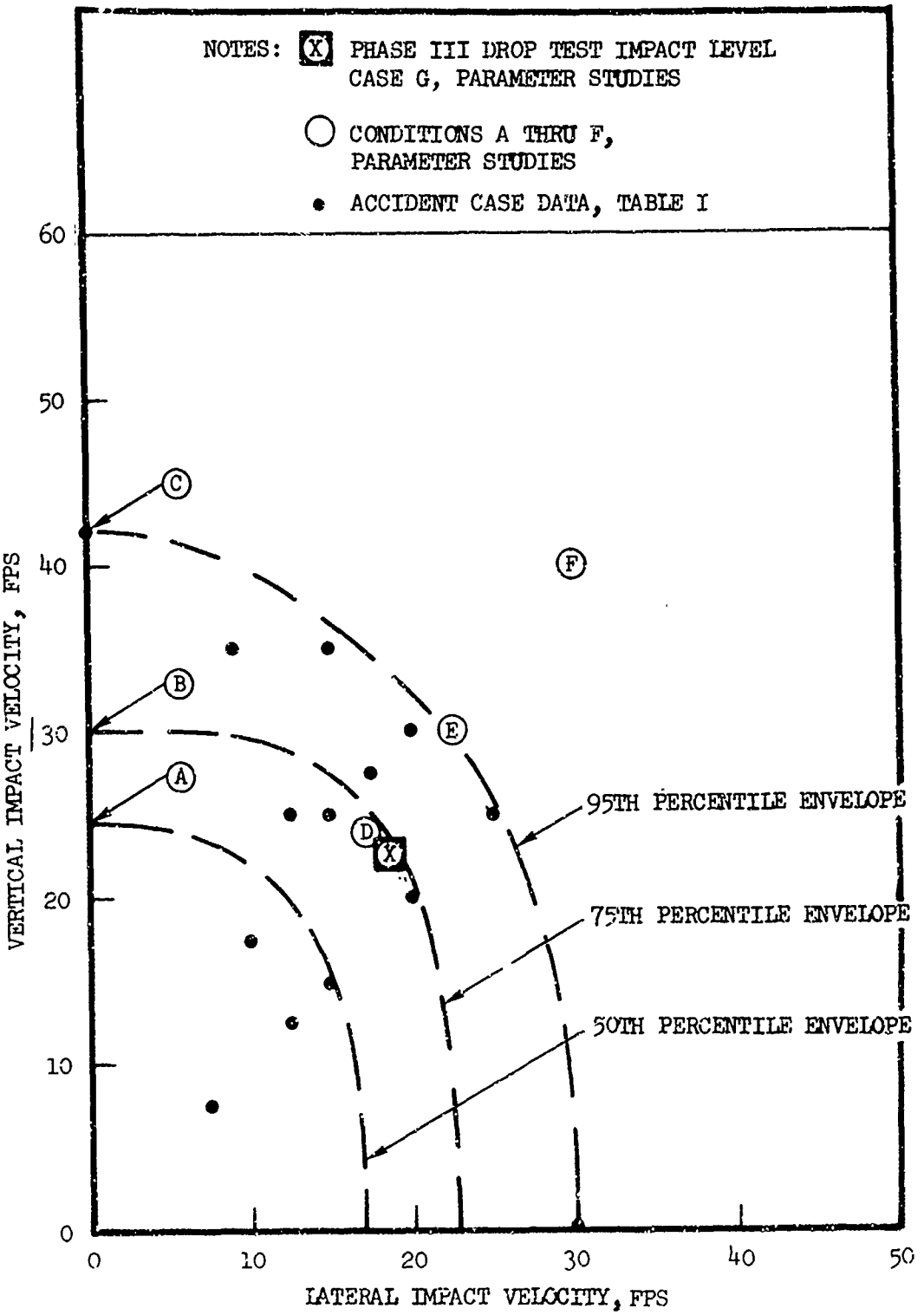

Figure 98. Combined Vertical-Lateral Percentile Potentially Survivable Accident Envelope.

"base point" or "reference" to which the various design configuration changes are compared to determine if adequate crashworthiness can be achieved. The values noted in Table XXIII are not intended as absolute measures of design limits since they are based on an analytical representation which by its very nature represents a compromise between reality and practicality. To provide flexibility and in recognition of analytical modeling limitations, the response deflections obtained during the parametric studies which are between the range of values noted in Table XXIII are considered to be of marginal crashworthiness capability.

TABLE XXIII. ANALYSIS DEFLECTION LIMITS (IN.)

Structural Elements	Acceptable if Deflection is Less than	Unacceptable if Deflection is Greater than	Analytical Results With Correlation Model
Engine vertical	.12	.16	.13
Engine lateral	.2	.24	.17
Transmission vertical	.75	1.17	1.17
Transmission lateral	.5	.6	.48
Pilot/Copilot seat vertical	.15	.2	.16
Medical Attendant seat vertical	.3	.4	.4

Based on operational data presented in Figure 95, the probability of spinal injury for a DRI measurement equal to 15 is nil while a DRI equal to 19.3 represents a 10% probability of spinal injury. For the purpose of this study, it is desired to achieve a probability of spinal injury $\leq$ 10% in order to be crashworthy.

INDIVIDUAL PARAMETER VARIATIONS

Table XXIV shows the results of the individual parameter variations. Included are response accelerations, DRI's and deflections. The individual parameter variations cover a wide spectrum including requirements of MIL-S-58095 (Reference 31) and UTTAS specifications (Reference 37). At the same time, the parameter studies cover changes to load levels and/or strokes for the landing skids, lower fuselage, seat, engine and transmission. Consequently, in some cases only one percentile accident condition was investigated.

TABLE XXIV. SUMMARY OF INDIVIDUAL PARAMETER VARIATION RESULTS

Case No.	Identification	* Percentile Accident	Occupant Response				Transmission Response				Engine Response			
			Forward		Rear		Vertical		Lateral		Vertical		Lateral	
			DRI	Δ(In.)	DRI	Δ(In.)	G_{Peak}	Δ(In.)	G_{Peak}	Δ(In.)	G_{Peak}	Δ(In.)	G_{Peak}	Δ(In.)
1	Basic Vertical Velocity Only	A	16	.115	27	.5	42.7	.932	-	-	32.4	.142	-	-
2	Same as Case No. 1	B	32.4	.25	40.7	.74	61.2	1.57	-	-	49.7	.25	-	-
3	Same as Case No. 1	C	57.5	.42	64.3	1.16	120	2.1	-	-	74.5	1.39	-	-
4	Basic Combined Vertical-Lateral Velocity	D	22	.164	29	.51	34	.982	8	.22	33.3	.145	10.6	.095
5	Same as Case No. 4	E	35.5	.25	41.1	.71	65	1.76	10	.39	47.7	.247	14.3	.126
6	Same as Case No. 4	F	60.4	.4	63.5	1.1	128	2.36	16	.69	72.1	1.52	36.8	.22
7	Increase Landing Skid Limit Load From 25,000 to 50,000 LB	E	21	.165	32.6	.6	96	2.55	14.3	.22	39.8	.182	18.7	.21
8	Increase Landing Skid Stroke From 12 to 20 inches	E	24	.176	30.5	.57	77	2.38	16	.26	36	.14	20	.1
9	Increase Lower Fuselage Load Limit From 60,500 to 121,000 LB	E	30	.22	41	.7	58	.96	13.5	.23	64	.32	22	.18
10	Same as Case No. 9	F	58	.515	55.5	1.14	122	1.92	15	.26	82	2.3	40	.35
11	Increase Lower Fuselage Stroke From 3.5 to 7 inches	E	26.5	.2	35	.64	48	1.25	12.7	.18	43	.21	14	.08
12	Same as Case No. 11	F	54	.39	59	1.07	89	2.0	13	.23	68	14	36	27.5
13	Increase Load Level and Stroke per Fuselage Bumper	F	53	.29	61	1.05	69	2.6	18	.31	35.4	.52	39.7	.207
14	Seat Load = 2015 LB, Stroke = 12 In. per MIL-S-58095	E	17	>12	15	>12	-	-	-	-	-	-	-	-
15	Same as Case No. 14 except load = 1878 lbs. Stroke = 20 In.	E	15.8	>20	15.2	>20	-	-	-	-	-	-	-	-
16	Transmission Load Limit = 20 G's Vertical, 18 G's Lateral	E	-	-	-	-	90	1.4	13	.2	-	-	-	-
17	Same as Case No. 16	F	-	-	-	-	133	1.88	14	.4	-	-	-	-
18	Engine Load Limit = 20 G's Vertical, 18 G's Lateral	E	-	-	-	-	-	-	-	-	40.8	.987	15.0	.305
19	Engine Load Limit = 20 G's Vertical, 18 G's Lateral	G	-	-	-	-	-	-	-	-	25.6	.189	12.0	.356
20	Engine Load Limit = 20 G's Vertical, 8 G's Lateral	G	-	-	-	-	-	-	-	-	26.0	.210	11.6	1.79

NOTE: *See Table XXII

Table XXIV shows the response of the engine, transmission, and forward and rear occupants for the condition defined in Table XXII. The occupant response is the DRI, not an acceleration. The DRI as noted earlier is based on the maximum spinal compressive deflection and differs somewhat from the acceleration value.

The transmission mounts are expected to fail for accident conditions B, C, E and F as a result of the deflections exceeding the mount deflection limit of 1.17 inch. For accident condition F the peak acceleration level occurs during a secondary impact at which time the transmission support mounts have bottomed and the transmission stiffness is associated with the adjacent pylon structure. The analysis also indicates that the transmission mount has experienced an unloading and subsequent reloading cycle. In condition F, the maximum transmission vertical deflection is 2.4 inches.

The engine is satisfactory in accident conditions A and D. However, for conditions B, C, E and F the engine support loads are such that the supports experience deflection in the inelastic regime and permanent deformation results.

The engine vertical deflections for condition C is shown in Table XXIV to be to 1.39 inches. This value is considerably lower than deflections noted in previous tests. However, an updated model of the engine mounts yields considerably more deflection (2.8 inches). The results, using the different engine mount configurations, are discussed later in this section and in the RESULTS OF THE PROGRAM Section under CORRELATION.

The DRI measurement at the forward fuselage station shows readings of 16, 32 and 57 for the accident conditions A, B and C, respectively. For condition A, the probability of spinal injury for operational data (Reference 2) is only .01. However, for conditions B and C, this probability increases to a value greater than .5. The DRI measurement for the aft occupant indicates that for all three percentile accident levels investigated, the probability of injury is in excess of .5.

Landing Skids

The landing skids offer the first line of resistance to the impact forces. The results of the drop test performed during this program indicated that prior to fuselage contact with the ground, the skids absorbed energy such that the vertical velocity was reduced approximately 10% from initial impact. This represents approximately 20% of the kinetic energy. The amount of energy absorbed is based on the reduction in vertical descent velocity. During a combined vertical-lateral impact the exact amount of vertical energy absorbed is difficult to determine due to such effects as binding. To ascertain the effect of changes in the landing skid load deflection characteristics, computer runs were made to evaluate individually an increased load limit (100%) and an increased stroke (67%). The

results of cases 7 and 8 in Tables XXIV and XXV show that the most significant reduction is obtained for the occupant responses. However, for accident condition E, the improvement is not large enough to reduce the probability of injury to below 10%.

TABLE XXV. LANDING SKID PARAMETER VARIATION RESULTS (ACCIDENT CONDITION E)

CONDITION	FORWARD		REAR		ENGINE		TRANSMISSION	
	DRI	Δ*	DRI	Δ*	G_{VERT}	$*\Delta_{VERT}$	G_{VERT}	$*\Delta_{VERT}$
Basic (Case 5)	35.5	.25	41.1	.71	47.7	.247	61.2	1.76
Load Limit (Case 7)	21	.165	32.6	.6	30.8	.182	96	2.5
Load Stroke (Case 8)	24	.176	30.5	.59	36	.14	77	2.38

* Units are in inches

Fuselage

The fuselage is considered to be the most significant region in which improved crashworthiness design can be achieved, and consequently several computer runs were performed at various percentile accident levels. These included:

- Increased fuselage load limit
- Increased fuselage stroke
- Two stage load limit fuselage

The results shown in Tables XXIV and XXVI indicate that the use of the two-stage fuselage significantly reduced the engine vertical accelerations from 72 G's to 35 G's and the engine deflections from 1.52 inches to .52 inches for accident condition F. The transmission, whose accelerations were nearly halved using the two-stage fuselage, shows an increase in deflection. The use of the higher fuselage load limit and stroke showed slight improvements compared to the basic case.

Seat System

The seat load stroke curve per Figure 3 of MIL-S-58095 (Reference 31) was incorporated into the model and the effect on the DRI's was noted. Seat

TABLE XXVI. FUSELAGE PARAMETER VARIATION RESULTS

Percentile Accident Condition	Configuration	Occupant				Engine		Transmission	
		Forward		Aft					
		DRI	Δ^*_{Seat}	DRI	Δ^*_{Seat}	$G_{Peak,Vert.}$	Δ^*_{Seat}	$G_{Peak,Vert.}$	Δ^*_{Seat}
Condition E	Basic (case 5)	35.5	.25	41.1	.71	47.7	.247	61.2	1.76
	Increased Fuselage Load Limit (case 9)	30	.22	41	.7	64	.32	58	.96
	Increased Fuselage Load Stroke (case 11)	26.5	.20	38	.64	43	.21	48	1.25
Condition F	Basic (cases 6)	60.4	.4	63.5	1.1	72.1	1.52	128	2.36
	Increased Fuselage Load Limit (case 10)	58	.52	65.5	1.14	82	2.3	122	1.52
	Increased Fuselage Load Stroke (case 12)	54	.39	59	1.07	68	1.4	89	2.0
	Two Stage Fuselage (case 13)	53	.29	61	1.05	35.4	.52	69	2.6

* Seat - Units are inches.

stroke lengths of 12 inches and 20 inches were studied. (12 inches is the minimum required stroke per Reference 31.) The results shown in Tables XXIII and XXVII indicate that the DRI's improve immensely. With a load level of 2015 lbs. the maximum DRI for condition E is 17 at the forward and 15 at the aft. Although the DRI indicate less than a 10% probability of spinal injury, the analytical results indicate that the seats are expected to exceed the minimum stroke requirement of 12 inches.

TABLE XXVII. SEAT PARAMETER VARIATION RESULTS (ACCIDENT CONDITION E)

CONFIGURATION	FORWARD		AFT	
	DRI	Δ(in.)	DRI	Δ(in.)
Basic (Case 5)	35.5	.25	41.1	.71
Per MIL-S-58095 12 in. Stroke (Case 14)	17	>12	15	>12
Per MIL-S-58095 20 in. Stroke (Case 15)	15.8	>20	15.2	>20

Transmission

The transmission load limit was raised to 20 G's (vertically) and 18 G's (laterally). These values correspond to the initial stiffness of the transmission on the mounts. After the mount bottoms, it is assumed that the stiffness increases as the transmission contacts adjacent support structure. It is this stiffness which actually results in the peak acceleration levels. For example, during the combined vertical lateral drop test the transmission experienced between 27 and 30 G's, which is considerably higher than the current crash loads design requirement (8 G's), and survived the impact in good condition. However, the longitudinal crash-loads requirement is also 8 G's and this was not reached during the Phase III drop test, indicating that the longitudinal is perhaps the most critical direction. The parametric results are shown in Table XXIV and XXVIII. For both condition E and F peak acceleration levels increase and the maximum deflections decrease due to the increased stiffness. The vertical deflections, however, are not reduced significantly below the minimum required value. The lateral deflections are reduced to acceptable levels.

TABLE XXVIII. TRANSMISSION PARAMETER VARIATION RESULTS					
PERCENTILE ACCIDENT CONDITION	CONFIGURATION	VERTICAL		LATERAL	
		G	Δ(in.)	G	Δ(in.)
E	Basic (Case 5)	61.2	1.76	10	.39
	Transmission Load Level (Case 16)	90	1.4	13	.2
F	Basic (Case 6)	128	2.36	16	.69
	Transmission Load Level (Case 17)	133	1.88	14	.4

Engine

The engine parameter studies vary somewhat from the other parameters (landing gear, transmission, fuselage) because at the onset of the parameter investigation, the engine was modeled as noted to obtain agreement with the Phase III drop test data. However, during the course of the parameter studies, an improved engine model was obtained which provided more consistent high-energy impact results. The improved model required:

- revised load-deflection curves
- revised unloading-reloading functions

Both of these changes were incorporated into the parameter studies and compared to the results obtained with the original engine model. Since the actual load deflection characteristics of the engine support structure beyond the elastic limit are not verified by existing test data, no attempt was made to revise previously obtained correlation and parameter results. However, the parameter studies do serve to illustrate the effect of the engine modeling on crash design criteria.

Tables XXIV and XXIX present the results of the engine parameter variations. As can be noted from cases 1 through 17, Table XXIV, the engine was modeled with stiff mounts, resulting in low deflections. The following sketch illustrates a basic difference between the correlated model (case 5) and parameter variation (case 18) at a potential combined 95th percentile level as determined from Figure 98.

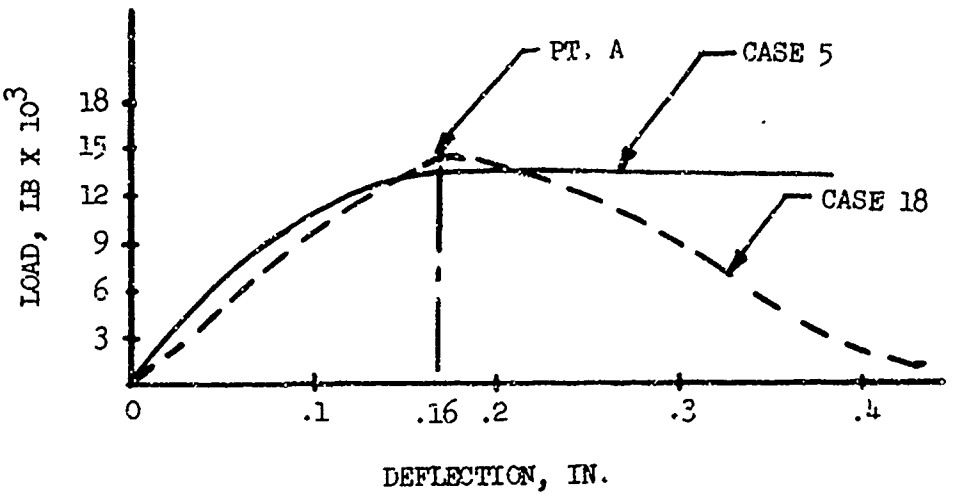

The basic case (case 5) deflects less since it will absorb more energy after the peak load (point A) is reached than will the engine modeled as in case 18. The engine loads in case 5 also exceed those obtained in case 18 since, in the latter configuration, there is a sharp reduction in the load-carrying capability of the structure; whereas in the case 5 configuration, the load-carrying capability remains uniform after reaching a peak value. Table XXIX summarizes these cases and verifies the above results.

Cases 19 and 20 were run so that a comparison could be made with the correlation results shown in Tables XIV and XV. The results of the parameter runs presented in Table XXVIII indicated that the proper modeling for the engine in the lateral direction is between 8 G's (case 20)and 18 G's (case 19). The test results indicate that the mounts deform less than 3/16". The use of an 8 G lateral engine mount would apparently result in too large an engine mount deflection as compared to the test.

The revised unloading-reloading cycle is more realistic for a structure which is initially stiff and then loses its load-carrying capability when buckled such as the engine is expected to do. As a result, the engine mount deflections will be greater than noted in the correlation run. The unloading-reloading cycle is described in detail in Volume II under the PROGRAM DESCRIPTION Section.

TABLE XXIX. ENGINE PARAMETER VARIATION RESULTS

PARAMETER	CONDITION	VERTICAL		LATERAL	
		G	Δ(in.)	G	Δ(in.)
Basic (case 5)	E	47.7	.247	14.3	1.26
Engine Load Level 20G Vertical (case 18) 18G Lateral	E	40.8	.987	15	.105
Engine Load Level 20G Vertical (case 19) 18G Lateral	G	25.6	.189	12.0	.356
Engine Load Level 20G Vertical (case 20) 8G Lateral	G	26	.21	11.7	1.79

COMBINED PARAMETER VARIATIONS

The results of the combined parameter variation study are shown in Table XXX. The results show that the crashworthiness of the UH-1H can be improved to a 95th percentile potentially survivable accident capability by improving the energy absorption capacity of the landing skids, lower fuselage and seats separately, or in conjunction with increasing the load carrying capacity of the transmission or engine. The analysis shows that an improvement to a 95th potentially survivable percentile accident combined vertical-lateral impact environment level requires one of the following approaches:

a)
- Increase landing strut stroke from 13.5 inches to 20 inches.
- Increase fuselage stroke from approximately 3.5 inches to 7 inches.
- Use seat requirement per MIL-S-58095 with + 15.5g load limit and a minimum stroke of 6 inches.
- Increase engine mount load limits to a minimum of 20 G's vertical and 18 G's lateral.

or, b)
- Increase landing strut stroke from 13.5 inches to 20 inches.
- Use fuselage bumper type structure at forward, mid and aft

TABLE XXX. SUMMARY OF COMBINED PARAMETER VARIATION RESULTS

Case No.	Identification	*	Percentile Accident	Occupant Response				Transmission Response				Engine Response			
				Forward		Rear		Vertical		Lateral		Vertical		Lateral	
				DRI	Δ(In.)	DRI	Δ(In.)	G_{Peak}	Δ(In.)	G_{Peak}	Δ(In.)	G_{Peak}	Δ(In.)	G_{Peak}	Δ(In.)
1	Increase Skid Load Increase Stroke Load	7 9 7	E	24	.16	33	.59	103	2.25	20	.31	46	.19	30	.25
2	Same as Case No. 1 Plus Seat Req't. per MIL-S-58095 (12 In. Stroke)	9 14	E	15.5	>12	15.5	>12	105	2.23	20	.305	45	.19	29.4	.25
3	Increase Skid Load Fuselage Bumper Seat Req't. per MIL-S-58095 (12 In. Stroke)	7 13 14	E	12.6	8.9	14	>12	25	.84	13.6	.21	26	.103	17.2	.11
4	Same as Case No. 3		F	16.2	>12	17.4	>12	60	.90	18	.276	56	.41	36	.255
5	Increase Skid Stroke Increase Fuselage Stroke Seat Req't. per MIL-S-58095 (20 In. Stroke)	8 10 15	E	11.8	3.6	12.5	5.66	50	1.8	18.8	.28	25.9	.095	22	.2
6	Same as Case No. 5		F	18.4	17	18.5	>20	127	2.65			63	.608		
7	Increase Skid Stroke Fuselage Bumper Seat Req't. per MIL-S-58095 (20 In. Stroke)	8 13 15	E	11	4.67	12.8	6.87	25.7	.84	9.2	.3	24	.114	27	.23
8	Same as Case No. 7		F	18.2	18.5	18.6	>20	57	.9	19	.27	58	.93	34	.2
9	Same as 5 Plus higher level transmission	16	E	-	-	-	-	30	1.04	18.3	.17	-	-	-	-
10	Same as Case No. 5 with 20/15 G Engine		E	-	-	-	-	-	-	-	-	27.5	.158	19.5	.150
11	Same as Case No. 9 with 15° Pitch, 30° Roll		E	13.6	5.0	13.9	8.4	8.7	.55	12.2	.47	23	.268	11.5	.2

*Reference Case from Table XXIV

section, each with a minimum energy absorption of approximately 22,500 ft-lbs.

- Use seat requirement per MIL-S-58095 with + 15.5 G's load limit and a minimum stroke of 7 inches.

It is estimated that to achieve the 95th percentile crashworthiness capability for a UH-1H, of the type tested in this program, an incremental weight increase of approximately 5% of the airframe, landing gears, seat system and major mass support structure (~125 lb) is needed. The aforementioned percentage value is based on an eleven (11) troop carrier UH-1H configuration less the weights (Reference 40) of the following items:

rotor blades, hubs and stabilizer	816 lbs.
engine	485 lbs.
transmission	379 lbs.
electronics, electrical equipment, instruments and hydraulics	720 lbs.
thirteen occupants and equipment	2860 lbs.
fuel	1374 lbs.

The estimated incremental weight increase is distributed among the structural elements approximately as follows:

fuselage	(2%)
landing skid	(1.6%)
seats	(0.9%)
engine mounts	(.5%)

The weight increases are based on first order linear approximations due to changes in thickness, area and stiffness for the various structural elements. For example, a change in load limit requires a new force level. Force is assumed to be proportional to the square root of stiffness (for a given energy level). In the case of a bending stiffness of a landing strut or the engine supports (assuming no change in modulus or length) the stiffness is proportional to cross sectional area moment of inertia, which, in turn, is a function of the strut diameter and thickness. For a linear system, doubling the force level will require an increase in the stiffness by a factor of 4. The increase in weight is then based on the required change in diameter and/or thickness to obtain the increased stiffness.

The best estimate of cost is to assume that the cost per pound of weight is the same as for the current vehicle. Using the same weight base of the vehicle airframe, landing gear, seat system, and support structure it can be expected that the increased energy absorption requirements to achieve a 95th percentile accident for the UH-1H vehicle will also add approximately 5% to the current vehicle cost. A preliminary draft of a cost effectiveness study (Reference 32) for a 9-13 place helicopter has indicated that the incorporation of crashworthy features ($\approx$ 200 lbs) will be cost effective within 5.4 years. The study is based on the structural damage and personnel injury history of the UH-1 aircraft series. The study takes into account the increased operating costs as a result of increased empty weight due to the addition of crashworthy structure.

From Table XXX it is interesting to note that the combinations which are considered to provide adequate, or near adequate, crashworthiness (cases 3, 5, 7 and 9) have resultant engine or transmission peak accelerations approximately equal to the acceleration levels experienced during the Phase III drop test. Both the transmission and engine survived that particular test in relatively good condition. Since the correlation between analysis and test at that impact level showed good agreement, there is added confidence that improved crashworthiness can be predicted by the mathematical model.

DESIGN CRITERIA AND CONCEPTS

The major considerations that influence the development of crashworthiness preliminary design criteria and concepts are:

- The crash condition statistical experience of impact velocities.
- Human tolerance to the loads imposed.
- The incremental structural weight cost and configuration changes needed to provide the desired crashworthiness capability.

CRASH LOADS AND ENVIRONMENT

Ideally, one would like to have occupant survival during a 99th percentile velocity impact. From a practical design viewpoint, however, it may not be possible to achieve such a high-velocity-impact capability without unduly penalizing the vehicle with added weight. It is important that the structure be designed to a given velocity percentile, whether it be the 80th or 95th, for any combination of vertical, lateral or longitudinal impact velocities, providing the given percentile has an equal probability of occurring. The consistency should be maintained regardless of the direction of impact, i.e., if the specified impact velocity should be the 80th percentile then the capability of the structure should be for the 80th percentile for any combination of vertical, lateral and longitudinal impact velocities. Figure 99 illustrates this three-dimensional family of impact velocity envelopes presented in statistical form. In contrast a hypothetical existing vehicle may have a capability envelope shown in Figure 100, which indicates that in the longitudinal direction it can meet a 75th percentile level, but because of nonconsistent design would only have a 50th percentile vertical capability and a 30th percentile lateral capability. If the given percentile of Figure 99 has an equal probability of occurring, the full capability of the hypothetical existing vehicle is much less than that implied by the 75th percentile longitudinal capability.

The impact velocity data compiled during Phase I and presented in Figure 98 illustrates that the combined impact velocity statistical representation is most likely a contoured surface. The determination of the exact shape of the surface has to be obtained from a thorough statistical evaluation. It may well be that the crash environment differs for the different types and classes of aircraft such as utility, attack, cargo and observation. These aircraft differ in weight and operational requirements. However, for the purposes of this study, the approximate accuracy of the accident data is sufficient to obtain significant results.

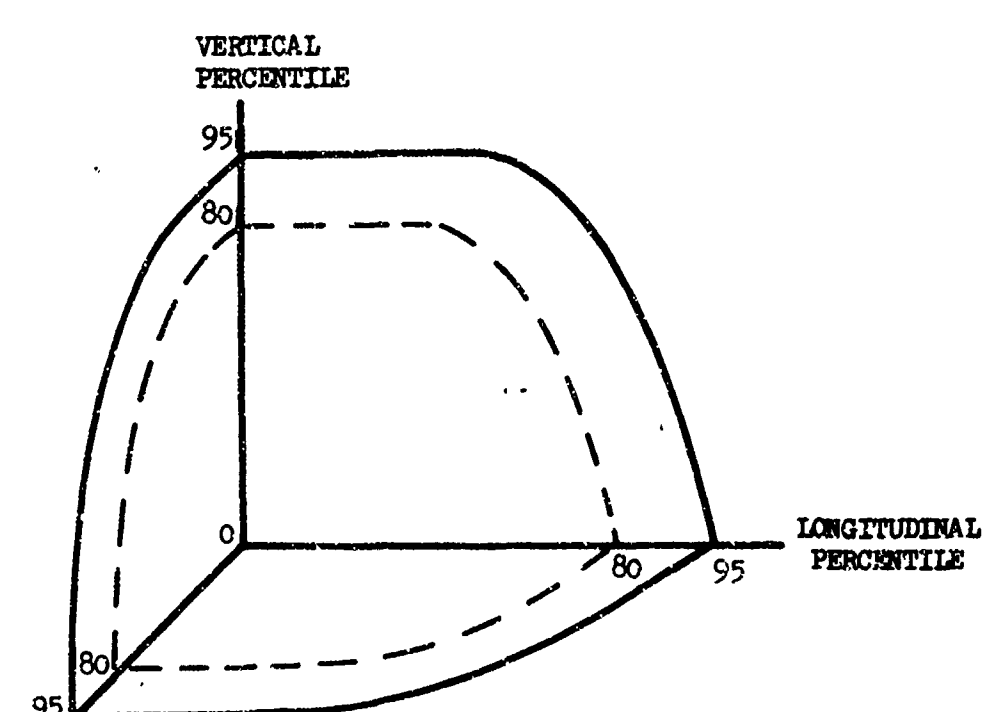

Figure 99. Three Dimensional Impact Velocity Statistical Presentation.

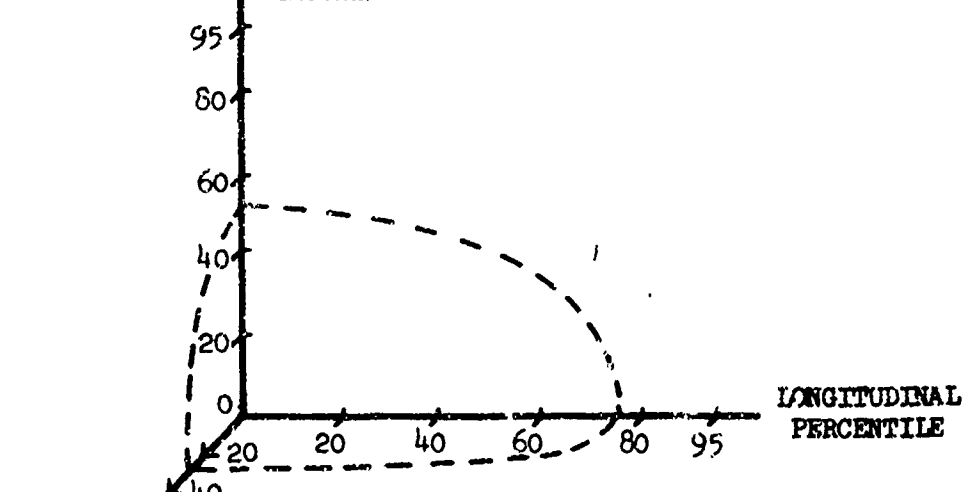

Figure 100. Example of a Three Dimensional Impact Velocity Airframe Capability.

HUMAN TOLERANCE TO IMPOSED LOADS

Human tolerance limits are a function of (a) peak acceleration, (b) duration of acceleration, and (c) rate of onset of initial acceleration that the occupant experiences. The occupant's posture, position and direction relative to the acceleration forces and the manner in which the occupant is restrained influence the acceleration levels that can be tolerated by the occupant.

Current criteria in this area are severely limited in the following respects:

- The data is based on acceleration measurements at the seat and not on the subject.
- The imposed loads or environment are based on estimated floor accelerations. This data does not take into account the location of the occupant relative to the impact load, nor does it consider the energy absorption or the transmissibility of the structure.
- There is very little verified modeling of the human body to account for critical body modes. The Dynamic Response Index (DRI) is one such model which can be used to determine the potential of a vertebrae compression injury. The Gadd Severity Index is available as a measure of brain damage.
- There is little data available on human tolerance to lateral loads, and consequently modeling of injuries due to lateral motion is sparse.

CONSISTENT CRASHWORTHINESS CRITERIA

Since occupant survivability is the objective of a satisfactory crashworthy design, it is desirable to maintain acceleration levels and the rate of change of acceleration at the occupant's location at or below human tolerance levels, while the structure surrounding the occupant's habitable shell remains essentially intact. This requires that the failure mode follow a desired and predictable sequential pattern. The weakest link in this concept is the lower fuselage structure, followed by the restraint system and then the support structure of the upper masses. Upon initial impact the acceleration levels that the occupant and structure experience are a function of the lower fuselage energy absorption capability, as well as the transmissability characteristics of the structure. To maintain a constant load factor requires that the stroke of the fuselage increase as the square of the impact velocity. However, as the stroke increases, the energy absorbed increases, which implies an increase in the weight of the lower fuselage, acting as an absorber. If the input energy exceeds the absorbing capability of the lower fuselage, the remaining energy must be absorbed by the structure

supporting the remaining vehicle mass and the occupants.

The allowable load factor will be reached or exceeded at a higher contact velocity, which requires the structure between the occupant and floor to deflect an additional increment of distance. The limiting impact is a function of the available stroke and acceptable weight increase for absorbing energy. Meanwhile the upper aircraft structure must also exhibit sufficient energy absorption capability to provide a habitable shell around the occupant. As with the lower structure, the energy absorption capability and the structural strength of the supporting structure must be compatible with the upper masses so that they will not collapse prior to the lower structure's performing its energy absorption work. The sequence of failure described above pointedly depicts the major problem in developing meaningful design criteria for aircraft crashworthiness. The design criteria must be established within limitations on parameters such as loading sequence, space, weight, and operating parameters to maintain acceptable acceleration levels and rate of change of acceleration for the occupants. Furthermore, the criteria must maintain compatibility between the various types of structures of which the major structural elements are:

(1) the crushable fuselage structure.

(2) the occupant retention system (seats).

(3) the major mass items such as engine and transmission.

If, in a crash situation, the aircraft drifted in addition to impacting vertically, the resultant velocity vector would be more significant than either velocity component. The structure, in this instance, would be less capable of handling the higher combined loading condition since it is designed for a unidirectional load. However, the general concepts regarding consistency of design, discussed earlier, would be as applicable for combined loading as for uniaxial loading conditions.

The proposed consistent crashworthiness design criteria approach as influenced by structural weight and configuration considerations is shown in Figure 101. The landing gear and crushable fuselage structure between the impact point and the seat support is the first area of interest in developing a crashworthy design. Loads resulting from deformation of the gear and structure in response to a given impact sink speed are compared with the occupant tolerance to loads. Providing strength in this area is beneficial up to a point. Should the load levels during the landing gear failure and fuselage crushing mode exceed that which can be tolerated by the occupant, then the energy absorbed does not serve a useful purpose because the occupant does not survive.

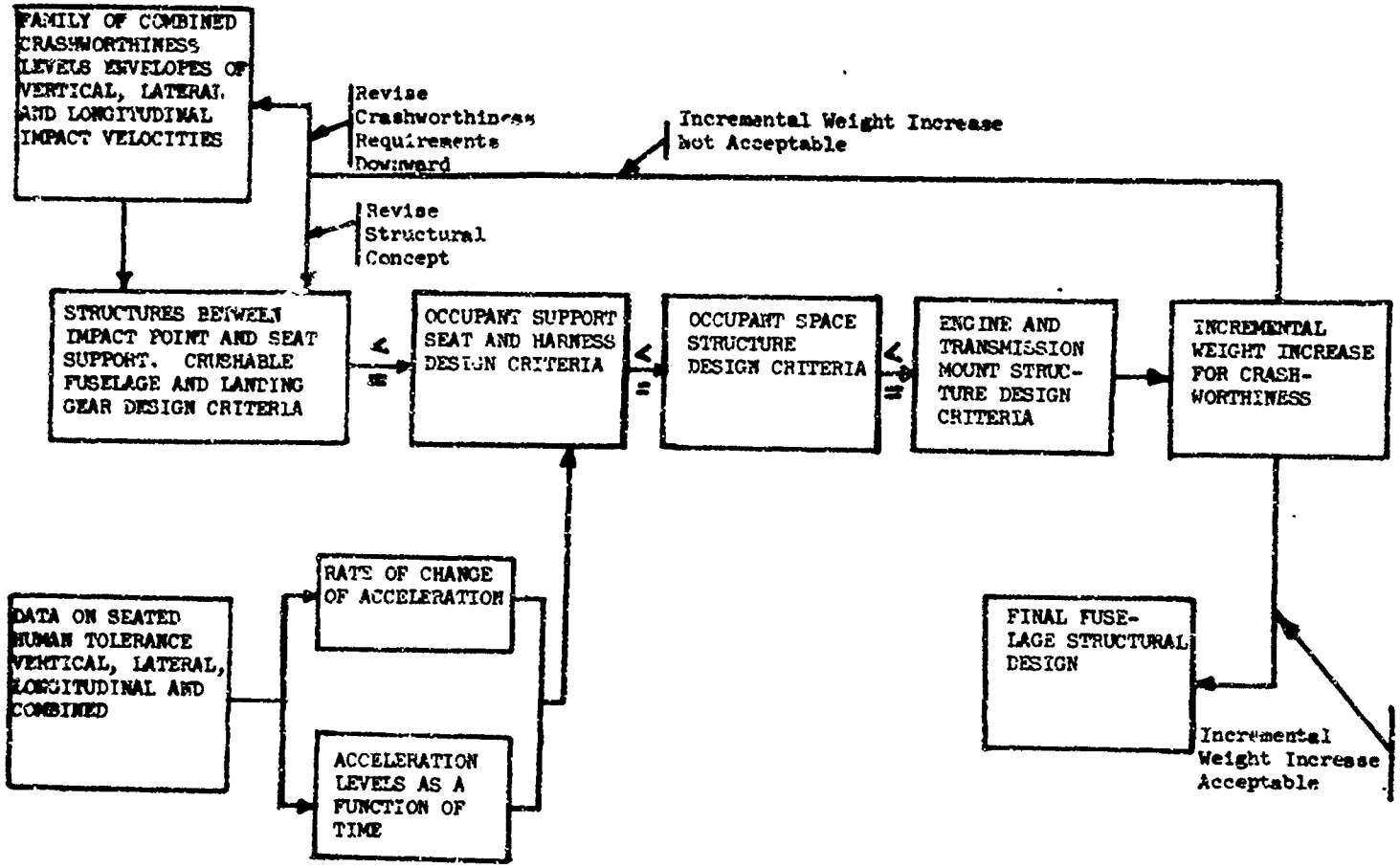

Figure 101. Consistent Crashworthiness Design Criteria Approach.

The maximum strength of the occupant seat support and restraint system should be such that they are retained even if the occupant is injured non-fatally. However, the strength of the seat support and restraint system should not be below levels which can be tolerated by the occupant. A consistent design would dictate that the strength of the occupant seat support and harness be equal to, or greater than, the loads imposed during the period of landing gear failure and fuselage structure crushing. Once these levels have been attained, additional energy can be absorbed by controlled failure of the seat structure. During the period that energy is being absorbed the structure surrounding the occupant must have, as a minimum, the strength to withstand the loads imposed without collapsing, thus protecting the occupant. This requirement dictates the strength of the structure supporting large mass items such as the engine, the transmission and the rotor system. Any structural configuration changes can result in weight changes. If it is an increase, its acceptability will have to be determined. If acceptable, the fuselage structural design has been set. However, it is unlikely that this will be the case initially, and other iterations will be required. The decision as to whether to revise the crashworthiness requirements downward or to revise the structural concept will depend greatly on what structural design options are available and can be used. Even in the event that the tradeoff studies indicate crashworthiness requirements have to be revised downward, this revision can be performed in a logical manner to provide the maximum consistent protection to the occupant commensurate with the weight and configuration requirement constraints.

The application of the proposed consistent crashworthiness design criteria approach (Figure 101) is demonstrated with the use of the results obtained from the parameter variation study and the flow diagram shown in Figure 102. For example, assume that it is the intention to design to the 95th percentile potentially survivable accident for a combined vertical and lateral velocity impact.

Crashworthiness of the current vehicle, based on the combined vertical lateral drop test and the envelopes presented in Figure 98 is somewhat lower than the 70th percentile. This assumption, of course, does not consider the vehicle's capability under other circumstances such as striking obstacles other than the ground. The test results indicated that with the exception of a high potential of spinal injury, as measured by the DRI, and exposure to head injury, due to unrestrained movement, the vehicle structure and occupants would have a reasonable chance to survive an impact of the magnitude experienced during the test. The occupant exposure to injury is increased by the lack of energy absorption capability of the troop seats which collapsed without absorbing any significant energy. Therefore, as a first step in the illustrative procedure (Figure 102) under the premises noted above, the vehicle is analyzed and determined to be crashworthy to a combined vertical-lateral 70th percentile. The first step, therefore, requires that the environment

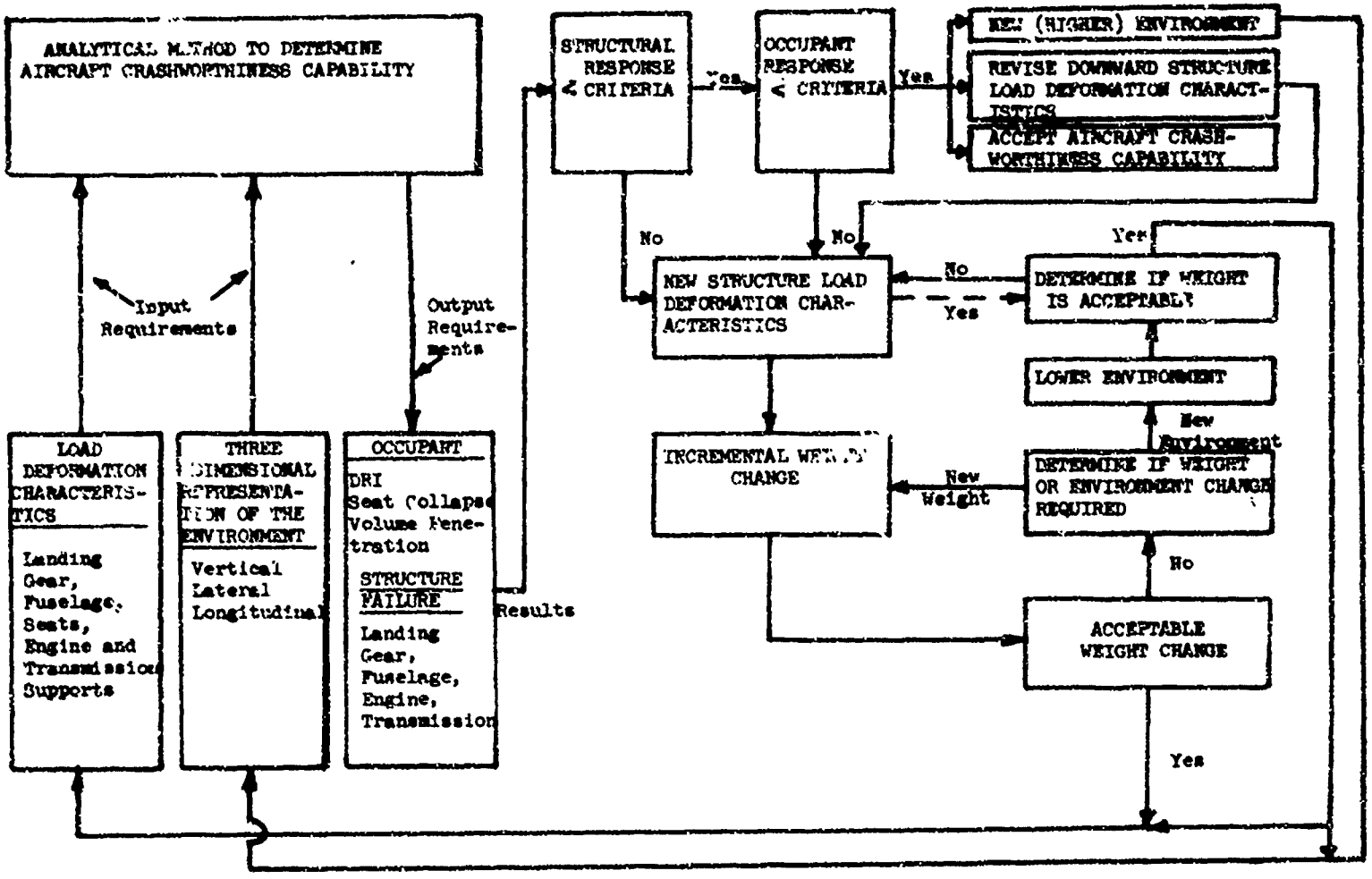

Figure 102. Flow Diagram - Procedure for Determining Crashworthiness Capability.

be statistically determined for all percentiles and that the load deformation characteristics of the structure be obtained. The statistical representation of the environment can be established from accident data. The load deformation characteristics are dependent upon the different types of structure used for the various elements of the vehicle and vary considerably in configuration. These data can be obtained via analysis and/or test. However, since the nonlinear deformation is the most significant aspect of crashworthiness structure, analytical procedures to be meaningful will require test verification.

The next step requires that the crashworthiness criteria for the structure and occupants be satisfied. This has to be accomplished using an analytical procedure which has been shown to be capable of accurately predicting structure and occupant responses during a combined velocity impact. Assuming that the structure and occupant responses meet their respective criteria then a crashworthiness capability of the aircraft for a specified design configuration and at a defined environment level ($\approx$ 70th percentile potentially survivable accident for illustrative purposes) has been established. The next requirement in the procedure is to decide if, a) the aircraft crashworthiness capability exists for a higher environment level, b) the crashworthiness capability is excessive and possibly a redesign in some areas will be more efficient (lower weight), or c) the results are satisfactory and no further analysis is required. Assuming that, as was the situation in this study, a 95th percentile capability was desired, then an analysis has to be performed using a new (higher) environment level and the results again compared to the design criteria. Naturally, if the criteria is again met then there is no need to continue the analysis except possibly to investigate the use of more efficient energy absorbing structural elements. However, as was the case in this study the present design configuration was inadequate at the 95th percentile potentially survivable accident level and, therefore, it was necessary to revise the load deformation characteristics of structural elements. For example, if the engine and transmission responses satisfied their respective criteria but the DRI's were excessive, then the energy absorption capability of the landing gears, lower fuselage and/or the seat system have to be revised upward in order to meet the energy requirements at the new environment level. This requires a determination of new load deformation data for the structural elements of interest. Changes to increase the energy absorbed may result in increased structural weight, as was demonstrated in this study. In the event the weight requirement increases to improve the aircraft's crashworthiness capability then a decision has to be made as to accepting or rejecting the incremental weight increase. A decision of this nature should be made on the basis of the relationship that exists between savings from reduced hardware damage and losses, medical expenses, and training expenses versus increased initial improvement cost and added operational expenses associated with increased weight and the detrimental effect of reduced mission capability. It is envisioned that a cost tradeoff can be established as a function of environment level by taking into account the

aforementioned factors. An acceptable weight change will then require that the load deformation input data be revised and the analysis be repeated to determine if, at the higher environment level, the responses meet their respective criteria. If the weight increase is considered excessive then a determination will have to be made on how the structure can be redesigned to absorb the required energy more efficiently (lower weight). This latter procedure, once again, requires that nonlinear load deflection data for various structural element types be available. However, if the structural weight cannot be reduced via a reasonable redesign then the aircraft has a crashworthiness capability to a lower environment level than is desired. Before re-evaluating the vehicle to a lower environment level a check should be made to determine if the previously added weight is still consistent with the requirements of the new environment level, since weight and cost are related to percentile accident. Once satisfied that the weight change is acceptable for a particular environment level then the analysis can continue. In the parameter studies previously discussed it was ascertained that for the UH-1H aircraft configuration analyzed, several structural design changes, if incorporated simultaneously into the design, would improve the aircraft's crashworthiness capability to a 95th percentile potentially survivable accident level, as defined by a particular combined vertical velocity (23 fps) and lateral (18.5 fps) velocity, and would require an increase in weight of approximately 5% of the current airframe weight. The airframe weight, as defined earlier in the discussion regarding the combined parameter variations, is considerably less than the total vehicle weight.

RESULTS OF THE PROGRAM

The results of the program are summarized as follows:

LITERATURE SURVEY AND CRITIQUE

A literature survey and critique of publications was completed. Thirty-two reports were reviewed. The literature was discussed with regard to applicability to ten areas of rotary-wing aircraft crashworthiness design. A literature index is provided in Volume II which further divides each report into specific content and areas of applicability. There are 27 such divisions. The basic contents of the publications was reviewed and commented upon.

ACCIDENT REVIEW

The accident analysis performed in this study consisted of the following data:

- 1 summary of 3657 U.S. Army rotary wing aircraft accidents between the period 1967-71.
- 1 summary of 185 U.S. Army rotary wing aircraft cases compiled in Reference 33.
- 209 narratives of major accidents from USAAAVS, the U. S. Naval Safety Center, and the Directorate of Aerospace Safety Center.
- 32 detailed accident cases from USAAAVS, the U. S. Naval Safety Center, and the Directorate of Aerospace Safety Center.

The detailed accident investigation was summarized in a comprehensive table which was divided into three areas of importance including kinematics, structural damage and personnel injury. The table is segmented into 56 columns. Included in the accident investigation were 13 photographs showing various aspects of postcrash damage.

The accident analysis revealed the following pertinent information:

- The most significant causes of injuries and fatalities are decelerative forces, the collapse of structure into occupiable areas, the impact of occupants with equipment or objects, and postcrash fire.

- The most frequent structural damage occurs to the main rotor system, transmission and tail structure. In 60% of the cases analyzed, the main rotor blade, tail rotor blade or tail boom contacted the ground, a tree or another aircraft prior to what is considered to be the helicopter crash impact. To a lesser extent the lower and upper fuselage structure, engine and seats sustained damage during the crash accident. Damage to these structural areas and items was noted in approximately one-third of the cases.

- The lateral rollover condition occurs in approximately one-third of the accidents reviewed. This type of helicopter behavior, after ground impact, occurs more frequently than such behavior as forward rollover, plowing, skidding or bouncing.

- A lateral impact velocity component is present in approximately 50% of the cases studied. Combined lateral-vertical impacts occur in 43% of the accidents reviewed. Combined longitudinal-vertical impacts occur in 32% of the accident cases.

- The crashworthiness design requirements for components/equipment in the proximity to the occupants should be equal to or greater than, "G" levels that can cause the occupant serious injuries.

- An analytical program must be capable of predicting the dynamic response of a rotary wing aircraft due to combined vertical, lateral, or longitudinal impacts. The accident records indicate that in over 70% of the accident cases analyzed the crash environment is multidirectional.

SUBSTRUCTURE TEST AND ANALYSIS

The energy absorption characteristic of a typical aircraft substructure (P2V-4 fuselage bumper) was obtained under dynamic loading conditions. The results were compared to available data from previously performed static loading tests. The results of the dynamic and static tests compared very favorably.

In addition, the fuselage bumper was analyzed using a general shell program (STAGS) which used the principle of minimum potential energy in conjunction with the finite difference method. The analytical results show general agreement in the deformation of the shell structure when compared to test data. However, the analysis showed considerably less energy absorbed by the shell than was measured in the test.

It is recognized that the response of a structure may vary as a function of the level of the impact velocity for a given energy ($\frac{1}{2}MV^2$), and thus test results could change somewhat if a different combination of masses and velocities were employed. However, for crash analysis purposes, we need only consider a very narrow range of impact velocities. Furthermore, a 10% change in mass requires only a 5% change in velocity to maintain the same level of energy.

The results obtained from both the test and analysis of the fuselage bumper are significant in that the problem of modeling helicopter structure during a crash environment, given the present state of the art, is put in proper perspective. The dynamic test of the bumper indicates that for some typical aircraft structure a simple static test will suffice when the static and dynamic load deformation characteristics are considered to be very similar. Some structures, on the other hand, will behave differently under dynamic loading conditions than under a static load environment. A notable example of such a structure is a column. Elastic buckling of bars is discussed in several references (38 and 39) from which much of the following information is obtained. A bar with its lower end stationary while the upper end moves with a constant velocity can be compared to an impact loading situation. Under this condition of rapid loading, the transverse motion of the column is retarded by the inertia of the mass. As a result, the dynamic deflection lags behind the values that correspond to infinitely slow loading. This lag between dynamic and static deflections is a function of curvature, velocity propagation of sound in the material, impact velocity, and slenderness ratio. The deflections eventually become large and the axial force in the column increases nonlinearly. Oscillations develop and the mass of the column is accelerated sufficiently in the transverse direction to reach the static value. The inertia forces cause the column to overshoot the static deflections which results in a drop in the compressive axial forces below the critical static load (Euler value). Studies of the problem of lateral buckling of an initially curved slender bar in which the load acts for a very short interval of time have shown that the column can safely withstand compressive forces larger than the Euler critical load provided the duration of the load is sufficiently short.

The results of the substructure test and analysis indicate that:

- Static tests are sufficiently accurate to define the dynamic load deformation characteristics for some typical aircraft structure. The fuselage bumper tested in this program is one such typical structure. However, for some structures, most notably columns or bars, static tests cannot accurately determine the dynamic load deformation.

- The current state of the art finite element methods have severe limitations when applied to crashworthiness studies. These analytical methods can accurately predict load deformation for different types of structures in the elastic regime. However, since during a crash impact elastic deformation accounts for only a small fraction of absorbed energy, an analysis to be useful as a predictive tool must account for plastic deformation.

- A reasonably accurate finite element, or difference method of determination of load deflection characteristics of aircraft structures which are subjected to impact loads, will require a substantial cost in engineering modeling and computer run time. The result f this study indicates that the analysis of an aircraft structure similar to the P2V-4 bumper, using finite difference methods would, as a minimum, cost twice as much as required to perform a dynamic test to obtain the structure's nonlinear load deformation characteristics. Modeling for nonlinear behavior requires accounting for changes in geometry, boundary condition and loading condition.

- The present analytical state of the art, although crude and costly, does offer advantages over testing in some respects. An analysis may not be capable of predicting the exact quantities; however, if the analysis can accurately predict correct trends, then this information can be utilized in determining quantitative design levels. Thus, the effects of design changes on the structural response of the aircraft can be reliably assessed. The ultimate design will probably require testing even if relatively accurate analytical methods could be developed.

COMPUTER PROGRAM

A computer program (KRASH) was developed which computes the time history response of N arbitrarily interconnected lumped masses. The program has the capability to:

- Define six degrees of freedom (DOF) at each representative location, including translational and rotational accelerations, velocities and displacements.

- Determine accelerations, velocities and displacements at each time interval.

- Determine forces and displacements for each member at each time interval.

- Treat up to 40 masses (240 DOF)* and plot results.
- Provide for general nonlinear stiffness properties in the plastic regime and determine permanent deformation.
- Provide for the application of different types of load-limiting devices.
- Determine how and when a rupture of an element takes place.
- Define mass penetration into an occupiable volume.
- Provide for ground contact by external structure including rotor blade contact.
- Provide for internal damping and ground coefficient of friction.
- Include a measure of spinal injury potential to the occupants, i.e., Dynamic Response Index.

QUALITATIVE ANALYSIS

A qualitative analysis was performed using program KRASH for the purpose of showing that the program is capable of predicting structural responses to combined vertical-lateral crash impact. The analysis was performed for three impact conditions. The results were compared with previously published data and the trends were consistent with expectations. The results were summarized in tabular form and included the peak decelerations of the engine, transmission and floor, fuselage deformation, and subjective estimates of component failures.

EXPERIMENTAL PROGRAM

A drop test was performed with a UH-1H helicopter. The impact velocities were 23 fps (vertical), 18.6 fps (lateral), and 0 fps (longitudinal). The drop test program consisted of:

Quantity	Item
2	preliminary swing tests
2	preliminary low-level drop tests
2	landing gear strain gage time histories
1	fuselage deflection rod
9	high-speed cameras including two mounted onboard the vehicle

*60 mass (360 DOF) without plotting capability

Quantity	Item
2	regular-speed documentary cameras
24	acceleration time histories
24	integrated velocity time histories
24	integrated displacement time histories
13	filtered (100-cps, low-pass) acceleration time histories
1	film approximately 20 minutes in length showing pretest activities, the drop test at high speed (500-1000 frames/sec), and posttest damage review.

The vehicle sustained the following damage during the test:

- failure of the landing skids
- deformation of the lower fuselage and side
- buckling of the floor
- collapse of the nine troop seats located at and aft of F. S. 81
- slight yaw rotation of the engine
- fracture of the tail boom
- fuel spillage (UH-1H test vehicle was not equipped with a crash resistant fuel system)

All the passengers exhibited a displacement in the direction of the lateral impact. From observation of the posttest damage and dynamic response analysis, using a DRI model, it was judged that a high potential for a vertebra compression injury existed for the rear left-side passengers. To a lesser degree, the copilot and pilot would be exposed to a similar injury. The movement of the passengers as a result of the impact indicated potential for other injuries resulting from seat collapse, flailing of the body, and possible contact with internal structures, i.e., seat braces aft of passengers at F. S. 117.

The results of the helicopter drop test show that:

- The impact velocities of 23 fps vertical and 18.6 fps lateral were high enough to cause permanent structural deformation, yet low enough that a meaningful correlation

could be achieved. The test conditions provided an excellent opportunity to exercise the capability of program KRASH to analyze large deformation nonlinear responses. Damage to the vehicle varied from "little" at the engine and transmission to "extreme" at the mid and aft fuselage. If the entire vehicle had experienced severe damage, the modes of failure would be difficult to identify and, consequently, the verification of the ability of the analytical program to describe a crash, would be greatly impaired.

- Measurements of accelerations should be obtained as near a rigid mass location as possible to provide meaningful correlation. Acceleration data from fuselage locations are representative of responses but not necessarily the forces that are acting. It is extremely unlikely that, for a lumped mass representation of the fuselage, the analytical and test accelerations at the floor can be directly compared. The test data is expected to show higher peak accelerations resulting from localized panel and plate responses. These responses, however, generally represent very little force.

- The reduction of test data to include low-pass filtering and integration of the acceleration response to obtain velocities and displacements should be included in the development of test plans. The low-pass filtering allows a comparison to be made between test data and analytical predictions which is not hampered by high-frequency oscillations, many of which are local responses. The integrated values, however, may present inaccuracies depending on the validity of the recorded data and the method of integration that is used.

CORRELATION

The UH-1H helicopter drop test data was correlated with an analytical model consisting of 31 masses (186 D.O.F.) and 38 springs. The results of the analysis compared favorably to the test data in the following areas:

- sequence of events
- times of occurrence of major events
- vehicle motion
- fuselage deflection and deformation
- engine and transmission time histories of acceleration, velocity and displacement.

- engine and transmission support mount deflections

Analytical results showed lower fuselage accelerations, both vertically and laterally, than did the test data. However, it is surmised that the accelerations obtained from the test include responses of local structural modes and are not representative of the force that is transmitted to the rest of the structure.

The correlation study indicated that the proper representation of the structure presented some significant modeling difficulties. For example:

1. The response of the major mass items (i.e. engine and transmission) is highly dependent on the load deflection characteristics of the lower structure (skids and fuselage) and the relationship between the stiffness of these major mass items with respect to the frequency of the force pulse transmitted via the floor. The analytical representation of the floor with a limited number of masses effectively acts as a filter and transmits a low-frequency ($\leq$10 cps) force to the attached structure. With the aid of the sketch of a half cycle sine pulse excitation (for a system initially at rest), one can see that the relationship between excitation frequency and natural period of the transmission or the seat or the engine masses on their respective supports is a significant factor. Damping, although a factor, is not as significant since we can realistically expect it to be in a narrow range, i.e., 5% to 10% of critical.

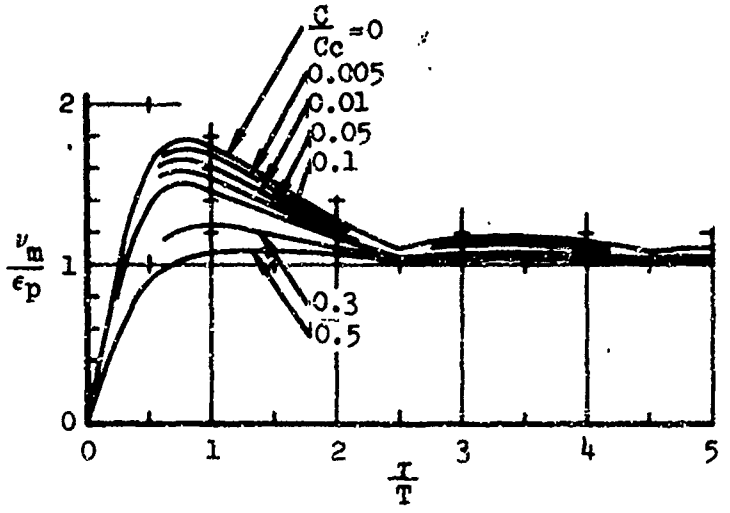

v_m = maximum response

ϵ_p = excitation

C/C_c = percent of critical damping

τ = excitation pulse

T = natural period of system

The maximum response of the upper mass elements is, therefore, a function of the stiffness regimes of the various elements at any time during the impact environment. In this respect, the nonlinear behavior of the lower fuselage, seat system, engine and transmission mounts is very critical in ascertaining the correct acceleration and deflection responses.

2. Correlation with a given set of test data may require a compromise between acceptable accelerations and deflections. The modeling of the engine mounts in this particular study illustrates this dilemma. The following sketch shows three choices of load deflections representing the engine mounts:

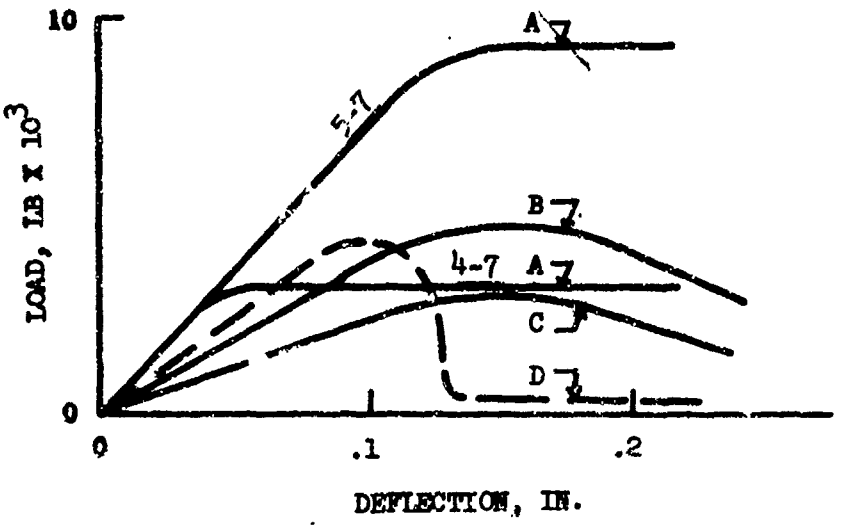

Strictly speaking, these are not actual vertical load versus vertical deflection curves. These are the axial loads versus axial deflections of beam elements 4-7 and 5-7, the engine supports, which in the model used are inclined from vertical. Due to this inclination, bending occurs which increases the vertical loads above those shown for a given vertical deflection.

For Case A, two separate curves were used for 4-7 and 5-7; for Cases B and C the two beam characteristics are identical. The following table shows the peak vertical acceleration on the engine, the time of its occurrence, and the maximum axial deflections of beams 4-7 and 5-7 for a drop test correlation run.

Case	Engine G Peak	Time of G Peak	Maximum Axial Deflection of Engine Support	
			4-7	5-7
A	25.9	.129	.040	.128
B	25.7	.134	.057	.168
C	17.6	.146	.47	1.00

As would be expected, going to progressively softer engine mounts lowers the vertical acceleration, increases the time at which the peak acceleration occurs, and increases the maximum axial deflections of the engine supports. The results of A and B appear to be quite similar, whereas C shows a drastic reduction of vertical acceleration and increase in beam deflection.

It is felt that the correct results are a compromise of the above cases. Based on drop test results, the engine vertical acceleration is about 25 G's at .110 sec. Engine deflections were not measured, but peak values appear to be less than .375 inches. Thus, the G levels from runs A or B are appropriate, although the times of occurrence are a little late. However, the deflection of element 4-7 is too low in cases A and B, and much too high (for both elements) in case C.

What is apparently required for correlation with test results is a load-stroke curve such as D, shown in dashed lines. The initial high stiffness would give the correct peak load, and the rapid reduction in load capability would give the necessary deflection. This case was not run since there is no test data available to verify the actual load deflection characteristics beyond the elastic limit . The discussion on the engine mount modeling is also applicable to the transmission mount representation .

The results of the analytical model of the UH-1H used in the correlation with the combined vertical-lateral velocity drop test data were also compared to higher vertical velocity (30 fps) drop test data, published in Reference 3. The use of this additional data provided a second level of impact energy with which to further evaluate structural nonlinear behavior. In particular, the engine and transmission mounts at the higher vertical impact condition sustained damage not obtained during the combined 23 fps vertical velocity and 18.5 fps lateral velocity drop test. Correlation of model KRASH analytical data with the two sets of test data further emphasizes the need to obtain, via test, proper load-deflection characteristics of the structure. The transmission modeling for the two different energy level conditions is used to illustrate this particular point. The sketch below shows two transmission load deflection curves used in the analysis to obtain agreement with both sets of independent test data.

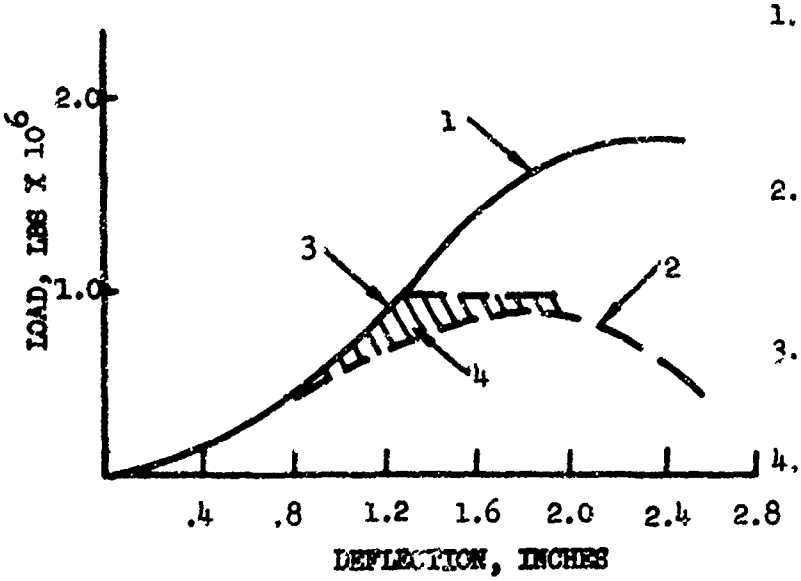

1. Transmission Load Deflection Curve for Correlation of Combined Vertical-Lateral Velocity Test.
2. Transmission Load Deflection Curve for 30 fps Vertical Impact.
3. Maximum Deflection Obtained Analytically (Correlation)
4. Appropriate Modeling Region

Without the higher energy level data (30 fps vertical velocity impact) it would be difficult to accurately predict the load deflection characteristics of the transmission after the soft mounts bottom. By the same token, with the lower velocity impact data it would be just as difficult to ascertain the transmission mount failure point. The combined vertical-lateral velocity impact test data indicates that the transmission survives intact despite experiencing approximately 27 G's in the vertical direction, which far exceeds the crash load requirement for the mounts. Thus, the cross-hatched region represents a range within which the results are expected to give reasonable agreement for both the lower energy (23 fps vertical velocity) and the higher energy (30 fps vertical velocity) impact levels.

In addition to correlation with the combined vertical-lateral impact test data, analytical results were compared to previous 30 fps vertical velocity drop test data. The results of the comparison showed good agreement in the following areas:

- The time of occurrence for peak floor accelerations.
- Peak floor acceleration levels (accounting for the effect of low-pass filtering)
- Initial peak transmission and engine acceleration levels.
- Maximum transmission mount deflection.

However, the analytical results understated the maximum engine deflection for reasons stated earlier.

The correlation results show that:

Computer program KRASH is capable of predicting structural responses of a helicopter during a combined vertical-lateral velocity crash impact.

The most significant limitation to analyzing structural responses during a survivable crash is the lack of available large nonlinear load deflection data for fuselage structure and major mass component mounting configurations. Stress analysis and static tests generally provide information defining the structure and support mounts' load deflection characteristics up to yield. However, during a crash environment, the nonlinear deflection of the structure represents the significant aspect of the problem.

The development of an analytical program requires verification with test data. The correlation between analysis and test crash data, to be meaningful, must include comparison of:

- Peak responses and deflections
- Vehicle motion
- Sequence of events
- Time of occurrence of major events
- Velocity and displacement changes
- Response shapes
- Fuselage deflection and deformation

The development of functional analytical models capable of predicting the structural response of rotary-wing aircraft during a crash condition is enhanced with the utilization of test data obtained at more than one impact energy level. Data obtained from a test in which all elements deform into the plastic regime impairs the ability to identify important load deformation characteristics of the various structural elements, i.e., the level at which the major mass elements supporting mount will behave nonlinearly.

Good correlation of analysis with test data from a 70th percentile potentially survivable accident with combined vertical and lateral velocities (approximately the level of the drop test performed in this study) and a 75th percentile potentially survivable accident (30 fps vertical) enhances the degree of confidence one can expect of the analysis.

PARAMETER STUDIES

The results of 31 parameter variation computer runs are included in this report. Individual parameter variations were made which include changes

to the following items at various percentile accident levels:

- Landing gear load limit
- Landing gear stroke
- Fuselage load limit
- Fuselage stroke
- Fuselage load limit and load stroke
- Engine mount stiffness
- Transmission mount stiffness
- Seat load stroke curve

The results of the individual parameter variation study were tabulated and summarized and then used to formulate a set of combined parameter trials. The combined parameter studies determined acceptable crashworthy design possibilities at the combined 95th percentile potentially survivable accident level and related the design changes to potential incremental weight increases.

The results of the parameter studies indicate that:

1. Improved crashworthiness criteria can be developed with the proper combinations of design changes to increase the energy absorption capability of the structure. In particular significant improvement can be made with increased landing skid stroke, improved fuselage load absorbing characteristics, and a substantial seat load stroke. Although improvements can theoretically be obtained via increased stiffness of the transmission and engine mounts, these areas may present conflicts with operational requirements. Furthermore, buckling of the engine mount appears tolerable since the occupants are not in immediate danger due to collapsing structure when the engine fails in a controlable manner.

2. The dynamic response of the occupants differ depending on their location with respect to the point of impact and on the motion of the vehicle subsequent to the initial impact. The parameter studies showed that the responses of the rear and forward seated occupants, with identical seat systems and weights, experience peak forces at much different times and that the maximum seat deflections also differ considerably.

3. A design change which alters the load deformation characteristics of the landing gear skid and/or lower fuselage can substantially change the response of the occupant and seat, the engine and the transmission. The design change can affect the time history of the response as well as the peak acceleration levels since in a dynamic system there is a great dependence on relative stiffnesses and natural frequencies of the various structural elements. To a lesser extent, total system responses are affected when individual and independent changes are made to the load stroke characteristics of the seat, engine and transmission. The prime factors which contribute to the level of response and the time of occurrence of their respective maximum values include:

   - structural load-deflection characteristics
   - structural element failure modes
   - environmental load levels
   - direction of the forces
   - vehicle motion after impact

These factors must be evaluated taking into consideration the interdependency that exists between the structural elements in a dynamic system. It is this interdependency that results in shifts in peak loads, deflections and failure times of occurrence when structural configuration changes are made.

DESIGN CRITERIA

Consistent crashworthiness preliminary design criteria approach is presented. The proposed approach is based on providing a predictable sequential failure pattern for the vehicle structure and its major masses. The approach maintains compatibility between the essential structural elements such as the crushable fuselage, the occupant restraint system, the engine and the transmission. With the aid of the parameter study results the use of the proposed design criteria approach is illustrated. The consequence of potential weight increases in order to achieve a crashworthy design at a higher environmental level is integrated into the procedure as is the use of analytical tools capable of predicting structural and occupant dynamic response during a crash. The demonstration of the application of the proposed consistent crashworthy preliminary design criteria showed that for design changes investigated during the parameter studies, the tradeoff between incremental weight versus improved crashworthiness can be graphically depicted as shown in the sketch on the next page.

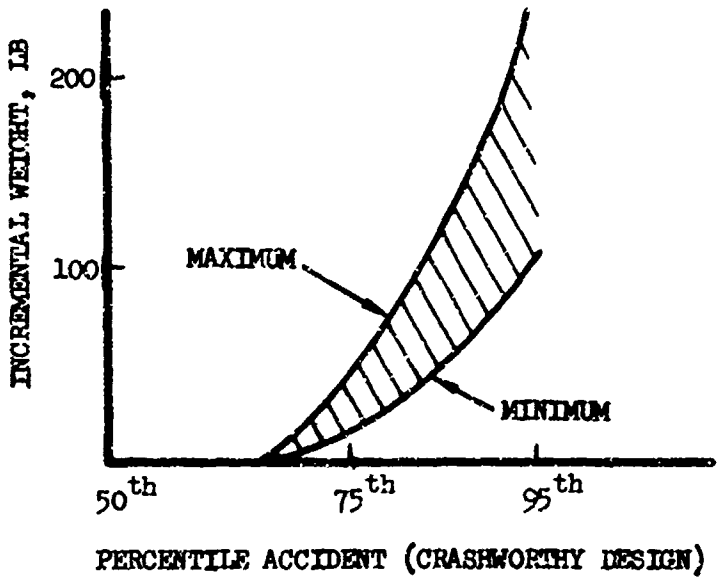
INCREMENTAL WEIGHT, LB
200
100
MAXIMUM
MINIMUM
50th
75th
95th
PERCENTILE ACCIDENT (CRASHWORTHY DESIGN)

CONCLUSIONS

1. Digital computer program KRASH is capable of satisfactorily predicting the dynamic responses of rotary-wing aircraft during a crash environment with a combined vertical-lateral impact velocity.

2. The most significant limitation to analytically simulating structural responses during a high energy impact is the lack of available large nonlinear structural element load deflection characteristics.

3. KRASH is capable of facilitating preliminary design, by assessing through parameter variation studies the effect of structural changes on the vehicle's crashworthiness capability. Parameter variation studies conducted during this effort provide pertinent data which can be utilized to assess the incremental weight requirements necessary to design to or near the 95th percentile potentially survivable accident.

4. The dynamic responses of the engine, transmission and occupants are greatly dependent on the degree of crushing that occurs within the lower fuselage and the manner in which the major mass support mounts plastically deform.

5. Consistent crashworthiness design takes into consideration the crash impact environment, human tolerance limits, structural load deformation characteristics, and incremental weight, cost and configuration penalties while treating the vehicle as an integrated system.

6. Main rotor blade impacts with the terrain and/or trees, penetration of occupiable spaces by the transmission and/or rotor blade and lateral rollover during ground impact each occur in at least 1/3 of the accident cases reviews. Program KRASH has provisions for:

   a) blade impact
   b) mass penetration into an occupiable volume
   c) lateral and longitudinal forces in addition to vertical forces

7. Current finite element analytical techniques are severely limited for use in complete vehicle crashworthiness analysis due to cost and size requirements. However, finite element methods can be utilized to determine substructure load deformation data for subsequent use in crashworthiness studies.

RECOMMENDATIONS

1. Perform additional correlation studies utilizing available test and accident data, for the purpose of improving analytical prediction capability.

2. Initiate a program to include analysis and test for the purpose of determining the nonlinear load deflection characteristics of pertinent forms of structural elements under dynamic loading conditions.

3. Institute a consistent crashworthiness preliminary design criteria approach which will provide for a predictable and desired sequence of structural failure that will afford the occupants the greatest opportunity for survival for an acceptable weight penalty.

4. Investigate the development of mathematical models for current and future U.S. Army helicopters. Analytical models once established and verified will be able to enhance structural design trade off studies and accident investigation analysis for different types of aircraft.

5. Perform research and development to ascertain design requirements for improved fuselage energy absorption during high rate vertical impacts, sideward impacts and lateral rollovers. Determine design requirements for transmission retention and maintainability of occupiable space.

LITERATURE CITED

1. Reed, William, Avery, James Ph.D., PRINCIPALS FOR IMPROVING STRUCTURAL CRASHWORTHINESS FOR STOL AND CTOL AIRCRAFT, Aviation Safety Engineering and Research; USAAVLABS Technical Report 66-39, U. S. Army Aviation Materiel Laboratories, Fort Eustis, Virginia, June 1966, AD 637133.

2. Turnbow, J. W., Carrol, D. F., Haley, J. L., Jr Robertson, S. N., CRASH SURVIVAL DESIGN GUIDE, Dynamic Science; USAAVLABS Technical Report 70-22, U.S. Army Aviation Materiel Laboratories, Fort Eustis, Virginia August 1969, AD 695648. (Most recent revision is USAAMRDL TR 71-22, AD 733358).

3. Gatlin, Califfor; Goebel, Donald; and Larsen, Stuart; ANALYSIS OF HELICOPTER STRUCTURAL CRASHWORTHINESS, Dynamic Science; USAAVLABS Technical Report 70-71, Eustis Directorate U. S. Army Air Mobility Research and Development Laboratory, Fort Eustis, Virginia, January 1971, AD 880680 and AD880678.

4. Greer, D. L., et al, CRASHWORTHY DESIGN PRINCIPLES, General Dynamics, Convair; FAA Technical Report ADS-24, Federal Aviation Administration, Washington, D. C., November 1965, AD 623575.

5. Reed, W. H., et al, FULL SCALE DYNAMIC CRASH TEST OF A DOUGLAS DC-7 AIRCRAFT, Aviation Safety Engineering and Research; FAA Technical Report ADS-37, Federal Aviation Administration, Washington, D. C., April 1965, AD 624051.

6. Reed, W. H., et al, FULL-SCALE DYNAMIC CRASH TEST OF A LOCKHEED CONSTELLATION MODEL 1649 AIRCRAFT, Aviation Safety Engineering and Research; FAA Technical Report ADS-38, Federal Aviation Administration, Washington, D. C., October 1965.

7. Fitzgibbon, Donald P., et al, CRASH LOADS ENVIRONMENT STUDY, Mechanics Research, Inc.; FAA Technical Report DS-67-2, Federal Aviation Administration, Washington, D.C., February 1967, AD 655920.

8. Greer, D. L., et al, DESIGN STUDY AND MODEL STRUCTURES TEST PROGRAM TO IMPROVE FUSELAGE CRASHWORTHINESS. General Dynamics, Convair; FAA Report DS-67-20, Federal Aviation Administration, Washington, D. C., October 1967.

9. Bigham, James P., and Bingham, William W., THEORETICAL DETERMINATION OF CRASH LOADS FOR A LOCKHEED 1649 AIRCRAFT IN A CRASH TEST PROGRAM, Boeing Airplane Company; FAA Technical Report ADS-15, Federal Aviation Administration, Washington, D. C., July 1964.

LITERATURE CITED (CONTINUED)

10. Turnbow, J. W., Ph.D., A DYNAMIC TEST OF AN H-25 HELICOPTER, Aviation Crash Injury Research Division; SAE Report 517A, National Aeronautic Meeting, April 1962.

11. Leredaht, B. H., et al, SOME NOTES ON THE PHYSIOLOGICAL TOLERANCE TO ACCELERATION, Douglas Aircraft Company, Report ES 40253, February 1961.

12. Stech, Ernest, and Payne, Peter, DYNAMIC MODELS OF THE HUMAN BODY, Frost Engineering Development Company; AMRL-TR-66-157, Aerospace Medical Research Laboratory, Wright-Patterson Air Force Base, Ohio, November 1969, AD 701 383.

13. PERSONNEL RESTRAINT SYSTEMS STUDY, BASIC CONCEPTS, Flight Safety Foundation; TCREC Technical Report 62-94, Task 9R95-20-001-01, U. S. Army Transportation Research Command, Fort Eustis, Virginia, December 1962.

14. Coleman, Rolf R., THE MECHANICAL IMPEDANCE OF THE HUMAN BODY IN SITTING AND STANDING POSITION AT LOW FREQUENCIES, Biomedical Laboratory; ASD Technical Report 61-492, Aeronautical Systems Division, Wright-Patterson Air Force Base, Ohio, September 1961.

15. Eiband, Martin A., HUMAN TOLERANCE TO RAPIDLY APPLIED ACCELERATIONS: A SUMMARY OF THE LITEPATURE, Lewis Research Center, NASA Memo 5-19-59E, National Aeronautics and Space Administration, Washington, D.D., June 1959.

16. O'Bryan, Thomas, and Hatch, Howard, Jr., LIMITED INVESTIGATION OF CRUSHABLE STRUCTURES FOR ACCELERATION PROTECTION OF OCCUPANTS OF VEHICLES AT LOW IMPACT SPEEDS, Langley Research Center, NASA-TN-D-158, National Aeronautics and Space Administration, Washington, D. C., October 1959.

17. UH-1 ACCIDENT SUMMARY, USABAAR Report, U. S. Army Board for Aviation Accident Research, Ft. Rucker, Alabama, 1963.

18. Mattox, Kenneth L., INJURY EXPERIENCE IN ARMY HELICOPTER ACCIDENTS, U. S. Army Board for Aviation Accident Research, Ft. Rucker, Alabama, September 1967, AD 658079.

19. Turnbow, James W., and Haley, J. L., Jr., A REVIEW OF CRASHWORTHY SEAT DESIGN PRINCIPLES, Arizona State University and AVSER Flight Safety Foundation, SAE Paper 851A, Air Transport and Space Meeting, April 1964.

20. Rich, M. J., VULNERABILITY AND CRASHWORTHINESS IN THE DESIGN OF ROTARY WING VEHICLE STRUCTURES, SAE Paper 680673, 1968.

LITERATURE CITED (CONTINUED)

21. Moseley, Harry, Colonel, et al, RELATION OF INJURY TO FORCES AND DIRECTION OF DECELERATION IN AIRCRAFT ACCIDENTS, Journal of Aviation Medicine, Vol. 29, October 1958.

22. Brinkley, James W., DEVELOPMENT OF AEROSPACE ESCAPE SYSTEMS, Air University Review, July-August 1968.

23. Weinberg, L. W. T., CRASHWORTHINESS EVALUATION OF AN ENERGY ABSORPTION EXPERIMENTAL TROOP SEAT CONCEPT, Aviation Safety Engineering and Research; USATRECOM Technical Report 65-6, U. S. Army Transportation Research Command, Fort Eustis, Virginia, February 1965, AD 614582.

24. Bruggink, G. M., and Schneider, D. J., M.D., LIMITS OF SEAT BELT PROTECTION DURING CRASH DECELERATIONS, Aviation Crash Injury Research; TCREC 61-115, U. S. Army Transportation Research Command, Fort Eustis, Virginia, September 1961, AD 265868.

25. Haley, J. L., HELICOPTER STRUCTURAL DESIGN FOR IMPACE SURVIVAL, U. S. Army Board of Aviation Accident Research, Ft. Rucker, Ala., November 1970.

26. Smith, H. G., and McDermott, J. M., DESIGNING FOR CRASHWORTHINESS AND SURVIVABILITY, Hughes Tool Co., American Helicopter Society Proceedings, November 1968.

27. Thompson, A. B., A PROPOSED NEW CONCEPT FOR ESTIMATING THE LIMIT OF HUMAN TOLERANCE TO IMPACT ACCELERATION, Aerospace Medical Journal, Vol. 33, No. 11, November 1962.

28. MIL-S-9479A, A GENERAL SPECIFICATION FOR AIRCRAFT UPWARD EJECTION SEAT SYSTEM, Amended December 1969.

29. MIL-T-27422B AIRCRAFT CRASH RESISTANT FUEL TANK MILITARY SPECIFICATION, Amended February 1970.

30. MIL-S-8698, HELICOPTER STRUCTURAL DESIGN REQUIREMENTS MILITARY SPECIFICATION, July 1954.

31. MIL-S-58095, GENERAL MILITARY SPECIFICATION FOR AIRCREW NON EJECTION CRASHWORTHY SEAT SYSTEM, August 1971.

32. Haley, J., PRELIMINARY DRAFT, COST EFFECTIVENESS OF CRASHWORTHY STRUCTURAL FEATURES IN A 9-13 PLACE HELICOPTER, USAAAVS, Technical Report 72-1, U.S. Army Agency for Aviation Safety, Ft. Rucker, Ala.

LITERATURE CITED (CONTINUED)

33. Haley, J., ANALYSIS OF HELICOPTER ACCIDENTS TO DEFINE IMPACT INJURY PROBLEMS, USAAAVS Report To Be Published, U. S. Army Agency For Aviation Safety.

34. STATIC TEST OF FUSELAGE TAIL BUMPER, Lockheed Aircraft Corporation, SRM 148, August 1948.

35. Phillips, N. S., A STATISTICAL EVALUATION OF THE INJURY POTENTIAL OF A "SQUARE WAVE" ENERGY ABSORBER, Beta Industries, USAAMRDL Technical Report 72-9, U. S. Army Air Mobility Research and Development Laboratory, Ft. Eustis, Virginia.

36. Carr, R. W., Phillips, N. S., DEFINITION OF DESIGN CRITERIA FOR ENERGY ABSORPTION SYSTEMS, Beta Industries Inc., NADC Report AC-7010, Naval Air Devel. Center, Johnsville, Warminster, Pa., June 1970, AD 871-040.

37. RFP DAAJ02-72-R-0254 UTILITY TACTICAL TRANSPORT AIRCRAFT SYSTEM, U. S. Army Aviation Systems Command, St. Louis, Mo., December 1971.

38. Timoshenko, S. P., THEORY OF ELASTIC STABILITY, McGraw-Hill Book Company, 1961.

39. Hoff, N. J., THE DYNAMICS OF THE BUCKLING OF ELASTIC COLUMNS, Journal of Applied Mechanics, March 1951, pages 68 - 74, Vol. 18.

40. Bell Helicopter Company Report 205-099-004, UNIT INERTIA LOADS - WEIGHT AND INERTIA DISTRIBUTION DATA.

41. Harris, C. M., Crede, C. E., VIBRATION AND SHOCK HANDBOOK, VOLUME I, Chapter 8, McGraw Hill Book Company, 1961

42. Lockheed Missile and Space Company, Inc. (LMSC), STAG'S USERS MANUAL, 003203.

43. Etkin, B., DYNAMICS OF FLIGHT, John Wiley and Sons, Inc., 1959.

44. Bell Helicopter Company Report 205-099-403, STATIC TESTS OF THE UHY-1D.

45. Bell Helicopter Company Report 205-099-991, BASIC STRUCTURAL DESIGN CRITERIA.

46. Bell Helicopter Company Report 205-099-003, STRUCTURAL DESCRIPTION REPORT.

47. Bell Helicopter Company Report 205-099-007, STRESS AND LOADS ANALYSIS.

48. Bell Helicopter Company Report 205-099-401, SKID GEAR DROP TESTS.